The University Of Sheffield.

Access To Thesis.

- A bound copy of every thesis which is accepted as worthy for a higher degree, must be deposited in the University of Sheffield Library, where it will be made available for borrowing or consultation in accordance with University Regulations.
- All students registering from 2008–09 onwards are also required to submit an electronic copy of their final, approved thesis. Students who registered prior to 2008–09 may also submit electronically, but this is not required.

Author: Martin R Braun Dept: Mechanical Engineering

Thesis Title: The Effect of Location and Climate Change on the Energy Consumption of Supermarkets in the UK Registration No: 110125309

For completion by all students:

Submit in print form only (for deposit in the University Library): ☑

Submit in print form and also upload to the *White Rose eTheses Online* server: In full ☑

Edited eThesis ☐

Please indicate if there are any embargo restrictions on this thesis. Please note that if no boxes are ticked, you will have consented to your thesis being made available without any restrictions.

Embargo details: (complete only if requesting an embargo to either your print and/or eThesis)	Embargo required?		Length of embargo (in years)
Print Thesis	Yes ☐	No ☑	____
eThesis	Yes ☐	No ☑	____

Supervisor: I, the supervisor, agree to the named thesis being made available under the conditions specified above.

Name: Stephen Beck Dept: Mechanical Engineering

Signed: S Beck Date: 18/6/15

Student: I, the author, agree to the named thesis being made available under the conditions specified above.

I give permission to the University of Sheffield to reproduce the print thesis in whole or in part in order to supply single copies for the purpose of research or private study for a non-commercial purpose.

I confirm that this thesis is my own work, and where materials owned by a third party have been used copyright clearance has been obtained. I am aware of the University's *Guidance on the Use of Unfair Means* (www.sheffield.ac.uk/lets/design/unfair)

I confirm that all copies of the thesis submitted to the University (including electronic copies on CD/DVD) are identical in content.

Name: Martin R Braun Dept: Mechanical Engineering

Signed: Date: 19/06/15

For completion by students also submitting an electronic thesis (eThesis):

I, the author, agree that the University of Sheffield's eThesis repository (currently WREO) will make my eThesis available over the internet via an entirely non-exclusive agreement and that, without changing content, WREO may convert my thesis to any medium or format for the purpose of future preservation and accessibility.

I, the author, agree that the metadata relating to the eThesis will normally appear on both the University's eThesis server and the British Library's EThOS service, even if the thesis is subject to an embargo. I agree that a copy of the eThesis may be supplied to the British Library.

I confirm that the upload is identical to the final, examined and awarded version of the thesis as submitted in print to the University for deposit in the Library (unless edited as indicated above).

Name: Martin R Braun Dept: Mechanical Engineering

Signed: Date: 19/06/15

THIS SHEET MUST BE BOUND IN THE FRONT OF THE PRINTED THESIS BEFORE IT IS SUBMITTED

Department of Mechanical Engineering

The Effects of Location and Climate Change on the Energy Consumption of Supermarkets in the UK

Martin R Braun

June 2015

A thesis submitted to the University of Sheffield in partial fulfilment of the requirements for the degree of Doctor of Philosophy.

Acknowledgements

The pursuit of a PhD can be frustrating and lonely at times, therefore any assistance and encouragement given to me is gratefully acknowledged. In particular I would like to say a big “Thank you!” to my academic supervisors, Prof Stephen B M Beck, Prof Martin Mayfield and Dr Hasim Altan, for their sustained, knowledgeable input during the research and writing process.

During the project I also received financial and logistical support from my industrial sponsor, Marks and Spencer, and also the permission to make this thesis available without restriction. In addition, I would also like to gratefully acknowledge Marks and Spencer’s willingness to share raw data and engineering knowledge. As I visited a number of stores and received the willing assistance of many employees there as well as from the energy management team, I would like to express my gratitude to all of them. In this connection I need to particularly thank Mr Paul Walton, who was my main contact at Marks and Spencer, for his valuable contributions during our quarterly progress update meetings and for readily progressing my requests internally in between. Another very supportive company was Emerson Climate Technologies Retail Solutions UK. In this company, I want to especially mention Mr Keith Bertie and Mr Matthew Maeer who took time out of their busy schedules to discuss and support my work.

Financial support for this work came from the University of Sheffield, Marks and Spencer, and the EPSRC, and is gratefully acknowledged.

Of course, without the support of my wife this project would not have been possible. So I thank her for her assistance and, in particular, for the many times she was willing to proofread parts of this thesis, papers, reports etc arising from my PhD project.

Abstract

This thesis reports on the investigation into how climate change may affect the energy consumption in supermarkets at various locations throughout Great Britain in the 2030s. Both complete supermarkets and refrigeration systems were studied. Information on questions on climate change impact can assist supermarket owners and operators with their long term planning regarding energy users, demand and infrastructure, and add impetus to the search for adaptation and mitigation strategies.

After reviewing relevant literature and evaluating different energy research tools, the fundamentals of climate change modelling were studied to understand the reliability of climate predictions. The guiding principle for selecting analysis tools was to use as simple an approach as possible which still yielded meaningful results. This led to the selection of simple regression and change point regression models for investigating whole supermarkets. This analysis was preceded by the identification of seven comparable grocery supermarkets with a good geographic spread. A refrigeration system software model was developed based on thermodynamic principles, also allowing examination of the effect of condenser fan control on energy use.

As climate change forecasts have a large error margin, the research findings should be treated as indicative only. To show the range of uncertainty, different values from the predicted temperature distribution were used. These results suggested that the electricity consumption for complete supermarkets will rise by between 0.6% and 4.7%, whilst gas use decreases by between 3.3% and 24.1%. This trend agrees with other research. The estimated increase of electricity use of between 1.7% and 13% from the refrigeration model indicates that this would account for most of the electricity demand rise. Future work should include investigating the condenser fan control, as the software model predicted an energy saving potential of approximately 4.5% by the use of better control algorithms.

Contents

List of Figures

Nomenclature

Abbreviation	Explanation
A	Surface area
A_i	Internal surface area
ANN	Artificial neural network
AOGCM	Coupled atmosphere-ocean circulation models
b_0	Estimate of regression intercept
b_i	Estimate of regression slope(s) ($i > 0$)
c_{air}	Specific heat capacity of air
c_v	Specific heat capacity at constant volume
c_p	Specific heat capacity at constant pressure
$c_{p,min}$	Minimum specific heat capacity at constant pressure
$\bar{c}_{p,vpr}$	Average of specific heat capacity in a vapour region
C_x	Coefficient for compressor (x^{th} coefficient)
C	Thermal capacitor
CDD	Cooling degree days
CFD	Computational fluid dynamics
COP	Coefficient of performance
$COSP$	Coefficient of system performance
CoV	Coefficient of variation
$CV(RMSE)$	Coefficient of variation of the root mean square error
DSY	Design summer years
E_{comp}	Power consumption of compressor(s)
E_{fan}	Power consumption of condenser fan(s)
E_{other}	Power input into devices other than compressors and condenser fans
E_{theo}	Theoretical work input into compressor(s)
$E_{theo,inst}$	Theoretical work input into installed compressors
E_{tot}	Total power input
EMIC	Earth system models of intermediate complexity
ENSO	El Niño/Southern Oscillation
ESM	Earth system models
EUI	Energy use intensity
EUI_{elec}	Annual electric energy use intensity
EUI_{pa}	Annual energy use intensity
EUI_{wkly}	Weekly energy use intensity
$\widehat{EUI}_{wkly}$	Estimated weekly energy use intensity
err_i	Individual error
err_{tot}	Total propagated error
F	F - static
g	Gravitational acceleration
GCM	General circulation model
GHG	Greenhouse gas
h	Specific enthalpy
$h_{i,air}$	Specific enthalpy of air in specific volume

Abbreviation	Explanation
h_{out}	Specific enthalpy at discharge port of compressor
h_{sh}	Specific enthalpy in superheated region
$h_{x,m}$	Specific enthalpy of model at point x in refrigeration cycle
h_x	Specific enthalpy at point x in refrigeration cycle
H_0	Null hypothesis
HDD	Heating degree days
HVAC	Heating, ventilation and air conditioning
$K_{tot,c}$	Total heat loss constant
K_{tot}	Total heat loss coefficient
m	Mass
$\dot{m}_{air,cdg}$	Mass flow rate of air through condensing part of condenser
$\dot{m}_{air,dsh}$	Mass flow rate of air through de-superheating part of condenser
$\dot{m}_{air,max}$	Maximum air mass flow rate
$\dot{m}_{air,rq}$	Required air flow rate
$\dot{m}_{inf,outside}$	Infiltration mass flow rate from outside
$\dot{m}_{inf,zone}$	Infiltration mass flow rate from another zone
$\dot{m}_{max,c}$	Maximum refrigerant mass flow rate of individual compressor
$\dot{m}_{ref}$	Overall mass flow rate of refrigerant
$\dot{m}_{rf}$	Required refrigerant mass flow rate
MBE	Mean bias error
MLR	Multiple linear regression
MVA	Multi variant analysis
n	Number of measurements Index of compression
N	Air infiltration rate
$n_{fan\%}$	Speed of condenser fan in % of maximum fan speed
n_{fan}	Speed of condenser fan
n_{max}	Maximum fan speed
NCM	National Calculation Methodology
OTTV	Overall thermal transfer value
p	Number of predictors Pressure
p_c	Condenser pressure (general) Absolute pressure at suction port of compressor
$\vec{p}_c$	Vector of condenser pressure
$p_{c,abs}$	Absolute condenser pressure
p_e	Evaporation pressure (general) Absolute pressure at discharge port of compressor
$p_{e,abs}$	Absolute evaporator pressure
PCA	Principle component analysis
q	Specific heat
$q_{h,in}$	Specific heat rate from the hot stream in heat exchanger
q_{HX}	Specific heat transferred in heat exchanger
q_c	Specific heat rejected by the condenser
q_e	Specific heat absorbed by the evaporator
Q	Heat
$\dot{Q}_1$	Heat rejection rate from condensing part of condenser

Abbreviation	Explanation
$\dot{Q}_2$	Heat rejection rate from de-superheating part of condenser
$\dot{Q}$	Actual heat transfer rate
$\dot{Q}_{air}$	Heat rejection rate to air through condenser
$\dot{Q}_c$	Heat rejected by condenser
$\dot{Q}_e$	Useful refrigeration effect Cooling load (or refrigeration effect)
$\hat{\dot{Q}}_e$	Estimated cooling load (or refrigeration effect)
$\vec{\dot{Q}}_e$	Vector of estimated cooling loads
$\dot{Q}_{e,max}$	Maximum refrigeration effect
Q_{heat}	Required heat/cooling supplied by HVAC system
$\dot{Q}_{infl,zn}$	Air infiltration rate from other zone(s)
$\dot{Q}_{infl,o}$	Infiltration rate of outside air
$\dot{Q}_{int\ gn}$	Rate of internal heat gain
$\dot{Q}_{max}$	Maximum possible heat transfer rate
Q_{net}	Net heat gain
$\dot{Q}_{net}$	Rate of net heat gain
$\dot{Q}_{srfc}$	Convection from surface
$\dot{Q}_{sys,sen}$	Load on HVAC system
r	Correlation coefficient
r^2	Coefficient of determination
R	Thermal resistor
RCM	Regional climate model
RCP	Representative concentration pathway
$RMSE$	Root mean square error
RH_{out}	Outside relative humidity
SBEM	Simplified building energy model
SCM	Simple climate model
SL	Secondary loop
SVM	Support vector machine
t	t – static Time
T	Absolute temperature
TMY	Typical meteorological year
TRY	Test reference year
u	Specific internal energy
U	Internal energy Fabric U-value
VSD	Variable speed drive
v	Specific volume
v_{in}	Specific volume at suction port of compressor
V	Velocity Space volume
$\dot{V}_{air}$	Air mass flow rate
w	Humidity ratio Specific work
w_{cmp}	Specific work input into compression process

Abbreviation	Explanation
$\dot{w}'_{cmp}$	Specific work input into compression process using $v\ dp$ integral
w_i	Weights of inputs for artificial neural network summation
w/c	Week commencing
W	Work
WG	Weather generator
$\vec{x}_k^T$	Transposed vector for which an estimate is to be made
$\bar{x}$	Arithmetic mean of all x_i
x_i	Independent variable of measurements, i^{th} input
X	Matrix of predictors (including leading column of ones)
$\bar{y}$	Arithmetic mean of all y_i
$\hat{y}_{gas}$	Estimated value of gas consumption
$\hat{y}_i$	Estimated value of the dependent variable for the ith data point
y_i	Dependent variable of measurements, i^{th} response
$\Delta\hat{y}_i$	Prediction interval

Greek Letters

Abbreviation	Explanation
α	Level of significance Activation function of ANN
β_0	True regression model intercept
β_i	True regression model slope(s) ($i > 0$)
ε	Effectiveness
ε_i	The error term for the ith measurement
σ	Standard deviation
σ^2	Variance
$\eta_{heat,c}$	Efficiency constant of heating system
η_{heat}	Efficiency of heating system
η_{isen}	Isentropic efficiency
ϑ	Temperature
$\bar{\vartheta}_2$	Arithmetic mean of de-superheating section of condenser
ϑ_{bal}	Balance point temperature
ϑ_{cdg}	Condensing temperature
ϑ_{cp}	Change point temperature
$\vartheta_{g,sat}$	Temperature of saturated vapour
$\vartheta_{in,i}$	Temperature of an internal surface
ϑ_{inside}	Interior temperature
$\vartheta_{l,sat}$	Temperature of saturated liquid
ϑ_{off}	Temperature of air leaving condenser
ϑ_{on}	Temperature of air entering condenser
$\vec{\vartheta}_{on}$	Vector of air temperature entering the condenser
$\vartheta_{outside}$	Outside temperature
ϑ_{sh}	Superheat temperature
ϑ_{suc}	Temperature at suction port of compressor
$\vartheta_{zn,air}$	Zone air temperature

Publications

Publications arising from the present investigation up to the writing of this thesis:

- BRAUN, M. R., ALTAN, H. & BECK, S. E. B. 2013. Using IBM SPSS Statistics to identify predictors of electricity consumption in a UK supermarket. *Energy and Sustainability 2013*. Bucharest: The Wessex Institute of Technology.
- BRAUN, M. R., BECK, S. B. M. & ALTAN, H. 2014. Comparing COP Optimization with Maximizing the Coefficient of System Performance for Refrigeration Systems in Supermarkets. *15th International Refrigeration and Air Conditioning Conference*. Purdue: Purdue University.
- BRAUN, M. R., ALTAN, H. & BECK, S. B. M. 2014. Using regression analysis to predict the future energy consumption of a supermarket in the UK. *Applied Energy*, 130, 305-313.

1 Introduction

Although the attribution of the quote "Predictions are difficult, especially about the future" is in some doubt (Pors and Kicia, 2007), its truthfulness is not. Therefore any study on how climate will change over the next couple of decades and how this will affect humankind will have to acknowledge the accuracy of this statement. This thesis, which explores the impact of climate change on energy use in supermarkets, is no exception.

Climate change predictions use models which try to mimic an extremely complex system with simplifying assumptions and this in the face of uncertainty. That this has been appreciated by the scientific community in this field is well documented in reports collected by the IPCC (see, for instance, Nakicenovic *et al* (2000)). Notwithstanding that, a substantial body of work has been produced in this field and models have been developed to predict the climate to the end of this century and beyond. Although the model designers have strived for accuracy, results from these models should be used more as one of many possible scenarios. However, being aware of different possible trends and their likelihoods will put decision makers in a better position to weigh the advantages and disadvantages of various options to arrive at more robust decisions.

As buildings have been said to account for approximately one third of all final energy use (Ürge-Vorsatz *et al*, 2012), a research field has developed to quantify the impact of climate change on energy demand. Probably the earliest work is a study by Loveland and Brown (1989) for the Office of Technology Assessment of the United States Congress in which the authors used building simulation software to estimate the change in energy use of five building types in six US cities. For the weather data, they used the then current typical meteorological years (TMYs) for those cities and a prediction of how these TMYs would change if the atmospheric CO_2 were to double. Their models suggested that, in general, the cooling load would increase by more than the heating demand would decrease, thus resulting in a net increase in energy use, but the exact amount would be location dependent. Subsequently, other regions have also been investigated and their results have been summarised by Li *et al* (2012). They found that, in addition to building simulation software, the degree day method was popular in researching heating and cooling demand in residential dwellings and office buildings. After reviewing over one hundred research outputs the authors came to virtually the same conclusion as Loveland and Brown (1989).

Their intuitively credible review findings were that, if the climate warmed up, heating demand would decrease, but cooling requirements would rise. Whether this meant that electricity and gas consumption would change and, if so, by how much depended on the location of a building and its type.

Although supermarkets belong to a building type with a high energy use intensity (EUI) (Tassou *et al*, 2011) the literature research summarized in the next chapter indicates that climate change impact on supermarket energy usage has not been investigated. Therefore this forms one of the research aims. These objectives can be summarized as follows:

- Quantify the possible influence of a changing climate in the UK on supermarket energy use. To be relevant to decision makers in supermarkets the time horizon is relatively short (the 2030s).

- Investigate the effects of location on the energy consumption in supermarkets. This includes not only considerations regarding the local climate, but also examines differences in operational procedures.

- Quantify the climate change impact on the refrigeration system separately, because this is a major temperature dependent energy consumer.

- Suggest possible energy saving measures to reduce the impact of climate change on the use of energy in supermarkets.

1.1 Context of research

This section frames the climate change impact assessment within the wider context in which supermarkets operate. In doing so it seeks to highlight the practical value of the research to senior management in supermarkets in the following two ways: Reputation and effectiveness of strategic decisions.

That a supermarket's reputation with its customers is of utmost importance is apparent when the statement: "[The] customer is the focus of all retail decisions." (Althouse *et al*, 1996) is considered. How this may affect decisions is exemplified in an article on confectionary placement in a supermarket by Piacentini *et al* (2000). These researchers argued that the main reasons for adopting a socially responsible approach to placement decisions was "ensuring customer satisfaction, rather than altruistic reasons". Another

motivating factor was profitability, or more specifically, the trade off between short-term and long-term profitability. The conclusion by the authors that the socially responsible selling of confectionery can be marketed and thus presents an opportunity for a competitive advantage may also be true for other decisions. This conclusion is supported by Whitehouse (2006) who reported that, in the retail sector some, felt that conducting business in a socially responsible way was another way to differentiate themselves from competitors. In this way, the increase in consumers' environmental consciousness may have encouraged the food retail sector to set the pace for the climate change agenda to the point that other sectors can learn from them (Oglethorpe and Heron, 2010). Amongst these Marks and Spencer seem to be a good example, as this company managed to bundle environmental concerns with other social-responsibility issues in a document they call 'Plan A' (Jones *et al*, 2009). In his article on corporate responsibility and sustainability Grayson (2011) used Marks and Spencer's 'Plan A' as a case study to show how to embed corporate responsibility and sustainability into a company. The research described below may very well feed into this activity, as it can be regarded as proof of the sponsor's desire to further understand long-term developments in the natural environment so that they can respond to it in a socially responsible manner.

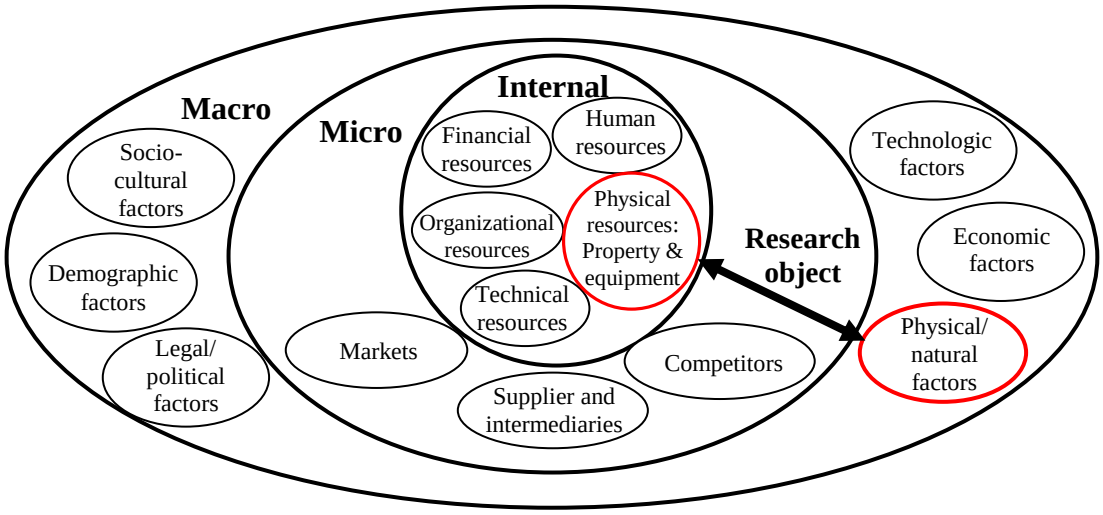

Figure 1.1: Environments relating to supermarkets

As regards the motives of engaging in socially or environmentally responsible practices it could be pointed out that, by law, company directors are required to maximise profits (Whitehouse, 2006, p 280). Therefore formulating and implementing strategies which take the wider context into consideration should benefit the company in one way or another, for

instance, by improving the company's reputation. Indeed doing otherwise may distract supermarkets from their core business - retailing products to consumers (Moore, 2001).

Figure 1.1 helps to highlight another way this research may be of value to supermarket decision makers. It shows that supermarkets engage in their main activity. i.e. the sales of goods and services from suppliers to end users for their personal use, in the following three types of environment (Cox and Brittain, 1996; Anderson, 1993):

- Macro environment
- Micro environment
- Internal environment

This diagram indicates the complex interactions between the different parts of these types of environment. It also highlights the subject of this research as the relationship between the physical/natural factors and items belonging to the physical resources. The macro environment considers aspects outside of the immediate control of the retailer (Anderson, 1993, 50). This could lead to the conclusion that the supermarket may not be able to change macro environmental factors, but may have to adapt to them. Adaptation measures may relate to the internal environment and may need to address the question of how to modify a supermarket's physical resources to cope with climate changes. One example of physical resources of supermarkets is their refrigeration systems, which have a design life span of between 10 and 15 years and may be affected by a change in temperature. Therefore choosing the 2030s as the time horizon for this research is appropriate in order to assist the decision makers in supermarkets with design and investment decisions regarding equipment like refrigeration plants.

1.2 Organisation of thesis

This thesis is organised as shown in Figure 1.2. This diagram indicates that, after this introduction, three chapters follow which are based on existing knowledge. The first of these is the literature review which summarizes literature on the impact of climate change on buildings and the energy analysis of supermarkets. The second chapter, discussing climate change predictions, is included to give an appreciation of the uncertainties attached to these and to introduce the background to the future climate estimates employed in calculating the energy consumption in the 2030s. This is followed by a survey of data-

driven and deterministic analysis tools in order to evaluate their individual advantages and disadvantages as a preparation for selecting an appropriate research methodology.

Chapters five to seven cover the research into the energy use in supermarkets and start with a description in chapter five of how seven similar stores throughout Great Britain were identified. This is followed in the same chapter by a discussion of the reasoning behind the selection of a method based on a statistical approach and how this methodology was then used to gather and analyse data. The sixth chapter, presenting the results, explains how the statistical models were constructed and what predictions these models yielded in terms of energy use change including error estimates. These results are discussed in chapter seven by comparing both the research approach and outcome with existing literature. It also examines errors and uncertainty, which influence the reliability of the results.

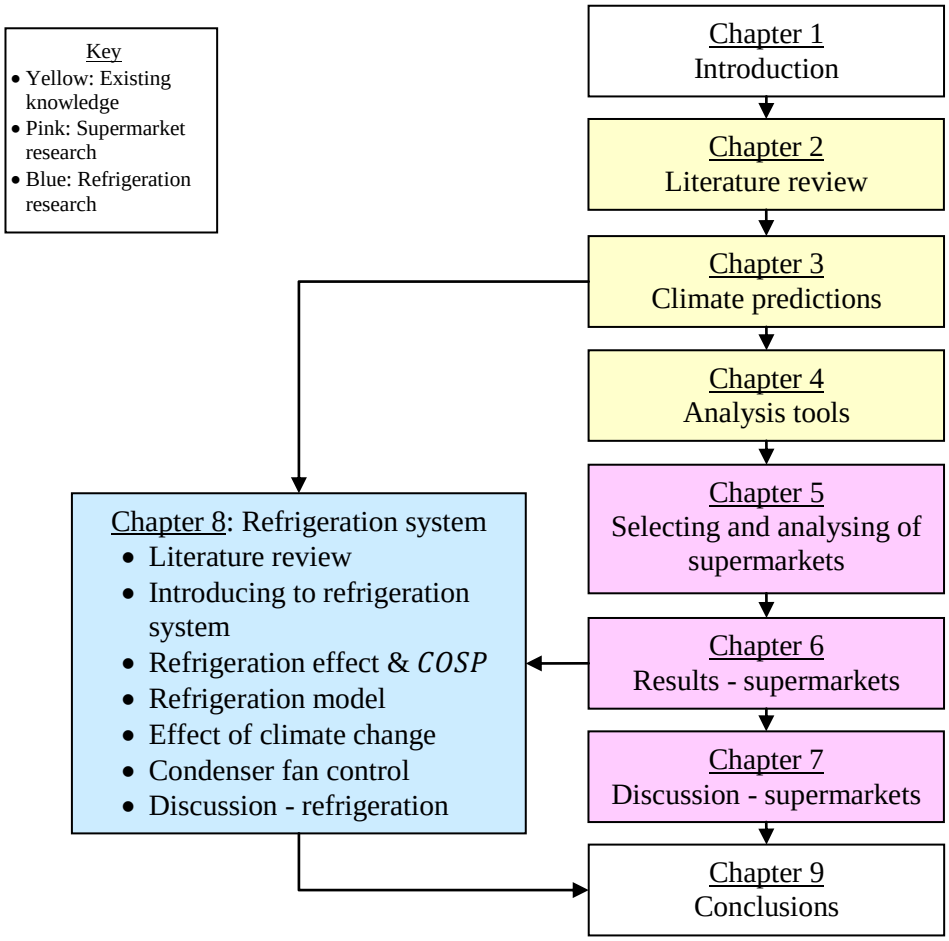

Figure 1.2: Thesis flowchart

Chapter eight is concerned with a refrigeration system installed in one of the selected supermarkets. The purpose of this chapter is to highlight how refrigeration systems, as a major temperature sensitive energy consumer, may react to a changing climate, thus adding

to the understanding of the behaviour of whole supermarkets developed in chapters five to seven. The description of the work on refrigeration systems begins, after a summary of the main topics of research in this field and a review of relevant thermodynamic theory, with a discussion of how the useful refrigeration effect of the installed plant, together with an efficiency figure, has been established. This is then expanded to construct a software model so that an estimate can be given of how the electricity consumption might change in the 2030s. The final piece of work covered in this chapter is the investigation into different approaches to condenser fan control.

The final chapter summarizes this thesis, discusses its main findings and offers some conclusions based on the work described. These conclusions include the major outcome form this work that, based on the climate change prediction employed here, the gas usage will drop by an amount significantly larger than the increase in electricity consumption. The research results of the refrigeration system suggest that most, if not all, of this increase in electricity demand may arise from the refrigeration system.

2 Literature review

This literature review chapter starts with describing the review rationale before relevant literature is summarized and evaluated. The first strand of research literature pursued here is regarding the impact of climate change on energy use in buildings, which is geographically organised. The second strand is concerned with how the energy use in supermarkets is analysed. For this topic the literature is divided into data-driven and deterministic tools.

2.1 Review rationale

The approach for researching the literature here is based on the systematic literature review method, a methodology found mainly in the medical field (Mulrow, 1994). The particular strength of this review approach is that it utilises a rigorous and structured way with the aim of identifying all relevant literature. This is in contrast to the more traditional approach which, according to Cronin *et al* (2008), lacks transparency. Hemingway and Brereton (2009) suggest that this leads to some bias because the traditional review method relies on the expert reviewer rather than on the peer review process. Since the systematic literature review has been designed with the medical literature in mind, not all of the stages of this process have been followed here. As this review was conducted from late 2012 to early 2013, a small scale literature search was conducted in November 2014 to include any relevant literature published since then.

What was found to be of particular help was the review protocol, which is included in Appendix A – Review protocol. This document sets out the background of the literature research and a focused research question, the search strategy (including search terms and resources), inclusion criteria and quality checks as well as the data extraction and synthesis procedures. This is complemented by a project timetable (Booth *et al*, 2012, pp. 58-60).

The draft protocol was submitted to the main PhD supervisor and to a health care professional teaching on the systematic literature review method. After the protocol had been approved, it was used to research a very narrow question which only allowed the inclusion of less than ten documents out of the 900 screened. In order to assess the body of literature more fully this initial question was widened to include the following two main questions:

- What does the existing literature say about the impact of the changing climate on the energy consumption in buildings?
- What methods have been used to investigate the energy consumption in whole supermarkets?

2.2 Impact of climate change on energy consumption in buildings

As Figure 2.1, which is based on the data reported in GEA (2012, pp 47, 48), shows buildings account for approximately one third of global energy end use. The energy demand arising from this sector, which is made up of residential as well as public and commercial buildings, arises mainly from heating and cooling (GEA, 2012, p 51). Therefore it is only logical that the effect of change climate on the consumption of energy in buildings has been studied for various locations.

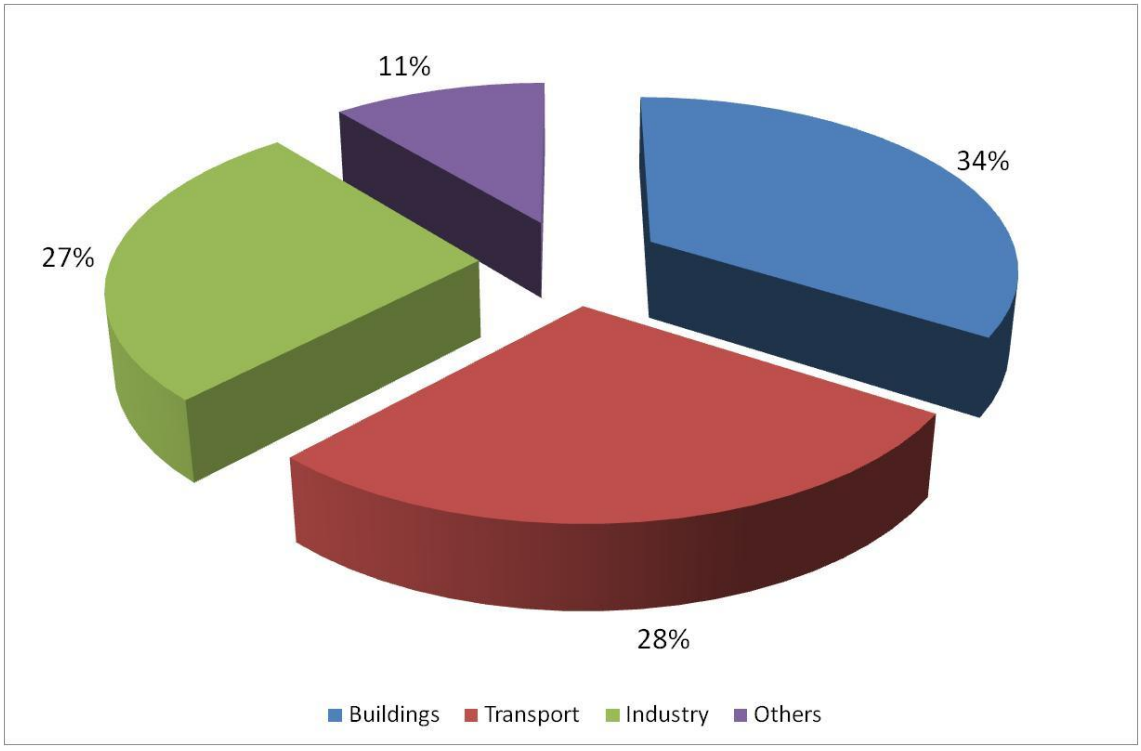

Figure 2.1: Sectoral breakdown of energy end-use

The literature relating to the impact of climate change on the energy use in building starts with a non-location specific section before it follows geographically grouped research outputs. Within these subsections the literature is chronologically arranged (except for the USA where a section relating to California has been included).

2.2.1 Global and summary studies

Isaac and van Vuuren (2009) modelled the global demand for energy for the residential sector by incorporating such diverse factors as HDDs (or CDDs for cooling), the population of a country and device efficiency. For their climatic data the researchers used IMAGE (Stehfest *et al*, 2014) output together with calibration and downscaling methods. Their model suggested an increase in demand for energy worldwide for both cooling and heating up to 2030 when heating demand was predicted to stabilize. However, cooling requirements were expected to continue to rise rapidly. The authors concluded that not all of this was owing to climate change, but also because of the increased comfort level demanded in homes. When exploring uncertainties, the authors pointed to uncertainties regarding future developments, lack of information about the present situation and their assumptions.

Li *et al* (2012) reviewed the literature on how climate change was expected to alter energy demand in the built environment. They found that the two most popular research approaches were the degree day method and the use of building simulation software. These methods were mainly applied to commercial buildings (e.g. office buildings) and residential dwellings. Their research showed that for higher temperatures the cooling demand was predicted to increase and the heating demand was thought to decrease. For severely cold climates this would likely lead to an overall reduction in energy use. For other climatic areas the overall effect was not so clear, but a shift towards higher electricity demand for cooling away from fuels for heating may result. The authors found studies suggesting that for office buildings the effect of climate change would be not as drastic as for residential dwellings, because of the higher internal loads in offices. Furthermore the authors reported that a number of papers also explored adaptation and mitigation measures, such as higher temperature set-points for air-conditioning or changes to the building envelope.

2.2.2 USA

The report by Loveland and Brown (1989) for the US congress was already referred to in the introductory chapter as probably the earliest work predicting the effect of climate change on energy use in buildings. In this work five building types (including a retail building) in six cities were simulated with the computer programme CALPAS3. The weather files of a TMY for the then present climate and for a climate scenario with double

the CO_2 levels were used to calculate changes in cooling and heating loads. One of the building types specifically excluded was food services (the paper also included food sales in this type of occupancy), because it was difficult to model this energy intensive building category and the total area of these types of commercial building was insignificant when compared with others. The overall conclusion was that the annual cooling load would increase more significantly than the heating load would decrease. However, the researchers were unable to indicate timing and duration of any annual demand patterns.

Scott *et al* (1994) first summarized studies undertaken for utility companies which had predicted that an average warming of 1°C may decrease heating demand by 2% and increase cooling requirements by a similar amount. The authors then criticized this approach using heating degree days (HDDs) and cooling degree days (CDDs) (see Section 4.5 for an explanation of the degree day method) as oversimplifying consumption predictions in commercial buildings, because this approach neglected any nonlinearities. For their building software model, these researchers not only used different future temperature scenarios, but also investigated the sensitivity to changes in humidity ratio and found significant nonlinear relationships between cooling energy and average temperature. The authors concluded that, for their study, the degree day method overpredicted heating and underpredicted cooling requirements, but also acknowledged that the overall effect of even simple climate change scenarios on the energy use in commercial buildings was difficult to predict.

One year later Matsuura (1995) published a paper detailing the research on a hypothetical town house and an office building simulated with a modified version of the software package BLAST in seven different cities throughout the United States. For the town house two different urban geometries were also evaluated. His simulation results showed that it was possible to fit linear regression models to one degree of warming for all cities. The author also found that, except for the two most southern cities, the overall energy demand would decrease for an average temperature increase. The author also noticed that the use and surroundings of the buildings were important. Further Matsuura suggests considering shading devices to reduce the summer cooling load.

In the same year as Matsuura, Rosenthal *et al* (1995) used the degree day method to investigate how warming of 1°C in 2010 would impact the total energy expenditure for space conditioning in the United States. Their research predicted that the overall monetary

impact would be a reduction in expenditure. The authors concluded that this trend remained the same, even if the considered increase was 2.5°C. The researchers acknowledged that their results were at variance with earlier studies and pointed out that earlier work had concentrated more on the increase in cooling rather than on the overall effect on cost. However, the research by Matsuura (1995) agreed with Rosenthal *et al* (1995) inasmuch as both pieces of research predict a countrywide reduction in energy demand.

Belzer *et al* (1996) published work using sample survey data to investigate commercial buildings. Their methodology started with deriving models based on degree days and energy bills. The regression models for electricity incorporated a temperature independent term and for gas consumption the model employed only an HDD dependent term. Next they extrapolated these models to the whole commercial building stock. This was followed by extrapolating these intermediate results to the year 2030. The researchers did not find any significant nonlinearity for their model, but acknowledged that, for CDDs, the fit of the model was not as good as for the HDDs. Their research supports the conclusion by Rosenthal *et al* (1995) inasmuch as it predicted that an average temperature increase would reduce the energy use in commercial buildings in the US, albeit only modestly.

Crawley (2003) used the different climate zones in the US (and one outside the US) to explore the global climate change impact on a small office building with the simulation software EnergyPlus. The researcher utilised modified weather files to represent the climate change for 2040, 2070 and 2100. His preliminary results showed that for a certain climate the overall energy use may not change, but a mere “fuel swap” from gas to electricity may occur.

A systematic study of all seven climate zones in the USA was performed by Wang and Chen (2014). They used the building simulation software EnergyPlus to calculate the change in energy use intensity of nine different types of building including residential and commercial buildings. To do this the researchers morphed current TRY data for three emission scenarios to simulate 2080s conditions with the monthly climate change prediction from the HadCM3 as input. Their research showed that the change in EUI is both building type and location dependent. For cities located in the colder regions of the USA an overall reduction in EUI can be expected, for the climate zones an increase was predicted.

2.2.2.1 California

Other research has been conducted relating to California only. For instance, Lebassi *et al* (2010) studied the historic climate change from 1970 to 2005 by means of temperature data from 159 locations in California. This research used HDDs and CDDs with a balance point temperature of 18°C because the authors felt this to be adequate to account for seasonal energy use variation. Their results showed that CDDs and HDDs differed significantly throughout California, which led to the authors differentiating between the coastal and inland effects. Based on their work these researchers suggested that the CDD for the lower coastal regions decreased whereas for inland locations situated at a higher altitude the CDD rose. This caused an uneven distribution of changes in peak electricity demand, ranging from a decrease in the southern coastal region to an increase in the more northern areas along the coast. Furthermore, the authors established that the reduction in HDDs was not matched by a corresponding increase in CDDs. According to these researchers this spatial distribution was due to the atmospheric and oceanic phenomena which dominated the climate in California.

Another example is the paper by Xu *et al* (2012) in which the authors downscaled weather data for 63 sites in California to predict the building energy use for the 2040s, 2070s and for the end of this century. After that they used these weather files to simulate a number of residential and commercial buildings in 16 climate zones in California with two different software packages. This phase was followed by combining the simulation results with estimates of building stock in California. The authors claimed very confidently that the use of heating would decrease and the energy consumed to cool buildings would rise significantly over the next century. They suggested that the actual building type should also be considered as the change in energy usage may be building type specific. In addition, these researchers reported that variations in energy use were location dependent, which corroborates the findings by Lebassi *et al* (2010).

2.2.3 Asia

Researchers in Asia, notably at the City University of Hong Kong, have also contributed to insight on the impact of climate change on energy use in buildings. Research output from this university used, amongst other methods, the principle component analysis (PCA) to investigate the impact of climate change on a typical office building in Hong Kong (Lam *et*

al, 2010a). Lam *et al* (2010a) explained that this approach was superior to the degree day method, as the PCA allows the incorporation of other weather variables in addition to dry-bulb temperature, and that it was also better than multiple linear regression (MLR) analysis as this method can cope with multicollinearity[1] better. Their research indicated that dry-bulb temperature, wet-bulb temperature and global solar radiation were the best predictors for their work leading to an estimate of an annual rise in cooling load of 9.1% translating into an increase in energy use of 4.3% for low radiative forcing (see Section 3.2.1 for an explanation of the term 'radiative forcing'). The researchers also estimated the model error with the coefficient of variation of the root mean square error ($CV(RMSE)$) (explained further in Section 5.7) using data for 2006-2008. They found the $CV(RMSE)$ for the heating load to range from 11.5% to 30.9% and for the cooling load to vary from 3.6% to 4.0%. A similar study on air-conditioning requirements in commercial buildings (Lam *et al*, 2010c) predicted a rise in electricity use for air conditioning of 18.4% for the 2069-2100 period (compared to 2008 consumption) for low radiative forcing. The $CV(RMSE)$ of their model varies from 9.2% to 23.5%.

Another approach used at this university was the overall thermal transfer value (OTTV) which was used on residential buildings (Wong *et al*, 2010). The OTTV gauges the heat transfer from the outside of the building to the inside through the building envelope, or vice versa, taking into consideration both walls and fenestration. The researchers also included the evaluation of energy saving measures in their study indentifying an increase in thermal insulation as the most effective option. The results showed that the building cooling load was expected to increase by 12.3% (compared with the period between 1979 and 2008) for 2071-2100 for low radiative forcing. It should be pointed out that the normalisation was different from that used in Lam *et al* (2010c) and therefore results are not completely comparable.

Morphed weather files together with a building simulation software package (EnergyPlus) were used for another piece of research investigating an office building and a residential building under climate change at this university (Chan, 2011). The researcher predicted that the increase in air-conditioning energy requirements of the office building would rise by 9.9% for a low forcing emission scenario for 2080-2099 (when compared with results based on then present weather files), whereas for the residential building, demand was

[1] "Multicollinearity implies a near-linear dependence among the repressors." (Montgomery *et al*, 2006, p 109)

expected to increase by 16.5% under the same conditions. The lower increase for the office building, the researcher surmised, would be due to the cooling load being significantly influenced by electrical equipment, which was not the case at the residential building.

A further paper from this university (Wan *et al*, 2011a) summarized work on predictions of the increase in average building energy use in Hong Kong with a PCA and a number of adaptation measures, which were simulated with VisualDOE4.1, relating to the building envelope, temperature set point and chiller efficiency. When using data from local weather stations and predictions based on MICRO3.2-H (Nozawa *et al*, 2007) the researchers found a continuous warming trend. This is expected to cause an electricity demand increase of 6.6% for the last decade of the 21st century for low forcing (compared with 1979-2008) without adaptation.

Wan *et al* (2011b) expanded the research done for Hong Kong to four other major cities in China. They also used a PCA which used the same three climate variables as in Lam *et al* (2010c) and, generally, the same approach as in Wan *et al* (2011a). The work done by the authors suggested an increase in the average cooling energy use from 11.4% to 24.2%, dependent on location, for low forcing for the rest of this century and a corresponding decrease in heating of between 13.8% and 26.6%.

The heating energy in the city of Tianjin was investigated by Xiang and Tian (2013) employing a PCA together with a TRNSYS software model of a reference building. Their PCA agreed with Lam *et al* (2010c) inasmuch as they used the same climate variables. Based on their PCA and their software model the researchers developed a third order polynomial regression model which predicted a heating energy reduction of 18.1% under low forcing conditions (i.e. under the same conditions as in Lam *et al* (2010c)) for the latter part of this century compared with the base period from 1971 to 2010. Because the data used to estimate the error was also used for the PCA, the validity of this method may be called into question and, therefore, is not stated here.

Chow *et al* (2014) investigated how better building regulations may alter the impact of climate change readiness in China. To this end they calculated the energy demand (although no calculation method was given in their paper) of an apartment block in each of four locations covering three climate zones in China. They found that the effect of the new regulations reduced the demand for heating, but pointed out that it depended on the climate

as to whether this was of significance, e.g. if the climate was so warm that heating requirements were already low impact, changes would be small. In addition, they mentioned that these measures may be counterproductive when it came to cooling as they could increase cooling demand.

2.2.4 Rest of the world – excluding Europe

Other research into climate change effects on areas of the world not covered so far include work by Zmeureanu and Renaud (2008), who examined the change in heating demands in Canadian houses by means of a simple regression model using HDDs as the independent variable and also a software model. Their statistical model incorporated a weather independent component not found in the normal degree day method. The data for the base year and future predictions was obtained from CCCMA (Environment Canada, n.d.). The results of this regression analysis compared well with the more detailed software model implemented in TRNSYS. This piece of research indicated that the reduction in the annual heating energy for 2040-2069 could range from 11% to 13.1% when compared with the data from 1961-1990.

Another example is the work by Roshan *et al* (2012) who used HDDs and CDDs to investigate how climate change may impact on Iran. These researchers chose the degree day method because they considered it simple and reliable. For their research the authors used data from 43 weather stations in Iran from 1961 to 1990 as their baseline and the output from the MAGIC/SCENGEN software (Wigley, 2008) for predicting the climate change impact. According to their research the annual heat requirements will reduce by about 20% with a simultaneous increase in cooling requirements of approximately 65% in 2075.

The sub-Saharan climate was studied by Ouedraogo *et al* (2012) with the simulation software package IES. The researchers used data from the Burkina Faso Meteorological Office from 1977 to 2010 to generate a current test reference year (TRY) and projected data from the Hadley Centre model HadCM3 for a future TRY. When comparing the HadCM3 projections with historical data, the researchers found a mismatch which they considered acceptable. A typical detached, three story office building was modelled in IES with internal gain due to people, lighting and electric equipment. This study found that the cooling load differed from room to room with the middle floor having the lowest load. The researchers also concluded that the yearly cooling demand would more than triple for the

period between 2060 and 2079 when compared with the demand of an actual, comparable building for 2007.

2.2.5 Europe – excluding the UK

The work reported by Cartalis *et al* (2001) investigated how the HDDs and CDDs may change in 2030 in Greece and how this translated into altered energy consumption patterns. The climate model used for this research, ESCAPE (Rotmans *et al*, 1994), together with an HDD set-point temperature of 15.5°C and 18°C for CDD, yielded different results for a "typical building construction" (Cartalis *et al*, 2001) of a one-zone building depending on the policy scenario employed. For the most aggressive reduction in greenhouse gasses, the researchers found that HDDs would reduce by just below 5% and CDDs would increase by just under 15% with a corresponding decrease in heating energy use of 4.7% and an increase for cooling of 14.9%. For a business as usual emission scenario heating and cooling energy was predicted to change by -10% and +28.4% respectively. The authors explained that, because of climate model uncertainties, their results should be treated with some caution. Other sources of uncertainties were not explored in this paper.

Frank (2005) employed the building simulation software HELLIOS to calculate the change in heating and cooling demand for a residential building and an office building in Switzerland. The base year period, for which the researcher used data from various sources (e.g. WM reference period (World Meteorological Organization, n.d.)), was modified to simulate rises of 0.7°C, 1°C and 4.4°C. He found that for each degree the temperature rose the heating energy demand in the residential building would drop by 8-13%. The increase in cooling demand, the author suggested, could be met by night time ventilation. The office building exhibited a similar drop in heating demand. However, due to a low starting value, the cooling demand was expected to rise by up to 1050% for a 4.4°C temperature increase.

Christenson *et al* (2006) used the degree day method to investigate how climate change would impact on buildings in four locations in Switzerland. In their paper they described how they had condensed data from eight climate models to upper and lower limits for the second half of the 21st century. They found that there was a large range of possible decreases for HDDs ranging from 13% to 87% in the period 1975-2085 with the temperature scenarios having a greater impact than location, building quality or balance point temperature. The CDDs had a much higher percentage increase, which was because

of a low starting point. These researchers also pointed out that the future projections were uncertain due a variety of possible socio-economic development paths.

Changes in heating and cooling demands in two climatic regions in Slovenia were researched by Dolinar *et al* (2010) with a TRNSYS software model. This model also allowed the investigation of different building properties. The authors explained that temperature, precipitation and global radiation were important inputs in constructing their climate scenarios. Their research suggested that for the subalpine region the 2050 heating demand would drop by 16% to 25% (compared with 1961-1990 figures), but for the Mediterranean area no significant change was expected. Similarly, the cooling demand increase was expected to be significantly higher in the subalpine zone than in the Mediterranean region. In addition to this, the researchers reported that for significantly warmer, more solar intensive climates, better insulated houses would perform better. However, if the temperature increase was only modest, standard buildings required less cooling energy.

Pilli-Sihvola *et al* (2010) sought to establish a relationship between climate change and electricity consumption across Europe. The authors collected electricity data for periods which varied from country to country, but generally included the period from 1989 to 2005. Then they made use of a multiple regression model to establish a link between electricity use on the one hand and seasonality, temporal trend, CDDs and HDDs on the other hand for Finland, Holland, Germany, France and Spain. The authors found a clear relationship between temperature and electricity demand for winter and also between the demand for cooling and temperature in summer for south Europe. Although the result for an individual country depended on the climate zone it was in, the overall result was a reduction in electricity use for Europe. In their section on conclusions the authors pointed out that, due to the long time horizon and uncertainty of the validity of their assumptions, any result should be treated as indicative only.

Research by Berger *et al* (2014) on urban locations in Vienna, Austria, and climate change investigated four office buildings (one built before World War One, one after World War Two, a highly glazed office block built post 2000 and a Passive House Standard office building). The regional climate model from the Max Planck Institute in Hamburg, Germany, was used to generate weather data input for the building simulation software package TAS from EDSL. The results showed an estimated reduction in overall future

energy demand of up to 15% for 2050 compared with the 1961 values and that EUI is more significantly related to the building type than to the location.

2.2.6 UK

When it comes to climate change and its impact on buildings, the UK is arguably among the best researched countries in Europe. One early example is the research reported by Jenkins *et al* (2008a) who simulated 2030 conditions with the ESP-r software package for a "typical office building" (Jenkins, 2009) at five different locations throughout the UK. In addition to the changing climate, efficiency improvements in lighting and small pieces of office equipment were also taken into consideration. When comparing both factors the results showed that the effect of more efficient equipment had a greater impact on energy demand than climate change. As the researchers found the spatial differences in climate change in the UK to be small (which seems to be at variance with official statistics, e.g. Jenkins *et al* (2008b)), they presented a conclusion for the whole of the UK, which was that climate change reduced the heating requirements more than it increased cooling demand.

De Wilde and Tian published two pieces of work on a theoretical office building located in Birmingham (de Wilde and Tian, 2009; de Wilde and Tian, 2010). They used the building simulation software EnergyPlus and future weather data based on UKCIP02 to investigate uncertainties in various input parameters such as changes to lighting levels, equipment efficiency and infiltration rate. When taking only climate change into account, their overall conclusion suggested that, although CDDs would rise, cooling energy would stay essentially the same. This was so because they considered only electricity for fans rather than complete air-conditioning systems. The heating requirements reduced more significantly pointing to an overall reduction of energy consumption due to climate change.

A CDD based regression analysis with a balance point temperature of 22°C was used by Day *et al* (2009) to forecast the cooling demand in London with climate data from local sources. They found that for London the CDDs would rise by almost 90% between 2004 and 2030 if no mitigation measures are adopted.

Collins *et al* (2010) examined the future energy requirements for the residential building stock with the assumption of a widespread up-take of air conditioning. In their study they used climate data based on UKCIP02 and the IES building software to simulate six

housing types at four locations in the UK. Their study also showed that heating demand was expected to fall whereas the cooling requirements were expected to increase due to the adoption of cooling systems. However, as the cooling demand started from a very low level, the overall effect would be a reduction in energy demand.

The updated version of the climate projection for the UK, UKCP09, along with IES was used by Gupta and Gregg (2012) to research the impact of climate change on four types of English houses in Oxford. Their work had the dual purpose of assessing the impact of the change in climate on thermal comfort and of evaluating adaption measures. The UKCP09 provides simulation results in the form of cumulative probability distributions for three different climate change scenarios. For the highest emission scenario and 90% probability, the researchers found a reduction in heating requirements by the 2080s of up to 75%. For the summer time, they identified a risk of overheating, possibly leading to the use of mechanical cooling equipment.

In addition to the academic community, other organisations have produced work concerned with the impact of climate change on buildings. One example is the summary report by Hacker *et al* (2005) in which the authors reported on the heat stress in six case study buildings and their carbon emissions as a function of the changing climate predicted for London, Manchester and Edinburgh. Their report concluded that many buildings in the UK would suffer from an increase in thermal discomfort and pointed to the absence of shading devices, controllable ventilation, insulation and thermal mass as high risk indicators. The authors suggested studying buildings in warmer climates to learn how to successfully adapt to the warming climate. The work summarised by Thompson *et al* (2015) may be considered an extension of the report by Hacker *et al* (2005) as it includes over 50 building adaptation case studies (including supermarkets). This document includes also recommendations for new building design such as the adoption of passive design features over energy consuming solutions.

2.3 Analysis of energy consumption in supermarkets

A major difference between a supermarket and other commercial buildings is the refrigeration system, which accounts for much if not most of the electricity consumption (Orphelin *et al*, 1997) and makes supermarkets highly energy intensive buildings (Hendron *et al*, 2012, pp 1-3). This has given rise to research in this area to see how refrigeration

systems may be made more efficient; Ge and Tassou (2000), Arias and Lundqvist (2006), Cecchinato *et al* (2010b), Llopis *et al* (2015) and others have published in this area.

Associated with the refrigeration in supermarkets is the cold aisle phenomenon caused by the open display cases. Related problems have been investigation with simple heat balancing equations (Orphelin *et al*, 1997), computational fluid dynamics (Stribling, 1997) or elaborate test set-ups including large scale smoke visualisation (Ndoye *et al*, 2011). Other researchers examined how a supermarket's internal conditions impacted on the cooling load of refrigerated display cases (see, for instance, Faramarzi (1999), Capozzoli *et al* (2006) or Bahman *et al* (2012)).

In contrast with research on specific problems in supermarkets referred to in the previous two paragraphs, this section surveys the literature on the energy consumption of whole supermarkets. The three main themes developed are data-driven methods, development of first principle models and software building simulation.

2.3.1 Research using data-driven approaches

Literature included in this sub-section proceeds from simple methods useful for benchmarking to change point regression analysis and more advanced multi variant analysis (MVA) including artificial neural networks.

2.3.1.1 Energy use intensity in supermarkets

The Energy Use Intensity (EUI) defined as the annual energy consumption per unit of area (usually given in kWh/m^2 per year) has been used by Tassou *et al* (2011) to investigate 2570 UK retail food outlets. DEFRA (2006, p.3) indicated that there were over 100,000 grocery retail stores in the mid 2000s and therefore only approximately 2.5% of all stores were investigated in Tassou *et al* (2011). Nevertheless the authors maintained that their sample was representative. In their work they based their classification on the sales area and followed the division found in DEFRA (2006, p. 24). Therefore they listed convenience stores (sales area of less than 280 m^2) as the smallest food outlet, followed by supermarkets with a sales area of between 280 m^2 and 1400 m^2. The category for stores with a sales area of between 1400 m^2 and 5000 m^2 was called superstores. This was followed by the biggest store format, hypermarkets, ranging from 5000 m^2 to over 10000 m^2. The researchers suggested that the variation of the electrical EUI from

approximately 500 kWh/m^2/pa for the larger retail food outlets to nearly 3000 kWh/m^2/pa for convenience stores was mainly due to a different product mix, or, in other words, smaller stores had a higher percentage of refrigerated food. Other factors responsible for this spread, the authors explained, may be owing to store formats, shopping behaviour and how the store was operated (including equipment used). Despite this spread, the researchers suggested an empirical model for the annual electrical EUI ($EUI_{elec} = 3600 \times Sales\ Area^{-0.18}$) for which no coefficient indicating the goodness of fit was given.

In his paper on energy saving measures in a supermarket in New Zealand Dazeley (2012) also used $EUIs$ to compare the actual impact of these measures. As the supermarket had an area of 6400 m^2 it can be classified as a hypermarket according to Tassou *et al* (2011), assuming that the sales area was not less than 5000 m^2. The EUI of this store before the implementation of energy saving measures had been 568 KWh/m^2/pa and therefore was under the expected value according to the model in Tassou *et al* (2011). The EUI for after the improvements was given as 414 KWh/m^2/pa. However, it was not quite clear how this figure was calculated as the author mentioned changes in store operation, but did not say how he treated them. The researcher attributed this change in EUI to the improvement measures, but did not mention if or how he controlled for weather variables (for one method of doing this see Fels (1986)).

Although $EUIs$ can help with benchmarking in a simple way, other factors may have to be taken into consideration so as to avoid oversimplifications. This is what Schraps (2005) pointed out and, therefore, she included the differentiation between ‘warm stores’ and ‘cold stores’. The author explained that the ‘warm stores’ had a higher cooling load owing to more baking ovens. However, this will not suffice if a more detailed analysis is required.

2.3.1.2 Change point regression

Change point regression models have a continuous graph with at least one point where the gradient suddenly changes and are more fully discussed in Section 4.2.2. This type of statistical model may be considered for a more complete analysis and has been applied to supermarkets and other buildings (Ruch and Claridge, 1992; Ruch and Claridge, 1993). For modelling energy use in buildings the outside temperature is normally used. Kissock *et al* (1998) discuss reasons why using only the ambient temperature is a valid approach.

Schrock and Claridge (1989) developed a change point regression model for a single-story supermarket in Texas based on data from March 1988 to April 1989. This store has a total area of approximately 3700 m^2, a ceiling height of 4.9 m and an annual electricity consumption (used also for some heating) of 834 kWh/m^2. The researchers found their approach superior to the simple regression models and divided the temperature range into heating and cooling regimes. The authors graphically determined the change point temperature for this model to be at 62°F (16.7°C) at which point the slope increased approximately six fold. The fit of this model in the cooling region was relatively good (r^2=0.755) (the meaning of the coefficient of determination r^2 will be explained in 4.2.1). However, in the heating region it was not as good (r^2=0.370). The problems the authors found when conducting this research included incorrectly set defrost timer clocks, not all lights which could be switched off during night time operations were switched off, and large pieces of equipment failed.

The same supermarket was also investigated by Ruch and Claridge (1992) using data for the period from June 1989 to May 1990. Their more rigorous approach to identifying the change point regression parameters employed a root mean square error ($RMSE$) algorithm resulting in a much better $r^2$of at least 0.915. Their research found the change point to be located at 15.6°C where the slope increased by a factor of approximately four. This may be owing to the more accurate statistical approach or due to the use of a different data set. When comparing Figure 3 in Schrock and Claridge (1989) with Figure 3 in Ruch and Claridge (1992) one finds that these two scatter plots look very similar, but are not identical. Ruch and Claridge (1992) also calculated confidence intervals for all model parameters and examined the residuals for heteroskedasticity[2]. From their data these researchers excluded holidays and data from a bad temperature sensor.

2.3.1.3 Multi variant analysis

If more than one independent variable needs to be included, an MVA may be appropriate. For supermarkets, MLR and change point principle component analysis have been used. In a study on how multiple regression can be used to identify appropriate indicators for benchmarking Chung *et al* (2006) investigated 30 supermarkets in Hong Kong. These supermarkets were described as being part of a building and having a total area of between

[2] Nonconstant variance of residual error (Ruch and Claridge, 1992)

75 m^2 and 650 m^2, which made most of them convenience stores according to the classification in DEFRA (2006, p. 24) (see also Figure 3 in Chung *et al* (2006) for the distribution of floor space). The researchers used an EUI which eliminated the temperature dependency and suggested that building age, floor area, opening hours, footfall and the energy conscientiousness of staff should be included in the model. This regression model had an r^2 of 0.708. However, it should be pointed out that the last three predictors would have been rejected at a 10% confidence level (Anderson *et al*, 2004, pp. 606, 669).

Chen (1991) and Ruch *et al* (1993) developed models based on principal component analysis (PCA) for the same supermarket as in Schrock and Claridge (1989) and Ruch and Claridge (1992). The authors gave the main advantage of PCA over MLR as the avoidance of multicollinearity thus avoiding misleading results for model coefficients. The cleansed data set included only 133 days from 19 June 1989 to 19 June 1990, because of a shortage of appropriate weather data. The change point temperature, which was found to be at 15.4°C (this value was approximately 0.2°C lower than in Ruch and Claridge (1992)), served to divide the supermarket operation into a base level regime before the change point and a cooling regime beyond this temperature. For the base level model the researchers found that outside temperature, sales and specific humidity gave an adequate model with an r^2 of 0.562. The predictor 'sales' was replaced with solar radiation for the cooling regime model resulting in an r^2 of 0.749. The reason suggested by the authors was that, at a lower temperature, where the energy consumption was relatively constant, customers opening freezer doors had a higher impact. When the outside temperature was greater than the change point temperature the slope increased by approximately a factor of four and the influence of solar radiation also became more important. Interestingly, the change point model developed by Ruch and Claridge (1992), using only outside temperature as its independent variable, had a higher r^2.

Artificial neural networks may be also classed as an MVA method as they normally have an input vector rather than just a single input variable. This method can be used if the underlying structure of the system studied is unknown. Input and output data provided is used to train the ANN. Datta *et al* (1997) reported on work in which they had applied the ANN method to a store in Airdire, UK. Their results from an ANN with eight inputs and three consumption related outputs were compared with MLR models showing that the correlation between the target output data and the predicted values for ANN was 0.955, but

for a second order regression model it was only 0.798 and for a linear model even worse. Datta and Tassou (1998) also detailed their approach of applying an ANN on a food retail store in Airdire, UK (presumable the same as in Datta *et al* (1997)). The researchers used two different training algorithms and calculated the mean absolute error as 4.6% for the best case.

Mavromatidis *et al* (2013) reported on work performed on a supermarket located in Kent, UK, with a sales area of 3300 m^2. Their aim was to train five networks with up to five input variables to predict the electric energy use in order to compare these predictions with the actual demand in order to detect abnormal stores operation. These networks achieved correlations of between 0.887 and 0.981. The authors suggested that ANNs required less expertise and effort than traditional methods. However, this approach may lead to models which have no real physical meaning.

2.3.2 The development of supermarket thermal models

Some researchers have decided to model supermarkets from first principles. The reason given by Arias (2005, pp 95-99) was that none of the complete building simulation software packages available then was capable of adequately modelling the idiosyncrasies of supermarkets (i.e.. refrigeration systems). Therefore he developed a computer programme based on seven supermarkets in Sweden. This software model derived values for the indoor climate based on internal gains, the interaction with cooling cabinets and cold rooms, and the outdoor weather, which was communicated to the inside through the HVAC system, the building envelope and infiltration (Arias, 2005, p. 105). The refrigeration models included direct and indirect refrigeration designs with the ability to model different compressors. The programme was able to assess the life cycle costs and the total equivalent warming impact so that supermarket designers may choose appropriate options (Arias and Lundqvist, 2005).

A much simpler theoretical model was developed by Ducoulombier *et al* (2006) who modelled a supermarket with two zones, one set at -20°C and the other at +20°C. This model incorporated three heat pumps, two for the cold area (for refrigeration) and one for the warm space (for comfort cooling), one electric heater (for heating the warm space) and one internal heat load. The aim of this simple model, the authors explained, was to derive a thermodynamic efficiency maximum. Their research suggested that better insulated supermarkets reduced the demand for heating and cooling of the warm space due to better

heat recovery opportunities. However, the authors qualified this statement by explaining that an improved heat recovery rate would increase not only overall efficiency figures, but also total required energy. Thus they concluded that this model helped with understanding the underlying principles even if it was unable to cater for the complexities of real supermarkets.

In their paper Hill and Levermore (2011) criticized the National Calculation Methodology (NCM) required by the UK Building Regulations, because the NCM does not include the energy requirements of supermarket refrigeration systems. They then developed a first-order dynamic model in Excel (Hill *et al*, 2012), which allowed the indoor temperature to change with time. Results from this model suggested that a building optimised to the NCM may not be as efficient as a supermarket with a refrigeration/HVAC heat exchanger installed.

Suzuki *et al* (2011) developed a supermarket model based on a food supermarket in Japan with a sales area of 1568 m^2 and an annual EUI of approximately 840 kWh/m^2, (this is below the expected value of 958 kWh/m^2 pa according to the empirical model developed by Tassou *et al* (2011)). This model used a heat balancing equation to investigate the impact of air leakage from refrigerated display shelves on the energy consumption. When comparing the model prediction with the measurements, the authors found good agreement for the hourly power consumption for lighting and refrigeration, but a larger deviation for the HVAC system. Notwithstanding that, the overall agreement between the overall calculated power consumption and the measurements was regarded as good. Regarding refrigerated display cabinets, the researchers concluded that air leakage from these had a considerable effect on both cooling and heating requirements.

Other researchers have decided to use existing software packages. One example of using building simulation software to investigate supermarkets is work reported by Khattar and Henderson (2000) who introduced a building simulation package for supermarkets called Supermarket Simulation Tool (SST). This computer programme was developed because common simulation software packages were unable to model refrigeration systems properly at that time. Thereafter they studied a hypermarket with a total area of 16200 m^2 (sales area: 12500 m^2). The simulated and actual electricity consumption in Khattar and Henderson (2000) exhibited good agreement and showed a temperature independent part before a steep temperature dependent increase occurred. On the other hand, the simulated

and actual gas plots in the same figure display a large discrepancy. The simulated data suggested that there was a certain point where gas consumption became temperature independent. When the temperature rose even further, estimated gas use increased rapidly due to summer dehumidification. Finally the authors offered some improvement suggestions and tested them with SST, presenting insights into, for instance, the limitation of evaporative condensers. The limitations of this software were not explored by the authors, but may arise from the simplifying assumptions of representing large areas, such as the sales floor, by only a small number of sections with only one zone temperature each (see also Section 4.6.1) thus disregarding the true temperature distribution.

Jenkins (2008) used the building simulation software ESP-r to simulate a supermarket in Edinburgh with weather files for Manchester. The total area, including a mezzanine floor, was 10950 m^2 (sales area: approximately 7800 m^2) with a building height of 6 m and an EUI of just under 500 kWh/m^2 (it is assumed that this is the annual consumption, although the paper does not state this explicitly), which was about 220 kWh/m^2 below the expected value according to the model in Tassou *et al* (2011). To calculate the overall energy use, the author had to add the average consumption of the refrigeration system separately, as this software package could not explicitly model a supermarket refrigeration system, a common deficiency of building simulation packages highlighted earlier by Khattar and Henderson (2000). After the model was constructed, the author used it to evaluate six improvement scenarios which added up to energy savings of 51% compared with the base model.

A software package developed by the US Department of Energy (DOE) (Crawley *et al*, 2001) includes the capability of modelling supermarket refrigeration systems since 2004 (Stovall and Baxter, 2010). EnergyPlus was compared with three other software tools: CyberMart (see also Arias (2005)), RETScreen and SuperSim (IEA Heat Pump Centre, 2012). Based on the capability tables in the report by the IEA Heat Pump Centre (2012), it can be concluded that EnergyPlus is the software with the most relevant features. The DOE also developed 15 benchmark buildings including a superstore with 4180 m^2 total area (Deru *et al*, 2011b).

EnergyPlus was extensively used in a project with the aim of designing a supermarket 50% more efficient than a base case supermarket (Leach *et al*, 2009; Deru *et al*, 2011a). This project also included a follow up study on why the building's performance did not meet

expectations (Deru *et al*, 2013). This superstore (4180 m^2 total area, sales area approximately 3400 m^2) was situated in Raleigh, North Carolina, USA. In their studies the project teams considered energy improvement measures relating to lighting technology, fenestration, building envelope, air conditioning equipment and energy generation. This necessitated EnergyPlus to be expanded to investigate all the options so that, in the end, over 75000 EnergyPlus models (Leach *et al*, 2009, p. iii) were constructed. This work suggested that 50% energy reductions could be achieved in a cost effective manner. For the case study an EUI of 662 kWh/m^2/pa was predicted (Deru *et al*, 2013), which is about 20% below the expected value according to the model in Tassou *et al* (2011). The follow up study for this supermarket (Deru *et al*, 2013) showed that, due to operational issues (e.g. the set points were not fully implemented or some overrides were not reset), the predicted energy savings were not fully realised.

Hill *et al* (2014) also used an EnergyPlus model to continue their argument for the inclusion of process related energy consumption in the NCM mentioned in the previous section. For this they concentrated on modelling the sales area of a supermarket with an approximate total building footprint of 3600 m^2. The researchers compared their model with measured heating and electricity data and discovered that it explained only 43% of this measured data. In their sensitively analysis the researchers compared the model with the NCM and found that, for air change rate and U-values, these two methods showed dissimilar behaviour. The authors reconfirmed their conclusion from Hill and Levermore (2011) that following the NCM may result in suboptimal building design.

2.4 Discussion and conclusions

The overall conclusion of the surveyed literature is that for a warming climate the heating requirement decreases and the cooling demand increases. However, by how much and how this translates into changes in energy consumption is location and building design dependent.

With the exception of Chung *et al* (2006), all the other research discussed above includes the dry-bulb temperature as an important, if not the only predictor in their models. For instance, the change point regression model by Ruch and Claridge (1992) achieved a good fit with the electricity consumption data by just using outside temperature. Also the PCA

by Lam *et al* (2010a), which originally considered five climate variables, incorporated the dry-bulb temperature in their final model with only two other variables.

A small number of studies investigated the same area or building. One example is the research into office buildings in Hong Kong. Lam *et al* (2010a) used a PCA to predict a rise of 4.3% for the low forcing climate scenario and the time period 2009-2100. Wong *et al* (2010), on the other hand, employed the OTTV method to forecast an increase of 6.1%. Another example is the change point regression model for a supermarket in Texas. Schrock and Claridge (1989) suggested that the change point temperature was at 16.7°C based on a graphical method, whereas Ruch and Claridge (1992) found it to be at 15.6°C ($RMSE$ method), and Ruch *et al* (1993) at 15.4°C ($RMSE$ method, different data inclusion criteria). This suggests that different research methods may lead to similar, but not identical results.

Sources of uncertainty identified included not only climate change models (Cartalis *et al*, 2001), but also problems during data collection. The latter was more explicitly explained in work relating to supermarkets and included holidays (Chen, 1991), data from a bad temperature sensor (Ruch and Claridge, 1992) and operational issues (Schrock and Claridge, 1989). One can expect to encounter similar problems during this research. Therefore a good understanding of climate model uncertainties will be advantageous in putting the research findings in context. Some of these uncertainties will be covered in Chapter 3 of this thesis. Issues related to data collection will be reported in Chapter 1.

A final point of interest is the error estimating coefficient $CV(RMSE)$. Lam *et al* (2010a) found that for their heating load model the $CV(RMSE)$ was approximately five times the $CV(RMSE)$ for the cooling load model and ranged from 11.5% to 32.6%. Lam *et al* (2010c) reported a similarly large $CV(RMSE)$ of between 9.2% and 23.5% for their electricity demand model. These values may well indicate that the models used perform rather poorly outside the researchers' data set.

The literature summarized above showed that the majority of the buildings already investigated for the impact of climate change on energy usage were office and residential buildings. Additionally, the literature on energy use analysis in supermarkets referred to throughout this chapter uses various tools to capture the effect of the refrigeration systems in supermarkets, but not the study of the impact of climate change on buildings. Therefore

the investigation here addresses this research gap by exploring how a change in climate may alter the energy demand in supermarkets throughout the UK.

3 Introduction to climate change prediction

As a precursor to quantifying the effect of climate change later, this chapter develops the reasoning behind selecting the UKCP09 projections and will particularity highlight sources of uncertainty. To accomplish this, the chapter starts by introducing some aspects of the earth's climate system which are then used to illustrate the uncertainties within the approach chosen by the UKCP09 team.

In order to understand the main thrust of this development it is advantageous to define the meaning of 'uncertainty'. According to ISO/IEC (2008) this expression refers to a parameter which "characterizes the dispersion of the values that could reasonably be attributed to" the quantity of interest. It is therefore not synonymous with the term 'accuracy' which denotes the closeness of measurements to the true value. This leads to the counterintuitive conclusion that a result could be certain, because the spread of measurements approaches zero, but not accurate, i.e. not close to the true value.

3.1 Climate system

The earth's climate system is a very complex collection of interactive systems exhibiting non-linear, erratic behaviour (IPCC, 2007, p 942). It is driven by solar radiation and can be divided into the five parts: atmosphere, hydrosphere, cryosphere, biosphere and geosphere (Baede *et al*, 2001, p 87). This section concentrates on only a few processes in the atmosphere, with the aim of showing the complexity and interconnectedness of the climate system.

As shown in Figure 3.1 the atmosphere can be divided into various layers. The lowest part (troposphere) stretches up to about 10 km and contains about 80% of the mass of the atmosphere. Here is also where the majority of weather phenomena occur. The layer above, the stratosphere, extends to approximately 50 km above the earth's surface and contains the ozone layer in its upper part (Baede *et al*, 2001, p 88). The mesosphere and thermosphere form the two outer layers of the atmosphere (Neelin, 2011, p 51; The Open University, 2002, p 17).

An area at the top of the atmosphere perpendicular to the solar radiation receives approximately 1366 W/m^2 from the 3.87×10^{26} W of radiation the sun emits. Since the

earth is roughly spherical and rotates, this instantaneous solar flux is averaged to 341.5 W/m^2 at the surface of the earth. The incoming radiation has a peak in the visible spectrum and a long tail in the infrared (IR) region. As it travels through the atmosphere it is partly reflected and absorbed and partly transmitted to the earth's surface. Absorption can occur in the upper stratosphere where ozone filters out ultraviolet radiation. Lower down in the atmosphere the long wave energy is mainly absorbed by clouds, water vapour and small particles (called 'aerosols') causing the atmosphere to warm up. The remaining part of the radiation together with some of the IR radiation from this atmosphere heats up the surface of the earth. This thermal energy is subsequently released by either long wave radiation or by the sensible or latent heat exchange necessary for the water cycle (Neelin, 2011, pp 44, 45). A basic energy consideration (if the heat flux from earth's core is neglected as it is comparably small (Davies and Davies, 2010)), as illustrated in Figure 3.1, leads to the conclusion that, in order for the average temperature on the earth to stay the same, the same amount of energy has to be released by the atmosphere as enters it.

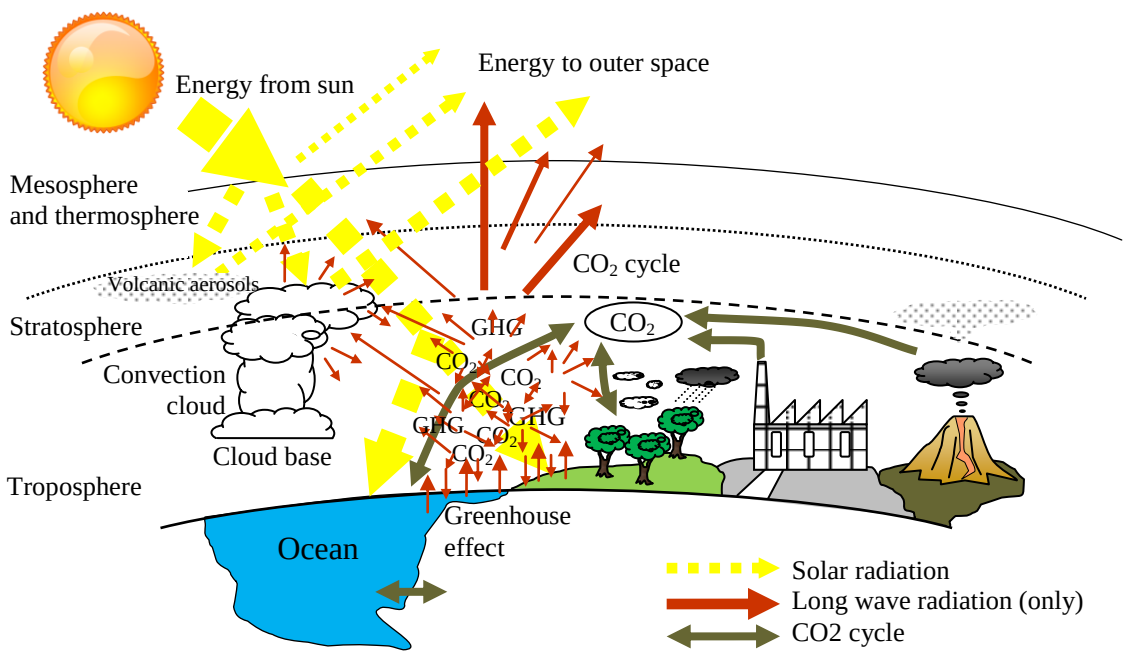

Figure 3.1: A sketch of some parts of the global climate system

The part of the water cycle which involves the atmosphere is of particular interest for the discussion here. The atmosphere is a mixture of gases, water vapour and aerosols. As mentioned in the previous paragraph the solar radiation, which reaches the earth's surface, both evaporates water and heats up the air close to the surface. The buoyancy effect causes this air-vapour mixture to rise. As it rises it expands and cools. This allows the small solid

particles in the atmosphere to transform this supersaturated air into clouds. If the droplets around these aerosols become too heavy, the clouds start to turn into precipitation. Clouds can be classified as low clouds, where the cloud base is below approximately 2000 m, medium clouds (cloud base above 2000 m, but below 6100 m) and high clouds (cloud base above 6100 m). Some clouds can rise as high as 12000 m, i.e. can reach the lower stratosphere (Met Office, 2006, p 2). Convective clouds have a typical horizontal expansion of up to approximately 1km and can have a height of 10km (Neelin, 2011, p 37). Convective motions create an irregularly shaped top. Winds move clouds to other areas where they can turn into precipitation (The Open University, 2002, pp 88-93; IPCC, 2013, p 576). Clouds influence the climate system in a number of ways. For example they alter radiative fluxes both in the atmosphere and on the ground. They also transport heat and moisture horizontally over large distances (Jakob and Miller, 2003).

Boucher *et al* (2013, pp 593, 594) summarize the current understanding of how clouds affect the climate and climate change. They first list effects on the current climate as warming the atmosphere when clouds are formed, reflecting both long and short wave radiation and causing up-draughts in clouds. Then they divide clouds into high-altitude and low-altitude clouds. Next, the dual effect of high clouds is explained as preventing sunlight from entering the climate system. At the same time they prevent infrared radiation from escaping into outer space with the result that changes in the amount of high clouds may have only a small overall effect on the surface temperature. On the other hand, the authors conclude that low clouds have a net cooling effect because they reflect more solar radiation back than they trap in IR radiation. Their overall conclusion is that based on available evidence: The net effect of the cloud feedback is likely to increase the effect of global warming. However, the magnitude of this is still uncertain.

The carbon cycle cannot be omitted when climate change is discussed. This cycle consists of the flux exchanges between the atmosphere, hydrosphere, biosphere and lithosphere. Within this cycle there are sub-cycles such as the growth and decay of plants. While growing, plants store some carbon in their structure which is released when they die off. The annual characteristic oscillation relating to a this cycle is evident in the CO_2 data (NOAA/ESRL, 2014) in Figure 3.2. Unlike the energy budget referred to earlier, there is no external source of carbon, so the total amount of carbon on the earth remains constant. Also the natural fluxes between carbon reservoirs are in balance when considering a long

enough time span. In addition to the annual oscillation, Figure 3.2 also shows an upward trend for the CO_2 concentration in the atmosphere. This has been traced back to the perturbation of the natural cycle due to human activities (Denman *et al*, 2007, pp 511-517; Warr and Smith, 1993, pp 79-82).

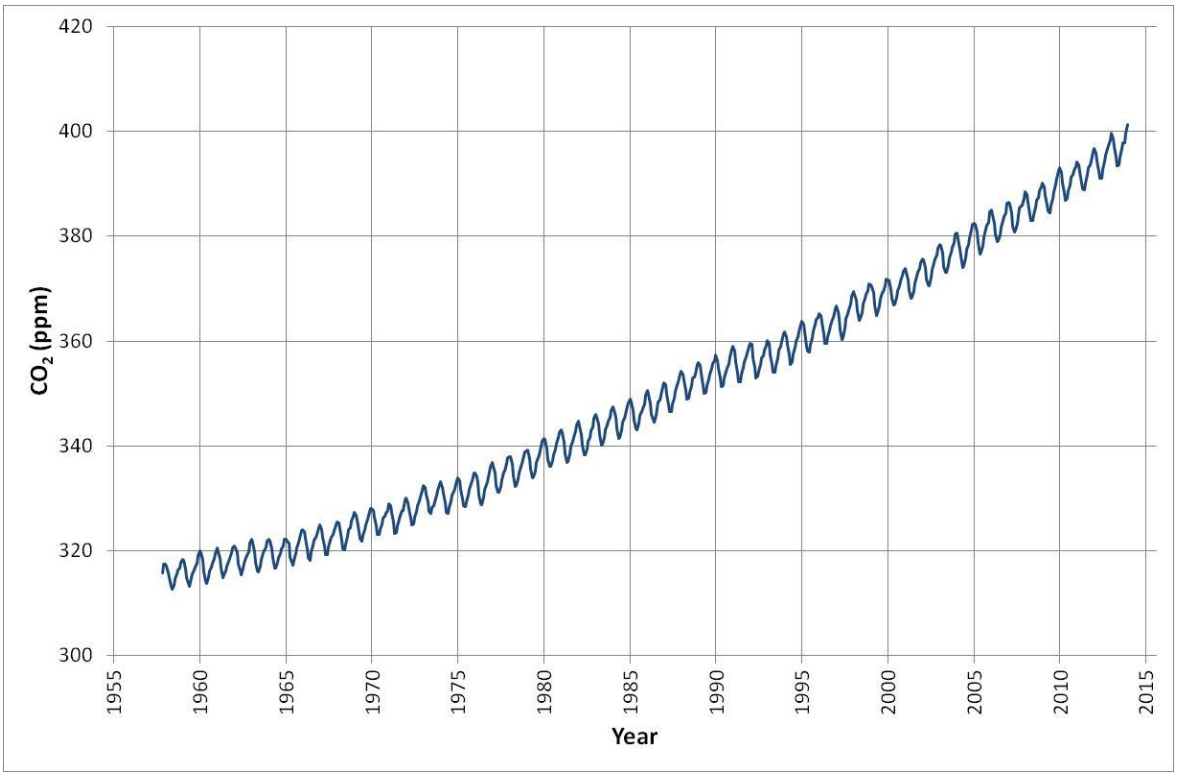

Figure 3.2: CO_2 concentration as measured on Mount Mauna Loa (based on NOAA/ESRL (2014))

The terrestrial atmosphere is made up almost entirely of N_2 and O_2 with CO_2 being only a trace gas. Nevertheless, this gas is very important, because it is involved in the greenhouse effect and, therefore, is also known as a greenhouse gas (GHG). The greenhouse effect, also illustrated in Figure 3.1, is the warming effect of all infrared absorbing parts of the atmosphere (IPCC, 2013, p 1455). Without this greenhouse effect, the earth would be too cold to live on, but if the greenhouse effect is too strong, the earth's temperature can rise uncomfortably high (compare, for instance, the runaway greenhouse effect on Venus (Trenberth *et al*, 1995, pp 57-59)).

As a final aspect of the climate system the El Niño/Southern Oscillation (ENSO) phenomenon is discussed here to illustrate natural climate variability and the development of understanding of how it affects the climate system. Although ENSO refers now to basin-wide warming of the eastern part of the tropical Pacific Ocean, originally the term El Niño just referred to the warm current off the Peruvian coast around Christmas. This

phenomenon was known some time before the 20th century. From the beginning of the 20th century to the 1980s, researchers discovered irregular oscillation of atmospheric surface pressure in the Pacific Ocean with a time scale of between two and seven years. It was debated whether this atmospheric phenomenon was related to the oceanic El Niño. Even after a coupled model was developed to predict the ENSO, this was still disputed, because the interaction was not fully understood. Only after further research a better, more complex ocean-atmospheric model could be developed with the result that now national weather services can routinely use ENSO events in their forecasts. These research findings showed the periodic atmosphere-ocean interaction included a warming phase during which the prevailing winds weaken, thus colder deep ocean water is prevented from upwelling with the effect of an increase in the sea surface temperature (Marshall and Plumb, 2008, p 266; Neelin, 2011, pp 14- 23; IPCC, 2007, p 945).

3.2 Climate predictions and their uncertainty

The main steps necessary to derive usable climate predications are described in this section. These steps along with some of the major associated uncertainties (both in the sense of the word defined earlier and with the meaning of 'lack of knowledge') are illustrated in Figure 3.3 (Eames *et al*, 2012; Eum *et al*, 2012; Rowell, 2006) and will also be discussed along with each process step.

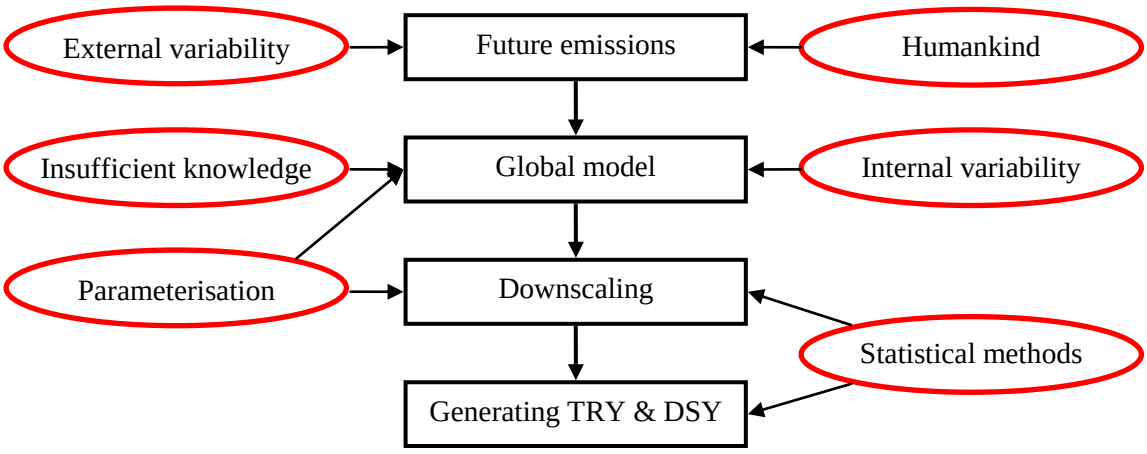

Figure 3.3: Process of generating climate prediction data and some associated uncertainties

3.2.1 Emissions

In addition to CO_2, which was introduced as a GHG in Section 3.1, other gases and aerosols can contribute to the greenhouse effect. Hence, to obtain usable climate change

data, the emission of GHGs and subsequent radiative forcing[3] was forecasted. The IPCC has expended considerable effort on this task, but is still forced to acknowledge that predicting "future anthropogenic GHG emission is impossible" and therefore has developed 40 scenarios to capture the uncertainty of a large number of known factors inherent in very complex, opaque dynamic systems (Nakicenovic *et al*, 2000, p 23). This section briefly outlines this work to illustrate the level of uncertainties this project had to deal with.

The process of arriving at emission scenarios started with reviewing literature on existing scenarios and their analysis. This was followed by constructing 'storylines' of credible, alternative future developments up to the year 2100. The next step was to quantify the emissions arising from these different development paths. The results were then reviewed, not only by the team members themselves, but also by a wider audience (Nakicenovic *et al*, 2000, p 25).

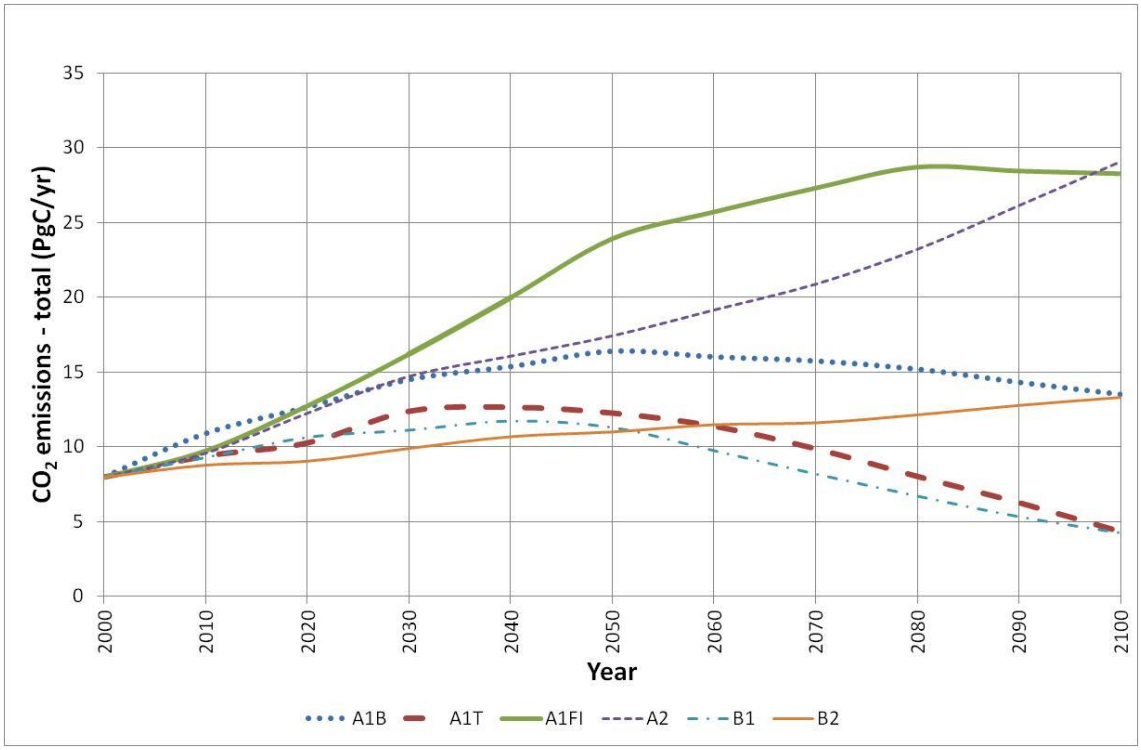

Figure 3.4: IPCC illustrative emission scenarios (based on Table II.1.1 in IPCC (2001, p 801))

The main drivers considered to formulate these four storylines were such diverse and difficult to predict factors as demographic predictions, economic and social development,

[3] "Radiative forcing is the change in the net, downward minus upward, radiative flux (expressed in W/m^2) at the tropopause or top of atmosphere due to a change in an external driver of climate change" (IPCC, 2013, p 1460).

energy use and technology, agriculture and climate policies. The four storylines, which were coded A1, A2, B1 and B2, have the following main characteristics (Nakicenovic *et al*, 2000, pp 28, 104):

A1: Very rapid economic growth and global integration, rapid introduction of new, more efficient technology, low population growth

A2: Very heterogeneous world where self-reliance and local identity are highly valued, population growth dependent on location

B1: Rapid change to a global service and information economy, low population growth

B2: Emphasis on local solutions to economic, social and environmental problems, moderate population growth

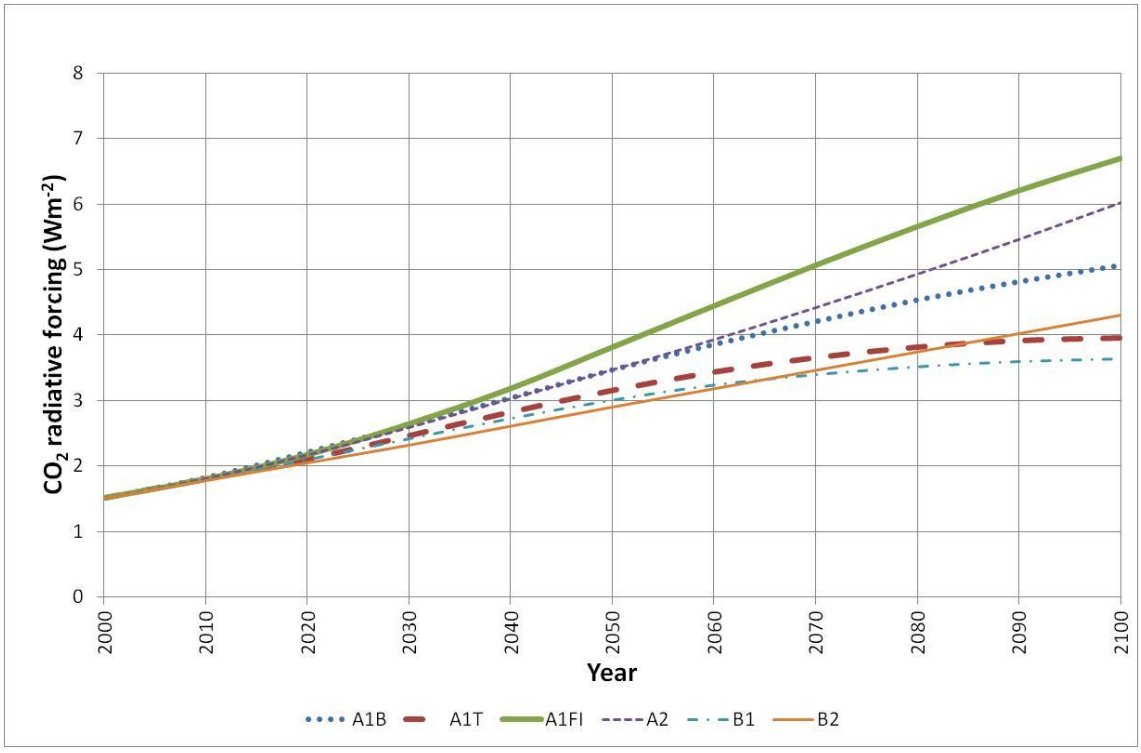

Figure 3.5: CO_2 radiative forcing (W/m^2) (based on Table II.3.1 in IPCC (2001, p 817))

These developments were then quantified in terms of GHG and sulphur emissions, which lead to significantly different emission scenarios. Although Nakicenovic *et al* (2000, p 46) emphasise that there is no single central or more probable scenario, they suggest the six illustrative scenarios which are shown in Figure 3.4. These scenarios are predicted to lead to radiative forcing as plotted in Figure 3.5. Comparing these two figures shows that, despite a significant spread in the emission scenarios (e.g. the emission of scenario A1FI is

twice the amount of B1 or B2 in 2050), the resulting radiative forcings are much closer together (the radiative forcing of A1FI is only approximately 30% higher than B2 in 2050). This suggests that the uncertainties associated with emission scenarios are significant, but their effect may be suppressed by the climate system, especially for near-term warming (Stocker *et al*, 2013, p 85).

For the sake of completeness, it should be mentioned that the approach of using emission scenarios was found impractical because of the differences in model requirements and Representative Concentration Pathway (RCP) scenarios were developed in their place. This approach starts with specifying the radiative forcing as a function of time and then works backwards to establish data sets usable for climate models (IPCC, 2013, pp 147-150). The implication of this approach is that it is less clear how these different RCPs relate to the real world.

3.2.2 Climate models

The global climate system is modelled by dividing the atmosphere and the ocean into smaller sections (except for in very simple models) and representing their internal processes and interactions with mathematical equations. These models can be classified according to their level of detail. The simple climate models (SCMs), for instance, consider only the ocean and atmosphere separately or split them into two hemispherical expansions to employ an energy balance approach to predicting the surface temperature (Meehl *et al*, 2007, p 797). The earth system models of intermediate complexity (EMIC) are a more involved class of models and consider processes in the atmosphere, ocean, sea ice, land surface, biosphere etc and their interaction at a relatively low resolution or in a simple, idealistic way. They have been extensively used for the IPCC's third assessment report (Randall *et al*, 2013, p 644-647). The next level of complexity contains the coupled atmosphere-ocean general circulation models (AOGCM), which provided most of the modelling power for the forth IPCC assessment report, and model the dynamics of the physical components at a finer scale than EMICs (Flato *et al*, 2013, p 746). Earth system models (ESM) are considered state-of-the-art and incorporate not only the physical interactions in the climate system, but also biogeochemical processes which interact with physical climate processes (Flato *et al*, 2013, p 746; Flato, 2011).

3.2.2.1 Model fundamentals

The purpose of this section is not to give a comprehensive introduction to climate models, but to discuss some aspects of the modelling approach in order to appreciate their limitations and uncertainties. Hence, it will briefly explain the fundamental idea behind climate models before it discusses parameterisation, one of the main sources of modelling uncertainty (Meehl *et al*, 2007, p 805).

The more complex models divide the atmosphere and the ocean into grid cells, for instance using the coordinates of latitude, longitude and height (or pressure for the atmospheric model) as illustrated in Figure 3.6 (Neelin, 2011, pp 146, 147; Flato *et al*, 2013, p 749). Each cell may be 200 km long or wide or even larger (Murphy *et al*, 2009, p 30; Neelin, 2011, p 150). The number of grid cells depends to a large degree on the available computing power (Randall *et al*, 2013, p 601). Each cell has one value for each variable associated with it (e.g. average temperature of cell). The arrows in Figure 3.6 indicate the flow of, for instance, mass into and out of a particular cell. The magnitudes of these flows are calculated by considering the balance of forces, fluxes etc acting on each grid cell. This allows the computing of new values for each cell for the next time step (Neelin, 2011, pp 146, 147).

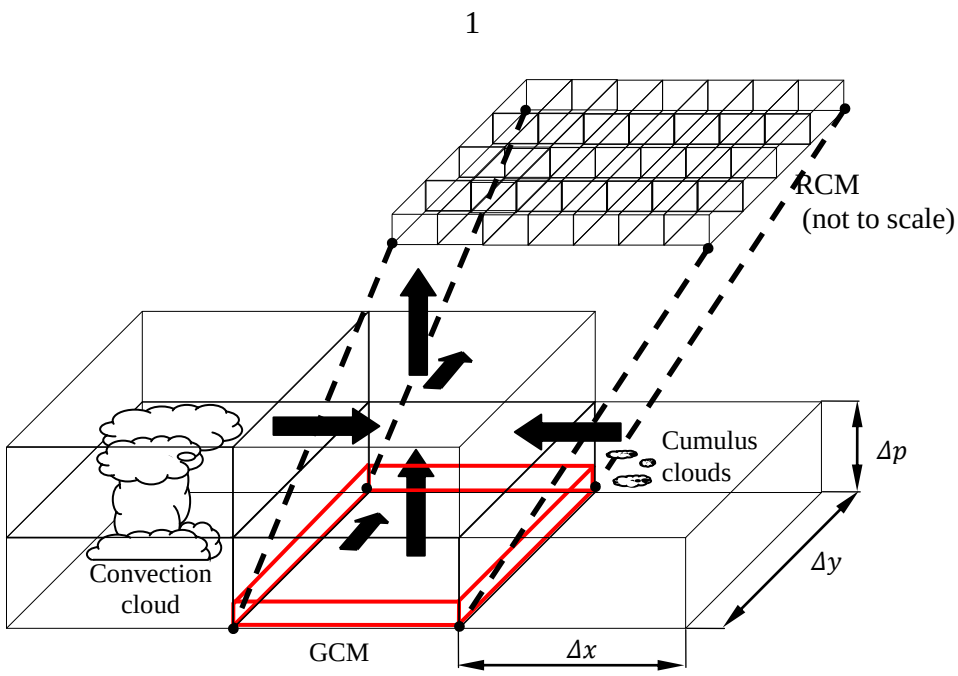

Figure 3.6: Example of climate model grids

Features smaller than the grid size, e.g. cumulus clouds, cannot be dynamically modelled and have to be approximated by parameterisation. The difference in parameterisation schemes and values are an important reason why different climate models yield different results (Randall *et al*, 2013, p 602). One example of parameterisation is subgrid-scale clouds. In early general circulation models, clouds were not explicitly considered at all, only precipitation was. The first scheme which included clouds considered the generation of clouds as a function of relative humidity in the grid cell and a convection parameter. The threshold for the relative humidity, above which cloud cover was assumed, was usually 80% and the cloud cover was calculated to rise as the relative humidity increased. The current parameterisation scheme is fully prognostic, that is to say that it has the form $\dot{y} = f(y)$, which translates to $y(t+1) = f(y(t))$ in a computer programme (Jakob and Miller, 2003; Tiedtke, 1993).

Parameterisation schemes in themselves are uncertain (Murphy *et al*, 2009, p 31). To illustrate this, the threshold value in the diagnostic cloud scheme mentioned above can be considered. If the relative humidity threshold value was lowered, clouds would appear earlier, which, in turn, would have a knock on effect on other parts of the model. In order to explore how much an individual parameter influences a particular model, a so-called perturbed physics experiment can be conducted during which the parameter is varied within meaningful limits (Meehl *et al*, 2007, p 805). Another approach is to run models from different modelling groups under the same initial assumptions and explore the inter-model uncertainties (or a combination of both methods) (Flato *et al*, 2013, pp 754, 755). In this way the certainty of a result can be increased, but not necessarily its accuracy (The terms ‘certainty’ and ‘accuracy’ should be understood according to ISO/IEC (2008)).

In addition to parameterisation there are other significant uncertainties linked with climate models ranging from a lack of understanding, exemplified by the history of the debate about the ENSO during much of the 20th century, and subsequent imperfect capture based on a faulty understanding, to computational costs, i.e. the grid has to have a certain minimum resolution to produce cost effective results. Some sources of uncertainty, for instance, phenomena relating to natural climate variability, may have been deliberately excluded, such as changes in solar radiation, knowing that they will affect the climate system to some degree. Others may be unpredictable, for example the eruption of a volcano (Flato *et al*, 2013, pp 809, 810; Murphy *et al*, 2009, pp 25-36).

3.2.3 Downscaling

As large scale models may not be able to represent the local climate adequately, downscaling methods need to be applied to assess the smaller scale impact of climate change. One method is to use regional climate models (RCMs) or another approach, often used in conjunction with them, is statistical downscaling. An RCM is a high resolution (typically 25 km) climate model which is nested within a coarser general circulation model (GCM) so that that this lower resolution model provides the boundary conditions for the RCM (see Figure 3.6). Statistical downscaling may use the results of an RCM (or other large scale data) and local weather (or climate) observations to establish statistical relationships (Christensen *et al*, 2007, pp 918-920; Flato *et al*, 2013, pp 813, 814).

Also the application of these downscaling methods introduces uncertainties and errors. For instance, the problems associated with an RCM are similar to those of a lower resolution model discussed in Section 3.2.2.1. However, as the grid size of an RCM is smaller, more processes can be resolved and fewer need to be parameterised. On the other hand, as the RCM is driven by a large scale model, the uncertainties associated with this model cascade into the RCM. Additionally, as simulation time progresses, the two models may become more and more decoupled, possibly leading to inconsistencies. Uncertainties associated with statistical downscaling may stem, for instance, from the need for sufficient observational data at the required scale, which may introduce sampling errors (Flato *et al*, 2013, p 815; Christensen *et al*, 2007, pp 918, 919).

3.3 UKCP09 and its application

The set of predictions published by the Department of Environment, Food and Rural Affairs in 2009 and abbreviated as UKCP09 (Street *et al*, 2009), is one of 16 different RCMs forecasting the climate change on a European scale (van der Linden and Mitchell, 2009). As the release date suggests, these predictions are not based on the latest modelling advances, which are described in IPCC (2013), but on the emission scenarios discussed in Section 3.2.1. The UKCP09 climate predictions are used to further illustrate some of the principles introduced in the previous sections.

Out of the six illustrative emission scenarios shown in Figure 3.4, above, three were chosen for UKCP09: A1F1, A1B and B1. As can be seen, A1F1 and B1 are the maximum and minimum graphs whereas the A1B trace follows an intermediate emission scenario.

Hence, they are usually referred to as high (A1F1), medium (A1B) and low (B1) emissions in UKCP09 literature (Murphy *et al*, 2009, pp 41, 42; Street *et al*, 2009). Murphy *et al* (2009, pp 41, 42) explain that there are essentially two sources of uncertainty attached to the use of these scenarios. The first is that there can be no likelihood given as to which is the most likely scenario. Furthermore the authors point out that these scenarios are based on assumptions which in themselves are uncertain. Therefore the authors suggest that UKCP09 users have to decide for themselves what the most appropriate scenario is (or scenarios are) for their application.

UKCP09 is based on the AOGCM called HadCM3 developed by the Met Office Hadley Centre (Murphy *et al*, 2009, p 31). The atmospheric component uses a 2.5° latitude by 3.75° longitude horizontal gird with 19 vertical layers and a 30-min time step (Pope *et al*, 2000; Gordon *et al*, 2000). This means that the base side area of four of these surface gird boxes is larger than the total area of the UK. The oceanic component uses a finer horizontal resolution of a 1.25° times 1.25° and twenty layers (Gordon *et al*, 2000). The coupling of these two models occurs once for every day simulated. The whole model is comprised of approximately a million gird points and contains 100 or more parameters. Because of the large number of experiments to be run on this model, it was simplified to a 'slab model' by just representing the top 50 m of the ocean as one layer. This model was called HadSM3 (Murphy *et al*, 2009, pp 30, 52).

Murphy *et al* (2009) described how two types of model uncertainties were quantified. To efficiently quantify the first source of uncertainty stemming from the parameterisation, the most important processes within the climate model were identified. These 31 key parameters (and their associated maximum, medium and minimum values where necessary) were then utilized in a perturbed physics experiment. This created 280 simulation runs which were then used as inputs to an emulator. This statistical tool allowed integration over the whole parameter space (Murphy *et al*, 2009, pp 50-53). The second type of uncertainty, the structural error of the model, was quantified by predicting the simulation outcome of twelve models from different modelling centres, which are partly based on different assumptions (Murphy *et al*, 2009, p39). Generally speaking the parameter uncertainty is the biggest single contribution to the total uncertainty, but the structural uncertainties are also significant so that all model uncertainties constitute up to three quarters of all the uncertainties (Murphy *et al*, 2009, p 153).

Natural internal variability also introduces some, albeit smaller, uncertainties in forecasting future climates and includes phenomena such as storms and interaction between the ocean and atmosphere (e.g. ENSO). An attempt was made to quantify these sources of uncertainty by combining multiple model runs with different, random initial stages (Murphy *et al*, 2009, p 153). Some natural external variability, however, such as volcanic eruptions are unpredictable with current scientific knowledge and therefore no attempt was made to include these in the models for UKCP09 (Murphy *et al*, 2009, p 28).

The results from the coarse GCM were downscaled dynamically for different scales including a 25 km grid for seven overlapping 30-year periods between 2010 and 2100 (Murphy *et al*, 2009, pp 15-19). This process established a statistical relationship between RCM simulations and the large scale model so that only the GCM was needed to create small scale climate predictions rather than new simulation runs by an RCM. The climate variables thus predicted were mean daily temperature (and derived variables such as mean daily maximum/minimum temperatures), precipitation (and wettest day), relative and specific humidity, total cloud cover, mean sea level pressure and various radiative fluxes (Jenkins *et al*, 2009, pp 19, 20). The uncertainties introduced during this stage vary from climate variable to climate variable, but are generally considerably smaller than model uncertainties from the driving GCM (Murphy *et al*, 2009, pp 73-78; Rowell, 2006).

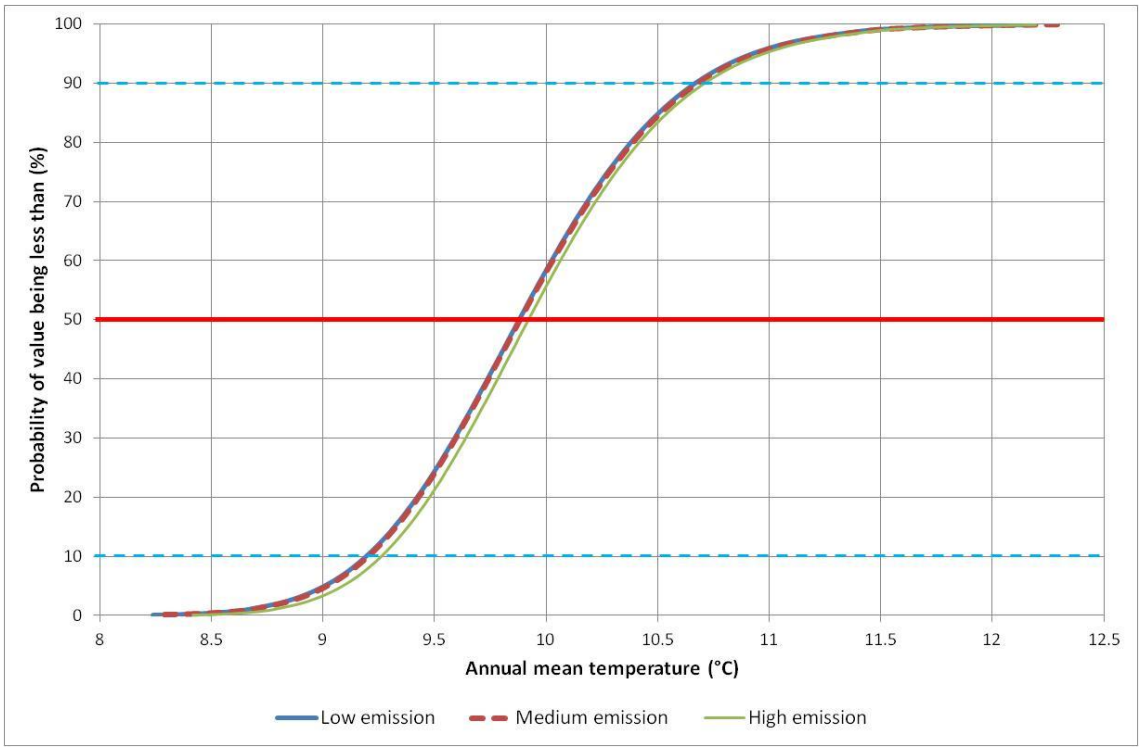

Figure 3.7: Predicted mean annual temperature for Glasgow (cell ID: 764) for the 2030s

The UKCP09 predictions do not give a single forecast value, but pass on the results of their work on uncertainties by providing probabilistic forecasts. One way of expressing this is by a cumulative distribution function which shows what the likelihood is that a value is below a certain point (Murphy *et al*, 2009). Figure 3.7 displays the annual averages of daily mean temperature for the high, medium and low emission scenarios for the time period from 2020 to 2049 for the UKCP09 grid cell ID: 764 (Glasgow). In this figure the lower, dashed horizontal line refers to the 10% likelihood that the future value will be below this line. Similarly '50%' denotes the central estimate and '90%' indicates a 90% likelihood for the temperature to stay below this value. The same figure also shows that the results for emission scenarios differ only slightly compared with difference between, for instance, the 10% and 90% values.

In order to use building simulation software to assess how climate change will impact buildings and their occupants, hourly data is needed for a specific set of climate variables. Two different approaches have been considered based on the UKCP09 data: data morphing and using the UKCP09 weather generator (WG). The first approach transforms the existing data from 14 different sites around the UK by shifting and/or stretching them (Hacker *et al*, 2009, p 22) to incorporate the climate change signal. The WG used for the second method is based on a statistical rainfall model and generates data for daily mean temperature, diurnal mean temperature range, vapour pressure, sunshine duration and potential evapotranspiration (Jones *et al*, 2010, p 8). This set of climate variables had to be complemented by wind speed and direction, air pressure and cloud cover. The main advantage of the second approach is that data can be generated for any location whereas morphing requires pre-existing data. (Eames *et al*, 2011). Mylona (2012) summarized and compared four research projects which had converted the output of the UKCP09 WG into usable TRY for building energy simulation and design summer years (DSY) for design considerations. The author found that, although these projects use the same data source, they produce "a wide variety of future TRYs and DSYs". Therefore the suggestion was made to conduct further research to quantify the spread of results when using these different TRYs and DSYs in different building software packages.

3.4 Discussion and conclusions

This chapter provided an outline of how future climate predictions are derived and what some of their uncertainties are. The complexity of the climate system makes the modelling

of it an extremely difficult task. Each model component introduces simplifications and uncertainties, which have to be born in mind when using model predictions. Efforts have been made to quantify sources of known uncertainties and it has been found that the parameterisation of GCMs is probably the biggest single contributor to uncertainties. In addition, there are also unknown uncertainties so Hall (2007) argues that the total amount of uncertainty will always be underestimated. On the other hand, it is worthwhile to include the comments by Murphy *et al* (2009, p 43), who say in their description of the UKCP09 project:

> Although it is important that prospective users understand the limitations and caveats, it is also worth emphasising that (a) current models are capable of simulating many aspects of global and regional climate with considerable skill […] ; and (b) they do capture, albeit imperfectly, all the major physical and biogeochemical processes known to be likely to exert a significant influence on global and regional climate over the next 100 yr or so.

In addition to modelling uncertainties, users are also interested in the accuracy of forecasts. This answer is difficult to provide because accuracy, as explained in the introduction to this chapter, is the difference between the true and measured (or, here, predicted) values. However, in prediction the true value is unknown and even measuring a value introduces uncertainties. Some researchers use the method of 'hindcasting' or retrospective forecasting. For instance, Reichler and Kim (2008) calculated a single index to quantify the goodness of a climate model. Their results showed that the HadCM3 belonged to the best models. However, it should be pointed out that data which helped 'tune' the model cannot be used to evaluate its accuracy (Flato *et al*, 2013, p 750) and, from the article by Reichler and Kim (2008), it is not clear if there was an overlap. Also the inability to reproduce the current slowdown in global temperature increase by almost all climate models used for the fifth IPCC assessment report highlights the limitations of climate models in terms of accuracy (Stocker *et al*, 2013, pp 61-63).

The above shows that it is very unlikely that a truly accurate and certain prediction of future emissions exits. Therefore the UKCP09 predictions were considered the best data for the purpose of this research because (a) the quality of the Handley Centre models is at least comparable to other models, (b) the data is relevant to the climate area of interest, (c) the process of how the data and their associated uncertainty estimates were generated is transparent, and (d) it is readily available.

The figures based on UKCP09 for the 2030s (e.g. Figure 3.7) period show little difference between the results for the three emission scenarios. This is consistent with the graphs for radiative forcing (for instance Figure 3.7), which showed only a moderate spread for the near term despite a larger range of emission scenarios. Taking this into consideration and the fact that the current trend of emissions follows the middle scenario quite closely (Stocker *et al*, 2013, p 64), it was decided to use just the medium emissions scenario set of predicted climate variables in further chapters.

4 Overview of energy analysis and simulation tools and their application

Chapter 2 mentioned a few energy analysis tools, but did not discuss their advantages and disadvantages. Therefore this chapter gives an overview of the more popular ones, including their pros and cons, and also offers some remarks about the more recent developments (see also Appendix B – Summary table of analysis tools). In addition, this chapter also includes a more in depth discussion of regression analysis tools and the conceptual idea behind software simulation packages based on the heat balance equation. This summary will be useful for the method selection process detailed in Section 5.4.

One way to classify these tools is illustrated by the Building Energy Software Tool Directory maintained by the US Department of Energy, which holds information of over 400 energy related building software tools and divides them into three categories based on their application (Building Technologies Office, 2014). It is also possible to divide energy analysis techniques into steady state and dynamic tools (Krarti, 2011, p 4-1). Other terminology was used by Foucquier *et al* (2013) who divided these techniques into white box (or physical models), black box (statistical methods) and grey box approaches (i.e. a combination of white and black box tools). Here the terms data-driven (ASHRAE, 2013) and deterministic (Wang *et al*, 2012) are used to classify these tools.

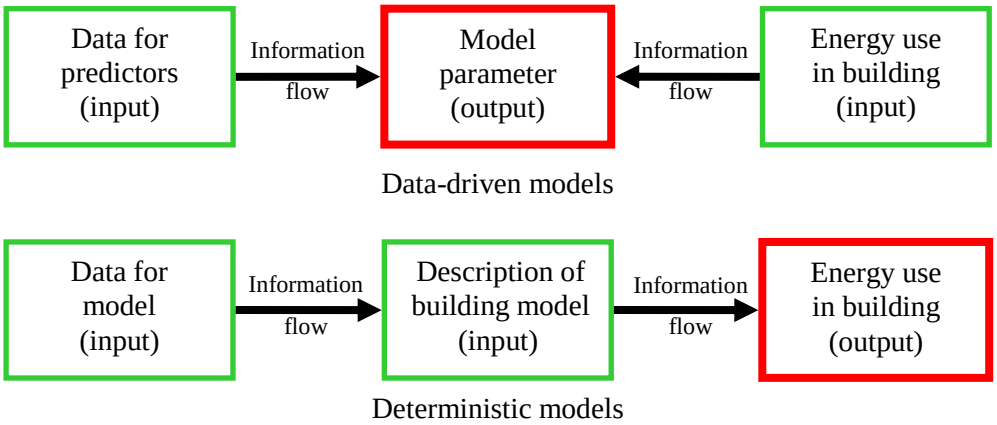

Figure 4.1: Comparing data-driven and deterministic approaches

As Figure 4.1 indicates, the main difference between these two approaches is that data-driven tools require both energy consumption and predictor data as inputs to calculate coefficients of a mathematical model. In other words, the information flow is towards the

model. Only afterwards can it be used for consumption prediction and similar tasks. A deterministic approach, on the other hand, requires a physical description of the building (this may be only one or two coefficients as in the case of the degree day method, which will be discussed later), its use and/or weather data to determine the energy use in a building as its output. Here the flow of information is towards the energy consumption. This difference also defines the application area. The data-driven tools are more geared towards energy use analysis for existing structures, whereas the deterministic approach is frequently used as a design tool.

4.1 Some data-driven analysis tools

Probably the simplest form of data-driven analysis tool is the ratio based normalized performance indicator. An example of this tool is the EUI for which the energy consumption is divided by the floor area (Wang *et al*, 2012) or space volume (Krarti, 2011, p 4-3) of a building. Such an indicator is frequently used for pre-audit analysis or for benchmarking (Beggs, 2002, pp 56-61). Although the indicator itself is easy to calculate, the interpretation of it may require a large database to determine the relative performance of a particular building against similar buildings (Krarti, 2011, p 4-2). An additional drawback is that it can include only a very limited number of influencing factors (Wang, 2015). In the example given above, no weather data is considered, limiting this approach to buildings in a similar climate zone (Chung, 2011).

A slightly more sophisticated tool is a plot in which the energy consumption data is plotted against a time axis. In addition to a cyclic (e.g. seasonal) pattern, such a graph may also allow the identification of the base load or a general time dependent trend. However, this tool may prove to be insufficient if there are important, time independent relationships as these may be difficult to recognize (Beggs, 2002, pp 61-63).

4.2 Regression analysis

A simple regression model in the form $y = a\,x + b$ overcomes the problem mentioned in the previous paragraph by exploring the possibility of a relationship between one response variable and a predictor variable. As such it requires the presence of (accurate) data. As the regression model equation shows, a large variety of independent variables is acceptable, such as heating degree days or production units in a factory. When using this tool it should be born in mind that any suggested relationship (or lack of it) should be substantiated by

other means to avoid erroneous conclusions regarding relationships (Beggs, 2002, pp 63-67). The change point regression analysis can be considered as an extension to the simple regression analysis as it uses only one independent variable, but can deal with nonlinearity (Krarti, 2011, pp 16-6 - 16-10). If more than one predictor needs to be incorporated, the MLR may be considered.

Simple, change point and multiple regression analysis have been widely accepted in correlating energy data to weather data and other influencing variables (Wang *et al*, 2012). The popularity of this method may be credited to the availability of tools, including visual tools, and easy interpretation of variables (Tso and Yau, 2007; Katipamula *et al*, 1998). Zhao and Magoulès (2012) mention research relating energy usage to one or more weather variables first in their list of applications indicating the popularity of this tool for this type of research. As a later chapter will show, this is also the application for regression analysis in this research.

4.2.1 Simple linear regression

If a set of n measurements exists in which y_i represents the ith response to the input x_i, then a simple linear regression model may be written as:

$$y_i = \beta_0 + \beta_1 x_i + \varepsilon_i$$

Equation 4.1

Where:

β_0 and β_1: Unknown model parameters

ε_i: The error term for the ith measurement

If b_0 and b_1 are estimates of the unknown model parameters β_0 and β_1 respectively, then an estimated linear regression equation can be expressed as in the equation below.

$$\hat{y}_i = b_0 + b_1 x_i$$

Equation 4.2

Where:

$\hat{y}_i$: Estimated value of the dependent variable for the ith data point

A common way of estimating b_0 and b_1 is to use the ordinary least square method which minimizes the following expression.

$$\min\left[\sum(y_i - \hat{y}_i)^2\right] = \min\left[\sum(y_i - b_0 - b_1\, x_i)^2\right]$$

Equation 4.3

These two parameters can be found by differentiating $\sum(y_i - \mathrm{b}_0 - \mathrm{b}_1\, x_i)^2$ with respect to b_0 and b_1 and then setting these two equations to zero to find the minimum. After some manipulation this yields the following two expressions.

$$b_0 = \bar{y} - b_1\bar{x}$$

Equation 4.4

$$b_1 = \frac{\sum x_i y_i - n\,\bar{x}\bar{y}}{\sum x_i^2 - n\,\bar{x}^2} = \frac{\sum(x_i - \bar{x})(y_i - \bar{y})}{\sum(x_i - \bar{x})^2}$$

Equation 4.5

Where:

$\bar{y}$: Arithmetic mean of all $y_i,\ i = 1 \ldots n$

$\bar{x}$: Arithmetic mean of all $x_i,\ i = 1 \ldots n$

These two parameters, i.e. b_0 and b_1, have their own confidence interval associated with them, because they are only estimates of the unknown parameters β_0 and β_1. Montgomery *et al* (2006, pp 28-30) show how these confidence intervals can be calculated.

The coefficient of determination, r^2, is frequently used to indicate how well the estimated equation fits the data set and is calculated as shown in Equation 4.6 (see also Figure 4.2). In this equation the numerator is referred to as the 'sum of squares due to regression' and the denominator as the 'total sum of squares'. The sum of squares due to regression can be considered a measure for the deviation from the mean (that is to say from $\bar{y}$) which can be explained by the estimated equation; whereas the total sum of squares measures the deviation with respect to y_i. Hence, the coefficient of determination can be interpreted as the proportion of deviation from the mean explained by the estimated equation. (Montgomery *et al*, 2006, p 35; Anderson *et al*, 2004, pp 527-530).

$$r^2 = \frac{\sum(\hat{y}_i - \bar{\mathrm{y}})^2}{\sum(y_i - \bar{\mathrm{y}})^2}$$

Equation 4.6

It should be noted that the coefficient of determination does not support any conclusion about a statistically significant relationship between the dependent and independent variables (Anderson *et al*, 2004, p 532). This can be established by two other statistics which are described in the section on multiple linear regression below.

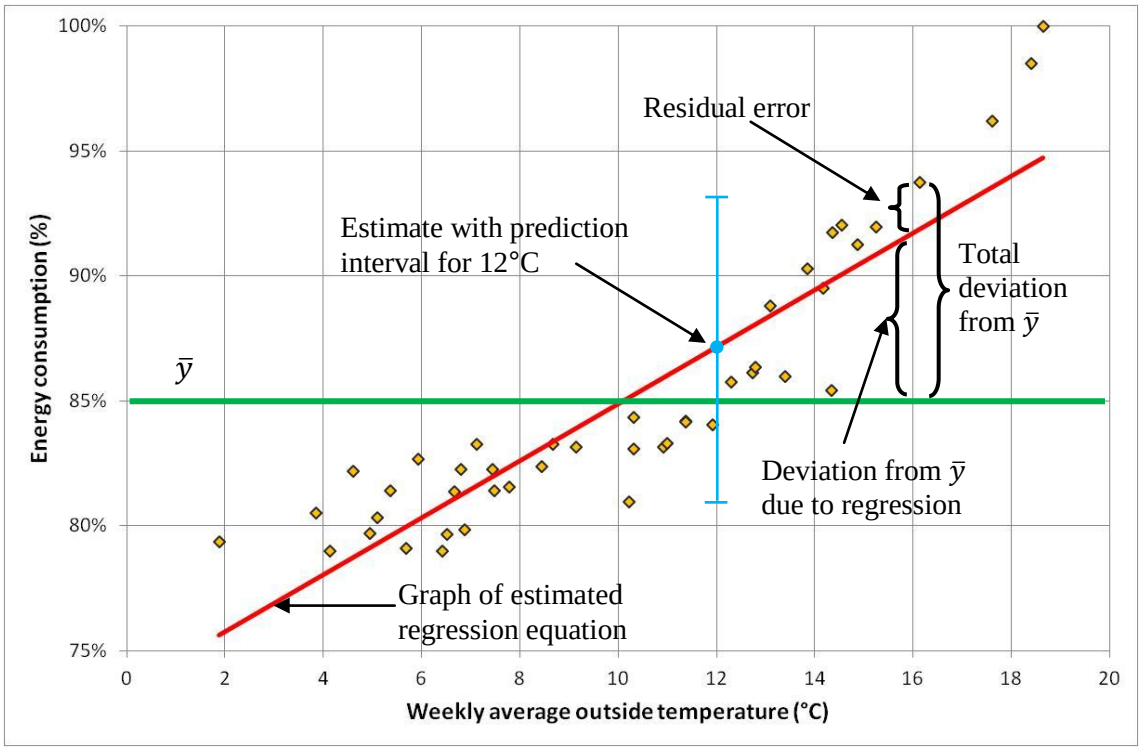

Figure 4.2: Example of a linear regression model

4.2.1.1 Estimation and prediction with simple regression models

Once a regression model has been derived, it may be used for prediction and/or estimations. In that way the expected value for the specific x_k may be calculated as $\hat{y}_k$. However, this value does not provide any information about the precision of this estimate. Therefore $\hat{y}_k$ should be accompanied by an estimate of the prediction interval. The method of calculating this interval for a simple regression model is shown in Equation 4.7 and indicated in Figure 4.2 for 12°C. Therefore the overall result may be stated as $\hat{y}_k \pm \Delta\hat{y}_k$ (Anderson *et al*, 2003, pp 555, 556).

$$\Delta\hat{y}_k = t_{\alpha/2}\sqrt{\frac{\sum(y_i - \hat{y}_i)^2}{n-2}}\sqrt{1 + \frac{1}{n} + \frac{(x_k - \bar{x})^2}{\sum(x_i - \bar{x})^2}}$$

Equation 4.7

Where:

$t_{\alpha/2}$: The value of the t distribution for the level of significance α

4.2.2 Change point regression

A simple regression equation may not be sufficient because of an abrupt change in the data. If this occurs, a change point model may be considered. Change point regression models with three parameters have been used to model the gas consumption in homes (Krarti, 2011, p 16-6; ASHRAE, 2013, p 19.25) and models with four parameters to analyse supermarkets (Ruch and Claridge, 1992). ASHRAE (2013, p 19.25) explains that four-parameter models are particularly suited for buildings with continuous heating and cooling, such as grocery stores. Julious (2001) suggests that in such a model the change point may be of primary importance, rather than the equation parameters. For a three-parameter model for heating, this may be the balance point temperature (defined in 4.5) when the consumption leaves the temperature independent region and becomes a function of the outside temperature (ASHRAE, 2013, p 19.23).

Both three and four-parameter models are shown in Figure 4.3. This figure shows that for a three-parameter model one part is temperature independent and is described by a single parameter (in this case $b_{3.1}$). For the section after the change point temperature ϑ_{cp} the line requires two parameters (i.e. b_1 and b_2). The four-regression model uses two straight line equations which join at the change point.

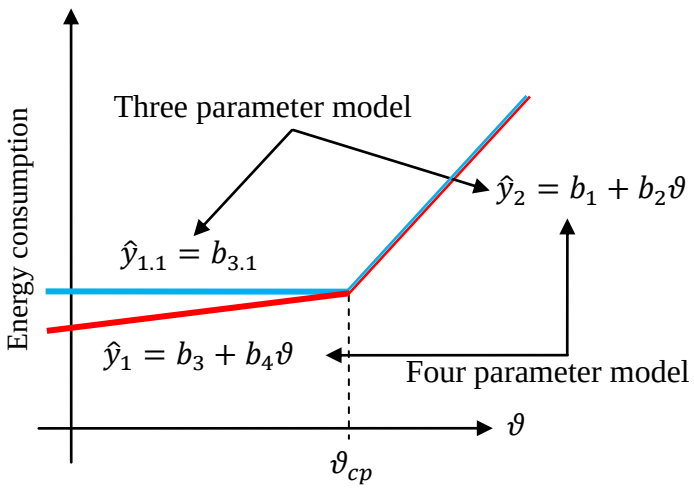

Figure 4.3: Change point regression models

In order to derive the parameters, the same least square approach explained in the previous section may be used. It should be noted that one of the unknowns derived for the model is the change point itself. Therefore the equation for the four-parameter model is as given in Equation 4.8. The coefficient of determination is calculated as described in Section 4.2.1.

$$\hat{y} = \begin{cases} b_3 + b_4\vartheta, & \vartheta < \vartheta_{cp} \\ b_3 + (b_4 - b_2)\,\vartheta_{cp} + b_2\vartheta, & \vartheta_{cp} \leq \vartheta \end{cases}$$

Equation 4.8

4.2.3 Multiple linear regression analysis

Both simple and change point regression have only the capability of regressing against one independent variable. MLR analysis, which can also include a change point (Katipamula *et al*, 1998), overcomes this problem by permitting the incorporation of any number of predictors (Lam *et al*, 2010b; Wang *et al*, 2012) and is thus one example of MVA, which all seek to establish a relationship between a set of independent variables and one dependent variables. Another example of MVA tools is the PCA. One drawback of both tools is that they require some statistical training for proper use (Pedersen, 2007; Wang *et al*, 2012). In addition, the same limitation of the simple regression with regards to only suggesting relationships and not establishing cause and effect needs to be kept in mind when interpreting results (Tso and Yau, 2007).

A general MLR model is shown below, which relates p independent variables (or predictors) to one dependent variable. These predictors may be different quantities (such as temperature and relative humidity), different powers of the same physical quantity (e.g. $\vartheta, \vartheta^2, \vartheta^3$ etc) or interaction between physical quantities (for instance the product of temperature and relative humidity).

$$y_i = \beta_0 + \beta_1\, x_{1,i} + \ \ldots + \beta_p\, x_{p,i} + \varepsilon_i$$

Equation 4.9

Where:

$\beta_0 \ldots \beta_p$: Unknown model parameters

Just as with the simple regression, the least square method can be used to estimate the parameters $\beta_0 \ldots \beta_p$ (Montgomery *et al*, 2006, pp 66-70). The coefficients are normally estimated by software packages such as Excel, IBM SPSS Statistics or R. These programmes also calculate the coefficient of determination (including an adjusted coefficient) and statistics for significance tests.

Problems may arise when using multiple predictors that are related to each other. This phenomenon is called multicollinearity and is detected by pairwise calculating correlation coefficients, r. If the absolute value of r is higher than 0.7 then there is the potential

problem of multicollinearity. Highly correlated predictors in a model may lead to spurious results, such as a model parameter having the wrong sign or that a test for predictor significance may be difficult to interpret (Anderson *et al*, 2004, pp 607, 608). This problem may be overcome by using principle component analysis (ASHRAE, 2013, p 19.26).

4.2.3.1 Significance tests

As mentioned above, the coefficient of determination does not support any conclusion about a statistically significant relationship between the dependent and independent variables (Anderson *et al*, 2004, p 532). This is usually established by two statistics, which test for overall and individual parameter significance. These statistics are based on the following assumptions (Montgomery *et al*, 2006, p 122; Anderson *et al*, 2004, p 536):

- The assumption of a linear relationship between the response and the predictor(s) is at least approximately valid.
- The error terms ε_i have a mean of zero.
- The error terms ε_i are normally and independently distributed.
- The error terms ε_i have a constant variance of σ^2.

The F test can be employed to establish overall statistical significance of all regression models if the residuals are normally distributed. If a model has p predictors, the F test examines the null hypothesis $H_0: \beta_1 = \cdots = \beta_p = 0$ by calculating the F test statistic as shown in Equation 4.10 (Anderson *et al*, 2004, pp 603-606).

$$F = \frac{\sum(\hat{y}_i - \bar{y}_i)^2 / p}{\sum(y_i - \hat{y}_i)^2 / (n - p - 1)}$$

Equation 4.10

In the case of a simple regression model Equation 4.10 simplifies to:

$$F = \frac{\sum(\hat{y}_i - \bar{y}_i)^2}{\sum(y_i - \hat{y}_i)^2 / (n - 2)}$$

Equation 4.11

This value is then compared with the critical value F_α from the F distribution with p degrees of freedom in the numerator and $n - p - 1$ degrees of freedom in the denominator

for a given level of significance α. If $F > F_\alpha$ then H_0 is rejected and a statistically significant relationship is assumed[4]. F_α is tabulated for different levels of significance and degrees of freedom (see for instance Anderson *et al* (2004, pp 672-675)). It should be noted that this test does not establish a cause and effect relationship or support the conclusion of a linear relationship between the response and predictor(s).

The so-called t test establishes the statistical significance of individual parameters. In the case of a simple regression this test yields the same result as the F test, because there is only one predictor variable. If there is more than one predictor, the t test statistics are calculated with Equation 4.12 (Anderson *et al*, 2004, pp 537-540).

$$t_j = \frac{b_j\sqrt{\sum(x_i - \bar{x})^2}}{\sqrt{\sum(y_i - \hat{y}_i)^2 \big/ (n - p - 1)}}, j = 1 \dots p$$

Equation 4.12

The t statistic allows the examination of the null hypothesis $H_0: \beta_j = 0$ by using the t distribution (also called student distribution). If $|t| > t_{\alpha/2}$, then H_0 is rejected and a significant relationship can be assumed[3]. Values of $t_{\alpha/2}$ as a function of the degrees of freedom and level of significance (i.e. α) are tabulated (see for instance Anderson *et al* (2004, p 669)).

Residual analysis is used to verify that the underlying assumptions mentioned earlier are met. For instance, an x-y scatter plot of the residuals against the predicted values may show whether the assumption of a linear relationship is reasonable. This plot can also show whether the variance is constant or not. A cumulative probability plot, on the other hand, may be used to verify normal distribution of the error terms. A plot against time (or sample number) can help identify autocorrelation, that is to say if error terms are somehow related to a time element (Montgomery *et al*, 2006, pp 123-134). This type of test can be useful to establish the validation of the selected predictor(s), because one frequent cause of autocorrelation is that an important repressor has been omitted (Montgomery *et al*, 2006, p 475).

[4] This result can also be stated by using p-values.

4.2.3.2 Estimation and prediction with multiple linear regression models

When making predictions based on a MLR model the expected value for, say, $\vec{x}_k$ is $\hat{y}_k$. The associated prediction interval can be calculated with Equation 4.13 so that the result may again be stated as $\hat{y}_k \pm \Delta\hat{y}_k$ (Montgomery *et al*, 2006, pp 76, 77, 99, 100).

$$\Delta\hat{y}_k = t_{\alpha/2,\mathrm{n-p}}\sqrt{\frac{\sum(y_i - \hat{y}_i)^2}{n-p}}\sqrt{1 + \vec{x}_k^T(X^TX)^{-1}\vec{x}_k}$$

Equation 4.13

Where:

$\vec{x}_k^T$: The transposed vector for which an estimate is to be made in the form $[1\ x_{1,k}\ \ldots\ x_{p,k}]$

X: In addition to the data for the predictors this matrix includes a column of ones as its first column

4.3 Further data-driven analysis tools

Another tool applied to building energy analysis is the artificial neural networks (ANN) approach (Datta *et al*, 1997; Zhao and Magoulès, 2012). This technique tries to imitate the learning capacity of the brain and its ability to store knowledge (Grossberg, 1988; Kalogirou, 2000; Tso and Yau, 2007). Such a network consists of three types of interconnected layers as shown in Figure 4.4 (it should be noted that there may be more than one hidden layer). The output of a hidden layer node is calculated by summing the weighted inputs and multiplying this sum by the activation function α (ASHRAE, 1997, p 30.24). Neural networks 'learn' from the relationship between input and output training data and adjust the weights of the summation to minimize the error terms. ANNs are capable of modelling non-linear processes and have been used for estimating the heating and cooling loads of buildings and for the prediction of air movement in various types of building (Kalogirou, 2000; Foucquier *et al*, 2013). They have also been combined with a genetic algorithm (which is a stochastic, heuristic optimisation procedure) to predict energy electricity use (Azadeh *et al*, 2007). The learning capabilities of these networks together with their fault tolerance are their advantages. To fully utilize these strong points though, the network needs to be properly configured and trained (Foucquier *et al*, 2013). That this is not always straightforward is apparent by the comment in *2013 ASHRAE*

HANDBOOK FUNDAMENTALS, where it says that "choosing an optimal network's configuration for a given problem remains an art" (ASHRAE, 2013, p 19.29). This estimate is at variance with the claim by Mavromatidis *et al* (2013) who state that this method "requires less expertise and effort compared to traditional modelling approaches".

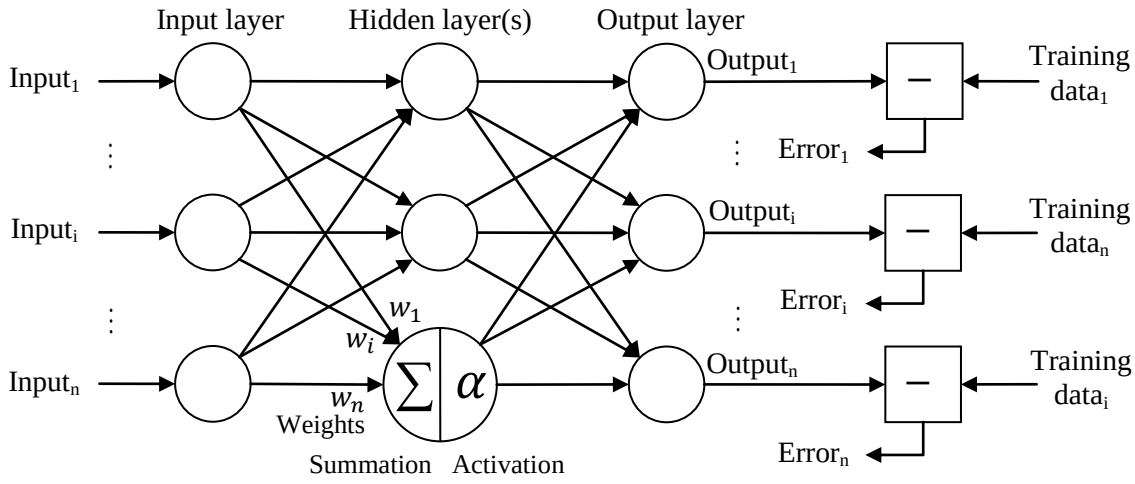

Figure 4.4: Schematic of an ANN

A more recent approach to predicting energy consumption is another neural network technique called 'the support vector machine' (SVM). This fairly complex prediction method treats nonlinearities highly effectively. However, according to Zhao and Magoulès (2012), SVMs are not easy to use. Nonetheless, it has been successfully applied to predicting energy use in buildings (Dong *et al*, 2005).

4.4 Some tools using the deterministic approach

Many, if not most, of the deterministic tools are based on the heat balance equation. One of these is the simplified building energy model (SBEM), which has been developed for the implementation of the EU directive relating to the energy performance of buildings (also known as 'EPBD') (European Commission, 2002). This method calculates the monthly or seasonal heating and cooling demand with the following equations (Wang *et al*, 2012; BSI, 2008):

- $Demand_{heating}$ = Heat loss of $area_{heating}$ – Gain utilization $factor_{heating}$ × Heat $gain_{heating}$
- $Demand_{cooling}$ = Heat $gain_{cooling}$ – Gain utilization $factor_{cooling}$ × Heat loss of $area_{cooling}$

The underlying assumptions of SBEM limit its accuracy. Furthermore, boundary conditions and input values need to be carefully specified in order to achieve reasonable results (Corrado *et al*, 2007).

Another method, which may be considered a variation of the heat balance method, employs a thermal network. This network is the discretization of the building into temperature nodes which are connected by thermal resistors and capacitors. Figure 4.5 shows a construction element model (e.g. of a wall) where the distributed thermal resistances and capacitance have been lumped into the three elements R_{in}, R_{out} and C_{mid} (Underwood and Yik, 2004, pp 33, 34). A five resistor one capacitor model has been suggested in EN 13790:2008 (BSI, 2008) to simulate the dynamic performance of buildings. The thermal network method is a very flexible tool, but may require some effort to achieve its full potential (ASHRAE, 2013, p 19.7).

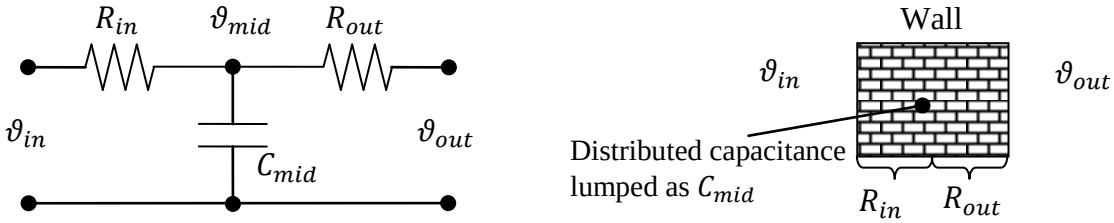

Figure 4.5: The thermal network of a construction element

In contrast to the thermal network, which combines heat flows, the computational fluid dynamics (CFD) method decomposes a zone into a three dimensional mesh with a large number of control volumes. This versatile tool can be used to study natural ventilation, help design HVAC systems or predict the dispersion of pollutants (Zhai, 2006). CFD has also been coupled with building simulation software (e.g. EnergyPlus) to improve the cooling and heating load prediction of such software while keeping computational burdens at a relatively modest level (Zhai *et al*, 2002). This is desirable because one of the drawbacks of this detailed approach is its high computational cost. Other disadvantages are the need to understand fluid dynamics to some degree and to have a good understanding of the software package used (Foucquier *et al*, 2013).

4.5 Degree days

A deterministic tool with a long history is the degree day method (Day, 2006, p 13). This steady state approach can be used to calculate the annual heating and cooling loads of

rooms or (small) buildings (Zhao and Magoulès, 2012) and has also been applied to a theoretical supermarket model (Ducoulombier *et al*, 2006). As this methodology can be employed to characterise the climate concisely (ASHRAE, 2013, p 19.16), it has also been used extensively in climate change impact studies (Li *et al*, 2012). One of the major attractions is its simplicity, therefore, even in the age of sophisticated simulation software packages, this method is still popular (Al-Homoud, 2001; Li *et al*, 2012). Another point in its favour is that its underlying concept is easily understood. A major drawback of the degree day method is that it relies on the validity of the steady state assumption (De Rosa *et al*, 2014).

It could be argued that the degree day method makes use of a very simple thermal network made up of only one resistor. When calculating the heating demand this resistor takes into consideration all heating loss mechanisms and therefore is referred to as the total heat loss coefficient. Day (2006, p 6) explains that this coefficient is made up of fabric transmission losses and the air infiltration rate, and then states an equation (see also Equation 4.14) on page 25 to calculate this coefficient.

$$K_{tot} = \sum U\,A + {}^{1}/_{3}\;N\,V$$

Equation 4.14

Where:

K_{tot}: Total heat loss coefficient

U: U-Value of building component

A: Area of building component

N: Air infiltration rate

V: Volume of space under consideration

The degree day method allows the estimation of the heating and cooling requirements based on the concept of the balance point temperature, ϑ_{bal}. For the heating demand in a building, this temperature is defined as (ASHRAE, 2013, p 19.16):

> [The] value of the outdoor temperature [$\vartheta_{outside}$] at which, for the specified value of the interior temperature [ϑ_{inside}], the total heat loss […] is equal to the heat gain from sun, occupants, lights, and so forth.

Based on this definition the yearly heating requirements can be calculated as shown in Equation 4.15 ASHRAE (1997, p 30.17).

$$Q_{heat} = \int_{1\,\mathrm{Jan}}^{31\,\mathrm{Dec}} \frac{K_{tot}}{\eta_{heat}} f(\vartheta_{bal})\, dt$$

Equation 4.15

Where:

$$f(\vartheta_{bal}) = \begin{cases} \vartheta_{bal} - \vartheta_{outside}, & (\vartheta_{bal} - \vartheta_{outside}) > 0 \\ 0, & \text{else} \end{cases}$$

η_{heat}: Efficiency of heating system

This integral is normally approximated with a sum of days when the average daily temperature is below the average balance point temperature, thus Equation 4.15 is approximated by Equation 4.16. In this equation the summation is also called ‘degree days’.

$$Q_{heat} \cong 24\ \frac{\mathrm{h}}{\mathrm{days}} \frac{K_{tot,c}}{\eta_{heat,c}} \underbrace{\sum_{\mathrm{days}} f(\bar{\vartheta}_{bal})}_{\text{Degree days}}$$

Equation 4.16

Where:

$$f(\bar{\vartheta}_{bal}) = \begin{cases} \bar{\vartheta}_{bal} - \bar{\vartheta}_{outside}, & (\bar{\vartheta}_{bal} - \bar{\vartheta}_{outside}) > 0 \\ 0, & \text{else} \end{cases}$$

$K_{tot,c}$: Total heat loss constant

$\eta_{heat,c}$: Efficiency constant of heating system

When the average balance point temperature is not known, ASHRAE (2013, p 19.17) suggests to assume 18.3°C as the balance point temperature which was also used in the first recorded application of degree days in the 1920s. In the UK, traditionally the temperature of 15.5°C is adopted. That these values are still being used despite changes in

building standards and internal gains may make them seem questionable and verification for individual cases may be advisable (Day, 2006, p 13).

One of the limitations of Equation 4.16 is that the total heat loss and the efficiency of the heating system are represented by constants. If these assumptions are significantly violated, then the results will be unreliable. Another weakness is that the balance point temperature is considered stable. However, as ASHRAE (2013, p 19.17) shows, the balance point temperature changes with the internal load over a day. The internal gains may change also over the year, which may affect the balance point temperature in an unpredictable way. Furthermore it should be noted that the equation above is only for sensible heat load.

Analogous to the heating degree days, a method for estimating the cooling requirements can be developed. Here the occupancy behaviour can have a significant impact on the total heat loss, because people may open windows with the effect of changing the heat loss factor substantially (ASHRAE, 1997, p 30.18). Therefore Al-Homoud (2001) suggests to use the degree day method only for heating calculations and preferably for skin-load dominated buildings as the degree day method does not consider internal loads rigorously.

Various methods have been developed to mitigate the shortcomings of the degree day calculations. One of them is the bin method, which has a number of bins for outside temperature or time intervals. This allows different balance point temperatures, loss and efficiency coefficients to be applied to each bin separately. The required heating (or cooling) energy is then the sum of all the bins (ASHRAE, 2013, p 19.19).

4.6 Computer simulation

Computer building simulation programmes are another example of deterministic tools. Before the advent of both these and powerful computers, building designers had to rely on manual calculation methods and/or rules-of-thumb. This posed the risk of misspecification of equipment leading to frequent oversizing with associated poor energy efficiency (Hong *et al*, 2000). This situation changed slowly in the mid to late 20th century with the development of increasingly sophisticated building simulation tools (Clarke, 2001, p 4; Hong *et al*, 2000). One of these software packages, EnergyPlus, has its roots in a programme written in the late 1960s for the US Post Office. Its successor, DOE-2, was eventually combined with another piece of simulation software (BLAST) sponsored by the

US government to form EnergyPlus (Crawley *et al*, 2001). As the documentation for this software package is detailed, it will be referred to throughout this section.

The literature review above indicated that the particular strength of this approach includes the evaluation of building design options and energy saving measures. However, Coakley *et al* (2014) pointed out that, despite sophisticated computer programmes, the performance gap can be as large as 100%. Therefore such a software model has to be calibrated if it is to be used for energy predictions rather than for comparing design options. The authors described this as a lengthy, opaque process.

As a preparatory step to simulating a building, a significant amount of data has to be gathered to model the building envelope together with its equipment and usage (some aspects are illustrated in Figure 4.6). Once a model has been built, the space load in each zone is calculated based on weather data and casual gains (e.g. people or small-scale electric equipment). The next step, referred to as 'system load calculations' in Figure 4.6, relies on the description of the distribution systems. If an air-conditioning system with a central plant is considered, this phase involves calculating the electricity use of the supply and return fans. After that the zone loads are combined to calculate the energy requirements of the central plant. These calculations are solved either simultaneously or successively (ASHRAE, 2013; Wulfinghoff *et al*, 2011; Wang *et al*, 2012).

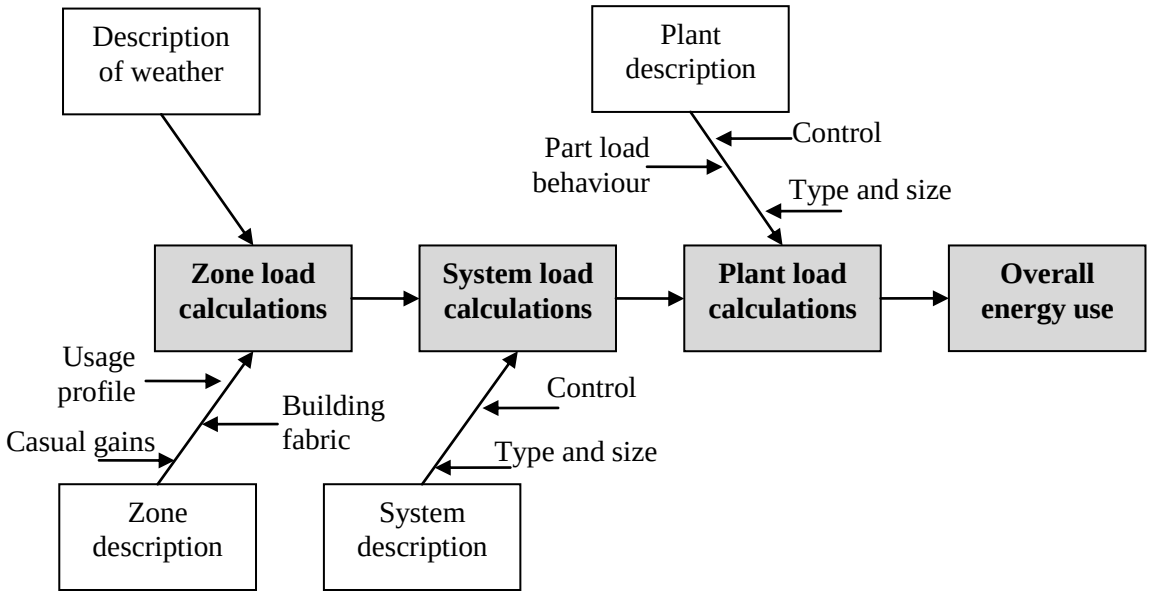

Figure 4.6: Outline of the calculation procedure in building energy simulation programmes

In order to calculate the thermal loads in zones, the heat balance equation is used with the following assumptions (Foucquier *et al*, 2013; Crawley *et al*, 2001):

- Each zone can be modelled with isotropic state variables. This means, for example, that the temperature in a zone is assumed to be the same throughout.
- Each surface has a uniform surface temperature, long and short wave irradiation.
- Heat conduction occurs only in one dimension.

The heat balance equation and the heat transfer equation for the zone surfaces have been described as "two essential equations" (Zhai *et al*, 2002) for a building simulation programme. However, here only the heat balance equation is developed, which was considered sufficient to further sketch out the logic and assumptions of this approach.

4.6.1 Heat balance equations

The heat balance method is based on the first law of thermodynamics and calculates the instantaneous net sensible load in each zone. To accomplish this, a set of heat balance equations are written for all enclosing surfaces and one for the air in the zone (see Figure 4.7). This allows the computation of surface and air temperatures, which are then used to determine the convective heat flows (ASHRAE, 1997, pp 19.4, 19.5).

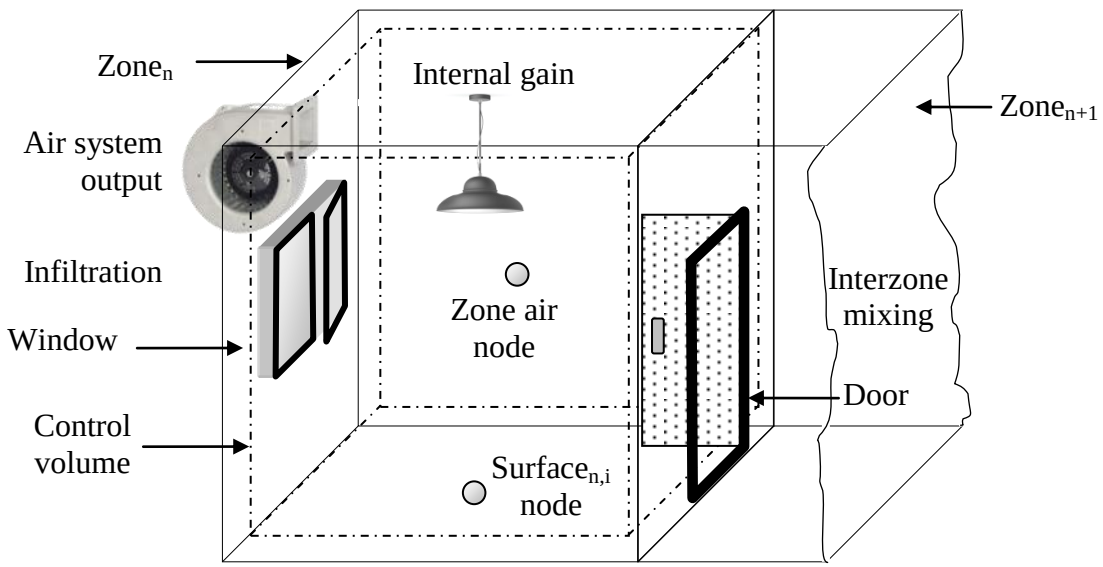

Figure 4.7: Diagram for the heat balance equation

The first law of thermodynamics can be written as in Equation 4.17.

$$Q - W = \Delta U$$

Equation 4.17

For the heat balance equation W is zero as the volume of the zone in Figure 4.7 remains constant. The term Q is the net heat added to the system. Further noting that

$$c_v = \left.\frac{\partial u}{\partial T}\right|_{V=\text{const}} \Longrightarrow \Delta u = \int_{T_1}^{T_2} c_v dT \xRightarrow{if\ c_v=\text{const}} \Delta u = c_v \int_{T_1}^{T_2} dT = c_v\, \Delta T = c_v\, \Delta\vartheta$$

Equation 4.18

Therefore Equation 4.17 can be re-written as

$$Q_{net} = m\, c_v\, \Delta\vartheta$$

Equation 4.19

Regarding Figure 4.7, the equation above can be expanded to yield the heat balance equation for one zone (US Department of Energy, 2013, p 7):

$$\dot{Q}_{net} = \sum \dot{Q}_{int\ gn} + \sum \dot{Q}_{srfc} + \dot{Q}_{infl,o} + \sum \dot{Q}_{infl,zn} + \dot{Q}_{sys,sen}$$

Equation 4.20

This leads to Equation 4.21 if the addition of $\dot{Q}_{net}$ changes the energy in the control volume shown in Figure 4.7.

$$\dot{Q}_{net} = mc_{air} \frac{d\vartheta_{zn,air}}{dt}$$

Equation 4.21

According to *EnergyPlus Engineering Reference* (US Department of Energy, 2013, pp 7, 8) the following individual terms in Equation 4.20 can be expanded as below:

- Convection from surface$_i$: $\dot{Q}_{srfc} = A_i\, h_{i,air}\left(\vartheta_{in,i} - \vartheta_{zn,air}\right)$
- Infiltration from outside air: $\dot{Q}_{infl,o} = \dot{m}_{inf,outside}\, c_{air}\, \left(\vartheta_{outside} - \vartheta_{zn,air}\right)$
- Infiltration from other zone: $\dot{Q}_{infl,zn} = \dot{m}_{inf,zone}\, c_{air}\, \left(\vartheta_{zn,n+1} - \vartheta_{zn,air}\right)$

Substituting these expressions into Equation 4.22 yields:

$$mc_{air} \frac{\mathrm{d}\vartheta_{zn,air}}{\mathrm{d}t} = \sum_{Surfaces} A_i\, h_{i,air}\left(\vartheta_{in,i} - \vartheta_{zn,air}\right) + \dot{m}_{inf}\, c_{air}\, \left(\vartheta_{outside} - \vartheta_{zn,\mathrm{air}}\right) + \sum_{Other\ zones} \dot{m}_{inf,n}\, c_{air}\, \left(\vartheta_{zn,n+1} - \vartheta_{zn,i}\right) + \sum \dot{Q}_{int\ gn} + \dot{Q}_{sys,sen}$$

Equation 4.22

With the assumption that the zone temperature is kept constant (Underwood and Yik, 2004, p 76) Equation 4.22 can be rearranged to finally calculate the system load. This equation,

or a similar equation, is used to calculate the energy used to condition, e.g., the room shown in Figure 4.6.

$$\dot{Q}_{sys,sen} = \sum_{Surfaces} A_i\, h_{i,air}\left(\vartheta_{zn,n} - \vartheta_{in,i}\right) + \dot{m}_{inf}\, c_{air}\left(\vartheta_{zn,n} - \vartheta_{outside}\right) + \sum_{Other\ zones} \dot{m}_{inf,n}\, c_{air}\left(\vartheta_{zn,n} - \vartheta_{zn,n+1}\right) - \sum \dot{Q}_{int\ gn}$$

Equation 4.23

4.7 Conclusion

This chapter introduced a number of data-driven and deterministic analysis techniques and considered in particular regression models and software simulation based on heat balance equations as an example of each. All of these tools and techniques have their individual strengths and weaknesses. How the discussion above influenced the decision process regarding the methodology choice for the whole supermarket research will be outlined in Chapter 5.

5 Selection and analysis of supermarkets

From this chapter up to Chapter 1, complete supermarkets are the object of study. Figure 5.1 shows the research covered in these chapters. The work involved in the first two steps is described first in the present chapter. The aim of these is to identify a number of supermarkets which satisfy the inclusion requirements; that is to say to select supermarkets which were as similar as possible. In this way the influence of differences relating to operational practice and local climate could be explored. In particular Sections 5.1 to 5.3 covers this two stage process by first describing how the sponsor's supermarkets were examined to narrow down the investigation to seven possible supermarkets. This is followed by a description of site visits to these supermarkets including their preparation. The discussion which follows shows why the seven supermarkets could be used to achieve the study aim mentioned here.

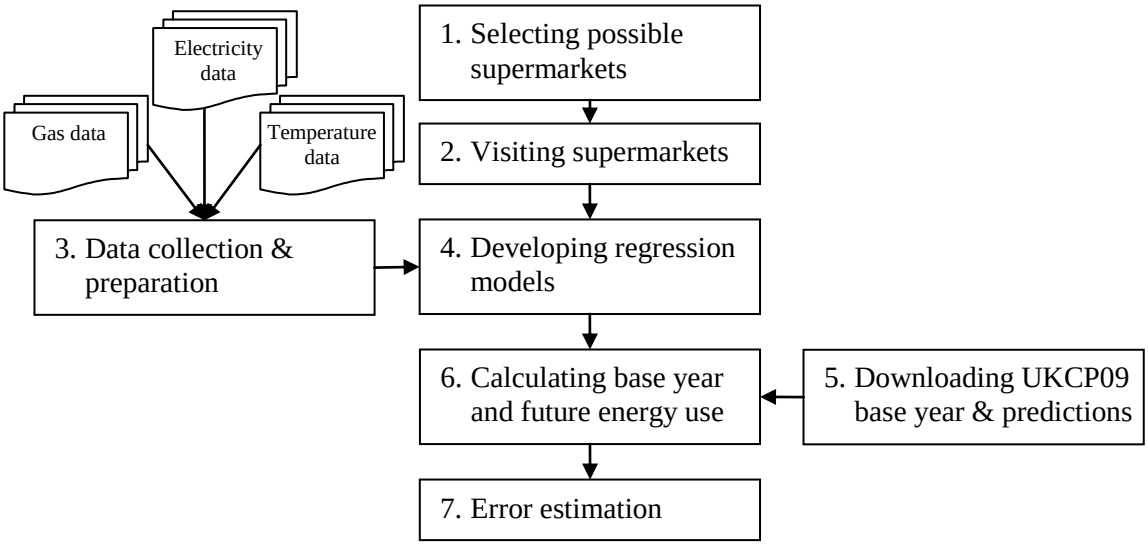

Figure 5.1: Research flow for the whole supermarket investigation

From Section 5.4, the discussion moves on to steps three to seven which are concerned with the actual analysis method and include a justification of the research method chosen. After that, a discussion on the preparation of the measured data follows. Next, an explanation of the way energy usage was estimated together with an error analysis completes this chapter.

5.1 Selection process

When the search for comparable stores began, the sponsoring supermarket reported a chain of 766 stores in the UK (of which 243 were franchised) (Marks and Spencer Group plc,

2014). The sponsor classified them according to their store format. The highest number of stores was in the 'High street' category. However, this format comprised an inhomogeneous building stock and, because the building type can have a significant impact on energy demand (see for instance Xu *et al* (2012)), this category was considered unsuitable for this study. In addition to this the same report indicated that, comparatively speaking, more stores were added to a different category. This type of store can be described as grocery supermarkets with a relatively large amount of refrigerated shelves.

Figure 5.2: Locations of selected supermarkets (map by Descloitres (2002))

The sponsoring company divided those 176 grocery supermarkets into small and large stores. The category containing the larger sized stores had about 100 entries with sales areas ranging from approximately 531 m^2 to 1910 m^2 averaging approximately 950 m^2. Their total annual EUI varied from 479 kWh/m^2 to 1540 kWh/m^2 (2012/13 figures). These approximately 100 stores were investigated as to building location and building type as well as to the presence of an in-store café and bakery. Here, the company's on-line store guide was used as it not only gave the address, but also indicated if a particular store had an in-store café and bakery. All of this was recorded in a spreadsheet. To investigate the building location the Street View (Google, 2009-2012) and satellite option on Google Maps (Google, 2013) were used and results were also noted in the same spreadsheet. If possible the exact location within a building or parade of shops was recorded too. It was

found that 45 of these large grocery supermarkets were located in retail parks of which 18 had both a café and bakery. As a final step it was ensured that all supermarkets had an R404/R744 type of refrigeration system. This led to the selection of seven supermarkets which had all these features in common.

As Figure 5.2 indicates, the supermarket locations are well spaced out throughout Great Britain, two towards the west, two inland and three to the east. It was also hoped to include Wales because the Met Office lists Wales as a difference climate region (Met Office, 2013), but no suitable supermarket could be located. The proximity of the two stores in Washington and Gateshead offered the potential of investigating other sources of deviation than different weather patterns.

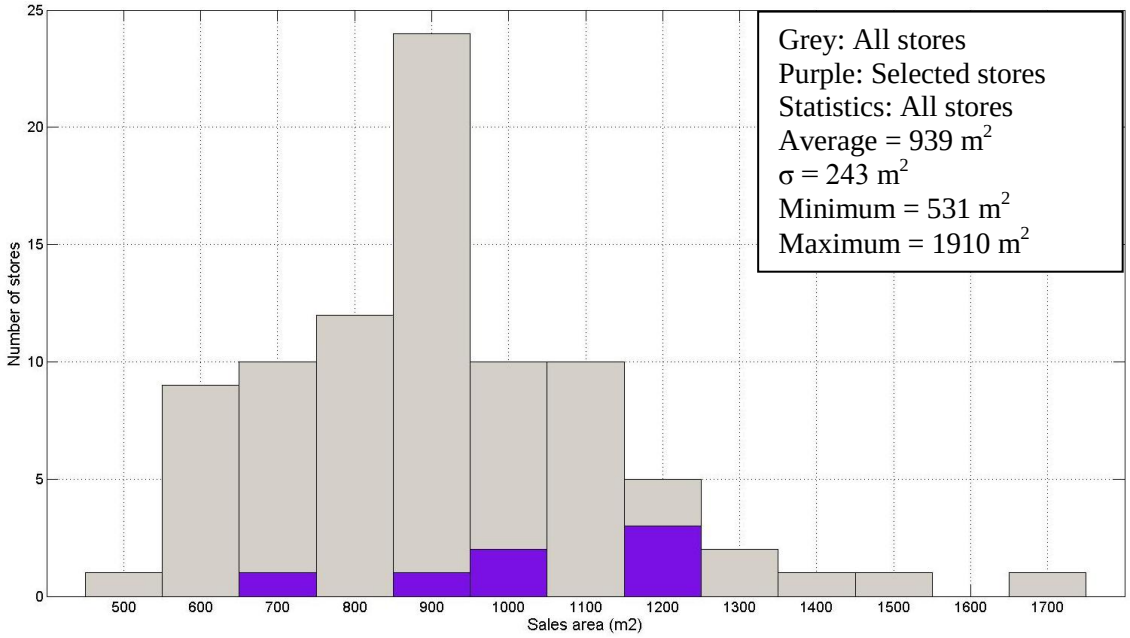

Figure 5.3: Histogram - Sales area of all supermarkets in the category considered vs the ones selected

The histogram in Figure 5.3 displays the distribution of the sales area of the nearly 100 large grocery supermarkets and, in purple, the selected stores. It shows that the sales areas of the selected stores tend to be larger than the average of 939 m^2. However, this was not considered significant as their sales areas are still considerably smaller than that of the largest store in this category.

For the histogram in Figure 5.4, the electricity and gas consumption (if applicable) was added up to give a total EUI for each supermarket. The histogram shows a relatively constant store count from the bin labelled 700 to 1100. Although all seven supermarkets are within this range, five of them are below the average EUI of 882 kWh/m^2. The two

stores which have a higher than average EUI are Washington (982 kWh/m^2) and Glasgow (1070 kWh/m^2).

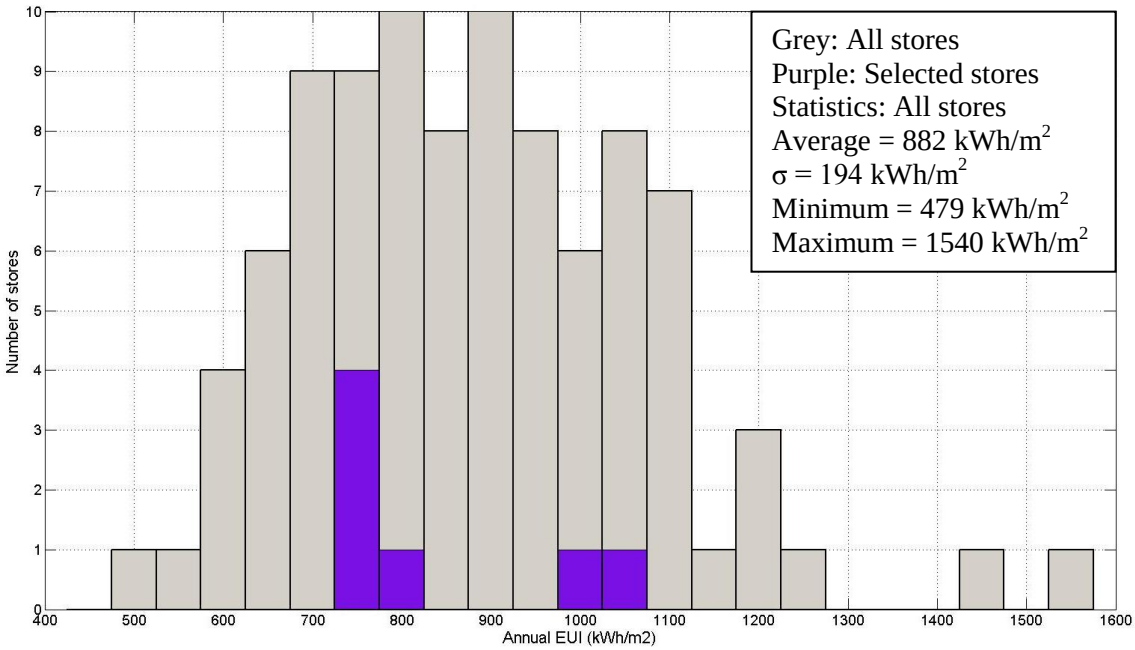

Figure 5.4: Histogram - EUI of all supermarkets in the category considered vs the ones selected

5.2 Visits to supermarkets

In order to verify the degree to which the selected supermarkets were actually comparable, site visits were conducted. These were preceded by devising a site visit protocol detailing the number of major energy consumers based on HVAC layout plans, lighting layout plans (if available) and other architectural drawings (these site visit protocols are included in Appendix C – Site visit protocols).

The sponsoring company employs regional energy managers whose task it is to assist stores with reducing energy consumption. Three of them were contacted to arrange to visit with them the supermarkets for which they were responsible. In this way it could be studied how the different regional energy mangers interpreted the energy consumption and how they identified and investigated abnormalities. Six of the seven supermarkets were visited starting early May 2014 and finishing early July 2014. The store in Hull had been visited before for a pilot study. During the visits the following tasks were performed:

- The actual numbers of energy consumers were compared with the number on the site visit protocol (this included documenting the installed refrigerated shelves).
- The timer settings were documented. (Timers are centrally programmed.)

- The times the night covers for the refrigerated display cases and freezers were removed and put back were recorded.
- The times the main baking time started and finished were noted down.
- If possible informal discussions were held with the store manager, the operations manager and the Plan A champion (see Grayson (2011) for a description of the role of the Plan A champion).

The major energy consumers, such as the HVAC system and lighting are centrally programmed and controlled via building timers. Therefore there is only a limited scope for how differences in operation can influence the energy use in individual supermarkets. The operational timings, which may have an impact on energy consumption and are listed in Table 5.1, are based on the estimates given by store personnel. This means that these values may be just approximate. Nonetheless it can be seen that some stores (i.e. Hull, Leicester and Newbury) put the night covers on the refrigerated display cases immediately after the store closes for the day whereas others allow for stocking during after store hours, which may be in addition to the preopening stocking time. One example of this is the Gateshead store, which has also different opening hours; thus the notation "Shut + 45 mins" was used to indicate that after the supermarket was closed to the public, stocking continued for approximately 45 mins. The table also records the times for the main bake of bread and cakes in the morning. This is significant because the ovens, which are in constant operation during this time, have a combined power consumption of 15 kW. Almost all stores start baking as early as possible and continue well after the supermarket has opened. The majority of stores suggested four hours for their main bake, with Glasgow and Washington being the outliers.

Table 5.1: Operational timings

Location	**Glasgow**	**Gateshead**	**Washington**	**Hull**	**Leicester**	**Newbury**	**Exeter**
Night cover							
Off	7:00	6:00	6:30 – 7:00	6:30	6 – 7:00	6:00	6 – 7:00
On	20:50	Shut + 45 mins	20:30 – 20:45	20:00	20:00	20:00	20:45
Total (h:min)	13:50	≈15:00	≈13:50	13:30	≈13:30	14:00	≈14:15
Main bake							
On	6:00	6:00	6:30	6:00	6:00	6:00	6:00
Off	11:00	10:00	9:30	10:00	10:00	9:30 - 10	10:00
Total (h:min)	5:00	4:00	3:00	4:00	4:00	3:45	4:00

After the visits the site visit protocols were updated, the main consumers were added up and recorded in Table 5.2. The volume-area ratio in this table shows whether or not a mezzanine floor was installed. For instance, this ratio shows that the supermarkets in

Glasgow, Hull and Exeter had only one floor whereas the other stores had a mezzanine floor. When dividing the installed lighting capacity by the total floor area, one finds that there is what may be considered only a modest spread from approximately 10 W/m^2 to just over 13 W/m^2. The larger spread observed in installed heating capacity density (between 105 W/m^2 and 179 W/m^2) may be partly due to the absence of precise data for the undercase heating modules for the refrigerated display cases and partly due to different cold aisle heating schemes. It should be noted that the installed comfort cooling is relatively small for all supermarkets (except for the Newbury store). This is so because the open refrigerated display cases also removed the room heat, hence normally no additional cooling is required for the sales floor, but heating is. The table also records the nominal size of the refrigeration plants. If two figures are given, then the supermarket has two plants, otherwise only one has been installed.

Table 5.2: Data of the selected supermarkets

Location	**Glasgow**	**Gateshead**	**Washington**	**Hull**	**Leicester**	**Newbury**	**Exeter**
Latitude	55.743	54.923	54.900	53.748	52.684	51.385	50.717
Longitude	−2.870	−1.620	−1.532	−0.425	−1.088	−1.318	−3.538
Weekly trading hours (h)	81	80	78	75	79.5	77	78
Total area (m^2)	1550	1730	1320	1820	1640	1710	1440
Sales area (m^2)	1030	1210	743	1250	1000	1190	929
Volume (m^3)	12000	7800	7090	13700	9210	8270	10400
Volume/total area (m)	7.74	4.51	5.37	7.55	5.61	4.84	7.22
Lobby (yes/no)	Yes	No	Yes	Yes	Yes	No	Yes
Installed lighting (kW)	17.5	21.8	15.4	19.1	18.7	21.8	16.9
Installed heating (kW)	277	232	227	191.5	215	256	227
Installed A/C cooling (kW)	50.1	65.7	12.9	59.5	23.1	83.4	29.5
Total length of ref. shelves (m)	97	89	71.4	94.4	90.1	88.2	102
Refrigeration plants (kW)	80 + 60	100	100	80 + 60	100	100	100

The number of cold room doors and how frequently they are opened may also influence the energy consumption in supermarkets. When visiting the selected supermarkets it was noted that, with the exception of Hull, all supermarkets had only one door to the cold room. In certain supermarkets, it was also observed that the light, which is controlled by a motion sensor, had been switched off indicating that the door had been open for a while. When visiting the Hull store it was noticed that, most of the time, at least one door was left open.

5.3 Discussion on the selection of supermarkets

So far this chapter described which seven grocery supermarkets were selected for further study. These stores belong to a building category with a relatively homogonous building stock, i.e. retail units in a retail park.

The EUI of all seven selected stores compares favourably with other supermarkets in the UK according to Tassou *et al* (Tassou *et al*, 2011). Based on their classification, all seven supermarkets can be categorized as mid-range stores with an expected annual EUI of between 997 kWh/m^2 and 1100 kWh/m^2. According to Tassou *et al* (2011) the lower limit is approximately 500 kWh/m^2 per year. The actual yearly EUI is between 463 kWh/m^2 (for Leicester) and 605 kWh/m^2 (for Glasgow). This comparison shows that, although the actual consumption figures are lower than the expected figures, they may be still considered comparable with other supermarkets in the UK.

Operational practice seems to have little impact on the supermarkets selected. The two supermarkets with the highest EUI have the night covers removed for approximately 13.75 hours. Other supermarkets with a lower EUI have the night covers removed for longer. Furthermore the main baking time is very similar across the supermarkets, and the two with the highest EUI have the shortest and longest times. The Hull store with the two door cold room is the median store for the EUI and still better than the overall average. Therefore it could be argued that keeping both doors shut may reduce the energy consumption, although not significantly.

The discussion above showed that the seven stores selected are comparable in size and energy consumption, and are also representative of the whole category. The operational practices investigated here seem not to influence the energy consumption significantly. Therefore research based on these supermarkets should yield meaningful results in answering the research question regarding the impact of climate change.

5.4 Method selection

In order to study the selected supermarkets, a number of different energy analysis methods are possible. The aim of the method selection process was to identify as simple an approach as possible which still yielded meaningful results. Li *et al* (2012) suggest that the two deterministic approaches, simulating buildings with software and the degree days

method, are the most popular research approaches for the impact assessment of climate change on energy use in buildings. Section 4.4 discussed simulation software models and showed in Figure 4.6 that there is a considerable amount of data from various sources to be collected before such a model can be built. For instance, in order to calculate the energy use in a building, hourly weather files and data regarding casual gains, e.g. from people, need to be available. However, how the number of customers will develop over the next couple of decades is not easy to predict and therefore may require a considerable amount of time to establish. Once the model has been constructed it needs to be calibrated to achieve more accurate and reliable results or else simulation results may deviate from the true value by as much as 100% (Coakley *et al*, 2014). The end product is a model which will be dealt with as a "black box", because the content of the model is not so important. What is of importance is that the model yields credible results. Depending on the level of detail this modelling and calibration can require a significant amount of time per building (Rivalin *et al*, 2014). Therefore this approach was not pursued further, because it was considered to not be time efficient.

The degree day method, also explained in Section 4.5, requires that a balance point temperature can be established. However, the data shows (see for instance Figure 5.8 on page 79) that heating is required all year round and, therefore, a balance point temperature (i.e. when heating is no longer required) cannot be established. The degree day approach can also be used for comfort cooling, but the purpose of refrigeration in a supermarket is to preserve food and not to provide comfort cooling. Hence, this method was also deemed unsuitable.

The data-driven approach uses measurements to establish a relationship between weather variables and energy consumption. According to Belcher *et al* (2005), there are 14 weather variables which could be considered for building simulations, some of which are derived from other variables. In order to achieve the objective of producing a simple, but relevant model, the automatic weather station Davis Vantage Pro2 was considered, which also received favourable reviews (Burt, 2009; Bell *et al*, 2015). However, the sponsoring company found this approach impractical. Therefore whether temperature alone would suffice or whether it should be combined with relative humidity was studied. The literature review supported using only temperature, because it showed that some researchers successfully applied a temperature change point regression to a supermarket (Schrock and

Claridge, 1989; Ruch and Claridge, 1992; Kissock *et al*, 1998). Some deterministic analysis tools also use only outside temperature as their input parameter (e.g. the degree day method discussed in Section 4.5). Furthermore a pilot study showed that the humidity ratio w (a function of the relative humidity and temperature) had a strong correlation with temperature (greater than 0.9). This strong correlation, which is called multicollinearity, can be problematic for MLR since it can produce predictions which are overly sensitive to small changes in the data (Montgomery *et al*, 2006, pp 109-111). Therefore it was deemed acceptable to use the outside temperature as the only weather variable.

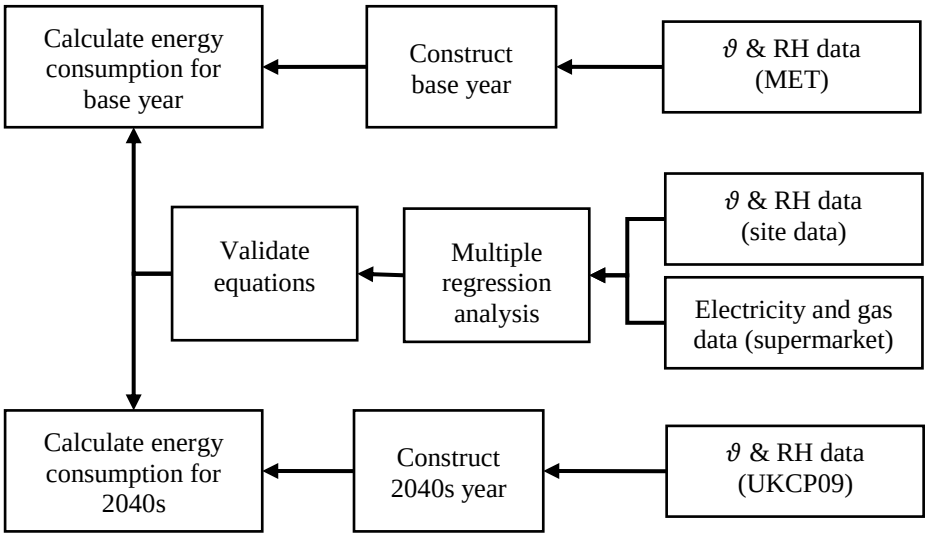

Figure 5.5: Method flowchart for the pilot study

The pilot study referred to in the previous paragraph was based on the supermarket in Hull and used the methodology sketched out in Figure 5.5. When comparing this method flowchart with the major steps depicted in Figure 5.1 it is evident that both approaches are very similar. Some of the minor differences are that the pilot study used relative humidity data for a multiple regression analysis and that the climate considered was for the 2040s rather than for the 2030s.

The scatter plot matrices in Figure 5.6 and Figure 5.7 relate to the original data for the pilot study, which is to say that outliers had not been removed. Both matrices plot the temperature against the humidity ratio w and confirm the strong relationship between the two variables. The panels in which these variables are used as predictors for the electricity and gas consumption also show little difference in their predictive power. Further examining the relationship between electricity use and temperature (or w) shows that it is

non-linear. On the other hand, the gas use and outside temperature (or w) exhibits more of a linear relationship.

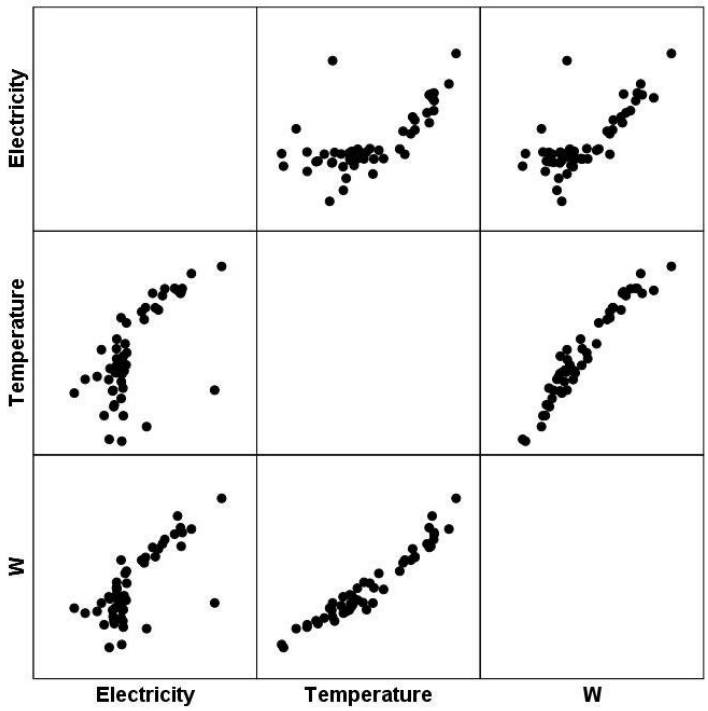

Figure 5.6: Scatter plot matrix for the original electricity data of pilot study

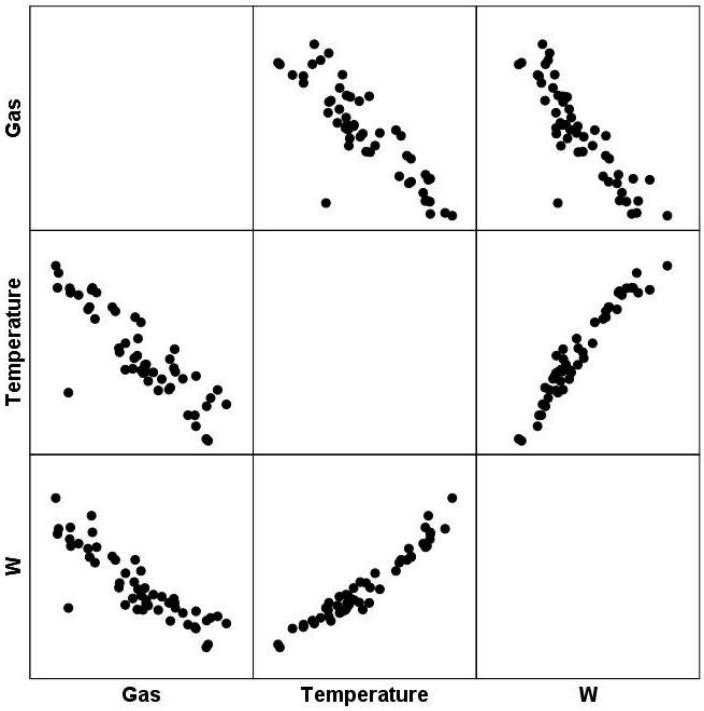

Figure 5.7: Scatter plot matrix for the original gas data of pilot study

In view of the issues raised above it was felt that simple regression should be used where possible and change point regression models where necessary. To decide when to apply a

change point regression model, a second order polynomial regression model was evaluated and, if the coefficient of determination improved over a simple regression model by more than 10%, a change point regression model was used, which was an approach also used for similar previous studies (e.g. Schrock and Claridge (1989); (Ruch and Claridge, 1992)). Although this threshold was somewhat arbitrary, it took the shape of the graphs into consideration. It was believed that using these relatively simple models satisfied the goal of simplicity with meaningful results in order to assess the impact of climate change on supermarket energy use.

5.5 Data collection and preparation

The goal of the data collection phase was to acquire data for electricity and gas consumption as well as for site temperature to analyse weekly consumption and to check daily patterns for differences and irregularities of operation and of building timers. To this end the consumption data were downloaded in 15 minute and weekly intervals from the supermarkets' energy loggers for the period from the week commencing (w/c) 1 July 13 to w/c 8 September 14. The period from w/c 1 July 13 to w/c 23 June 14 was used for the actual data analysis and the remaining data for error estimation. Weekly data, rather than daily or monthly data, were used because supermarkets tend to operate on a weekly cycle, therefore averaging over a week removes the dependency of the consumption on the day of the week.

Table 5.3, which shows a summary of the downloaded consumption data for all seven supermarkets, makes frequent use of the term 'EUI', which is given in kWh/m^2 and in W/m^2. The annual area EUI, which makes the comparison of the selected supermarkets with the energy use prediction in Tassou *et al* (2011) easier, is computed by dividing the annual consumption figure by the sales area. The annualized EUI, EUI_{pa}, is calculated by dividing the annual consumption by the total supermarket area and the weekly trading hours. Weekly opening hours, rather than annual trading hours, were used as only inter-supermarket differences had to be eliminated. The average of the EUI_{wkly}, which is the average weekly energy use intensity, is listed as 'Av EUI_{wkly}' in Table 5.3.

The energy use data in Table 5.3 is listed from north (i.e. Glasgow) to south (i.e. Exeter). The average EUI_{wkly} for electricity has an average of 90 W/m^2 and exhibits a linear relationship with the total supermarket area. This relationship has a correlation coefficient

of −0.854. The coefficients of variation ($CoVs$) have been calculated after the exclusion of data inconsistencies, such as outliers, to avoid a false impression of the magnitude of data spread and shows relatively little variation amongst the supermarkets. The electricity consumption for 25 and 26 December was considered the supermarket base load as the store was closed for these two days. Apart from the outlier at Newbury (the 2013 value for this supermarket was 24% higher than the one for 2012) the base consumption figures are also consistent with each other with low correlation to building area and volume.

Table 5.3: Energy consumption data of supermarkets

Location	**Glasgow**	**Gateshead**	**Washington**	**Hull**	**Leicester**	**Newbury**	**Exeter**
Electricity							
Annual (kWh)	647000	595000	542000	581000	556000	593000	552000
Base load (kW)	35.0	31.6	28.6	31.6	33.5	42.7	34.7
Annual area EUI (kWh/m^2)	417	364	361	336	334	309	381
EUI_{pa} (W/m^2)	5150	4300	5260	4260	4210	4670	4920
Av EUI_{wkly} (W/m^2)	99.0	82.7	101	81.9	81.0	89.8	94.6
CoV (%)	6.26	6.62	7.15	6.26	6.08	5.50	5.05
Gas							
Annual (kWh)	394000	328000	N/A	408000	254000	242000	210000
Annual area EUI (kWh/m^2)	254	201		236	153	126	145
EUI_{pa} (W/m^2)	3140	2370		2990	2000	1910	1870
Av EUI_{wkly} (W/m^2)	60.4	45.6		57.5	38.5	36.7	36.0
CoV (%)	31.3	26.8		35.1	38.1	35.4	42.0

The gas data in Table 5.3 has a distinct north-south divide with Glasgow, Gateshead and Hull making up the northern cluster and the other three supermarkets the southern cluster. This can also be seen by the strong linear relationship (r = 0.825) between a supermarket's latitude and its average EUI_{wkly}. The relationship between annual average temperature and average EUI_{wkly} is much weaker (r = 0.505). The CoV, which also excluded inconstancies, has a relationship with latitude (r = −0.829) that is similarly strong to that of the average EUI_{wkly}, which may be related to the fact that daylight is also a function of latitude. Its associated standard deviation follows the supermarket volume almost perfectly (r = 0.978 for a linear model).

The plots of the gas and electricity consumption of the supermarket in Glasgow in Figure 5.8 are in 15 minute intervals and for four days, one for each season. Other stores show

virtually identical graphs, therefore only the operation of the Glasgow store is discussed here. Before about 06:00 the gas consumption is zero and the electricity use is at its base load level. Then at approximately 06:00 staff arrives for stocking and baking which causes a jump in electricity consumption. The HVAC timer enables some of the heating at about the same time causing a peak in gas use. The store lights are switched on just before 08:00 and the rest of the heating is turned on at 08:00 resulting in another sharp increase in both gas and electricity use. There tends to be a rise in electricity use after 12:00 which may be because of higher energy demands from the in-store café. The gas consumption reduces as the day progresses until just after 18:00. The peak at this time is because the HVAC plant is switched off for energy conservation from 16:00 to 18:00. When it is turned on again, the heating demand results in this peak in gas use. When the store closes at 20:00, the trading lights and HVAC plant are switched off resulting in a steep decrease in energy consumption. After all personnel have left (at about 20:30), the remaining lights are switched off, therefore the electricity consumption returns to its base load level.

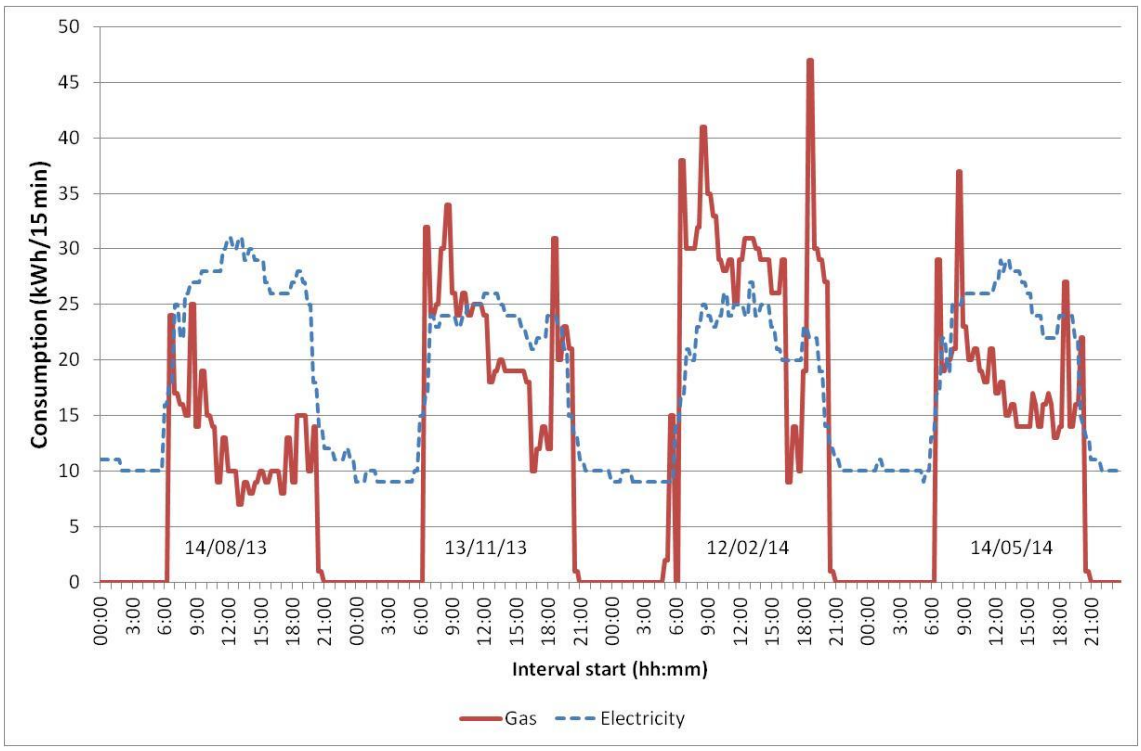

Figure 5.8: Gas and electricity consumption in 15 min intervals for the store in Glasgow

During the download of the weekly data the following problems were encountered. Firstly, it was discovered that the gas data for the Washington store could not be retrieved and therefore only its electricity data was analysed. The $CoVs$ for the consumption and temperature data were calculated by dividing the standard deviation of a variable by its

average. When comparing the CoVs of weekly gas data, another problem was detected. It was noted that the coefficient of variations for Hull was significantly higher than for the remaining supermarkets. An investigation showed that the boiler had been out-of-order for 3 months during the period of interest. Therefore the data for 2012, which was used for the pilot study mentioned above, was substituted for the analysis, and data from the w/c 30 June 14 to w/c 8 September 14 was used for error estimation.

An attempt was made to remotely access the site temperature sensors in order to download consumption data in 15 minute intervals for the same period. However, this was not possible for the supermarkets in Newbury and Exeter, therefore hourly data from a nearby MET Office weather station was substituted as supplied by the sponsoring company. The temperature data was then averaged for each week.

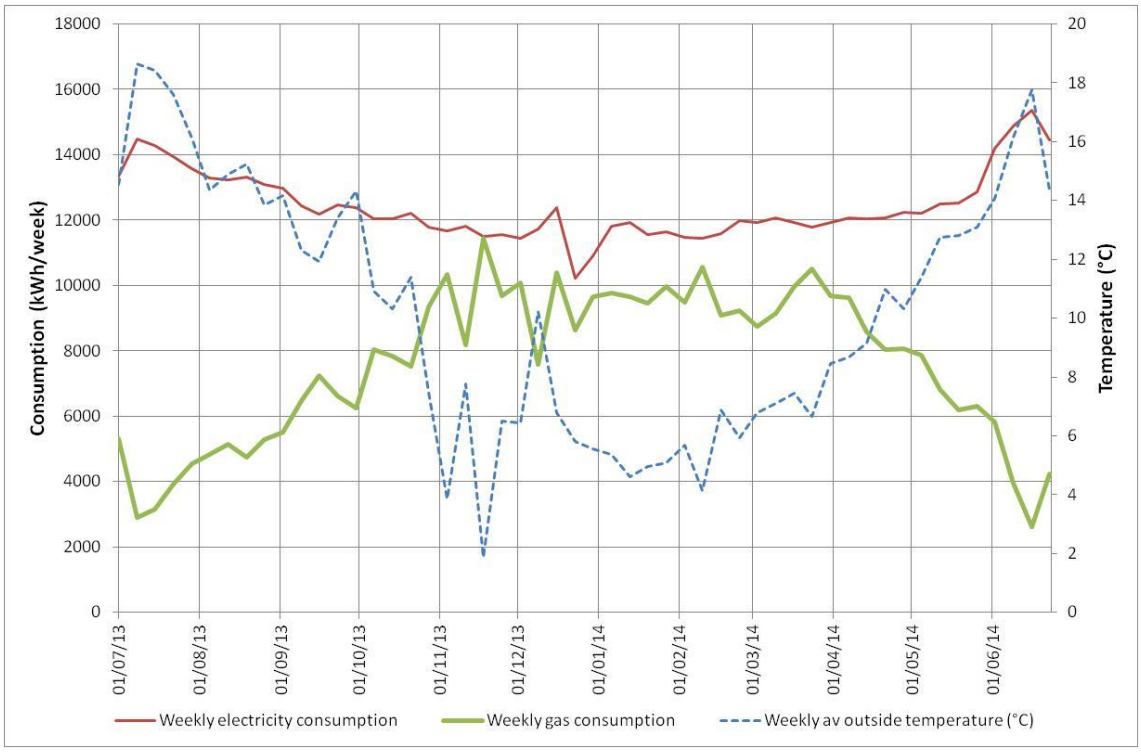

Figure 5.9: Line graph of weekly energy use and average temperature for the Glasgow supermarket

The traces in Figure 5.9 show the weekly consumption data and weekly average outside temperature for the supermarket in Glasgow. Again, the other supermarkets have similar plots so that only the line graph from this one store is displayed and discussed here. The electricity consumption is relatively constant throughout the year, which is consistent with the CoV of only 6.26% mentioned in Table 5.3. This is understandable when the electricity trace in Figure 5.8 is considered, which shows a constant base load during the night and a

temperature independent load portion (e.g. trading lights) during the day. The gas consumption in Figure 5.9 shows a much larger variability which agrees with the much larger coefficient of variation of 31.3%. This trace is essentially a scaled mirror image of the weekly temperature averages. One exception is the time around Christmas where both the electricity and gas consumption first rises and then drops because of staff stocking overnight and then the supermarket having reduced opening hours up to New Year's Day. As this behaviour is temperature independent, it was excluded from the data sets for all supermarkets.

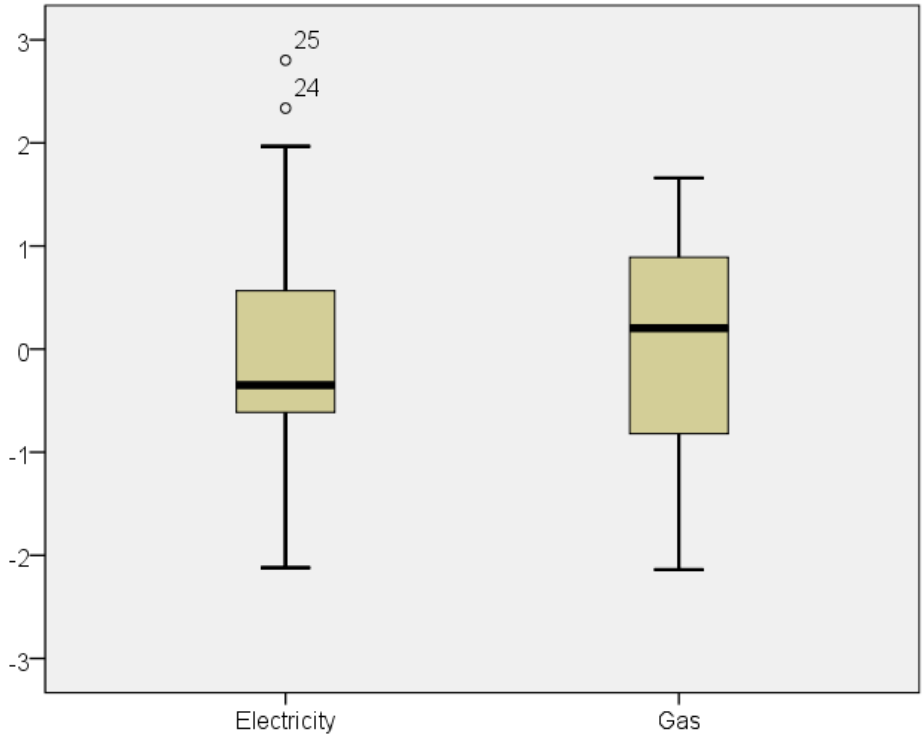

Figure 5.10: Box plot of consumption data for the Glasgow supermarket

In addition to graphs against time, box plots (for an example see Figure 5.10) were also employed to detect outliers. These plots use ranked data and are constructed around the data set median. The lower limit of the box is the median of the lower half of the data set, i.e. from the smallest value to the data set median, and the second limit is the corresponding median of the upper half. The line in the box is the median of all the data. The lines extending out of the box mark the minimum and maximum values except when they are 1.5 times of the box height away from the box limits. These points are considered outliers and need be investigated (Anderson *et al*, 2003, pp 108, 109).

The box plots in Figure 5.10 are for the supermarket in Glasgow and help to illustrate how these plots were used. Before the consumption data were plotted in these graphs, they were normalised so that gas and electricity data had an average of zero and a standard deviation of one. In this way different data sets could be more easily compared. Once a plot indicated an outlier, the reason for it was investigated. In the case of Figure 5.10 it is apparent that the electricity data contains outliers at week 24 and 25. On further investigation it was found that in week 23 (w/c 02/06/14) new refrigerated display cases were installed. Therefore the data from week 23 onwards were excluded to ensure data integrity.

In this way, during the data preparation stage data points were excluded for the following reasons:

- Christmas period (all stores): Here the supermarkets restock during the nights prior to Christmas (higher than normal energy use) and then have reduced opening hours up to New Year's Day (lower than normal consumption of energy).
- Addition of refrigerated display cases (Glasgow).
- Faulty repair resulting in higher energy consumption (Gateshead).
- Building timers for heating incorrectly set (Newbury).

Table 5.4: Result of the data preparation phase

Location	**Glasgow**	**Gateshead**	**Washington**	**Hull**	**Leicester**	**Newbury**	**Exeter**
Electricity							
Data points left (No)	45	37	49	49	49	47	49
Data points deleted (% No)	13.5	28.9	5.77	5.77	5.77	9.62	5.77
Data points deleted (% consumption)	14.3	29.9	5.23	5.72	5.24	9.58	5.49
Gas							
Data points left (No)	49	50	N/A	50	49	46	49
Data points deleted (% No)	5.77	3.85		3.85	5.77	11.5	5.77
Data points deleted (% consumption)	7.28	6.35		3.25	6.09	11.5	7.73

The overall result of the data preparation phase was a reduction in data points by between 3.85% and 28.9%. As Table 5.4 shows, the largest decrease was for the electricity data for the Gateshead store. Only the supermarkets in Gateshead and Glasgow had more than 10% of their electricity data deleted and only the Newbury store had more than 10% of its gas data points removed. The percentage of the total consumption of the deleted data points,

which may more accurately reflect the impact of these deletions, shows only a slight deviation from the percentage of the number of removed data with the result that, for ten of the thirteen data sets, more than 90% of the original data was available for analysis. Even in the extreme case, more than 70% could still be included in the analysis, therefore it could be concluded that, for all supermarkets, useful data sets existed (the only exception was the missing gas for the Washington store).

5.6 Estimation of energy use

Next, the scatter plots of the data sets, prepared as described in the section above, were used to develop regression models. To this end, Excel was used to first assess the adequacy of simple regression models. As mentioned above, if a second order model improved r^2 by more than 10%, a change point regression model was considered. If the r^2 for the change point model was greater than for the quadratic polynomial model, then the change point model was used. The coefficients for the change point regression models were calculated with the Matlab function 'lsqcurvefit', which solves non-linear data fitting problems with the least square approach (the least square approach was explained in Section 4.2.1). The model was checked against the underlying assumption and its error was estimated as described in the next section.

Table 5.5: Grid cell number of UKCP09 grid

Location	**Glasgow**	**Gateshead**	**Washington**	**Hull**	**Leicester**	**Newbury**	**Exeter**
Grid cell No	764	1004	1004	1240	1393	1625	1657

The estimation of the future energy consumption was based on the UKCP09 predictions by the MET Office (Met Office, n.d.). Cumulative probability distributions for the monthly mean air temperature for the 2030s (which is an abbreviation for the period from 2020 to 2049) were downloaded from the UKCP09 website for the appropriate 25x25 km grid cells (see Table 5.5 for the grid cell numbers). A sample graph for the gird cell containing the supermarket in Glasgow is shown in Figure 3.7. A preliminary study showed that, for this time interval the temperature data does not vary greatly for different emission scenarios. Therefore only the emission scenario 'medium' was used for further analysis. From the downloaded cumulative probability density function, monthly temperature values for 10%, 50% (i.e. central estimate) and 90% probabilities were extracted. The probability values show the likelihood that a temperature stays below a certain temperature.

In order to generate the weekly figures from the monthly data provided by the UKCP09 website, the Matlab function 'spline' was considered and actually used for the pilot study. However, Baltazar and Claridge (2006), who studied how to best fill missing hourly data, recommended simple linear interpolation for small data sets. Therefore this technique was used to generate weekly predictions based on these monthly values and for values for the base period (1961-1990). Next, the energy consumption models for each supermarket were used to calculate the base period energy use and predicted energy consumption. Finally, the increase over the base period consumption was calculated. The Matlab programme for this is included in the Appendix D – Matlab programmes.

5.7 Verification of regression models and their results

When constructing and using the regression models, three different sets of verification checks were employed. The first set of tests was concerned with checking the regression models against the underlying assumptions mentioned in Section 4.2.3.1. In particular, the assumption of normal distribution of the residuals was verified, as this influences the validly of the F-test.

The second verification step was concerned with calculating a prediction interval for the estimated values. The method used was explained in Section 4.2.1.1. In order to compute the propagated error, Equation 5.1 was used (Popula, 1991, p 479). This then was compared against the predicted change to see if detection seemed to be reasonable.

$$err_{tot} = \sqrt{\sum_i err_i^2}$$

Equation 5.1

Where:

err_{tot}: Total propagated error

err_i: Individual error

For the last set of tests the mean bias error (MBE), $RMSE$ and the $CV(RMSE)$ were calculated based on data from w/c 30 June 14 to w/c 8 Sept 14. These statistics have been used for data-driven energy models and in deterministic models to indicate how well the model performs (Lam *et al*, 2002; Coakley *et al*, 2014). The MBE is a measure of the overall bias of the model and is calculated as shown in Equation 5.2.

$$MBE = \frac{\sum_n (\hat{y}_i - y_i)}{n}$$

Equation 5.2

The $RMSE$, which is computed according to Equation 5.3, shows by how much the estimated values deviate from the measured values. When it is normalised by dividing it by the annual average consumption, the coefficient of variation of $RMSE$, abbreviated as $CV(RMSE)$, is obtained. The annual average consumption was preferred to the average of the period from w/c 30 June 14 to w/c 8 Sept 14, because this approach avoided seasonal bias. Coakley *et al* (2014) list a small number of acceptance criteria for the MBE (e.g. 5% for monthly data) and the $CV(RMSE)$ (e.g. 15% for monthly data) when used in calibrating building simulation models.

$$RMSE = \sqrt{\frac{\sum_n (\hat{y}_i - y_i)^2}{n}}$$

Equation 5.3

5.8 Summary of selection and analysis of supermarkets

This chapter described the research steps mentioned in Figure 5.1 and how they were executed in order to estimate the change in energy use. This investigation started with indentifying a small number of supermarkets from total of 766 which had common features relevant for energy use. After visiting these supermarkets to verify installed energy consumers and record two local operation procedures, consumption and temperature data were collected and prepared for analysis by removing outliers. In addition, this chapter covered how regression models were developed and how these models were verified.

6 Results of whole supermarket analysis

The results from the research described above are presented in this chapter which is divided into three sections. The first shows the outcome of the process which allowed the development of the regression models for the supermarkets. Although this section concentrates on the store in Glasgow, as all the relevant features of the model generation process can be exemplified by this supermarket, it also includes the results of the other supermarkets. After that the estimated changes in gas and electricity use are given along with error estimates. The final part in this chapter is concerned with an error analysis based on real consumption data.

6.1 Energy consumption models

Figure 6.1 and Figure 6.2, which show the scatter plots for the supermarket in Glasgow, divide the data clouds into included and removed data points. The excluded data in Figure 6.1 are outliers in the true sense of the word. For instance, the excluded data points for the Christmas and New Year period include two points which have a lower than expected consumption (because of shorter opening hours) and one with a higher than average consumption (due to overnight stocking). Another example is that, after new refrigerated display cases were installed, the electricity use increased appreciably as shown by the outliers marked as 'New display outliers'.

When examining the included data one notices a non-linear relationship which is well captured by the change point regression model resulting in a high coefficient of determination (for r^2 see Table 6.1). This change point regression model, based only on the data points marked 'included', is represented by the turquoise line in Figure 6.1. The reason for this change point is likely due to the control algorithm of temperature sensitive electric equipment (If it were owing to the building fabric, a linear relationship would be expected.). This equipment may be the air conditioning units, but it is more likely that it is the refrigeration system, because the air conditioning units are standard products which should behave in an identical manner and the analysis showed that three supermarkets can be adequately represented by linear models. Further investigation should confirm if this chance point is related to the point when the minimum head pressure of the refrigeration system is insufficient.

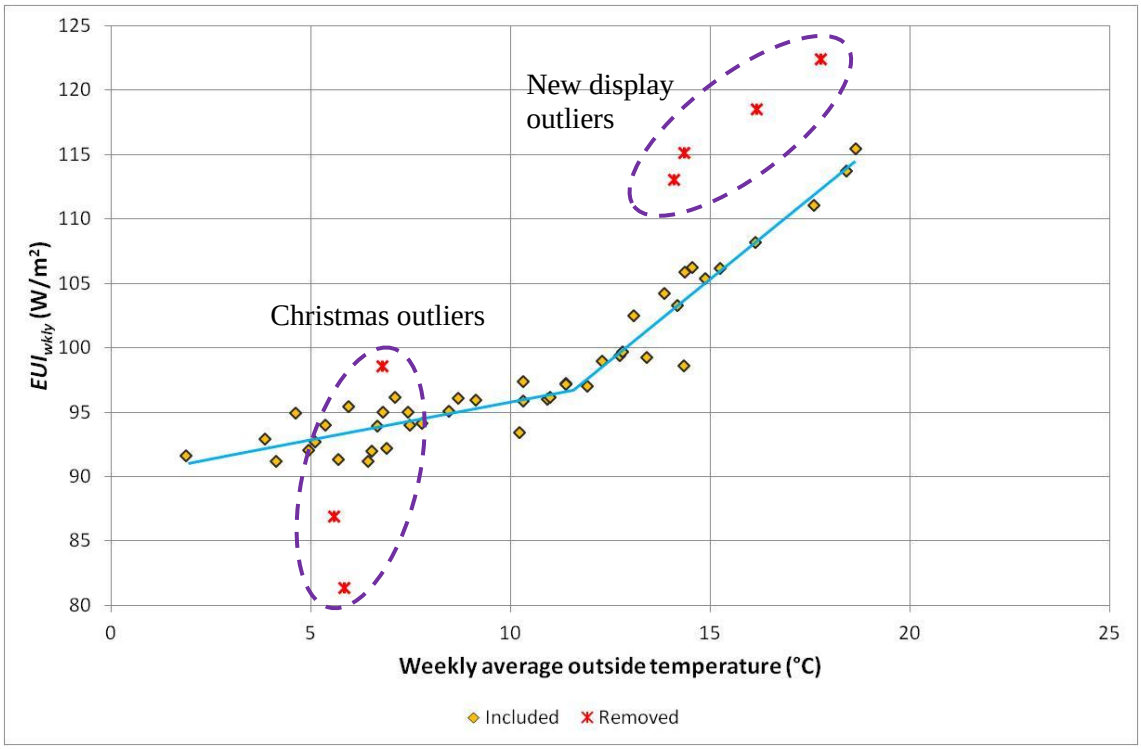

Figure 6.1: Scatter plots of electricity consumption vs outside temperature for the supermarket in Glasgow along with the model of this supermarket (turquoise line)

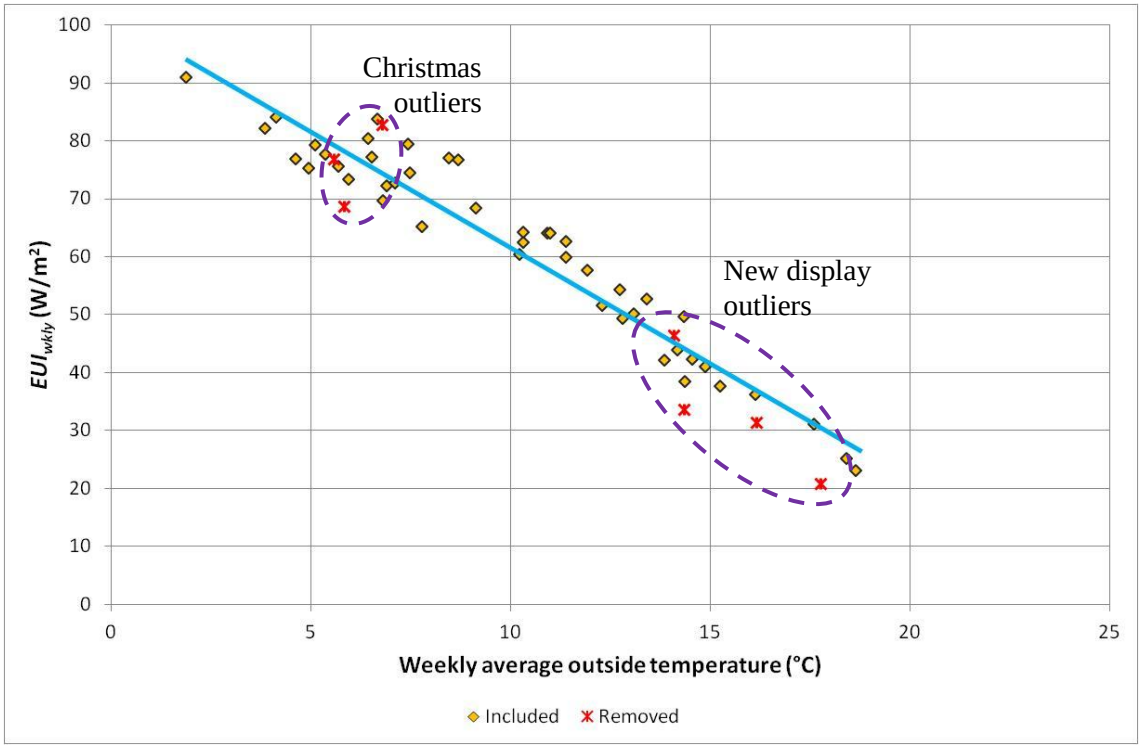

Figure 6.2: Scatter plots of gas consumption vs outside temperature for the supermarket in Glasgow along with the model of this supermarket (turquoise line)

The scatter plot displayed in Figure 6.2 shows that the excluded gas data are much closer to the expected value, indicated by the regression line, than the electricity outliers. The included data points in this scatter plot exhibit a relatively linear relationship, therefore a

simple linear regression model, shown as a straight turquoise line in Figure 6.2, portrays this behaviour well (for r^2 see Table 6.2). Interestingly, after the additional open refrigerated display cases were installed, the gas use was generally lower than the expected value. This seems counterintuitive as it is to be expected that more heat is removed from the sales area because of the additional shelves and therefore one would assume a higher heating demand and, in turn, an increase in gas use.

The results relating to the development of the regression models listed in Table 6.1 and Table 6.2 are given in a north-south axis. The headings 'r^2 (Linear)' and 'r^2 (Square)' in these tables refer to the coefficients of determination for a linear regression model and for a quadratic polynomial regression model respectively. The rows entitled 'Improvement: Square (%)' in Table 6.1 and 'Improvement (%)' in Table 6.2 on page 91 were included to make clearer the decision process regarding which models were used. These improvements are correlated with the store volume given in Table 5.2 with a correlation factor of 0.891 for electricity and −0.767 for gas. If a change-point model, rather than a simple regression model, was used, b_0 is the intercept and b_1 the gradient before the change-point temperature ϑ_{cp}, and b_0' and b_1' are the intercept and gradient, respectively, after this temperature. All F tests for the selected models show that statistically significant regression models were selected. The residual analysis showed that all error terms were normally distributed to a reasonable degree.

Table 6.1: Models of electricity consumption in the selected supermarkets

Location	**Glasgow**	**Gateshead**	**Washington**	**Hull**	**Leicester**	**Newbury**	**Exeter**
r^2 (Linear)	0.826	0.859	0.945	0.676	0.563	0.674	0.642
r^2 (Square)	0.934	0.956	0.954	0.878	0.607	0.705	0.743
Improvement: Square (%)	13.1	11.2	1.03	29.8	7.77	4.73	15.7
r^2 (Change point)	0.950	0.973		0.896			0.766
Improvement: Change point (%)	15.0	13.3		32.5			19.3
b_0 (W/m^2)	90.0	73.9	82.3	78.0	71.4	78.9	88.0
b_1 (W/m^2/°C)	0.578	0.582	1.55	0.0875	0.739	0.840	0.452
ϑ_{cp} (°C)	11.6	16.0		15.0			14.5
b_0' (W/m^2)	67.5	39.2		39.2			58.6
b_1' (W/m^2/°C)	2.52	2.75		2.68			2.48
F-test	714	1250	803	407	60.75	92.9	154

Table 6.1, which displays results for the electricity consumption models, shows that, for four supermarkets, a change point regression model improved the predictive power by between 13.3% and 32.5% over that of a simple regression model. Although the slope change ratio for these models varies between 4.36 (Glasgow) and 30.6 (Hull) the slope after the change point temperature is approximately the same. The change point temperature fluctuates between the low and mid teens. For the other three supermarkets, the slopes can be considered consistent with each other as they vary only by a factor of approximately 2.

Figure 6.3 displays results for the electricity consumption models and thus visually represents the model parameters listed in Table 6.1. In this figure the change point models are blue whereas the linear models are red. These graphs indicate that, in addition to temperature, other parameters need to be considered in order to produce valid EUI_{wkly} predictions. One of these factors may be location as suggested by comparing the graphs for the Hull and Gateshead stores (both of which are located close to the east coast of England and the graphs are relatively close together) with those for the models for the supermarkets in Glasgow and Exeter (these supermarkets are situated towards the west of Britain and their regression models also show some proximity).

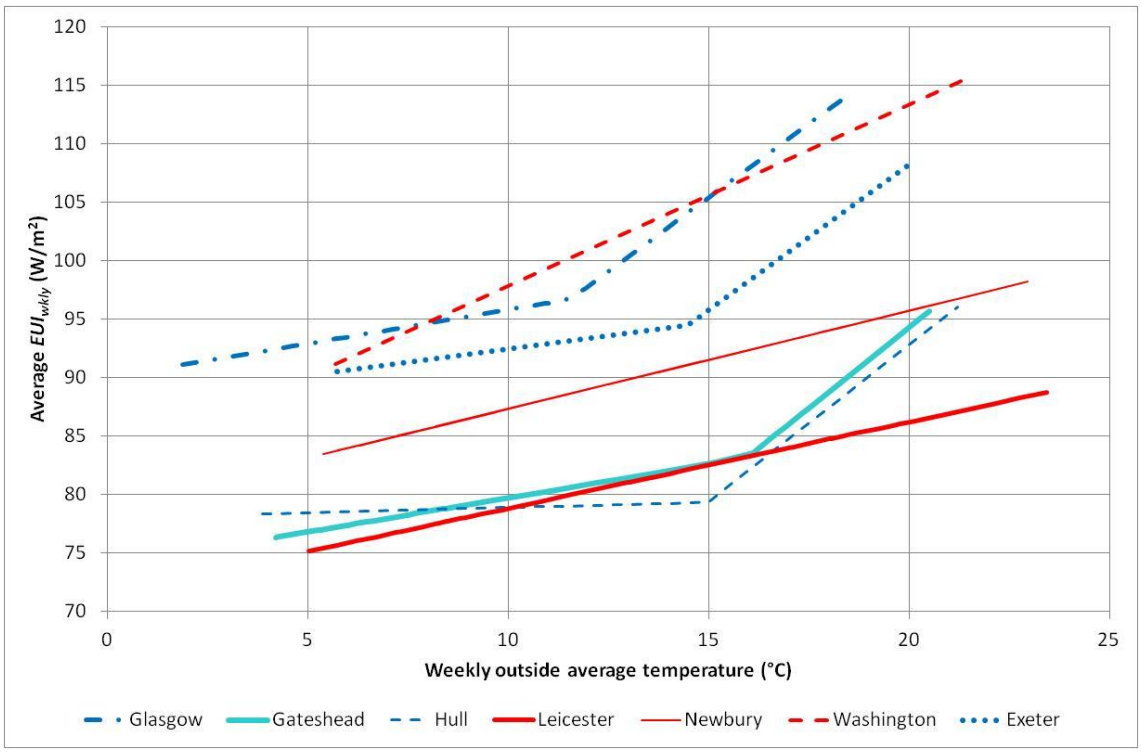

Figure 6.3: Summary graph of all models for electricity consumption

Table 6.2: Models of gas consumption in supermarkets

Location	**Glasgow**	**Gateshead**	**Washington**	**Hull**	**Leicester**	**Newbury**	**Exeter**
r^2 (Linear)	0.934	0.833	N/A	0.843	0.930	0.846	0.886
r^2 (Square)	0.951	0.893		0.846	0.939	0.912	0.888
Improvement (%)	1.94	6.67		0.391	0.975	7.19	0.154
b_0 (W/m^2)	102	70.1		111	75.7	69.4	77.7
b_1 (W/m^2/°C)	-3.94	-2.27		-4.16	-2.83	-2.56	-3.54
F-test	651	239		263	653	242	366

Table 6.2 summarises the gas consumption model results and shows that the spread of r^2 (Linear) is much smaller for gas than for electricity, and has an average of 0.879. Therefore only linear models were used. The two supermarkets for which the second order regression would have offered the greatest improvement were those without a lobby. Both the slopes and the intercepts of these models have a strong correlation (r for a linear model is at least 0.959) with the building volume, consistent with basic thermodynamic principles. It can also be observed that both coefficients vary by a factor of less than 2 indicating a good degree of consistency amongst models.

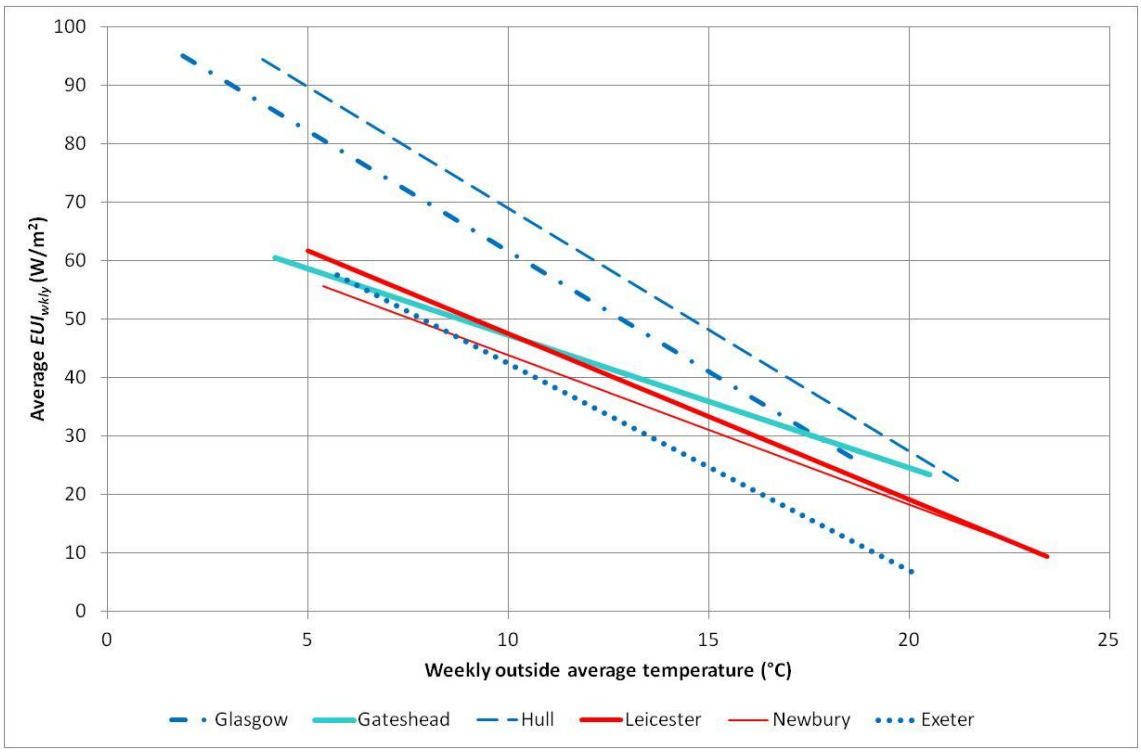

Figure 6.4: Summary graph with all models for gas consumption

Figure 6.4, which relates to Table 6.2, shows two groups of models. The graphs for the supermarket without a mezzanine floor at Glasgow, Hull and Exeter (shown as non-solid lines) are virtually parallel lines, whereas the other three (shown as solid lines) are not. As

already mentioned, the intercepts of all of these models have a strong correlation (r = 0.959) to the building volume. The slope is also closely correlated to the building volume (r = 0.968), but the relationship with the volume-to-total-area ratio is even stronger (r = 0.977). Based on this the following equations can be suggested to compute the coefficients in the model for gas consumption, $\widehat{EUI}_{wkly} = b_0 + b_1\vartheta_{outside}$.

$$b_0 = 14.2\frac{\mathrm{W}}{\mathrm{m}^2} + 0.00694\frac{\mathrm{W}}{\mathrm{m}^5}\,Volume$$

Equation 6.1

$$b_1 = 0.0100\frac{\mathrm{W}}{\mathrm{m}^2\,°\mathrm{C}} - 0.526\frac{\mathrm{W}}{\mathrm{m}^3\,°\mathrm{C}}\frac{Volume}{Total\ area}$$

Equation 6.2

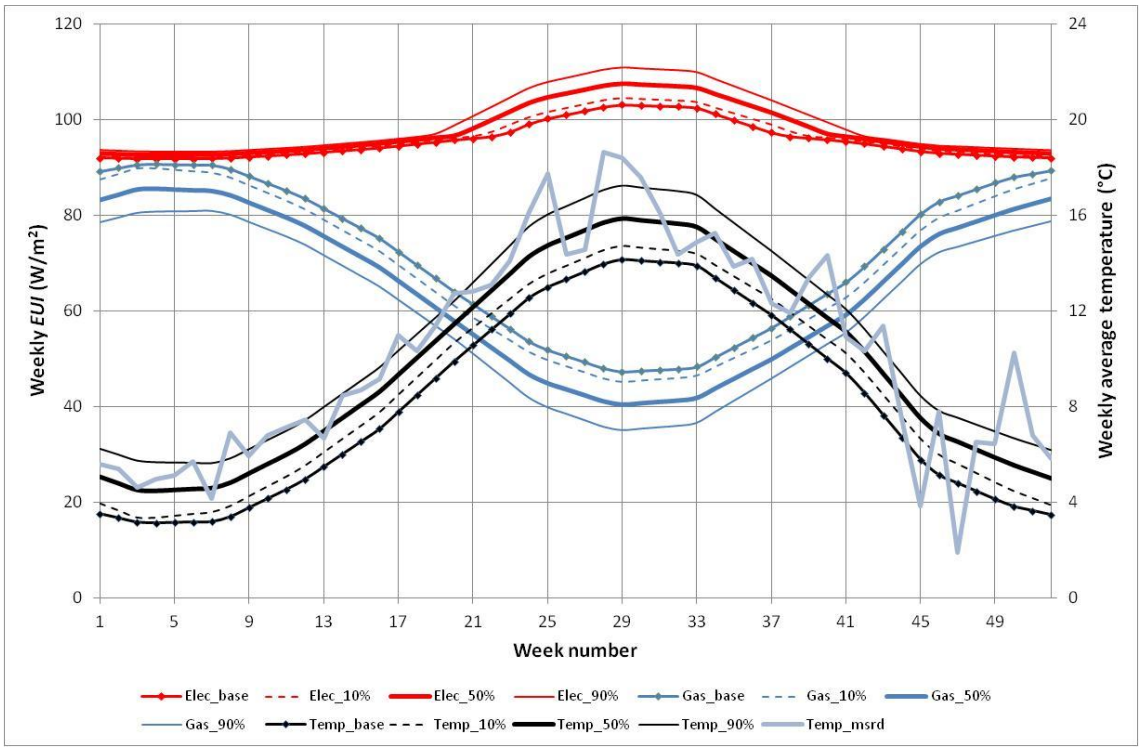

Figure 6.5: Weekly temperature and predicted energy use for the supermarket in Glasgow

The model parameters given in Table 6.1 and Table 6.2 were used to estimate the gas and electricity use for the base period and the 2030s. Figure 6.5, which displays the weekly results for the supermarket in Glasgow, also includes temperature graphs. The gas data is, in effect, a scaled mirror image of the temperature data. The electricity data, on the other hand, has an interval from approximately week 20 to about week 40 when the electricity plots first fan out before converging again. This is due to the non-linear change point model. The black lines are for the data from UKCP09 and the grey trace for the measured temperature data. In addition to the seasonal variation, also seen in the UKCP09

temperature data, the measured data includes a stochastic element. Because of the non-linear behaviour of the electricity use in supermarkets, this may be of significance, but this was not pursued further, as this element, by definition, is random and was considered too difficult to model reliably. The measured temperature shows that the UKCP09 weather data are within the model data range so no extrapolation had to be used. This is only the case for this supermarket and for the one in Hull. For the other five supermarkets the lower temperature is not covered by the measured temperature.

Table 6.3: Changes in energy use (including errors) and temperature as percentage of the respective base years

Location	**Glasgow**	**Gateshead**	**Washington**	**Hull**	**Leicester**	**Newbury**	**Exeter**
Electricity-gas ratio (Base period) (%)	1.35:1	1.53:1	N/A	1.1:1	1.54:1	1.91:1	2.15:1
Electricity							
Change 10% (%)	0.722	0.559	1.23	0.554	0.598	0.638	0.628
Error 10% (%)	0.431	0.327	0.519	0.614	1.26	0.965	0.649
Change 50% (%)	2.11	1.40	2.92	1.68	1.61	1.72	2.00
Error 50% (%)	0.421	0.320	0.507	0.601	1.24	0.950	0.641
Change 90% (%)	3.78	2.84	4.73	3.32	2.76	2.94	3.71
Error 90% (%)	0.411	0.314	0.498	0.593	1.22	0.939	0.636
Gas							
Change 10% (%)	-3.37	-3.34	N/A	-4.45	-3.54	-3.71	-5.41
Error 10% (%)	1.91	2.73		3.32	2.35	3.33	3.01
Change 50% (%)	-8.90	-7.92		-10.6	-9.55	-9.98	-14.2
Error 50% (%)	1.86	2.66		3.25	2.30	3.27	2.98
Change 90% (%)	-15.0	-12.82		-17.7	-16.3	-17.1	-24.1
Error 90% (%)	1.82	2.62		3.21	2.27	3.23	2.95
Av temperature							
Base (°C)	8.15	8.24	8.24	9.22	8.88	9.36	9.86
Current (°C)	10.3	11.1	12.2	12.5	13.1	12.4	11.8
Change current (%)	26.4	34.7	48.3	36.0	48.0	32.2	20.6
Change 10% (%)	7.44	9.16	9.16	8.40	7.11	7.04	6.72
Change 50% (%)	19.7	21.7	21.7	20.1	19.2	18.9	17.7
Change 90% (%)	33.2	35.1	35.1	33.3	32.8	32.4	30.0

6.2 Changes in energy consumption in the 2030s

This section gives the future energy estimates in two formats (in Table 6.3 as well as in Figure 6.6 and Figure 6.7) so that different types of comparison can be made more easily. The results are stated as changes relative to the base period of the relevant parameter for each respective location. The error bars, shown as whiskers on the bar graphs in Figure 6.6 and in Figure 6.7, indicated the propagation error. The chart type bar graph was chosen to emphasise that the estimates include values up to the maximum value, but are not necessarily equal to this maximum. For instance, the estimate for Glasgow labelled '90%' in Figure 6.6 is 3.78%. This means that the likelihood that the increase does not exceed

3.78% is 90%. It is possible that the increase will be less than that. The error bars in these bar charts take only uncertainties introduced through the modelling process into account (see Section 5.7). They show that, for the central estimates and the 90% estimates, changes in energy consumption should be detectable. For the 10% likelihood cases the detection is more doubtful.

The predictions presented here suggested that the percentage change in electricity consumption are smaller than for gas consumption and, when taking the electricity-gas ratio in Table 6.3 into consideration, it can be concluded that this is also true for the absolute amount. This is also consistent with the lower $CoVs$ of electricity as shown in Table 5.3. The underlying reason for both of these results is that heating, and therefore gas use, is more temperature sensitive, whereas electricity is also used for temperature independent consumers, such as lighting.

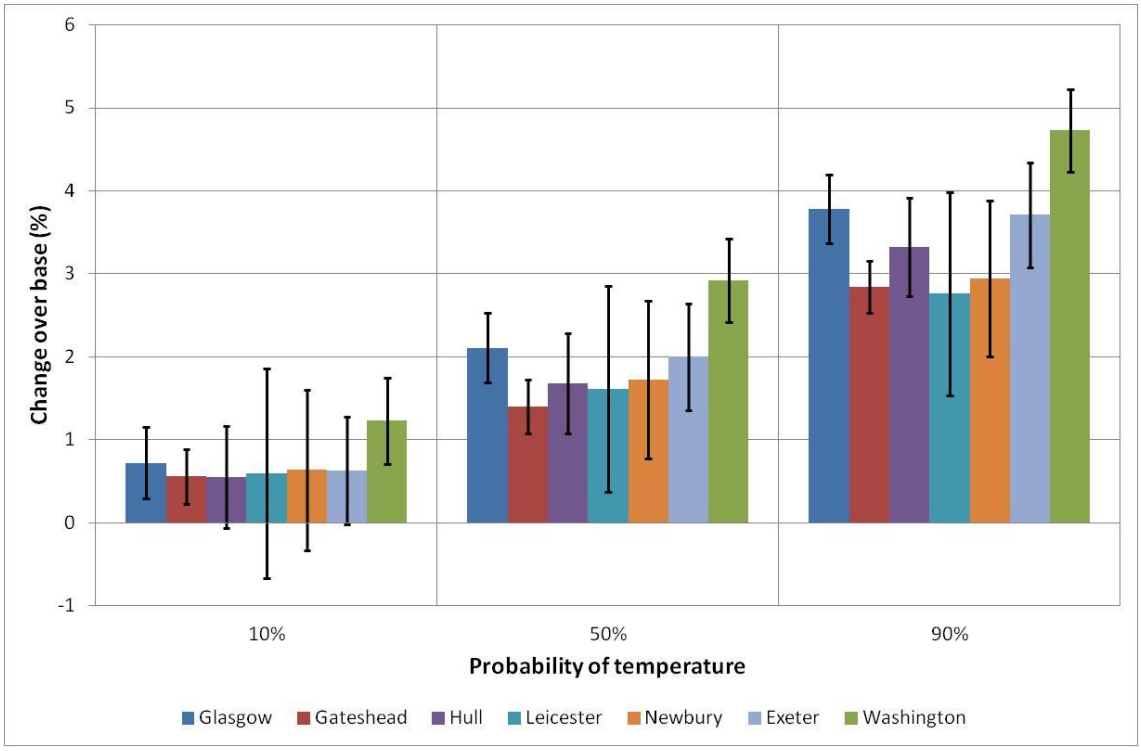

Figure 6.6: Changes in electricity consumption in the 2030s relative to the relevant base period

The reduction in gas consumption depicted in Table 6.4 is relatively consistent over the three probability values. Although the spread increases, the ranking of the supermarkets stays the same. The figures show that the reduction tends to be the largest in the supermarkets without mezzanine floors, which is consistent with the steeper slopes seen in

Figure 6.4. The change ranges from a minimum of -3.34% (10% probability) to a maximum of -24.1% (90% probability).

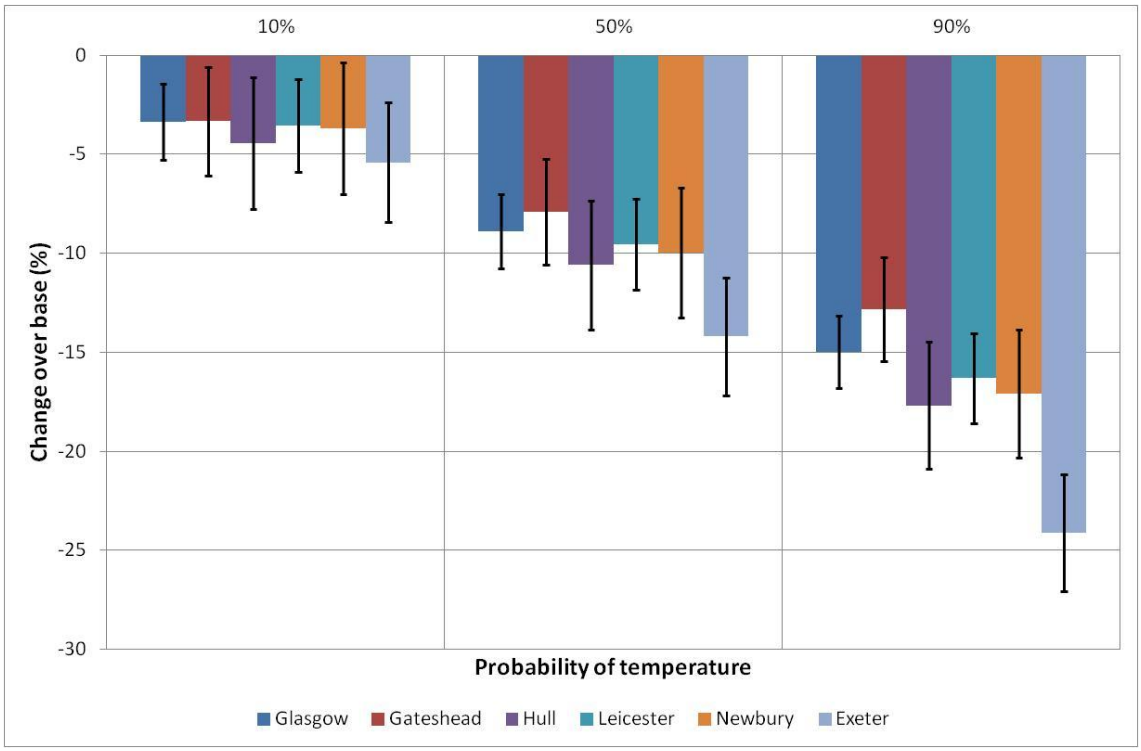

Figure 6.7: Changes in gas consumption in the 2030s relative to the relevant base period

When comparing the electricity consumption of the store in Hull with the one in Leicester in Figure 6.6, one notices the effect of the change point model for Hull. For the 10% temperature change, the value for Hull is just below the figure for Leicester. However, when considering the 50% case, the roles are reversed, and this is even more apparent for the 90% probability. That this is not due to a steeper temperature increase can be seen when examining the temperature increase in Table 6.3. Although the increase for Hull is always greater than that for Leicester, the gap narrows with increasing probability of temperature maximum. Because of modelling the electricity use of only a small number of supermarkets with non-linear regression models, location dependency is difficult to attribute. Looking at the span of predictions, one finds that the largest increase in electricity of 4.73% for a 90% likelihood is for the smallest supermarket (in Washington), whereas the largest supermarket (in Hull) has a maximum increase of 3.32%. The largest store has also the lowest overall electricity increase estimate of 0.554%.

When comparing the temperature increases for the 2030s with the average of the measured temperature, both listed in Table 6.3, one finds that the measured average is at least as high

as the 50% probability temperature values. If the predictions for the 2030s are correct, then the period for which the supermarkets were examined may be a good indication of future average energy consumption.

6.3 Error estimate based on measured consumption data

In addition to the error estimates based on error propagation as described in the previous chapter, the $MBEs$ and $RMSEs$ were also calculated. The estimates of the propagation error shown in Figure 6.6 and Figure 6.7 indicated that, expect for the 10% case of electricity change for the stores in Hull, Leicester, Newbury and Exeter, a change in energy usage should be attributable to a change in climate, everything else being equal. The $MBEs$ and $RMSEs$ were based on the measured data from w/c 30 June 14 to w/c 8 Sept 14, and are shown in Table 6.4. The $MBEs$ for the electricity indicate that, for the chosen period, the models tend to underpredict electricity use. The $CVs(RMSE)$ is below 10%, except for Glasgow where the higher error is due to the installation of more refrigerated shelves. For the gas data the models tend to overpredict consumption. The $CVs(RMSE)$ for gas is above 10% for all locations, and for the three southern supermarkets it is greater than 25%, due to the low annual consumption.

Table 6.4: Models of gas consumption in the selected supermarkets

Location	**Glasgow**	**Gateshead**	**Washington**	**Hull**	**Leicester**	**Newbury**	**Exeter**
Electricity							
MBE (W/m^2)	-11.8	-5.11	2.45	-1.90	-6.35	0.56	-6.01
$RMSE$ (W/m^2)	12.0	5.29	6.60	2.43	7.38	2.04	6.82
$CV(RMSE)$ (%)	12.2	6.50	6.49	2.96	9.07	2.27	7.19
Gas							
MBE (W/m^2)	9.02	5.53		6.15	9.13	9.16	8.80
$RMSE$ (W/m^2)	9.28	6.91		6.81	11.17	10.72	9.27
$CV(RMSE)$ (%)	15.0	15.6		11.72	28.65	29.2	26.3

The results of the MBE and $CV(RMSE)$ estimates displayed here are larger than the values of the propagation errors, but, except for the electricity consumption in the Glasgow store and the gas consumption in the three southern supermarkets, they are within or close to the targets mentioned in Section 5.7. The reason (additional refrigerated shelves) for the changes in the Glasgow supermarket is credible. However, why the three stores in the south have such large $CVs(RMSE)$ is not clear. One reason could be that the annual gas consumption for these three supermarkets is significantly lower than for the more northern stores. Another reason may be that the data used for the error estimate were collected for

the summer months, i.e. out of the main heating season, and expanding the data to include winter months should yield more accurate results.

6.4 Summary of whole supermarket analysis

In this chapter the results of the data analysis, described in the previous chapter, are shown and the gas and electricity consumption models were used to predict the change in energy usage for seven UK supermarkets. Throughout this chapter the data from the supermarket in Glasgow are used to illustrate the important steps in developing regression models for the electricity and gas use in the selected supermarkets. These models are simple linear regression models for the gas use data and for three out of the seven electricity data sets. The maximum change in electricity use is approximately 4.7% for the 60 year interval investigated and approximately 24% for gas demand. The propagation error showed that for the 10% probability case detection of changes in energy demand is doubtful, but is more likely for the high probability values. The error estimate based on measured data indicates that the estimates for the electricity demands are more reliable than the gas predictions.

7 Discussion on whole supermarket analysis

The results presented in the previous chapter are discussed here in the following order: First it is shown how the results have addressed the question regarding the impact of climate change and location on energy use in supermarkets. This is followed by a discussion of sources of errors and uncertainties. The third section of this chapter critically evaluates the methodology used here against other possible approaches. After that, the results are compared with work from other researchers. A discussion on practical implications completes this chapter.

7.1 Comparison with research aims

The analysis of the selected seven similar supermarkets proposed answers to the questions regarding how (a) climate change and (b) location influence energy consumption in supermarkets. The UKCP09 central estimate for the 2030s predicts an increase in annual average temperature of approximately 20% over the base period with little spread among the supermarkets (CoV = 7.38%). This translates into a predicted maximum rise in the average electricity use of 2.9% for all seven supermarkets (CoV = 26.1%), and a maximum drop in average gas consumption of 14% (CoV = 21.3%) for these temperatures. Although the seven supermarkets consume between 10% and 115% more electricity than gas, the predictions suggest that there will be a reduction in overall energy demand. The electricity estimate for the temperatures at 10% and 90% probabilities give an average deviation from the central estimate of −1.2 percentage points (for the 10% temperature values) and +1.5 percentage points (for the 90% temperature values). For the same temperatures the gas consumption deviated from the central estimate by +6.2 percentage points (for the 10% temperature values) and −7.0 percentage points (for the 90% temperature values) on average.

The research also looked at how location may influence energy consumption. One aspect is the differences in climate and weather. Here the temperatures have a span of 1.71°C (CoV = 7.51%) for the base period climate and 2.80°C (CoV = 7.92%) for the measured temperatures. Although the minimum for both temperature ranges occurs in Glasgow, the maximum for the base year climate is in Exeter and for the measured temperature in Leicester. Neither set of temperature values follows a straight north south trend. This may be partly due to difference in local topologies and partly due to how the data had been

acquired and prepared. For instance, the current temperature has generally been measured at the supermarket. However the UCKP09 data are given as one value for each 25 x 25 km square based on measurements from the MET weather stations network. Therefore it can be said that temperature is not a strict function of location and, by extension, energy use by temperature sensitive equipment is only loosely related to latitude and longitude.

Another aspect of local influence may be the way a specific supermarket is operated. When visiting the stores it was noticed that most large energy consumers, such as lighting or gas boilers, were centrally controlled, hence differences were minor. The two operational practices investigated were the main baking time and the times the night covers were removed and replaced. The main baking time estimated by the baking staff is approximately four hours for five of the seven supermarkets. Therefore establishing a relationship between a supermarket's EUI and the baking times was not possible. The reported practice regarding refrigeration night covers varies from supermarket to supermarket (see Table 5.1), but a linear regression model indicated that a store's EUI does not seem to be related to its night cover placement practice. An operation practice not thoroughly investigated was the routine closing of the cold room doors. As only the supermarket in Hull has more than one door, it could have been suspected that it performed the worst of all the supermarkets. However, the model graphs in Figure 6.3 as well as Table 5.3 showed that this idea cannot be substantiated by the current research. At best it could be argued that keeping both doors shut may reduce the energy consumption, although not significantly. Taking the findings summarized in this paragraph into account it can be concluded that local variations in operational procedures have no appreciable effect on the gas and electricity consumption in the researched supermarkets.

Another indication that the differences in local operation procedures seem to have only a small overall effect is that the differences in gas use models were adequately explained with thermodynamic principles and building dimensions. Part of this reasoning is that air behaves similarly to a perfect gas. This means that, for a given temperature rise, the required amount of heat is proportional to the volume of the thermodynamic system, everything else being equal. However, for Gateshead and Newbury, this model seems to start to break down as the second order model improves the fit by over 5%. This behaviour may be due to the lack of a lobby resulting in the outside temperature having a more direct

influence. This may need further investigation to see if this is also the case for electricity consumption.

7.2 Other approaches

The coefficients of determination for the electricity model range from 0.563 (simple regression model for Leicester) to 0.973 (change point regression model for Gateshead) and for the simple regression models for gas use from 0.843 (Hull) to 0.934 (Glasgow). These figures indicate that the models chosen have the potential to explain a high percentage of the data variation. A similarly high r^2 was also reported by Ruch and Claridge (1992) for their electricity change point regression model for the supermarket they investigated. The relatively low coefficient for some of the electricity models here may be because of equipment problems at those stores (e.g. the site temperature sensors for Newbury and Exeter were not accessible) and not because of the approach chosen.

Methodologies employed by Ruch *et al* (1993) to investigate electricity used in a supermarket were MLR and PCA. The researchers found that the values for r^2 were comparable with each other and were given for the PCA, which included temperature, humidity and solar radiation, as 0.562 for the range before the change point temperature, and 0.740 for the temperature range afterwards. However, when they are compared with the coefficients of determination for the electricity models here, one finds that the PCA coefficients do not improve the predictive power.

First principle models were developed by Arias and Lundqvist (2005) and Suzuki *et al* (2011). Although their models showed a good general agreement with measured data, there were discrepancies between estimated and actual consumption. Both papers gave only graphical indications of the model error and not MBE or $RMSE$ values. Therefore comparing them with the models used in the investigation above is difficult. However, it can be said that the time invested to investigate only the response to temperature change would have been too high.

Another alternative approach is using building simulation software outright. As pointed out earlier, constructing models in those software packages is not a trivial task and even after these have been carefully constructed, they may not be accurate and therefore they need to be calibrated (Coakley *et al*, 2014; Deru *et al*, 2013). Research which uses this approach frequently takes advantage of the software's ability to investigate mitigation and adaptation

options (Jenkins *et al*, 2008a; Wan *et al*, 2011b; Wan *et al*, 2011a; Deru *et al*, 2013). As no such further investigation was part of this study, such an approach would have been time inefficient. Taking the discussion above into consideration, it may be concluded that the methodology selected yielded results of a level of credibility comparable to other options in a time efficient manner.

7.3 Errors and uncertainties

In this section the errors associated with measured data are discussed first, which is followed by considering uncertainties relating to predictions. The first two sources of error acknowledged, but not further pursued here, are associated with the measuring devices. These measuring devices include the on-site temperature sensors or the MET office stations (for Newbury and Exeter). To increase the intercomparison of the results, these sensors could be compared with each other, particularly those at the two supermarkets in Gateshead and Washington which are close together, so that differences in energy performance can be more thoroughly investigated. The second source relates to non-linear models, which may yield different results for different temperature distribution with the same mean value. This is to say that larger data spans (e.g. through the introduction of some randomness to temperature data) may produce higher electricity demand. However, how great such a data spread should be is a problem difficult to solve.

Another source of error arises from faulty equipment or the way the equipment is operated. During the site visits and data collection phase, it was discovered that building timers were incorrectly set, equipment had broken down or repairs were carried out incorrectly. Other researchers reported similar problems (Ruch and Claridge, 1992; Schrock and Claridge, 1989). The possibility of not all of these problems having been detected is indicated by the low coefficients of determinations for, e.g., Leicester.

The error estimates from the statistical models were summarized in two different ways. The first was by computing an error estimate based on error propagation, which showed a modest error. The second way was by calculating the $MBEs$ and $RMSEs$ for a period outside the analysed period. These error values were considerably greater than the propagation error estimates, especially for the gas consumption. However, other researchers found their $CVs(RMSE)$ to be of similar magnitude (Lam *et al*, 2010a; Lam *et*

al, 2010c), therefore, although the results should be treated with appropriate caution, they should be still considered useful and comparable with other research outputs.

Sources of uncertainty may relate also to changes to supermarkets and future shopping behaviour. One example is the additional refrigerated shelving units installed in Glasgow, which had a significant impact on electricity consumption. Improved supermarket refrigeration systems summarized by Tassou *et al* (Tassou *et al*, 2011) are an example of technological changes which may well alter the energy use in supermarkets. Other alterations may relate to the advances in technology for which Jenkins (2009) investigated the impact on an office building. He found a significant difference in energy use between the scenario with the present day equipment and one with more efficient equipment. These potential developments and changes in shopping behaviour should be taken into account to obtain a more complete picture of future energy demand in supermarkets.

Chapter 3 introduced major uncertainties in climate change predictions ranging from insufficient understanding of the natural climate system to limited computer power. Although some of the known uncertainties have been made explicit in the UKCP09 predictions, many are difficult to account for and, therefore, any prediction based on these will suffer from the same shortcomings.

The discussion above acknowledged a few sources of uncertainties and tried to put them into the context of research into climate change impact assessments. It is apparent that the results presented in the previous chapter have a potentially large error margin and should be regarded as indicative only. They can only be validated when measurements are available. However, it should also be pointed out that the discussion in this section mentions published research literature which reported errors of comparable magnitudes.

7.4 Comparison with other research

Early research into climate change impact on buildings suggested that, depending on location, an increase in cooling load and corresponding decrease in heating demand can be expected (Loveland and Brown, 1989). This assessment has been substantiated and quantified in other research (Li *et al*, 2012). The work reported here agrees with this assessment by suggesting an increase in electricity use of between 1.4% and 2.9% for the central estimates. As electricity is not used for heating, but rather for comfort cooling and refrigeration, it is likely that this increase is due to a higher cooling load. The heating

demand, on the other hand, is predicted to drop by between 7.9% and 14.2% for the central estimates. When comparing the absolute total amount, one finds that there is actually a decrease in energy demand and not a 'fuel swap' suggested by Crawley (2003) and more in line with work by Pilli-Sihvola *et al* (2010) who predict a larger drop in heating demand than a rise in cooling demand for Central and North Europe.

The geographical spread of the predicted change in energy usage is larger for electricity than for gas. This is similar to work done on different types of dwellings in four locations in Great Britain (Collins *et al*, 2010). This research suggests a drop in gas consumption for three of the four locations of 26%, and of 32% for the other. The estimates presented in the previous chapter predicted a decrease for five of the six stores included in the gas consumption analysis of between 7.9% and 10.6%, with the remaining one dropping by 14.2%. However, the percentage increase in electricity use reported by Collins *et al* (2010) due to a rise in cooling load, is higher both in magnitude and in spread. This is owing to low initial figures for the current demand. Although the change in electricity use in the supermarkets investigated here does not exhibit such a high increase, its associated CoV shows a sensitivity to differences in these small changes. The location dependant energy change in Great Britain reported for an office building by Jenkins *et al* (2008a) also agrees with the results for gas here both in magnitude (average: -10.7%) and spread (average: 9.6%). However, the increase in electricity use suggested in this paper (average magnitude: 31.6%, average spread: 14.6%) is much higher. This may be because supermarkets have a higher electricity EUI owing to the refrigeration system and higher lighting density.

Four out of the seven supermarkets could be modelled with nonlinear change point regression models. Scott *et al* (1994) found indications that this may be true for commercial buildings in general. The work done on change point regression for supermarkets (Schrock and Claridge, 1989; Ruch and Claridge, 1992) corroborate the change point regression models developed here. These previous studies investigated a superstore with a sales area at least 2.5 times the size of the supermarkets researched here. The change point temperatures (15.6°C in Ruch and Claridge (1992) and (16.7°C in Schrock and Claridge (1989)) are also comparable for three out of the four change point models here. Only the one for Glasgow indicates that the quasi temperature independent temperature range finishes relatively early at 11.6°C. The slope ratio in Ruch and Claridge (1992) is 4.4 and the slope after ϑ_{cp} is 19.4 kWh/m^2/°C there. Except for the slope ratio for

Hull, both parameters are comparable with the results here. For instance, the slope after the change point for Gateshead is 16.4 kWh/m^2/°C (please note that Table 6.1 uses different units). Based on the research here it may be suggested that there is an upper limit for a linear regression model after which change-point regression models should be considered.

7.5 Practical implications

One of the practical implications is that the heating consumption for supermarkets in retail units may be predictable with a relatively simple model using only building geometry. This may be helpful in verifying the correct operation of the heating systems and in detecting any abnormalities.

Another useful insight gained through this research is that the electricity consumption over the next decade or so should not drastically increase due to climate change. This statement should be regarded as tentative and read in conjunction with the section on errors and uncertainties. In addition, research indicated that dwellings may use considerably more electricity (e.g. Collins *et al* (2010)), therefore utility companies may have to cater for this demand in novel ways to make more effective use of the energy infrastructure.

The drop in gas consumption for heating suggested by this research may open up other avenues of gas use. One possibility is the use of combined heat and power (CHP) plants to combat the increase in electricity use. The change in consumption calculated here is from the base period from 1961 to 1990, so some reduction in gas use may have occurred already.

One implication of the randomness in supermarket operation (e.g. incorrectly set timers, fault repairs, equipment breakdowns) could be that, if a large enough sample is used, including this randomness gives a more authentic picture of energy use in supermarkets than detecting and excluding outliers.

7.6 Conclusions of whole supermarket analysis

The discussions in this chapter compared the results with the research aims and put it into context by comparing them with other relevant research literature. The chapter showed that for the central estimate the yearly electricity demand would rise by 2.9% and the gas use would drop by 14% over a 60 year interval ending in 2030s.

This chapter also indicated that location and temperature are somewhat related, but because of local microclimate there is no strong north-south correlation. Also the influence of local variation in operation could not be match with variation in energy use in the different supermarkets.

When comparing the investigation here with other research projects it was found that the method chosen of a level of credibility comparable to other options. The discussion on the geographic spread found in other research papers showed also that the variation found here was comparable to them. In addition, this chapter showed that the change point regression models used for some supermarkets are comparable to the ones published in research literature.

8 The R404A/CO_2 refrigeration system and climate change

As the literature review indicated in Section 2.3, the refrigeration system usually makes up a large proportion of the electricity consumption in a supermarket. Therefore it is useful to investigate such a system in isolation to more fully appreciate how supermarkets respond to climate change. This is the main aim of this chapter, which is organised in the following way. The first section concentrates on literature introducing the main strands of research into supermarket refrigeration. The next section discusses the basic principles of vapour compression systems. This is followed by an explanation of how the useful refrigeration effect $\dot{Q}_e$ was derived and how it was used to calculate the coefficient of system performance ($COSP$) for a complete refrigeration system in steady state. Based on this work, a software model was developed and implemented in Matlab. After its verification, this was used to achieve the main aim of this part of the research: estimating the response of a refrigeration system to climate change. The section thereafter employed the Matlab model to investigate the energy savings potential of a different approach to controlling the condenser fans. The final section in this chapter discussed the results and drew conclusions based on the work presented in this chapter.

8.1 Major topics of supermarket refrigeration system research

Research into supermarket refrigeration systems includes investigation of different topologies and HVAC integration strategies (Cecchinato *et al*, 2010b; Cecchinato *et al*, 2012). This field of research also covers secondary loop (SL) refrigeration systems in which the primary system is a vapour compression system and the SL system serves as a distribution system. This type of refrigeration system has also been installed in the supermarket discussed below. Wang *et al* (2010) reviewed such systems and found that one of the driving forces behind the move towards them was the Montreal Protocol, which enforced the phasing out of chlorinated hydrocarbon refrigerants. Replacement refrigerants may be flammable or toxic, so limiting them to a closely controlled primary system seems advisable. After discussing flammable refrigerants at some length the authors mentioned two R&D challenges. The first one is the degradation of the system's efficiency due to the introduction of a circulation system including pump(s) and the second is the higher initial costs.

Tassou *et al* (2010) published a review on emerging technology for food refrigeration including also a description of refrigeration systems for supermarkets which were considered modern at that time. Such systems used the refrigerant R404A, a multi-compressor pack with an air-cooled condenser and variable head pressure control. The authors found that capacity control for the compressor bank of such systems was achieved by cylinder unloading, on-off cycling of individual compressors and by using a variable speed drive for a trim compressor. This description fits the system analysed below very well, thus it can be concluded that it is representative of a significant percentage of currently installed systems. Therefore results from investigating this system should be not peculiar to this supermarket, but should be valuable for supermarkets in general.

8.1.1 Refrigerated display cabinets

The distinguishing feature of energy consumption in supermarkets compared with other commercial buildings is the influence of refrigerated display cabinets. That is why Hill *et al* (2014) argued to include the refrigeration system and the impact of these open refrigerated display cases in the NCM, a statutory energy assessment. These researchers found that the NCM severely underpredicted cooling and heating demands which were, in fact, twice as much as lighting for the supermarket used for their case study. However, according to the NCM, lighting seemed to be the largest item in an energy audit. Heating and cooling, on the other hand, were virtually nonexistent according to this methodology.

The effect of indoor relative humidity on the refrigerated display units was examined by Howell *et al* (1997). These researchers found for the supermarket in Florida they investigated that, if the indoor relative humidity was reduced from 55% to 50%, energy savings of 4.7% were possible for the whole store. Subsequently Bahman *et al* (2012) built on this work investigating energy saving potentials when assessing refrigeration and HVAC energy consumption together. The methodology developed for researching this supermarket in Florida was based on a moisture balance equation. These researchers discovered that the measured indoor annual average was 51.1% relative humidity, which was below the design value of 55% relative humidity. Their paper reported on the results of reducing the humidity as low as 40%. The authors found that the overall energy used was reduced despite a higher annual energy demand from the air condition system. Kosar *et al* (2005) investigated reduction of the indoor relative humidity to 35% in supermarkets in general and found that, even then, energy could be saved.

8.1.2 Modelling of supermarket refrigeration systems

Refrigeration systems in supermarkets form a subset of all the commercial vapour-compression systems. Ding (2007) reviewed then recent developments in simulating vapour compression systems. He found that the mathematical models for compressors depended on the aim of the research and divided them into steady state and dynamic models. In conjunction with the steady state models, the author referred to the polytropic exponent, mass flow rate and motor efficiency as necessary model inputs. Evaporator and condenser models were also divided into steady state and dynamic models and, for the latter method, Ding found the following three approaches: lumped parameter models, zone models and distributed models. Regarding the algorithms he observed that the more abstract simultaneous solving method and the sequential module method, which had a more physical meaning, were used. In his review of future developments the author included knowledge transfer into industry and associate problems as well as nanofluids for refrigeration as topics for further research.

The paper reviewing modelling approached by Ding (2007) discussed in the previous paragraph did not include the thesis by James (1976) who researched a produce freezing plant for energy conservation. This researcher used a first principle approach based on the conservation laws to model the steady state and transient behaviour of an air condition system as well as a quick freezing and liquid chilling plants. According to the author his work was particularly useful for improving the control settings of the air conditioning system. He also found ways to improve the capacity control of the freezing plant, but admitted that the model for the chilling plant only offered more insight without yielding definite results.

Ge and Tassou used the energy simulation software package TRNSYS to simulate supermarket refrigeration systems (and whole supermarkets, e.g. Ge and Tassou (2011)). One example of their work for which these researchers used TRNSYS was the modelling of a multi-compressor refrigeration system (Ge and Tassou, 2000). In the corresponding paper the researchers described the mathematical models in quite some detail taking into consideration points such as the heat transfer between the inlet and outlet of the compressors. The researchers used their model to investigate the benefits of variable speed drives and variable head pressure control. These improvements had become the norm when they published their paper referred to earlier (Tassou *et al*, 2010).

When discussing climate change and refrigeration systems, only the effect of the refrigeration system as a contributing cause to climate change is normally examined. One example, is the paper by Wang *et al* (2010) mentioned above which discussed the need for replacement refrigerants for ozone depleting chlorinated hydrocarbon refrigerants. Another example is Lucas (2006) who explored the consequences for professional practice and changes to life style because of necessary changes in refrigeration technology arising from the need for replacement refrigerants. Earlier examples are summarized in Devotta *et al* (2005).

The effect of the changing climate on refrigeration systems, however, does not seem to be an area of active research. Therefore the main aim of this chapter is to investigate the impact of climate change on refrigeration systems. A secondary research question revolves around how the condenser fan control could be improved. For this research the supermarket system in Hull was investigated as a typical refrigeration system. A first principle model was chosen for this as such a model allows the investigation of improvement ideas, e.g., in conjunction with the condenser fans more easily then a data-driven model. As mentioned in an earlier chapter, the same type of system has been installed in all the investigated stores. Therefore results of the research here should be relevant to other supermarkets as well.

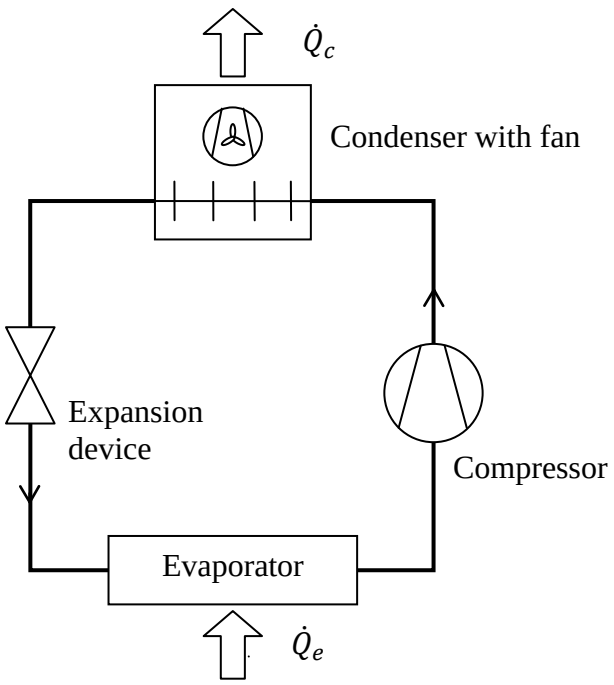

Figure 8.1: Schematics of a simple vapour compression system

8.2 Introduction to refrigeration systems

The aim of refrigeration is to generate and maintain a space at a temperature lower than its surroundings. This can be achieved through various ways, but, currently, the most common approach for supermarkets are vapour compression cycles (Arora, 2010, pp 1-7; Gordon and Ng, 2000, p 15). All of these cycles use thermodynamic processes and principles. To illustrate how they may be applied to refrigeration systems a simple, steady state vapour compression system with a pure substance refrigerant and the components as shown in Figure 8.1 is considered. These four components are also included in the subsequently analysed installed system and the software model.

8.2.1 Vapour compression cycles

The p-h diagram in Figure 8.2 is of a hypothetical, pure refrigerant (a similar approach was used by Riffe (1994)) containing three vapour compression cycles. The cycle indicated by the dashed black line (1 → 2 → 3 → 4 → 1) is the fully reversible Carnot cycle. This cycle consists of two isothermal processes (4 → 1 and 2 → 3) and two processes for which the entropy remains constant (1 → 2 and 3 → 4). During the process 4 → 1, the refrigerant absorbs heat from the higher temperature surroundings by being partly vaporized. This vapour-liquid mixture is then adiabatically and without any losses compressed to point 2, at which point the refrigerant is a saturated vapour. Next, heat is rejected during the process 2 → 3 to the lower temperature surroundings. A fully reversible expansion process, i.e. 3 → 4, returns the refrigeration from the saturated liquid line to the two phase region at point 4. It has been shown that this theoretical cycle constitutes the maximum limit for thermal efficiency for a given temperature difference so that actual cycles can be compared against it (Çengel and Boles, 2007, p 625; Stoecker and Jones, 1983, pp 187-188).

One of the reasons why this cycle is not used in practice is that compressors can be damaged when dealing with wet vapour (Arora, 2010, pp 135, 136; Gordon and Ng, 2000, p 19). Therefore the Carnot cycle is amended by replacing the process 1 → 2 with the isentropic compression process 1’ → 2’. This process along the constant entropy line does not acknowledge any losses, such as heat or friction losses. This deviation is shown as the process 1’ → 2” in Figure 8.2. To capture this deviation, the isentropic efficiency may be used, which is defined as the ratio between the isentropic work and the actual work (Arora, 2010, p 148). Another approach, which allows the exploration of the underlying thermodynamic principles, is to assume this process to be polytropic (Arora, 2010, p 172).

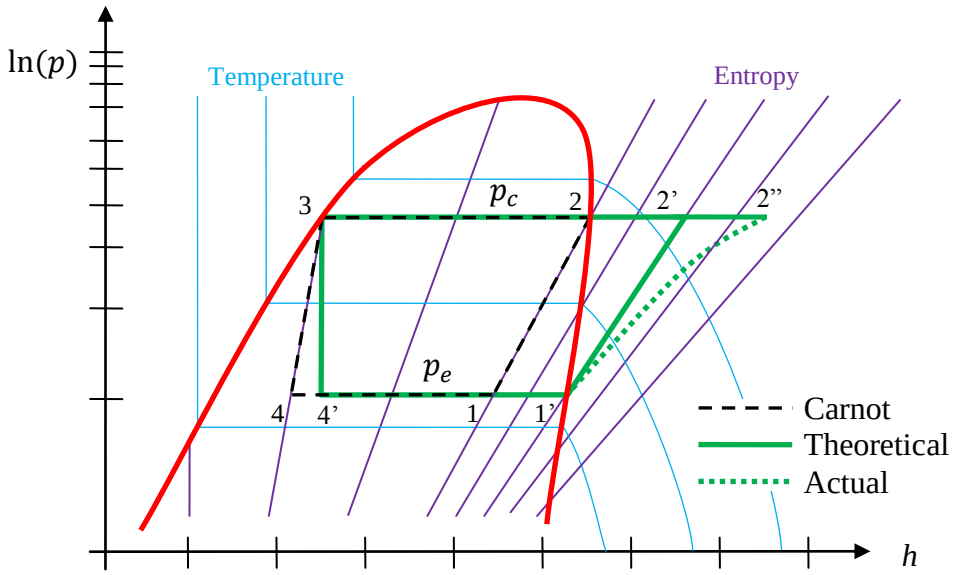

Figure 8.2: Vapour compression cycles in *p*-*h* diagram

8.2.1.1 Analysis of compression process

The analysis of the different processes and system components makes use of the laws of thermodynamics, in particular the first law. This is sometime also referred to as the "law of the conservation of energy" (ASHRAE, 1997, p1.2) and can be written as in Equation 8.1.

$$\sum Energy_{in} - \sum Energy_{out} = \Delta Energy$$

Equation 8.1

In the analysis here only steady state conditions are considered, therefore the change in energy term is zero. The same implications apply for a steady state mass flow rate through an open system. With these two simplifications Equation 8.1 may be re-written as in Equation 8.2 (Stoecker and Jones, 1983, pp 21, 21; Arora, 2010, p 31).

$$\left(h + \frac{V^2}{2} + gz\right)_{in} - \left(h + \frac{V^2}{2} + gz\right)_{out} = q - w$$

Equation 8.2

Where:

h: Specific enthalpy

V: Velocity

g: Gravitational acceleration

z: Elevation

q: Specific heat

w: Specific work

in: Index indicating variables associated with energy entering a system

out: Index indicating variables associated with energy leaving a system

The simplifying assumptions for the compression process include that the compression process is adiabatic, during which the change in kinetic and potential energy are negligible (Stoecker and Jones, 1983, p 22) so Equation 8.2 can be modified to yield Equation 8.3.

$$w = w_{cmp} = h_{out} - h_1$$

Equation 8.3

A way of characterising an actual compressor is by using isentropic efficiency, η_{isen}. Referring to Figure 8.2 the η_{isen} can be defined as in Equation 8.4 (Arora, 2010, p 125). This efficiency is particularly relevant for compression processes which are (at least nearly) adiabatic (Çengel and Boles, 2007, p 379).

$$\eta_{isen} = \frac{Isentropic\ work}{Actual\ work} = \frac{h_2' - h_1'}{h_2'' - h_1'}$$

Equation 8.4

Another method of calculating the specific work input to an isentropic compression for steady flow is to integrate the $v\ dp$ work using the equation below (Arora, 2010, p 109):

$$p \times v^{\gamma} = \text{constant}$$

Equation 8.5

Where:

p: Absolute pressure

v: Specific volume

γ: Specific heat ratio

Such an approach yields Equation 8.6:

$$-w'_{cmp} = \frac{\gamma}{\gamma - 1} p_e \, v_{in} \left[\left(\frac{p_c}{p_e} \right)^{(\gamma-1)/\gamma} - 1 \right]$$

Equation 8.6

Where:

w'_{cmp}: Specific work input into the compression process ($v \, dp$ integral)

p_e: Absolute pressure at suction port of compressor

v_{in}: Specific volume at suction port of compressor

p_c: Absolute pressure at discharge port of compressor

8.2.1.2 Analysis of condensing process

The refrigerant is first de-superheating in a condenser either from point 2" Figure 8.2 (for an actual compression process) or from point 2' (for an isentropic process) and then passes point 2 when the actual condensing process starts. Depending on the condenser the process finishes at the saturated liquid line (point 3) or extents into the sub-cooled region (not shown in the diagram). For the analysis here the saturated liquid line marks the end of the condensation process. With this in mind Equation 8.2 can be simplified when noting that the specific work is zero and neglecting changes in potential and kinetic energies to give Equation 8.7.

$$q_c = h_{sh} - h_3$$

Equation 8.7

Where:

q_c: Specific heat rejected by the condenser

h_{sh}: Specific enthalpy in the superheat region (either at point 2' or 2")

h_3: Specific enthalpy at outlet of condenser

The heat q_c is rejected into the air stream forced through the condenser by the fan indicated in Figure 8.1, which increases the enthalpy of the air by $h_{sh} - h_3$. Noting that the specific heat constant at constant pressure, c_p, is defined as (Çengel and Boles, 2007, p 179):

$$c_p = \left.\frac{\partial h}{\partial T}\right|_{p=constant}$$

Equation 8.8

it is possible to write an equation that relates the change in enthalpy, which is equal to the rejected heat q_c, to the change in air temperature. Equation 8.9 is for the case where c_p is constant.

$$q_c = c_p \left(\vartheta_{off} - \vartheta_{on}\right)$$

Equation 8.9

Where:

ϑ_{off}: Temperature of air leaving condenser

ϑ_{on}: Temperature of air entering condenser

The power required to remove this heat is governed by the fan laws, which show that the fan power consumption is proportional to the cube of the volumetric flow rate of the air (ASHRAE, 2008, p 20.4).

Major differences between the theoretical and actual processes in the condenser include the drop of pressure along the condenser, which makes the condensing process non-isothermal for pure substances (Stoecker and Jones, 1983, p 203). If the refrigerant is not a pure substance, then the condensing process may not be isothermal, even if it were isobaric (ASHRAE, 1997, p 1.10). Another possible difference is the sub-cooling in the condenser, that is to say that the refrigerant is cooled beyond the saturated liquid line, which may be a design feature of an actual cycle, to ensure that only liquid enters the expansion device (Stocker *et al*, 2001, p 203).

8.2.1.3 Analysis of the expansion process

The most severe deviation from the Carnot cycle is probably the irreversibility through the throttling valve. When assuming that the changes in potential and kinetic energy can be neglected, Equation 8.2 can be simplified to yield Equation 8.10 if neither heat nor work enters or leaves the valve throughout the process (Arora, 2010, p 123).

$$h_3 = h_4$$

Equation 8.10

Where:

h_3: Specific enthalpy of the refrigerant entering the expansion valve

h_4: Specific enthalpy of the refrigerant leaving the expansion valve

ASHRAE (1997, pp 1.12-1.13) analyses an actual refrigeration system and suggests that there is no heat exchange between the expansion valve and its surroundings. However, Arora (2010, p 151) explains that there is some heat transfer to the expansion device in real systems with a corresponding increase in exit enthalpy.

8.2.1.4 Analysis of evaporation process

The refrigerant evaporates in the isothermal process from 4' to 1' (or from 4 to 1 in the Carnot cycle is considered). This latent heat provides the desired refrigeration effect. The specific refrigeration effect q_e can also be calculated based on Equation 8.2. Again, neglecting any changes in kinetic and potential energy and noting that there is no work done by or on the system, Equation 8.11 can be derived (Arora, 2010, p 123).

$$q_e = h_1' - h_4'$$

Equation 8.11

Where:

q_e: Specific heat absorbed by the evaporator

h_1': Specific enthalpy at the outlet of the evaporator

h_4': Specific enthalpy at the inlet of the evaporator

The mass flow rate, $\dot{m}_{rf}$, to give the required total refrigeration effect $\dot{Q}_e$ can be calculated as shown below (ASHRAE, 1997, p 1.9).

$$\dot{Q}_e = \dot{m}_{rf} \times q_e \rightarrow \dot{m}_{rf} = \frac{\dot{Q}_e}{q_e} = \frac{\dot{Q}_e}{h_4 - h_1}$$

Equation 8.12

Deviations from the theoretical evaporation process in Figure 8.2 are very similar to the one discussed for the condenser, such as the pressure drop along the evaporator. In the case of an evaporator the vapour may be deliberately superheated (rather than sub-cooled) to avoid wet compression (Stoecker and Jones, 1983, p 203).

Other losses in the refrigeration system include heat exchanges along connecting pipes and other system devices, and pressure drops along these. The refrigerant may also contain an amount of lubricant required for the compressors, moisture and noncondensable gases, thus changing its behaviour. (Arora, 2010, pp 148-153). The example in ASHRAE (1997, pp 1.12-1.14) shows that the component with the highest losses is the compressor due to, for instance, friction losses, motor inefficiencies and heat exchange with its surroundings.

8.2.1.5 COP and COSP

The two efficiencies figures which will be used to throughout this chapter are the coefficient of performance (COP), which is for the core refrigeration system, and the coefficient of system performance ($COSP$), which also includes other components. A later section will discuss them and their relationship with each other more closely. Below is the definition for the COP (ASHRAE, 1997, p 1.3) and $COSP$ (Evans *et al*, 2014).

$$COP = \frac{Useful\ refrigeration\ effect}{Net\ energy\ supplied\ from\ external\ sources\ to\ core\ system}$$

Equation 8.13

$$COSP = \frac{Useful\ refrigeration\ effect}{Energy\ supplied\ from\ external\ sources\ to\ complete\ system}$$

Equation 8.14

8.3 Introduction of the installed system and its $COSP$

The two cascaded R404A/CO_2 refrigeration systems investigated here are installed in the Hull supermarket mentioned in the previous chapters. These systems have a nominal cooling capacity of 60 and 80 kW (Searle Manufacturing Company, 2008, p 69). Although this study concentrates mainly on the larger of these two refrigeration systems, data for both systems were downloaded and used for intercomparison to detect errors in data acquisition and preparation. The reason for this selection was that the electricity consumption of the condenser fans could be studied more effectively as there are twice as many in the larger system. The two refrigeration systems are located in the plant area behind the supermarket (see Figure 8.3). The wall of this area, which is north facing, also has an outdoor temperature sensor installed approximately 2 m above ground.

The focus of the explanations below is on describing how the necessary specific enthalpies and the overall mass flow rate were calculated so that the useful refrigeration effect $\dot{Q}_e$ and the $COSP$ of the complete system could be estimated.

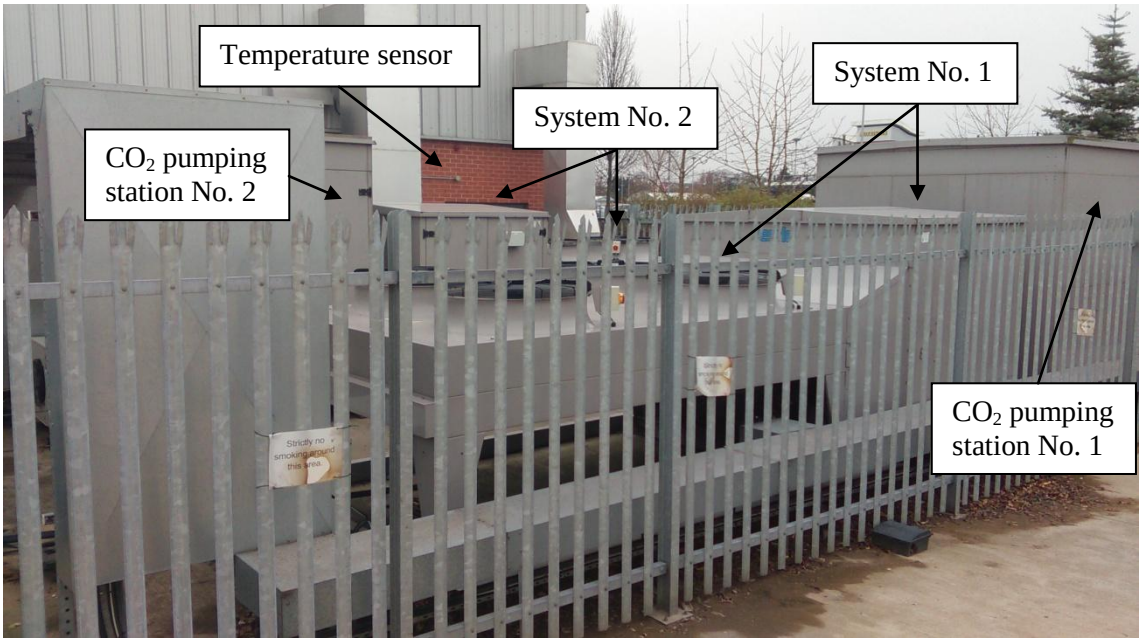

Figure 8.3: Refrigeration systems in Hull (including condensers and CO_2 pumping stations)

8.3.1 Description of system

The main components of the 80 kW system are listed in Table 8.1. In addition to the position of these components within the system, Figure 8.4 also indicates schematically the position of the temperature and pressure sensors used throughout this section. The yellow circles with numbers in Figure 8.4 correspond to those in Figure 8.5 (shown later in this chapter) and were added to more easily identify the thermodynamic processes. The CO_2 system, shown in blue in Figure 8.4, is considered as the load of the refrigeration system and is not further analysed. The CO_2 vessel is maintained at approximately 30 bar_g corresponding to a temperature of about -4.4°C.

Table 8.1: Main components of the installed refrigeration system

Short	Component	Model	No	Remarks
N/A	Refrigerant	R404A	1	
C1	Compressor	Bitzer, 4DC-5.2Y	1	VSD: 20 Hz – 60 Hz
C2	Compressor	Bitzer , 4PCS-10.2Y	1	50%/100% capacity control
C3	Compressor	Bitzer, 4J-13.2Y	1	
C4	Compressor	Bitzer, 4DC-5.2Y	1	
N/A	Condenser	GEA, MGC222H-09-EC3	1	No sub-cooling section
Fan	Condenser fan	Searle, 231-9091-EC 43	4	1.9 kW/fan, VSD, all fans some VSD signal
$HX_{e,1}$, $HX_{e,2}$	Evaporator heat exchanger	Alfa Laval, AlfaChill 120	2	
EEA	Electronic expansion valve	Carel, E3V	2	
HX_{sub}	Heat exchanger	Ecolfex, GBS800H, 44 plates	1	

The suction line accumulator of the actual system contains a heat exchange coil to boil off any liquid refrigerant from the evaporator. However, as the quality of the refrigerant leaving the evaporator is not measured, the accumulator is thought of as a simple flash tank with the assumption that the expansion valve is controlled in such a way that the quality of the refrigerant is close to unity. This simplification may overestimate the useful refrigeration effect $\dot{Q}_e$. All the sub-cooling is attributed to the heat exchanger, shown as HX_{sub} in the centre of Figure 8.4.

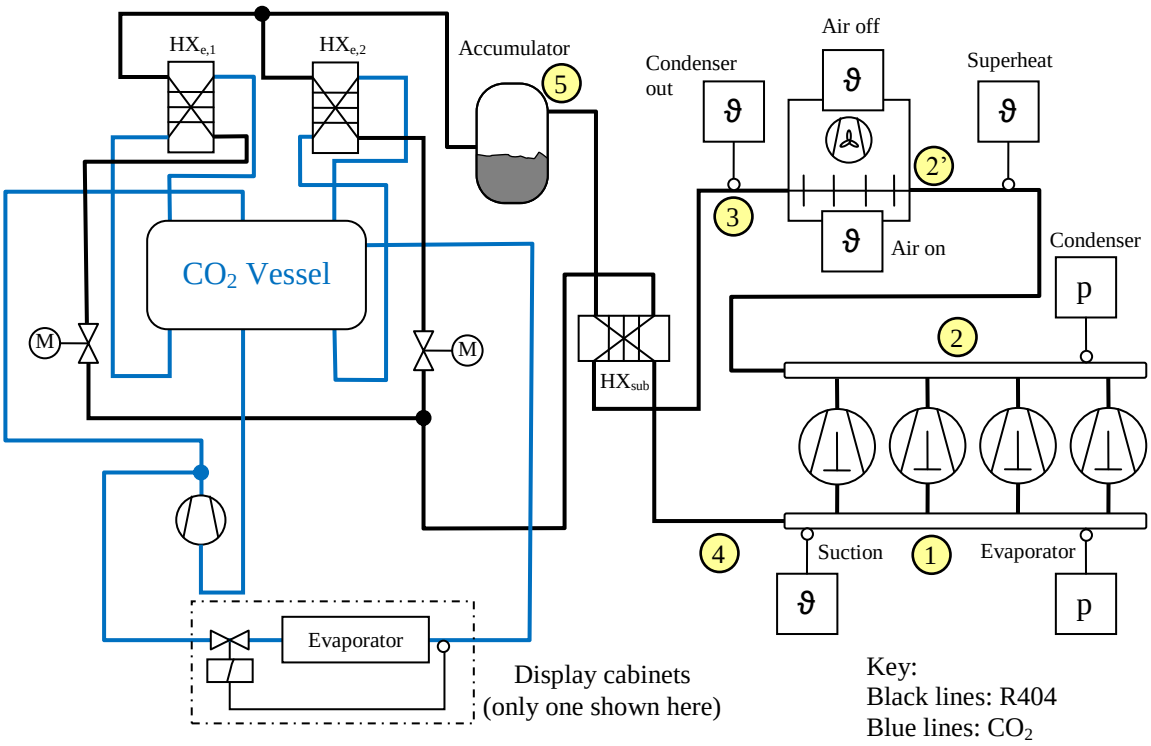

Figure 8.4: Schematics of the installed refrigeration system with sensor positions

The controller for the refrigeration system controls both the compressor bank of the four reciprocal, semi-hermetic, 4-cylinder compressors and the four condenser fans. The speed control signal is the same for all four fans. Originally, only compressors C1 to C3 were fitted. C4 was added later (but before this analysis started) to boost the system's cooling capacity. Compressors C3 and C4 have only on/off controls, C2 has the capacity to offload two of its four cylinders (Bitzer Kühlmaschinenbau GmbH, 2014, p 8) and C1 is controlled via a variable speed drive (VSD) which operates from 20 Hz to 60 Hz (Searle Manufacturing Company, 2008, p 69).

The control input for the compressor bank is the suction pressure, which has a set-point of 3.5 bar_g, (corresponding to a refrigerant temperature of -9.1°C). For the condenser fans the

condenser pressure is monitored and has a target value of 10 bar_g and a control band of ±0.5 bar. The condenser fans also have a night set back which limits the maximum fan speed to 53% of its maximum (Searle Manufacturing Company, 2008, pp 69-71).

8.3.2 Data acquisition and preparation

Data for the period from 1 June 2014 to 30 Nov 2014 were remotely downloaded from the following on-site devices. Firstly, the readings of the sensors shown in Figure 8.4 and mentioned in Table 8.2 are routinely recorded by controllers (one controller for refrigeration system No. 1 and one for system No. 2) and therefore could be remotely downloaded in 15 s intervals (lowest resolution) from these controllers. Secondly, data from two power meters, each measuring the electricity consumption of one complete system, were also downloaded in 15 s intervals. These power readings cover the compressors, condenser fans, CO_2 pumping station, controls and auxiliary equipment such as control room heaters and lights. As they have been considered the power supplied to the complete refrigeration system, they have been used as was. The third data source was the temperature sensor in the plant area on the north side of the building (see Figure 8.3). Temperature (as well as relative humidity) data from this sensor were downloaded in 1 min intervals as changes in these values were expected to be captured within this time frame.

Table 8.2: Measuring devices and sensors per refrigeration system

Device	Model	No
Pressure sensor	RDM, PT4-18S	2
Temperature sensor (Refrigeration system)	RDM, PT1000	3
Temperature sensor (Condenser)	RDM, PT1000	2
Power meter	Elcomponent, AEM33 485 DIN	1
Temperature sensor (outside temperature	RDM, PT1000	1

Before averaging the data, it was investigated if the averaging span had an effect on the quality of the compressed data. In order to do this power consumption data for two months were averaged over the following three different intervals: of 10 min, 15 min and 20 min. It was found that the 20 min interval reduced data points too much so that the behaviour could not be studied in sufficient detail. Therefore the 15 min interval was chosen to reduce the number of data points as much as possible without losing resolution.

After this was determined, data from these data sources were combined in monthly spreadsheets and averaged over 15 min intervals. For the control data of the compressors C2 to C4 this included converting the text form, i.e. ‘on’ and ‘off’, into ‘0’ and ‘1’ before

averaging them for a 15 min interval for each compressor to obtain an average on time them. For C1 the VSD signal was converted into a percentage value of the full load at 50 Hz using Equation 8.15. This value was then multiplied with the converted on/off value before it was averaged over a 15 min interval.

$$precentage_{full\ load} = 0.007\ \times VSD + 0.4$$

Equation 8.15

8.3.3 Description of the R404A refrigeration cycle

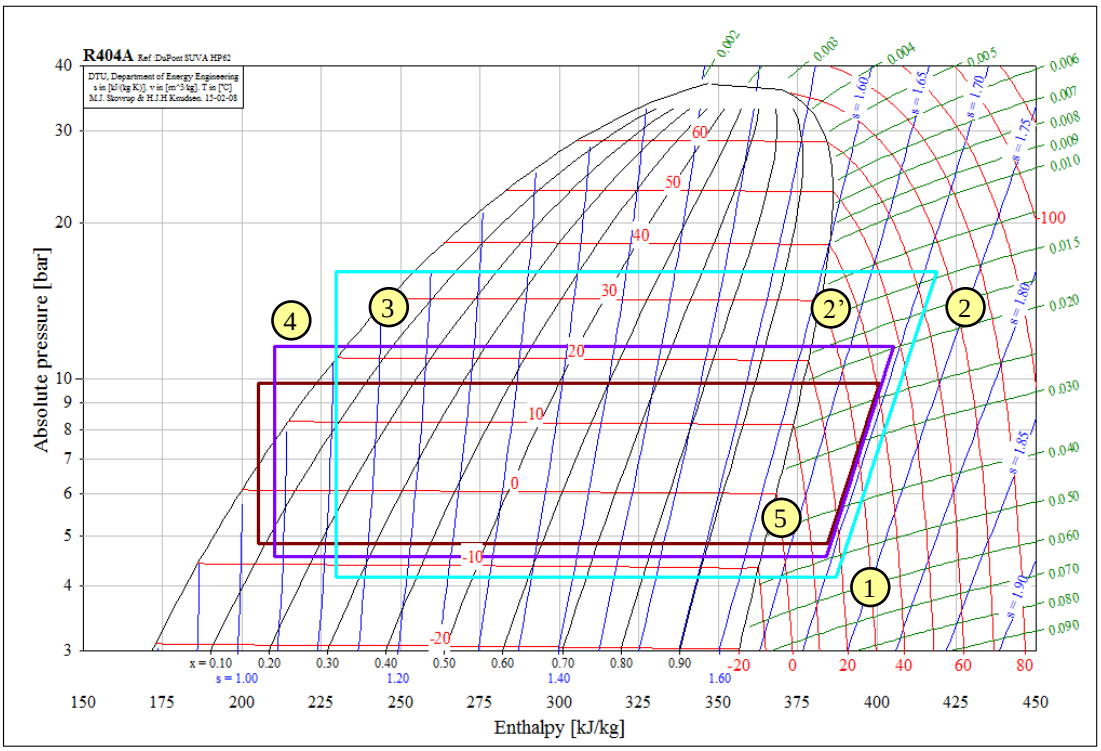

Figure 8.5: R404A cycles (Δp_{min}: brown, Δp_{av}: purple, Δp_{max}: turquoise)

Table 8.3: Main pressures and temperatures in the refrigeration cycles

$\Delta p_{c,e}$	p_e (bar$_g$)	ϑ_{suc} (°C)	$\vartheta_{g,sat}$ (°C)	p_c (bar$_g$)	ϑ_{dis} (°C)	$\vartheta_{cond,out}$ (°C)	ϑ_{sub} (°C)
Min	3.80	15.9	-6.90	8.80	48.0	17.7	3.98
Average	3.51	15.1	-8.48	10.53	46.2	21.4	7.54
Max	3.15	17.7	-11.2	15.5	64.0	34.4	20.2

The three refrigeration cycles in Figure 8.5 show the full operation range of the refrigeration system under consideration by displaying the cycles for the minimum, average and maximum pressure difference between the evaporator (or low pressure) side and the condenser (or high pressure) side of the system. The numbers in the yellow circles indicate how the data from the sensors in Figure 8.4 have been interpreted. From this diagram it is apparent that none of the second order effects mentioned in Section 8.2 have

been taken into consideration. Table 8.3 lists the data which were used to construct these cycles and is based on measurements and R404A refrigeration data for the software CoolPack (Skovrup *et al*, 2012).

8.3.3.1 Suction point

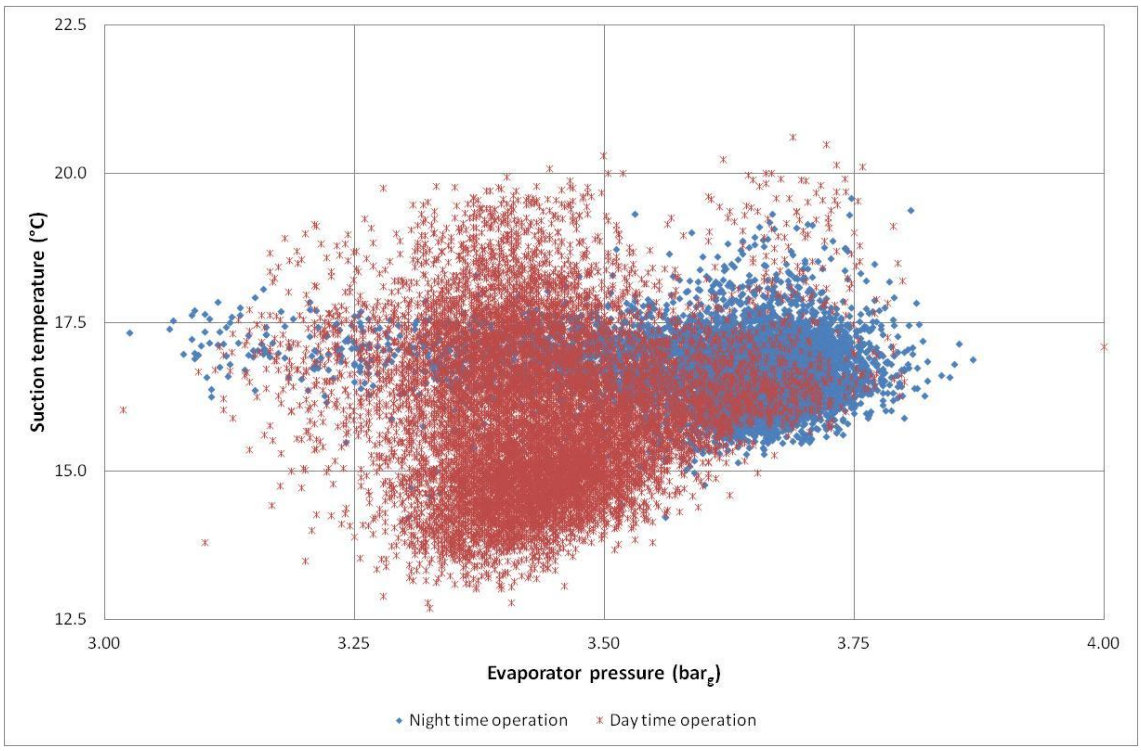

Figure 8.6: Pressure vs temperature scatter plot for the suction point

The description of the cycle starts with the suction inlet of the compressor (referred to as '1' in Figure 8.5) because this is the point monitored by the controller. The scatter plot in Figure 8.6 displays data for this point which is also considered the low pressure output port of the heat exchanger HX_{sub}. The day time operation, which relates to the set back of the condenser fan speed mentioned above, extends from 06:00 to 20:00. The rest of the time the refrigeration system is in night time operation mode (see Section 8.3.3.5 for more explanations). The diagram shows that the set point of 3.5 bar_g is achieved well (overall average: 3.51 $bar_{g,}$) and that over 95% of the data points lie within a ±0.25 bar band.

Table 8.4 lists some statistics for the suction point which indicates that the coefficient of variation CoV (=σ/Av) is small (less than 4% for all cases). This table also shows that the pressure tends to be lower than average during the day corresponding to a higher evaporation temperature, which may be owing to a higher load through the day. The converse is true for the night time operation.

Table 8.4: Evaporator pressure and temperature statistics

	Overall				Day time operation				Night time operation			
	Min	***Av***	σ	**Max**	**Min**	***Av***	σ	**Max**	**Min**	***Av***	σ	**Max**
Evaporator pressure p_e (bar_g)	2.89	3.51	0.14	4.00	3.02	3.44	0.10	4.00	2.89	3.62	0.11	3.87
Suction temperature ϑ_{suc} (°C)	12.4	16.3	1.13	20.62	14.4	16.0	1.33	20.6	14.2	16.7	0.57	19.6

To derive the enthalpy equation for this operational area of the refrigeration cycle, R404A enthalpy data for the pressure range from 3.1 bar_g to 4 bar_g and for the temperature interval from 12°C to 21°C were exported from the CoolPack software package (Skovrup *et al*, 2012). The following multiple regression analysis yielded Equation 8.16 with an r^2 of 1.00 and a maximum residual of 0.027 kJ/kg (which is 0.007% of the average enthalpy value of interest).

$$h_1 = 376\frac{\text{kJ}}{\text{kg}} + 0.892\frac{\text{kJ}}{\text{kg °C}}\,\vartheta_{suc} - 1.44\frac{\text{kJ}}{\text{kg bar}_\text{g}}\,p_c$$

Equation 8.16

8.3.3.2 Compression

The compressor bank increases the pressure of the vapour and transports the refrigerant through the system. To work out the overall mass flow rate the Bitzer software (BITZER Kühlmaschinenbau GmbH, 2013) was used to calculate the coefficients for the maximum mass flow rate, $\dot{m}_{max,c}$, as a function of the condenser and evaporator temperatures for each compressor. This software presents the results in the polynomial form as specified in the standard BS EN 12900: 2013 (BSI, 2013) which is also shown in Equation 8.17. The ten coefficients of for these equations are given in Table 8.5.

$$\dot{m}_{max,c} = C_1 + C_2\,\vartheta_{suc} + C_3\,\vartheta_{cdg} + C_4\,\vartheta_{suc}^2 + C_5\,\vartheta_{suc}\,\vartheta_{cdg} + C_6\,\vartheta_{cdg}^2 + C_7\,\vartheta_{suc}^3 + C_8\,\vartheta_{cdg}\,\vartheta_{suc}^2 + C_9\,\vartheta_{suc}\,\vartheta_{cdg}^2 + C_{10}\,\vartheta_{cdg}^3$$

Equation 8.17

Where:

ϑ_{suc} : Temperature at suction port of compressor

ϑ_{cdg}: Condensing temperature

Table 8.5: Mass flow rate coefficients according to BS EN 12900:2013

Compressor	C_1	C_2	C_3	C_4	C_5	C_6	C_7	C_8	C_9	C_{10}
4J-13.2Y	1740	61.8	-6.19	0.822	-0.133	5.74e-04	4.32e-03	-1.14e-03	-4.50e-05	4.18e-06
4PCS-10.2Y (50%)	659	23.3	-1.75	0.310	-0.035	-1.763e-02	1.64e-03	-3.47e-04	-2.224e-04	6.45e-05
4PCS-10.2Y (100%)	1320	46.6	-3.49	0.620	-0.070	-3.54e-02	3.28e-03	-6.93e-04	-4.46e-04	1.30e-04
4PCS-10.2Y	659	23.3	-1.74	0.310	-0.035	-1.78e-02	1.64e-03	-3.46e-04	-2.23e-04	6.54e-05
4DC-5.2Y	756	26.8	-3.31	0.352	-0.089	-6.036e-03	1.78e-03	-8.12e-04	2.52e-05	4.77e-05

The individual maximum mass flow rates thus calculated were multiplied with the respective averages of the compressor on time and added up to obtain the overall mass flow rate $\dot{m}_{ref}$. The average overall mass flow rate was computed to be 1140 kg/h with a minimum of 0 and a maximum of 2350 kg/h.

8.3.3.3 Discharge point

Figure 8.7 displays the scatter plot for the discharge point of the cycle (noted as '2' in Figure 8.5). As Figure 8.4 indicates, the sensor measuring the refrigerant temperature is sited somewhat away from the discharge point. Therefore this temperature is referred to as superheat temperature, ϑ_{sh}, rather than discharge temperature.

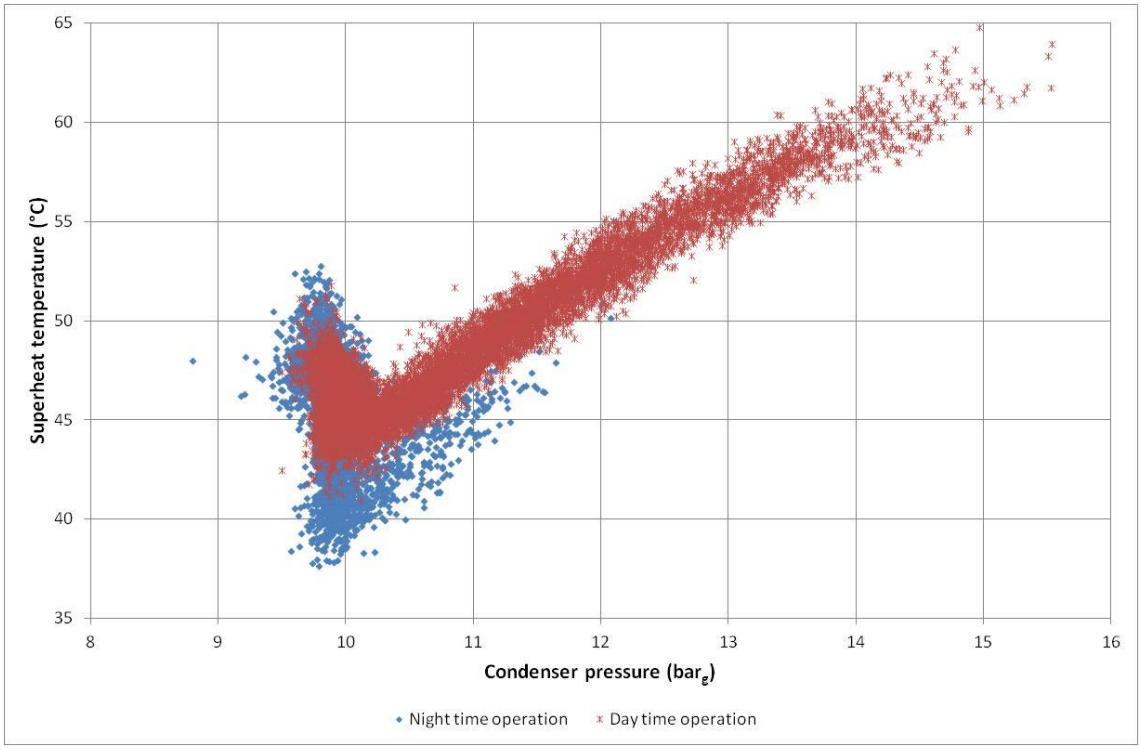

Figure 8.7: Superheat temperature vs condensing pressure scatter plot for the discharge point

The night time operation data points in Figure 8.7 have a smaller spread than the day time operation, which is also confirmed by the smaller standard deviations in Table 8.4 for both the discharge pressure p_c and temperature. The day time and night time plots show that the superheat temperature has a minimum between 9.5 bar_g and 10 bar_g. This corresponds to the control set point for the condenser fans and can be explained with a feedback from the increase of the air flow rate through the condenser. After this minimum the discharge temperature rises with increasing pressure, for the day time operation almost linearly (r^2 = 0.945 for a linear model when the discharge pressure is above 10.3 bar_g). That the graph for the day time extends to higher pressure values is partly due to higher refrigeration loads during the day (for instance, night blinds removed) and partly due to higher outside temperatures during the day time affecting the condenser. The discharge enthalpy is not necessary for the calculation of the $COSP$ and therefore will be discussed in Section 8.4.2.7 when the compression software model is developed.

Table 8.6: Discharge point pressure and temperature statistics

	Overall				**Day time operation**				**Night time operation**			
	Min	***Av***	***σ***	**Max**	**Min**	***Av***	***σ***	**Max**	**Min**	***Av***	***σ***	**Max**
Condenser pressure p_c (bar_g)	8.80	10.5	1.01	15.5	9.50	10.9	1.14	15.5	8.80	9.95	0.210	12.1
Superheat temperature ϑ_{sh} (°C)	37.6	47.5	3.79	64.8	41.0	48.8	4.11	64.8	37.6	45.6	2.25	52.8

8.3.3.4 Condensing

The condenser rejects heat to the surroundings which is described by the thermodynamic processes from point 2 to point 3 in Figure 8.5. Depending on the fan speed the operation of the condenser can be divided into three different modes (ignoring radiation and conduction). For low condenser pressures the fans are at a standstill and therefore the heat is rejected through natural convection. During the transitional range, when the fan speed increases, the rejection rate is a function of the fan speed and the approach temperature difference. The final mode of operation occurs when the fans run at maximum speed and an increase in heat rejection can only be achieved by increasing the condenser temperature.

If the vapour enters the condenser in a superheated state, then the vapour has to be first de-superheated to the temperature ϑ_{cdg} at the start of the two phase region before it can be condensed. Although the refrigerant is a zeotropic mixture, the glide during the

condensation process is small (maximum glide: −0.433 K, data from CoolPack (Skovrup *et al*, 2012)). Because the condenser has no sub-cooling section (GEA Searle, 2015) the refrigerant leaves the condenser as a saturated liquid.

The temperature ϑ_{cdg}, necessary to compute the mass flow rate (see Equation 8.17), was calculated based on the saturated vapour and liquid data from the CoolPack software (Skovrup *et al*, 2012) for the pressure range from 8.8 bar_g to 15.5 bar_g. It has a maximum residual of 0.0558 (or 0.2% of the average ϑ_{cdg}) and an r^2 of 1.00.

$$\vartheta_{cdg} = -0.0853\ \frac{°\text{C}}{\text{bar}_\text{g}^2}\ p_c^2 + 5.01\ \frac{°\text{C}}{\text{bar}_\text{g}}\ p_c - 21.1°\text{C}$$

Equation 8.18

It was assumed that no pressure drop occurs across the condenser, therefore an equation for the specific enthalpy of the refrigerant leaving the condenser could be derived as a function of the discharge pressure. In order to accomplish this, data for the saturated liquid were exported from CoolPack (Skovrup *et al*, 2012) and the equation below was computed with Excel (r^2=1.00) for the pressure range between 8.8 bar_g and 15.5 bar_g.

$$h_3 = 179\ \frac{\text{kJ}}{\text{kg}} + 7.05\ \frac{\text{kJ}}{\text{kg bar}_\text{g}}\ p_c - 0.0907\ \frac{\text{kJ}}{\text{kg bar}_\text{g}^2}\ p_c^2$$

Equation 8.19

The maximum absolute residual for this equation was found to be 0.0724 or 0.03% of the average enthalpy value for saturated liquid, which was 239 kJ/kg.

8.3.3.5 Condenser cooling

All four condenser fans (1.9 kW per fan) were controlled by the same signal from the controller. According to the user's manual (Searle Manufacturing Company, 2008, p. 70) this signal is limited to 53% for night time operation (from 20:00 to 06:00), but when examining the actual values, it was apparent that day time and night time operation had been swapped around (see Figure 8.8).

According to the actual controller settings and the explanations in the user's manual (Searle Manufacturing Company, 2008, p 70) the signal for the fan speed is related to the compressor pressure in the following way. The control signal is zero until a condenser pressure of 9.5 bar_g is reached, then the signal increases up to its maximum at 10.5 bar_g. During the night this maximum is 100% whereas for the day time operation this signal is

limited to 53%. When examining the variable speed drive (VSD) signal in Figure 8.8, it is apparent that, for this transitional period, the data spreads and the relationship between the condenser pressure and the VSD signal is not linear. The ramifications for modelling will be discussed in Section 8.4.2.4.

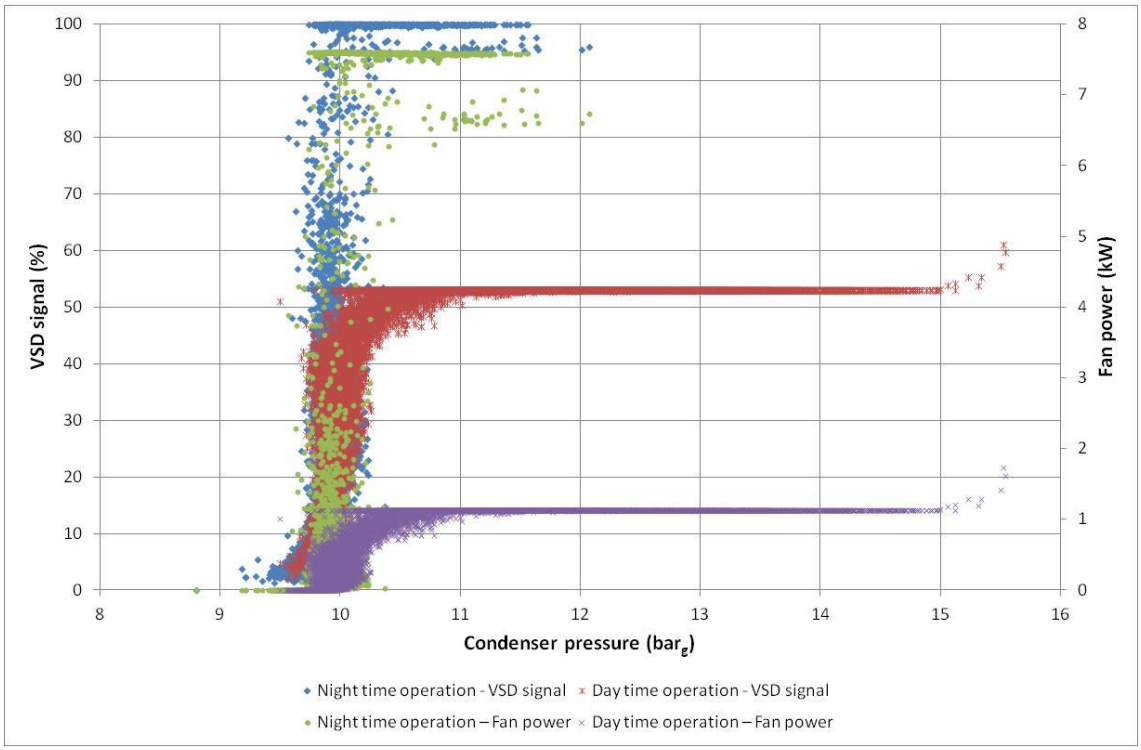

Figure 8.8: Scatter plot of the fan VSD signal and power vs the discharge pressure

In addition to the VSD signal Figure 8.8 also displays the electric power consumed by the condenser fans. As the power increases by the third power of the fan speed (ASHRAE, 2008, p 20.4) and the VSD signal is proportional to the fan speed, Equation 8.20 was used to calculate the fan power. Figure 8.8 shows that the electric power for the day time levels off at a much lower value than for the night time operation. This level is 15 % (= 0.53^3) of the full load power during the night.

$$E_{fan} = 4 \times 1.9 \text{ kW } (VSD\ signal)^3$$

Equation 8.20

8.3.3.6 Sub-cooling/Superheating

After the liquid refrigerant enters the heat exchanger it is sub-cooled from point 3 to point 4 in the diagram in Figure 8.5. This is accomplished by superheating the refrigerant vapour in the low pressure side of the heat exchanger from point 5 to point 1 in Figure 8.5. As plate heat exchangers are generally considered efficient (Gut and Pinto, 2003) and this

particular heat exchanger is covered by a 19 mm layer of insulation (Searle Manufacturing Company, 2008, p 90), no energy losses were considered. Therefore the heat flux into the high pressure side was equated to the heat flux out at the low pressure side. This allowed the calculation of the specific enthalpy of the sub-cooled liquid h_4 (point 4 in Figure 8.5) by subtracting the difference between the enthalpy at the suction point, h_1, from the enthalpy of the saturated vapour, i.e. h_5 (see Equation 8.21).

$$h_4 = h_3 - (h_1 - h_5)$$

Equation 8.21

Data for the saturated vapour from 3.2 bar_g to 3.8 bar_g from CoolPack (Skovrup *et al*, 2012) were used to work out the equation for h_5 (see Equation 8.22). The coefficient of determination was 1.00.

$$h_5 = 350\ \frac{\mathrm{kJ}}{\mathrm{kg}} + 3.83 \frac{\mathrm{kJ}}{\mathrm{kg\ bar_g}}\ p_e$$

Equation 8.22

For this equation the maximum absolute residual was 0.0261 kJ/kg which is 0.007% of the average enthalpy of the saturated vapour used to work out Equation 8.22.

8.3.3.7 Expansion

The expansion through the electronic expansion values used in this system was thought of as being a constant enthalpy process and therefore the specific enthalpy h_4 into the valves was the same as the one leaving them. As Figure 8.5 shows, the inlet fluid was in the sub-cooled region. This is necessary to avoid flashing in the expansion valves (CAREL INDUSTRIES, 2012). After the expansion process was completed the refrigerant was in the two phase region.

8.3.3.8 Evaporation

The refrigerant leaving the electronic valves enters the plate heat exchangers $HX_{e,1}$ and $HX_{e,2}$ which serve as evaporators (see Figure 8.4). As the quality of the refrigerant coming out of the evaporators is not measured, it was assumed that the refrigerant was a saturated vapour at the exit of the heat exchangers. Based on this assumption the useful refrigeration effect can be calculated as follows.

$$\dot{Q}_e = \dot{m}_{ref}\ (h_5 - h_4)$$

Equation 8.23

As mentioned in Section 8.3.3.2 the temperature ϑ_{suc} at the end of the evaporator was required to calculate the mass flow rate. The equation which was used to compute this temperature, Equation 8.24, was based on the saturated vapour data from CoolPack (Skovrup *et al*, 2012) for the pressure range from 3.1 bar_g to 3.8 bar_g and had an r^2 of 1.00. The largest absolute residual of this equation was 0.0008°C or 0.01% of the average temperature of the saturated vapour of the range of interest.

$$\vartheta_{suc} = -0.564\ \frac{°\text{C}}{\text{bar}_\text{g}^2}\ p_e^2 +\ 10.5\ \frac{°\text{C}}{\text{bar}_\text{g}}\ p_e -\ 38.6°\text{C}$$

Equation 8.24

The values in Table 8.7 are the averages of the saturated liquid and saturated vapour temperatures at the same pressure. This table shows that during the day the temperature was lower corresponding with the lower average pressure mentioned in Table 8.4. This may be because of higher refrigeration loads during the day. Or in other words, the refrigerant and the CO_2 in the evaporator had to have a higher temperature difference to provide a higher refrigeration effect.

Table 8.7: Average evaporator temperatures

	Overall				**Day time operation**				**Night time operation**			
	Min	***Av***	***σ***	**Max**	**Min**	***Av***	***σ***	**Max**	**Min**	***Av***	***σ***	**Max**
Av evaporator temperature (°C)	-13.0	-8.78	0.881	-5.68	-12.1	-9.22	0.640	-5.68	-13.0	-8.05	0.702	-6.84

8.3.4 Power consumption and $COSP$ of refrigeration system

The graphs in this section show the results of the calculations detailed above. For instance, Figure 8.9 and Figure 8.10 display the electricity consumption scatter plots of the complete system (as defined in 8.3.2) against the outside temperature. The data points of each plot were divided into four approximately equal amounts. This allowed visual gauging of how the data are spread around the average values for $\dot{Q}_e$ of 58.4 kW (day time operation) and 31.7 kW (night time operation). Figure 8.9 indicates that the lowest data cloud has a large spread, but the upper data clouds are more tightly packed. The situation for Figure 8.10 is the reverse inasmuch as the data cloud towards the higher end of the refrigeration effect has a larger spread.

The four data clouds in Figure 8.9 have a progressively steeper gradient as the $\dot{Q}_e$ increases. If all four data clouds are combined, a second order polynomial trendline has an r^2 of 0.678. This may mean that the increase in power consumption accelerates as the temperature rises.

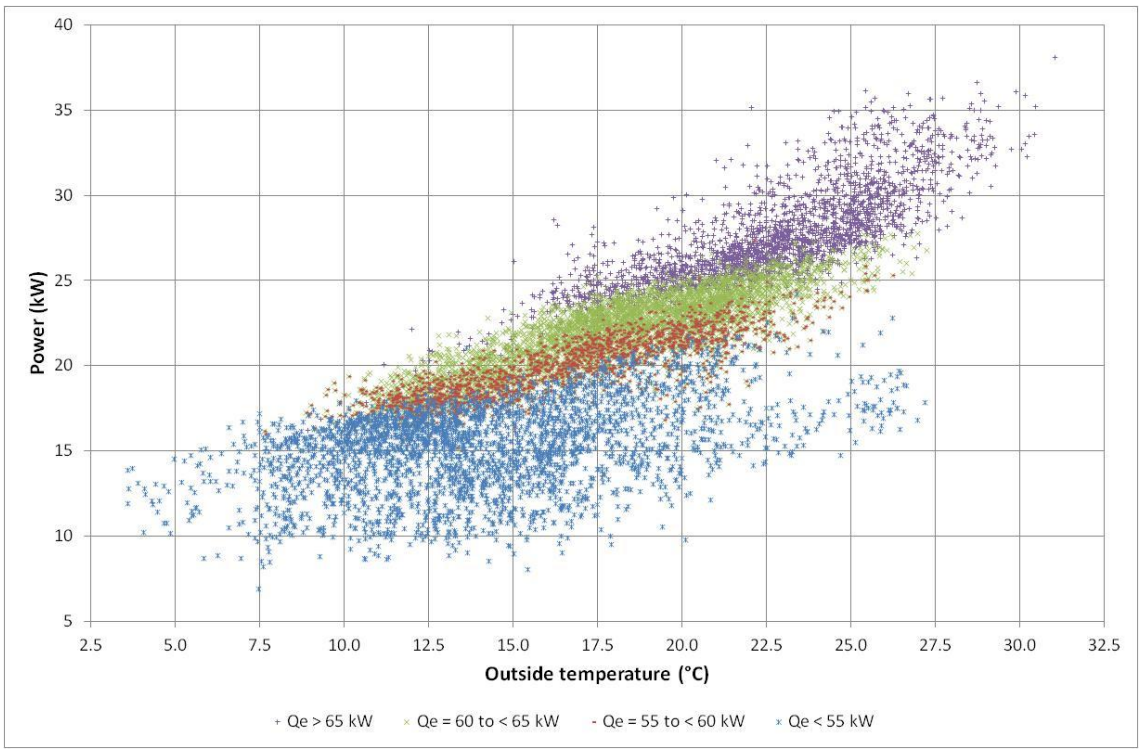

Figure 8.9: Power consumption of the complete refrigeration system in day time operation mode

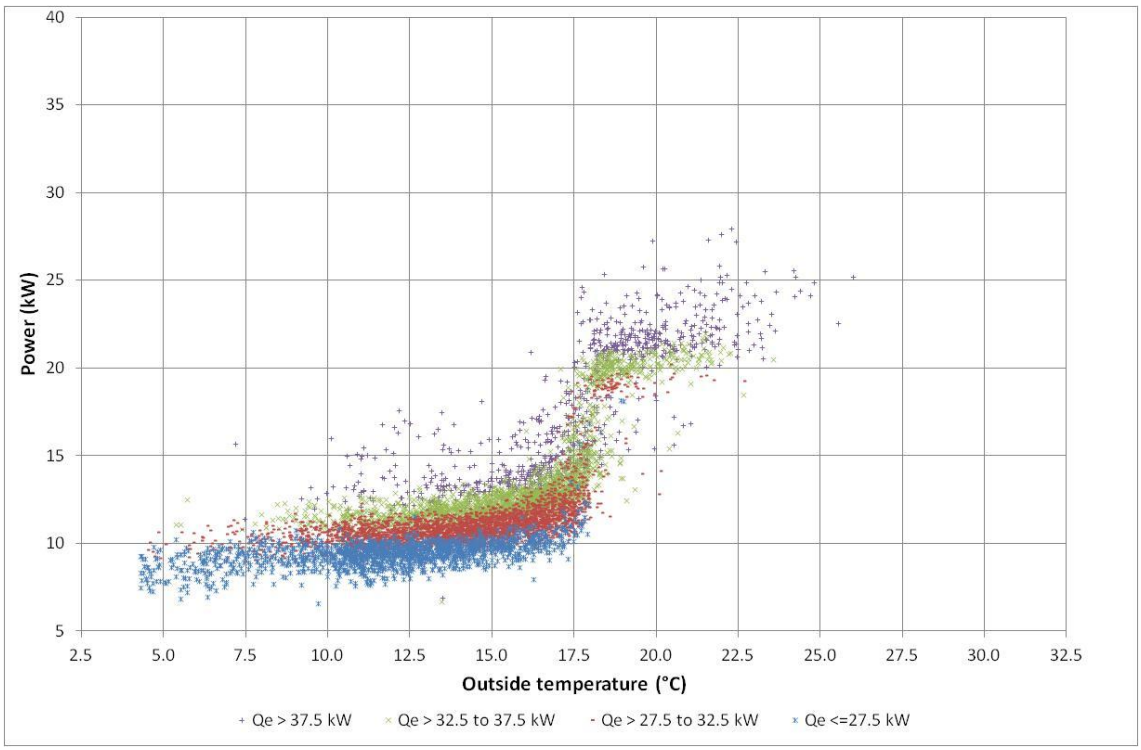

Figure 8.10: Power consumption of the complete refrigeration system in night time operation mode

The blue scatter points in Figure 8.9 include data when the refrigeration system was in day time mode, but the supermarket was still closed. Under these conditions the relationship between temperature and power consumption is fairly linear ($r^2 = 0.763$ for linear model). This relationship is still visible for temperatures above 22°C where some blue data points continue on a straight line.

In Figure 8.10 the step change in power consumption between 17°C and 19°C is approximately 8 kW. Allowing for a small temperature difference between ambient temperature and the condenser temperature, this can be explained by the control strategy for the condenser fans. As shown in Figure 8.8 the condenser fans quickly ramp up to full speed between the condenser pressures of 9.5 bar_g and 10.5 bar_g, corresponding to a refrigerant temperature in the 2-phase region of between approximately 18.5°C and 22°C.

Examining all of the power consumption data shown in Figure 8.9 and Figure 8.10 against outside temperature with change point models found that, for the refrigeration system No. 1, such a model has a change point at 14.9°C where the gradient increases by a factor of 4.38. The refrigeration system No. 2 can also be modelled with a change point regression equation and has a change point at 15.0°C. Here the gradient increases by a factor of 3.8. These refrigeration change point models have a slightly better coefficient of determination (0.676 for system 1 and 0.556 for system 2) than a second order polynomial model (0.657 for system 1 and 0.540 for system 2).

The coefficient of system performance in day time mode is displayed in Figure 8.11. It shows a non-linear relationship with the outside temperature. Up to approximately 11.7°C the $COSP$ is approximately 3.0 and virtually independent of the outside temperature. After that the $COSP$ can be modelled as a linear function when outliers are ignored. The overall model given by Equation 8.25 also ignores outliers and has an r^2 of 0.787.

$$COSP = \begin{cases} 0.0128\ {}^{1}/_{°C}\ \vartheta_{outside} + 3.00, & \vartheta_{outside} < 11.7\ °C \\ -0.0555\ {}^{1}/_{°C}\ \vartheta_{outside} + 3.80, & \vartheta_{outside} \geq 11.7\ °C \end{cases}$$

Equation 8.25

The $COSP$ for the night time operation also contains a virtually temperature independent range (up to 16°C) where the $COSP$ is approximately 2.8. Figure 8.12 shows that the $COSP$ drops steeply between 17°C and 19°C to about 1.8. This corresponds to the sharp increase

in power consumption of the condenser fans mentioned earlier. The data points beyond 19°C suggest that the $COSP$ becomes relatively temperature independent again.

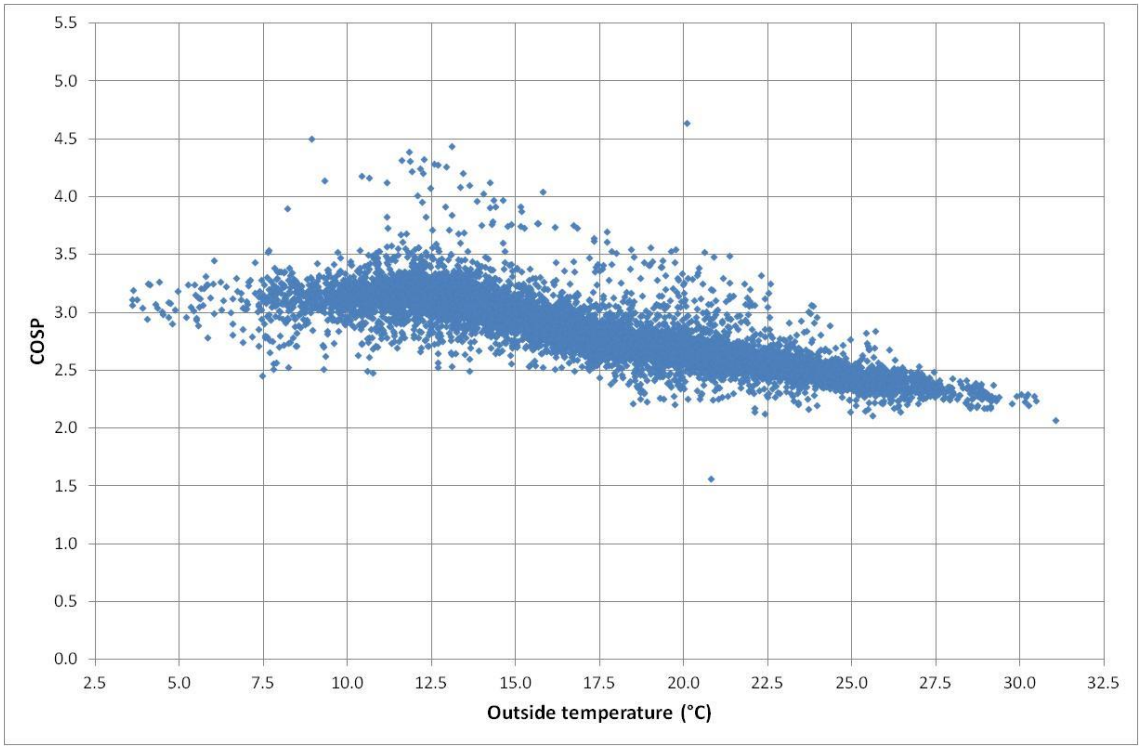

Figure 8.11: $COSP$ of the complete refrigeration system in day time operation mode

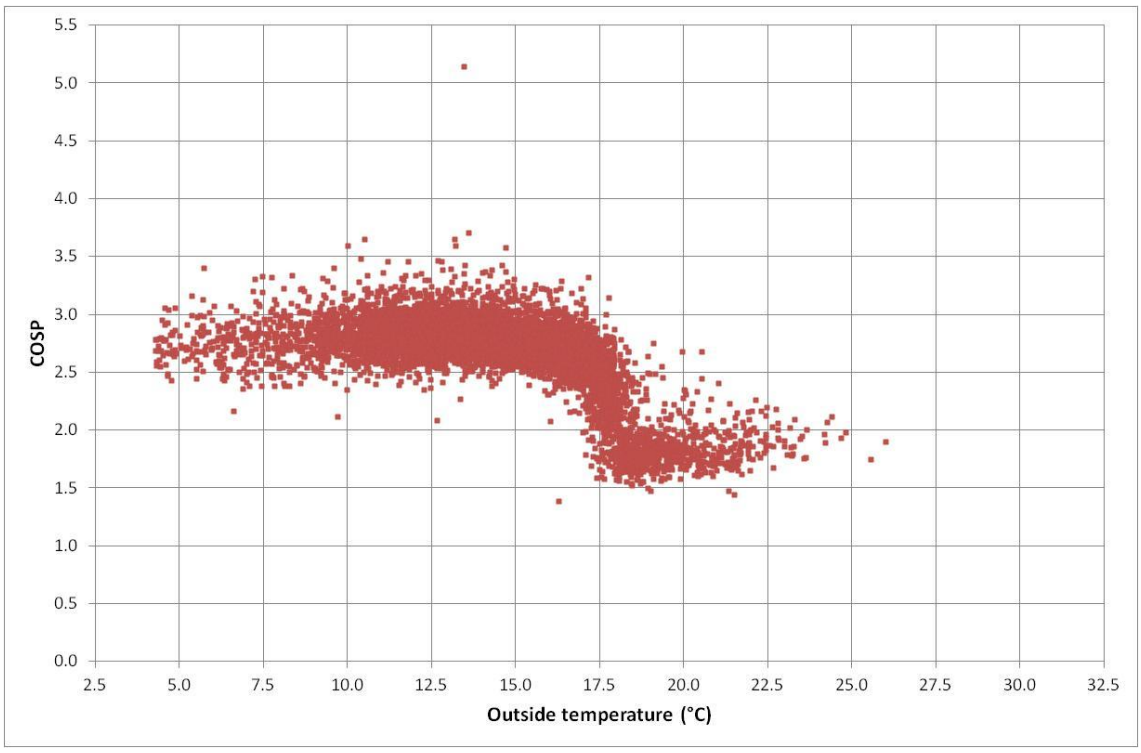

Figure 8.12: $COSP$ of the complete refrigeration system in night time operation mode

8.3.5 Discussion of the installed system

Based on the measurements and calculations above the maximum refrigeration effect $\dot{Q}_{e,max}$ is 84.3 kW. This occurs when the mass flow rate of C1 has been calculated to be 106% of its nominal maximum, C2 and C3 are constantly on and C4 constantly off for the corresponding 15 min interval. The outside temperature was measured to be 26.1°C, which is close to the design ambient temperature of 27°C (Searle Manufacturing Company, 2008, p 4). This means that this value has been computed for the original system (i.e. without compressor C4) virtually under design conditions. Using the assumption that the nominal cooling capacity of 80 kW occurs at design conditions, it can be concluded that the model in Figure 8.4 and the calculations based on it overestimate the cooling effect by between 5% and 6%. This may be owing to the simplification and assumptions used for the calculations, such as that the accumulator being modelled as a simple tank without heating and the assumption that the refrigerant arrives with a quality of close to unity in this tank.

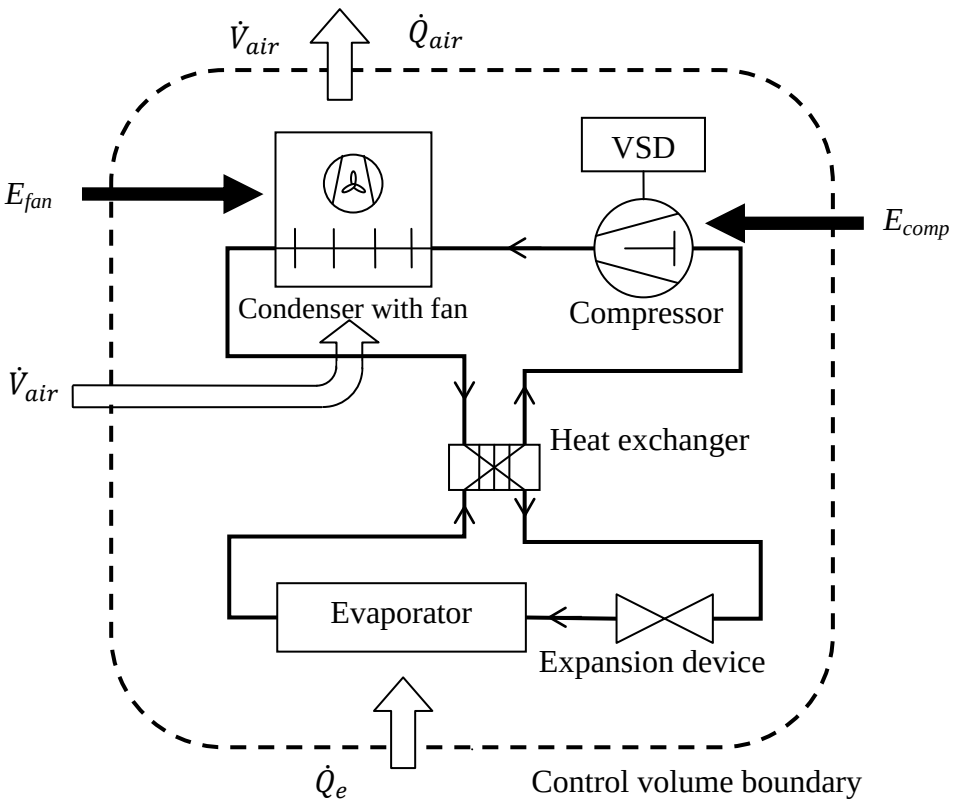

Figure 8.13: Refrigeration system simulated by the software model

8.4 R404A refrigeration model

The software model described below is based on the refrigeration system described in the previous section. The development of certain model parameters was also based on measured data for the installed system analysed above. R404A data from the software package CoolPack (Skovrup *et al*, 2012) were employed to help calculate specific enthalpies. The usual simplifying assumptions for a steady state system were applied (for a list see, for instance, Arora (2010, p 121)). Other simplifications are mentioned in the relevant component sub-sections.

The refrigeration system was modelled under steady state conditions with the five components displayed in Figure 8.13 using Matlab (MathWorks, 2011). This diagram indicates that the CO_2 distribution system was regarded as the load of this refrigeration system. It also shows that the bank of four compressors was represented as just one compressor with a VSD. This was because the mass flow rates of the individual compressors were combined in the analysis above to give only one overall refrigerant flow rate. The heat rejection from the condenser relies on forced convection only. The natural convection below the condenser fan set-point was modelled as a constant rejection rate.

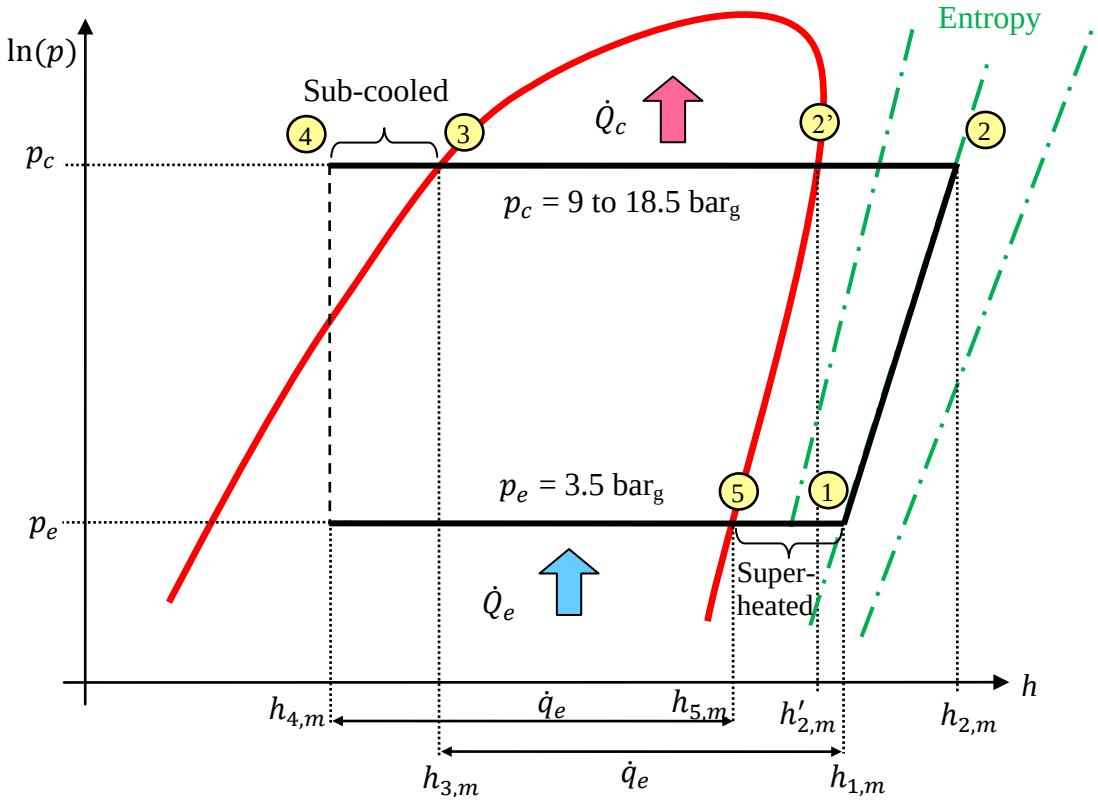

Figure 8.14: The *p-h* diagram for the software model Description of software model

8.4.1 Description of software model

The corresponding p - h diagram in Figure 8.14 indicates that the refrigeration cycle followed standard simplifying assumptions for a pure refrigerant. This means that evaporation and superheating were modelled as isobaric processes with a constant pressure of 3.5 bar_g, which is also the suction set-point of the compressors. The compression was thought of as an isentropic process with the implication that work input is a function of $h_{1,m}$ as the gradient of the entropy change decreases with increasing superheating (note logarithmic y -axis). The processes in the condenser and the sub-cooling were also modelled isobarically. The pressure range used here starts at 9 bar_g, which is approximately the minimum pressure of the installed system (see Table 8.3), and extends to 18.5 bar_g corresponding to the maximum ambient temperature for which the installed system was designed (Searle Manufacturing Company, 2008, p 4).

8.4.2 Description of main programme

The main programme has three loops as illustrated in Figure 8.15. The two outer loops are for the independent variables $\dot{Q}_e$ and ϑ_{on} for which the energy consumption E_{tot} is calculated. Their values are passed on to the programme in two vectors: $\vec{\dot{Q}}_e$ for the useful refrigeration effect as the load of the system and $\vec{\vartheta}_{on}$ for the ambient temperature, which is the temperature of the air entering the condenser.

The main purpose of the third loop is to determine whether the air flow through the condenser is able to remove the rejected heat from the condenser at a given condenser pressure. It starts with the minimum value for p_c and loops through until it reaches its end value. Whilst doing this it calculates all the required enthalpies and the refrigerant mass flow rate $\dot{m}_{rf}$ as described in the next few sections. With these and other variables the main programme calls a separate function to calculate the fan speed. This function returns an error if the maximum air flow rate is insufficient. This causes the main programme to record a high value (i.e. 9e99) in the vector storing all values for the fan power for this inner loop. Otherwise the programme calculates the fan power consumption E_{fan} with the value for the speed of the condenser fan n_{fan} returned by the function.

Once the third loop has calculated all the possible combinations, the lowest possible compressor power consumption is identified taking into consideration only values for

which the function did not return an error. This is than stored in a vector for displaying the results after all values in $\vec{\dot{Q}}_e$ and $\vec{\vartheta}_{on}$ have been processed.

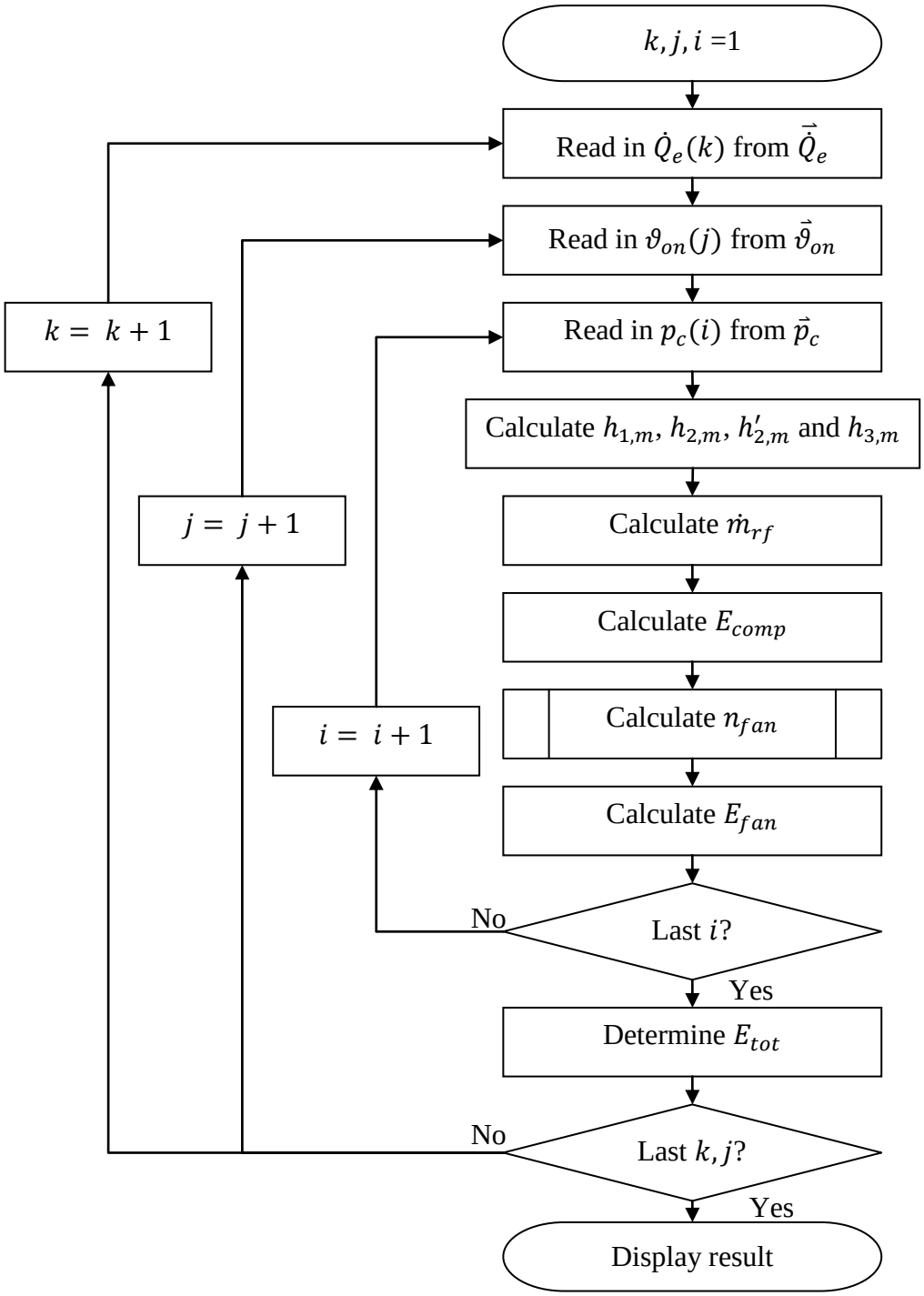

Figure 8.15: Flowchart of main programme of the Matlab model

8.4.2.1 Heat exchanger

The liquid-to-suction heat exchanger in Figure 8.13 transfers the heat energy from the high temperature, high pressure stream to the low temperature, low pressure stream and

achieves sub-cooling the liquid and superheating the vapour at the same time (Stoecker and Jones, 1983, pp 200 - 202). This allows using $h_{1,m}$ and $h_{3,m}$ to calculate the specific refrigeration effect $\dot{q}_e$, instead of $h_{5,m}$ and $h_{4,m}$ as indicated in Figure 8.14 eliminating the need for $h_{4,m}$. To derive the relationship between these two streams, Equation 8.2 can be applied to a control volume around the cold refrigerant stream section. If

$$\dot{q}_{h,in} = h_{3,m} - h_{4,m}$$

Equation 8.26

Where:

$\dot{q}_{h,in}$: Specific heat rate from the hot stream

$h_{3,m}$: Specific enthalpy of the hot stream entering the heat exchanger

$h_{4,m}$: Specific enthalpy of the hot stream leaving the heat exchanger

then the following equation can be written.

$$h_{3,m} - h_{4,m} = h_{1,m} - h_{5,m}$$

Equation 8.27

Where:

$h_{1,m}$: Specific enthalpy of the cold stream leaving the heat exchanger

$h_{5,m}$: Specific enthalpy of the cold stream entering the heat exchanger

The model used here is based on the effectiveness-NTU method (Incropera and DeWitt, 1985, pp 561-562). The effectiveness ε is defined as in Equation 8.28.

$$\varepsilon \equiv \frac{\dot{Q}}{\dot{Q}_{max}}$$

Equation 8.28

Where:

$\dot{Q}$: Actual heat transfer rate

$\dot{Q}_{max}$: Maximum possible heat transfer rate

When noting that

$$\dot{Q}_{max} = \dot{m}_{rf} \; c_{p,min} \left(\vartheta_{l,sat} - \vartheta_{g,sat}\right)$$

Equation 8.29

and that the specific heat constant in the vapour region of interest, $c_{p,vpr}$, is smaller than the specific heat constant in the liquid region of interest and therefore is equal to $c_{p,min}$, one can derive Equation 8.30 for the specific heat q_{HX} which takes the refrigerant from $h_{5,m}$ to $h_{1,m}$. Because $c_{p,vpr}$ changes only by 0.0421 kJ/kg/J (about 5%) from the saturated vapour point to the maximum recorded suction temperature, the average $\bar{c}_{p,vpr}$ of 0.872 kJ/kg/K was used.

$$\dot{q}_{HX} = h_{1,\mathrm{m}} - h_{5,\mathrm{m}} = \varepsilon\, \bar{c}_{p,vpr}\left(\vartheta_{l,sat} - \vartheta_{g,sat}\right)$$

Equation 8.30

From the measurements for the installed refrigeration system, ε as a function of $\dot{Q}_e$ could be constructed. This is shown in Figure 8.16 and the corresponding equation, Equation 8.31, has an r^2 of 0.864.

$$\varepsilon = 0.857 + 1.68 \times 10^{-3} \frac{1}{\mathrm{kW}} \times \dot{Q}_e - 5.52 \times 10^{-5} \frac{1}{\mathrm{kW}^2} \times \dot{Q}_e^2$$

Equation 8.31

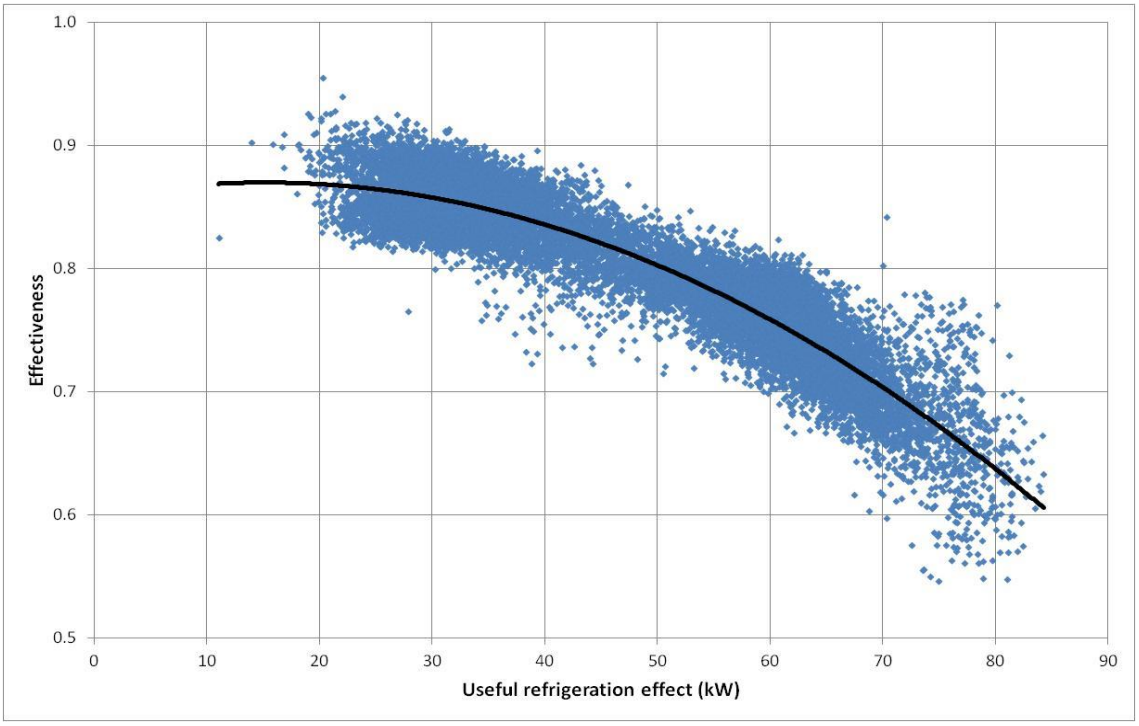

Figure 8.16: Heat exchanger effectiveness vs useful refrigation effect

The input temperatures were approximated by temperatures for the saturated vapour, $\vartheta_{g,sat}$, of -8.8 °C and the statured liquid, $\vartheta_{l,sat}$ as a function of the discharge pressure. Based on R404A data for the pressure range from 9 $\mathrm{bar_g}$ to 18.5 $\mathrm{bar_g}$ the following equation was

derived ($r^2 = 1$). This equation is slightly different from Equation 8.18, because the pressure range is different.

$$\vartheta_{l,sat} = -19.14\ ℃ + 4.69\ \frac{℃}{\mathrm{bar_g}}\ p_c - 0.0772\ \frac{℃}{\mathrm{bar_g^2}}\ p_c^2$$

Equation 8.32

8.4.2.2 Modelling compression

Before the compression process was modelled as isentropic it was investigated to see if this assumption gave a reasonable approximation of the measured data. To test this assumption the difference between h_2 and h_1 in the actual system was multiplied by the mass flow rate of all four compressors to compute the theoretical work input to the installed system, $E_{theo,inst}$. These results were compared with the measured power consumption for when the fan VSD signal was less than 25% (corresponding to a maximum fan power consumption of 119 W) so that the calculation related to the compressor consumption.

A constant entropy compression process follows the chain lines in Figure 8.14, in which logarithmic plot they are shown as straight lines with decreasing slopes towards higher enthalpy. Therefore the $slope$ had to be calculated first as a function of h_1 in order to be able to calculate h_2 afterwards. Using R404A data (Skovrup *et al*, 2012) Equation 8.33 was developed.

$$slope = 0.124\ h_1 - 24.8\ \frac{\mathrm{kJ}}{\mathrm{kg}}$$

Equation 8.33

With the $slope$ from this equation the estimated discharge enthalpy h_2 was calculated with Equation 8.34. This allowed the calculation of the theoretical power input as described above.

$$h_2 = slope\ \times ln\left(\frac{p_{c,abs}}{p_{e,abs}}\right) +\ h_1$$

Equation 8.34

The scatter plot in Figure 8.17 shows that a linear model describes the relationship between the theoretical work input according to the measure data, $E_{theo,inst}$, and the actual compressor power[5] well (r^2 =0.957) . This supports the idea of modelling this process as

[5] The actual power is the power supplied to the compressor motor, controllers and other ancillary equipment, and thus is not related to the isentropic efficiency.

isentropic. The scaling factor and offset can be attributed to the compressor motors and other system components.

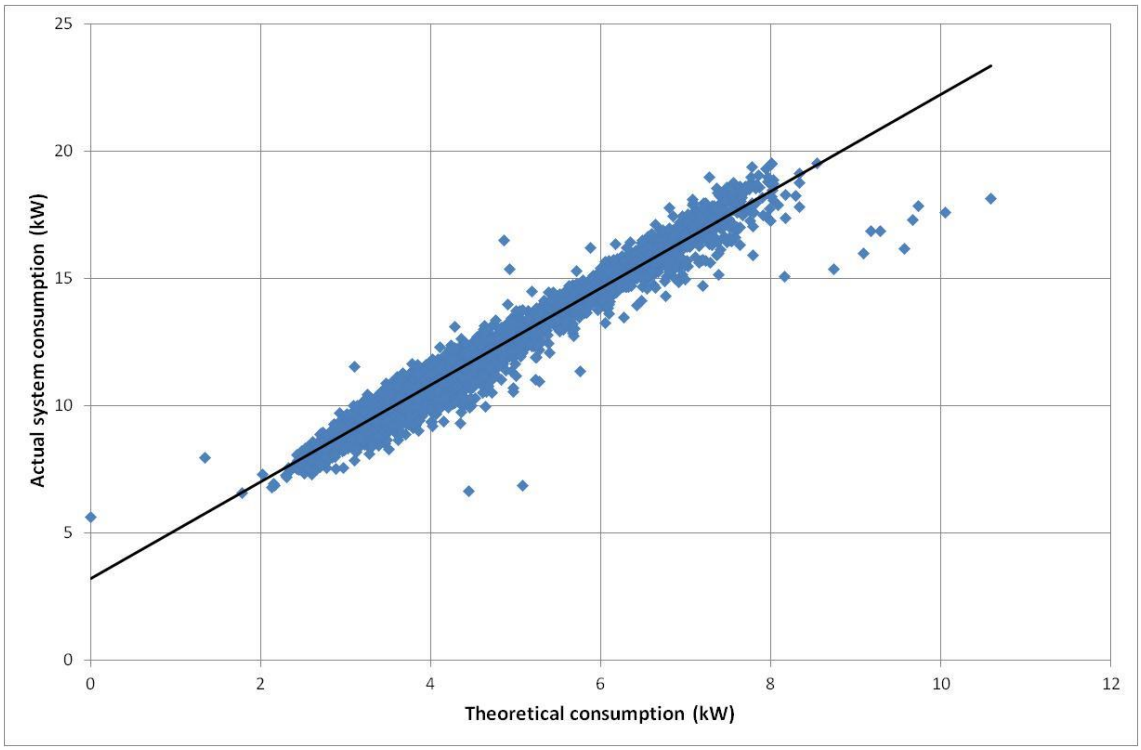

Figure 8.17: Scatter plot of the actual system consumption (excluding condenser fans) vs the theoretical power consumption

The actual compression process is more involved. What looks like an isentropic process may be the effect of two phenomena which cancel each other out. On the one hand, the friction in the compressor will add some heat to the refrigerant, thus increasing its enthalpy. On the other hand, the refrigerant will have lost some heat energy through the compressor head and connecting pipe work so that the overall effect looks like an isentropic compression (Arora, 2010, p 125). Nonetheless, the discussion above showed that the assumption of isentropic compression is supported by the measured data.

Based on this investigation $h_{2,m}$ was calculated as shown below. In this equation the $slope$ was also calculated with Equation 8.33.

$$h_{2,\mathrm{m}} = slope \times ln\left(\frac{p_{c,abs}}{3.5\ \mathrm{bar_g} + 1\ \mathrm{bar}}\right) + h_{1,\mathrm{m}}$$

Equation 8.35

Another approach to calculating $h_{2,m}$ could have been to use Equation 8.3 and Equation 8.6. Equating these two equations and solving them for $h_{2,m}$ yields Equation 8.36.

$$h_{2,m} = \frac{\gamma}{\gamma - 1}\ 4.5\ \mathrm{bar_g}\ v_{in} \left[\left(\frac{p_{c,abs}}{4.5\ \mathrm{bar_g}} \right)^{(\gamma-1)/\gamma} - 1 \right] + \mathrm{h_{1,m}}$$

Equation 8.36

However, James (1976, p 4.20), who used a similar approach, had to first estimate his constants and then adjust them to fit actual data. Therefore it was decided to derive Equation 8.35 based on the p-h diagram rather than using the $v\ dp$ integral. The chosen method yields acceptable results and was considered simpler than the $v\ dp$ integral approach.

8.4.2.3 Condenser

The constant pressure process in the condenser shown in Figure 8.14 first de-superheats the refrigerant from $h_{2,m}$ to $h'_{2,m}$ and then condenses it to $h_{3,m}$ by rejecting the heat to the air which is forced through the condenser. This means that the refrigerant temperature in the condenser is not constant. Nonetheless Stoecker and Jones (1983, p 248) suggest treating the condenser processes as isothermal. Here, however, a more realistic approach has been chosen to account for the de-superheating process. Out of the three steady-state methods described by Ding (2007), the one used here is based on the zone method with only two zones: The de-superheating zone and the condensing zone (see also Figure 8.18).

From Figure 8.18 it is evident that the total heat rejected, $\dot{Q}_c$, and therefore the heat taken up by the air stream through the condenser, is the sum of $\dot{Q}_1$ and $\dot{Q}_2$. Hence, a Matlab function (see Figure 8.20) was written that checks if the air mass flow rate is sufficient to cope with the condenser load $\dot{Q}_c$. This is done by assuming that the condenser temperature at a certain point is higher than the temperature of the air leaving this point by a constant offset k of 2 K. This together with the assumption of an isochoric process (see Equation 8.9) allowed the calculation of the required $\dot{m}_{air,1}$ and $\dot{m}_{air,2}$.

$$\dot{m}_{air,cdg} = \frac{\dot{Q}_1}{c_{air}\left(\vartheta_{l,sat} - k - \vartheta_{on}\right)}$$

Equation 8.37

$$\dot{m}_{air,dsh} = \frac{\dot{Q}_2}{c_{air}\left(\bar{\vartheta}_2 - k - \vartheta_{on}\right)}$$

Equation 8.38

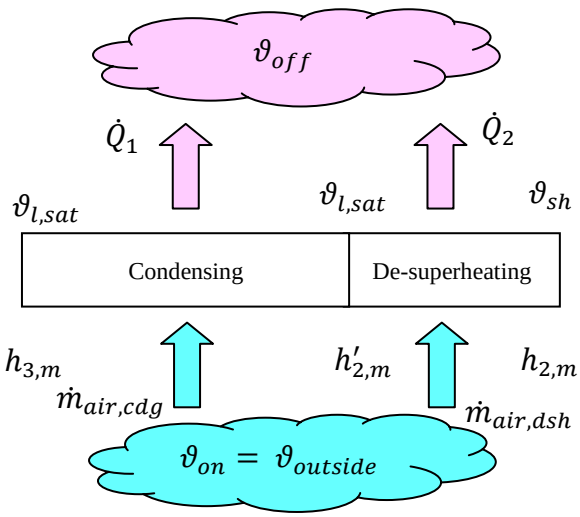

Figure 8.18: Condenser model

If a linear temperature distribution can be assumed, then the average temperature for the de-superheating section may be written as:

$$\bar{\vartheta}_2 = \frac{\vartheta_{sh} + \vartheta_{l,sat}}{2}$$

Equation 8.39

The total required air mass flow rate is then the sum of $\dot{m}_{air,cdg}$ and $\dot{m}_{air,dsh}$.

8.4.2.4 Condenser fan

The air mass flow rate $\dot{m}_{air}$ through the condenser is coupled to the condenser pressure through control laws (Searle Manufacturing Company, 2008, p 70). The actual control values, which were remotely accessed, were the target value of 10 bar_g and the control band of ±0.5 bar. The data clouds for day and night time operation in Figure 8.19 indicate, that, in the pressure range of interest, the VSD signal quickly rises from close to zero to maximum, but the dependency on the condenser pressure is not as strong as the description in the user's manual suggests. It is also apparent that the relationship between the VSD signal and the condenser temperature is non-linear. It was decided to use a logistic function to model this behaviour, because this type of function allows modelling of the steep rise at the beginning of the active region before the tapering off. The parameters for the two curves in Figure 8.19 were graphically determined and differ only by the factor n_{max}.

$$n_{fan\%}\,(p_c = 9.5 - 10.5\ \text{bar}_\text{g}) = \frac{n_{max}}{1 + 0.25\,exp\left(-15\ {}^{1}/_{\text{bar}_\text{g}}\ (p_{c,g} - 10\ \text{bar}_\text{g})\right)}$$

Equation 8.40

Where:

$n_{fan\%}$: Speed of condenser fan in % of total maximum fan speed

n_{max}: Maximum fan speed (day time operation: 53% of total maximum fan speed, night time operation: 100% of total maximum fan speed)

$p_{c,g}$: Condenser pressure in bar_g

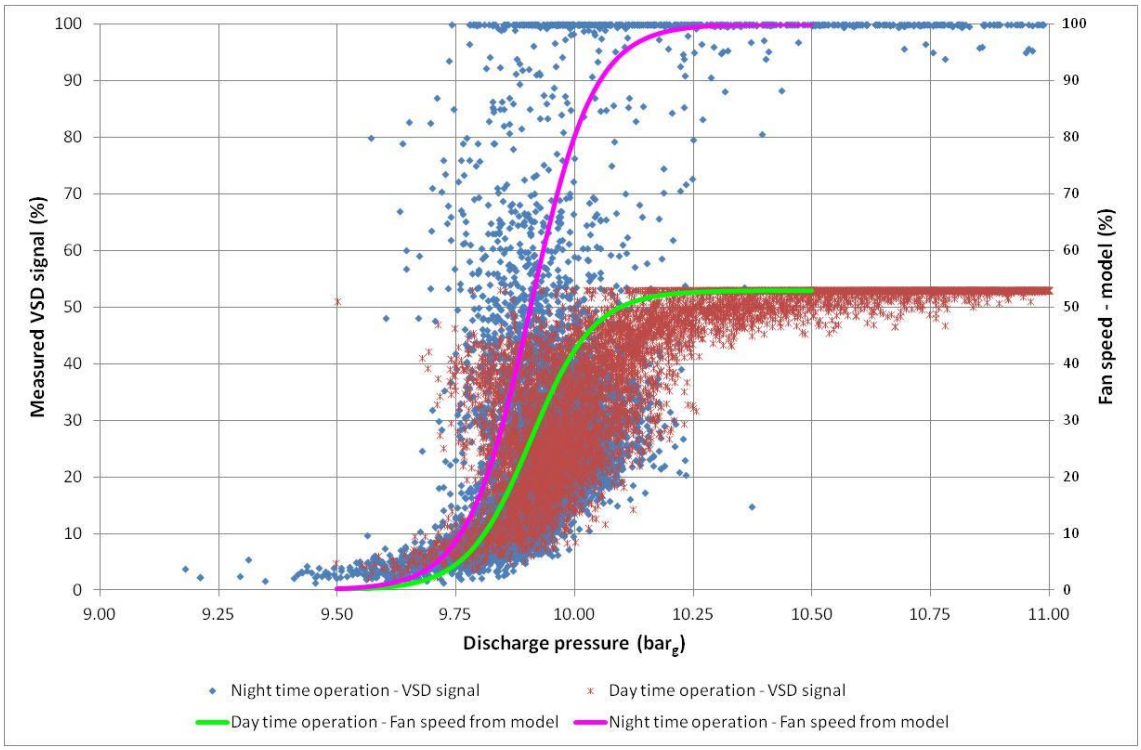

Figure 8.19: VSD signal for the fan with fan model for the software simulation overlaid

This equation allows the stating of the overall equation for the fan speed as shown in Equation 8.41. The air mass flow rate can then be calculated as $n_{fan\%} \times \dot{m}_{air,max}$, where $\dot{m}_{air,max}$ is 27.9 m^3/s (GEA Searle, 2015).

$$n_{fan\%} = \begin{cases} 0, & p_c < 9.5\text{bar}_\text{g} \\ \dfrac{n_{max}}{1 + 0.25\, exp\left(-15\left(p_c\, {}^{1}/_{\text{bar}_\text{g}} - 10\ \text{bar}_\text{g}\right)\right)}, & 9.5\text{bar}_\text{g} \leq p_c \leq 10.5\text{bar}_\text{g} \\ n_{max}, & p_c > 10.5\text{bar}_\text{g} \end{cases}$$

Equation 8.41

The Matlab function which calculates the fan speed (see Figure 8.20) converts $n_{fan\%}$ to its corresponding mass flow rate in order to calculate the maximum value of heat the air can

remove. This allows the simulating of the natural convective mode below 9.5 bar_g with a constant value for $\dot{Q}_c$ of 15kW (this estimate was based on the measured data).

If the error variable returns a one, 9e99 is recorded for this condenser pressure indicating that the condenser pressure is insufficient. Otherwise the power consumption E_{fan} computed with Equation 8.42 (ASHRAE, 2008, p 20.4) is entered.

$$E_{fan} = 7.6 \text{ kW } n_{fan}^3$$

Equation 8.42

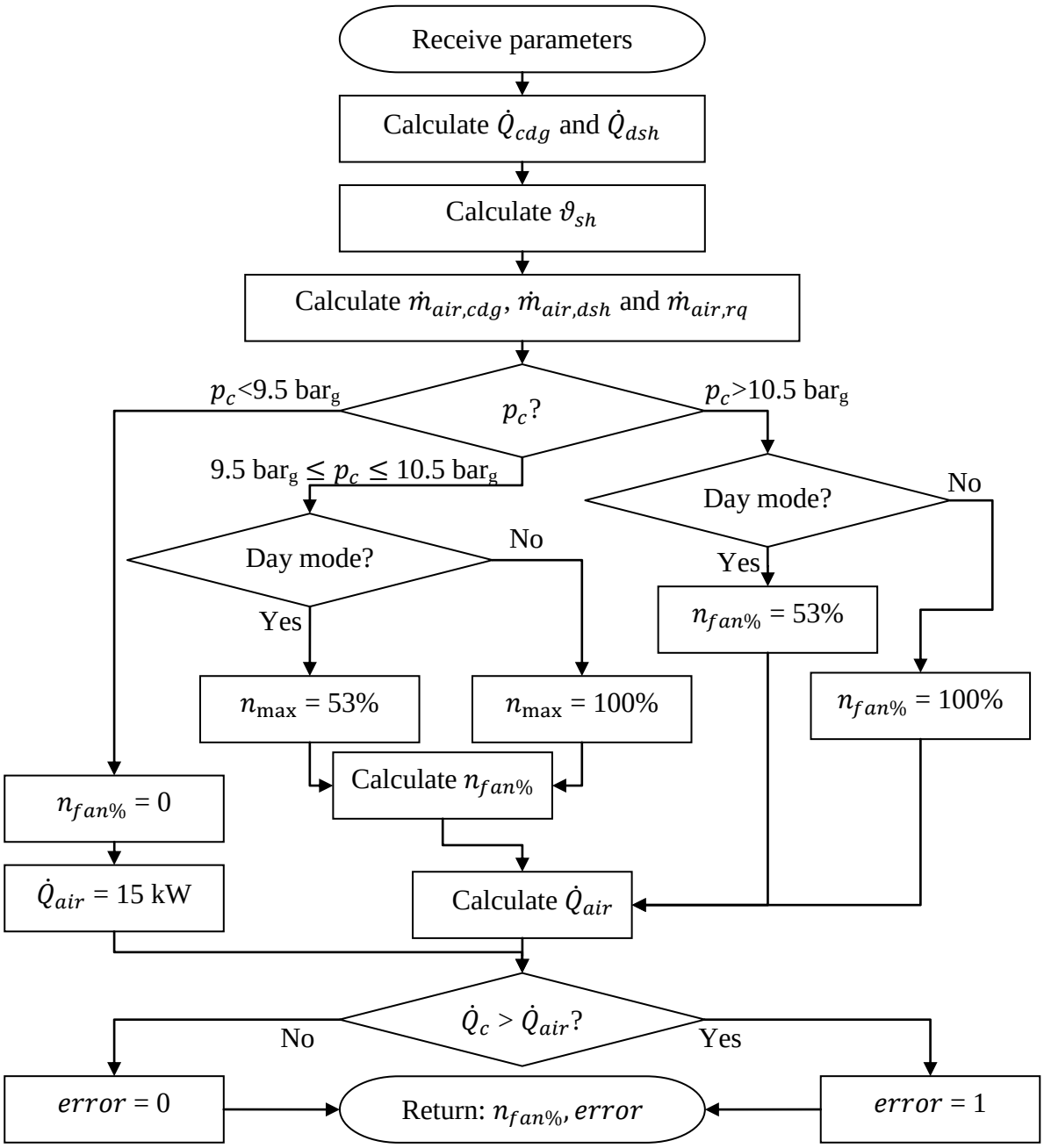

Figure 8.20: Flowchart for calculating the condenser fan speed

8.4.2.5 Expansion device

The electronic expansion valve was modelled as an isenthalpic throttling process. This means that when passing through this restriction the pressure and temperature of the refrigerant is reduced, but the enthalpy remains the same. Therefore the enthalpy $h_{4,m}$ in Figure 8.14 at the end of the sub-cooling process can be used to calculate the useful refrigeration effect. As mentioned earlier, $h_{1,m}$ and $h_{3,m}$ are used in conjunction with the useful refrigeration effect, because the difference between them is the same as between $h_{5,m}$ and $h_{4,m}$.

8.4.2.6 Evaporation and mass flow rate

In this Matlab model the isobaric evaporation process takes the refrigeration effect $\dot{Q}_e$ as the input argument, which allows the calculation of the required mass flow rate as shown in Equation 8.43 (ASHRAE, 1997, p 1.8).

$$\dot{m}_{rf} = \frac{\dot{Q}_e}{h_{1,\mathrm{m}} - h_{3,\mathrm{m}}}$$

Equation 8.43

8.4.2.7 Power consumption of compressor

As the compression process is treated here as isentropic, the theoretical power input E_{theo} into the refrigeration cycle can be calculated with the following equation (ASHRAE, 1997, p 1.8).

$$E_{theo} = \dot{m}_{rf}\left(h_{2,\mathrm{m}} - h_{1,\mathrm{m}}\right) = \dot{Q}_e \frac{h_{2,\mathrm{m}} - h_{1,\mathrm{m}}}{h_{1,\mathrm{m}} - h_{3,\mathrm{m}}}$$

Equation 8.44

8.4.3 Calibration

After the model was debugged, it was calibrated against the measured data. The first step in this process was to relate E_{theo} to the measured consumption of the compressors. In order to achieve this the Matlab programme was modified so that it could calculate the E_{theo} with $\dot{Q}_e$, $\vartheta_{outside}$ and a variable indicating day/night time operation as input vectors.

The measured data includes not only the compressor consumption, but also the power consumption of the condenser fans and auxiliary equipment. Because the model adds the fan power to the total power input separately, an equation could be developed estimating the power consumption of the compressors and auxiliary equipment as a function of the E_{theo}. This idea led to the evaluation of the following three possible scenarios for the VSD signal: less than 20%, 30% and 40%. For a VSD signal of less than 40% the fan power consumption is ($0.4^3 \times 7.6$ kW =) 0.49 kW, which is less than 10% of the total measured power consumption. For the equations in Table 8.8 outliers (such as cooling load = 0 and C2 above 90%) were eliminated.

Table 8.8: Possible equations for E_{comp}

VSD signal	Equation	r^2
<20%	$E_{\text{comp}} = 1.93 \times E_{theo} + 3.07$ kW	0.955
<30%	$E_{\text{comp}} = 1.94 \times E_{theo} + 3.13$ kW	0.966
<`40%	$E_{\text{comp}} = 1.98 \times E_{theo} + 3.07$ kW	0.965

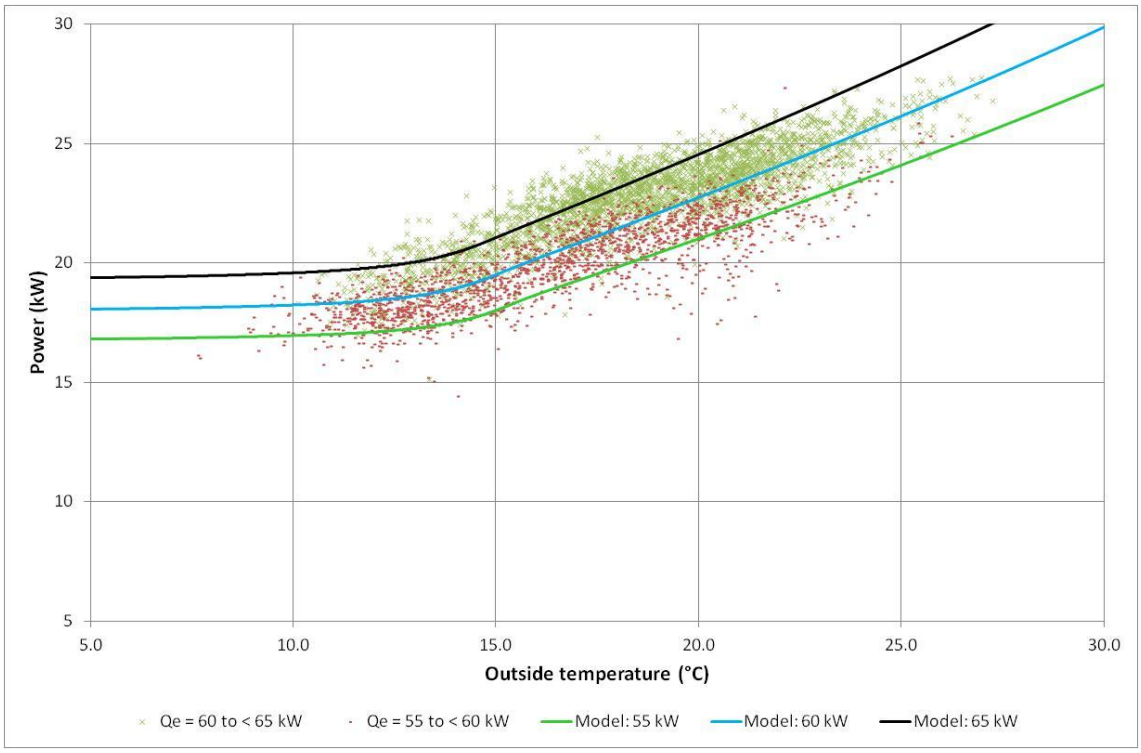

Figure 8.21: The measured data overlaid by the modelled data (day time operation)

The coefficients of determination in Table 8.8 show a good agreement for a linear model. In order to decide which set of coefficients give the best results, the model was run in day mode for cooling loads equal to 55 kW, 60 kW and 65 kW, and for the following values in night mode: 27.5 kW, 32.5 kW and 37.5 kW. These values were selected because they are

the bands used in Figure 8.9 and Figure 8.10 and, therefore, a meaningful comparison between the model output and the measured data was straightforward. These tests showed that the equation for the 20% VSD signals yielded the best results. However, the average fan power from the model was 62.7 kW, whereas the average consumption based on the VSD values was only 20 W. The difference was subtracted from the intercept to give Equation 8.45.

$$E_{\text{comp}} = 1.93 \times E_{theo} + 3 \text{ kW}$$

Equation 8.45

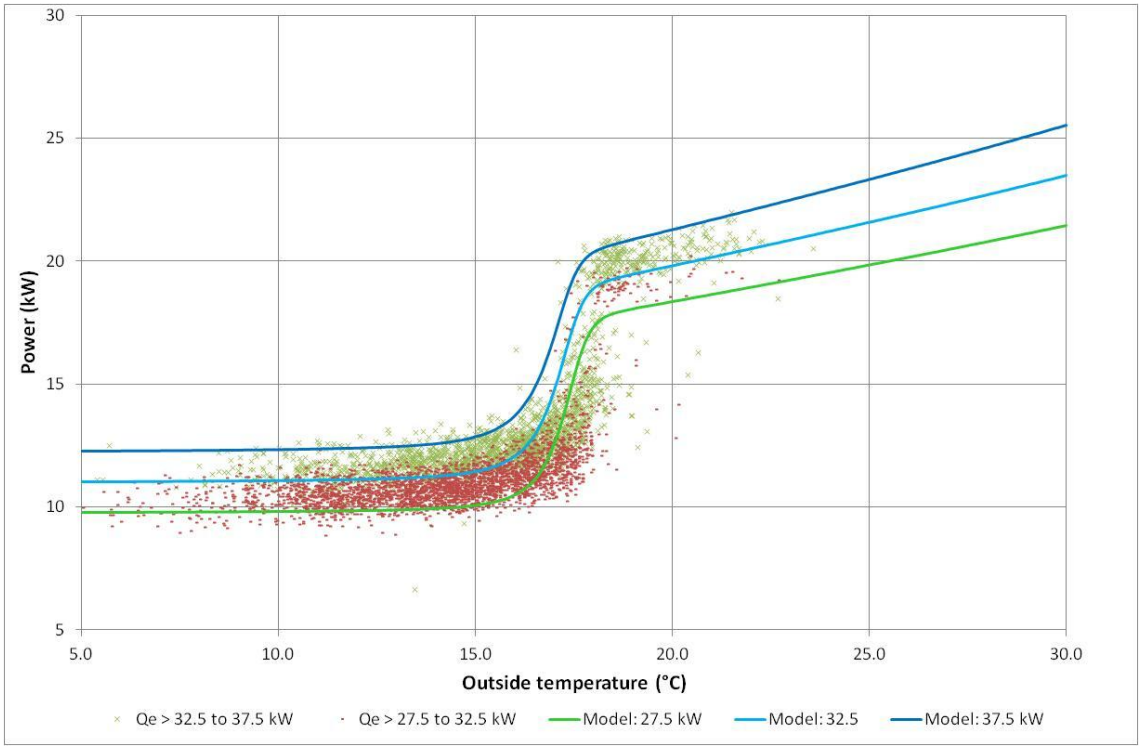

Figure 8.22: The measured data overlaid by the modelled data (night time operation)

Finally, Equation 8.45 was used to verify a good fit of the model for day and night time operations. Figure 8.21, which shows the results for the day time operation, indicates that the lower limit at 55 kW bounds the data cloud well. For a temperature range of between 13°C and 23°C data points spill over the upper model prediction. The graphs for the night time operation shown in Figure 8.22 also generally show a good agreement.

8.4.4 Error estimation

To further evaluate the accuracy of the model, error scatter plots were developed and the $RMSE$ and the MBE were calculated. The values in the scatter plots in Figure 8.23 and Figure 8.24 were normalised against the maximum measured value, i.e. also the estimated

power consumption is expressed in percentages of the measured maximum. Both figures display a green centre line, which indicates when the value from the software model exactly agrees with the measure value. The chain lines indicate the ±10% and the dashed line the ±20% limits.

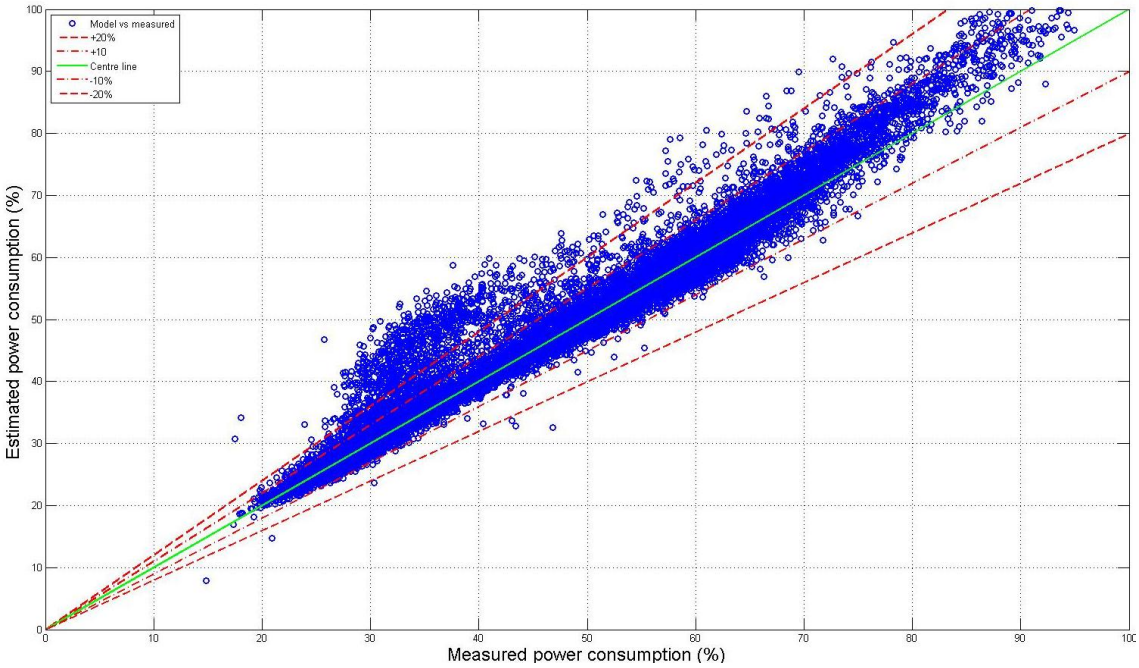

Figure 8.23: Scatter plot of the estimation from the model vs the measured data from the refrigeration system No. 1

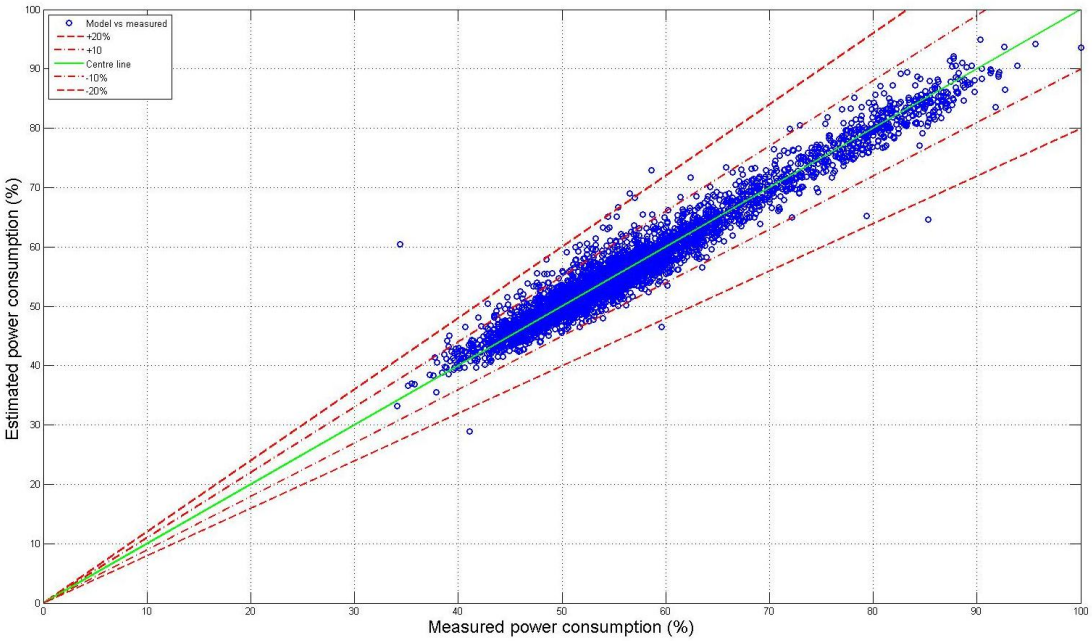

Figure 8.24: Scatter plot of the estimation from the model vs the measured data from the refrigeration system No. 1 for the data points where the fan VSD signal less than 20%

Figure 8.23 shows that the majority of data points (88.5%) lie between the ±10% boundaries. From approximately 75% (measured consumption) onwards the model tends to overestimate the consumption. From approximately 28% to about 40% the model overestimates the consumption for a number of data points, which may be due to the way the fan control has been simulated. The scatter plot in Figure 8.24 uses only the data points for when the fan VSD signal is less than 20%. Similar to Figure 8.23, most of the data points are within the ±10% limits, and only a few exceed the ±20% boundaries.

The $RMSE$ was calculated for all the data points and found to be 1.43 kW or 8.22% of the average measured consumption. The MBE is 0.480 kW indicating that for the data set used the model tends to overpredicts the energy consumption.

8.4.5 Summary of software model results

The model developed above contains a number of simplifications such as using a constant air temperature difference for the condenser or an isentropic process for the compressor. In addition, the control of the fans could not capture the spread of the measured data well. Notwithstanding that, almost 90% of simulation results for the measured data fall within the ±10% error band and the overall $CV(RMSE)$ is 8.22%, therefore it can be concluded that the model captures the main features of the refrigeration system with adequate accuracy.

8.5 Response to climate change

This section describes how the change in energy consumption of the refrigeration system due to climate change was estimated. It contains a method section explaining how the software model developed above was used and what further assumptions were made. The part headed 'Results' displays the results based on the medium emission scenario for the 2030s. The discussion which follows restricts its comments to this chapter. A discussion relating the results here to other chapters can be found at the end of this thesis.

8.5.1 Method of estimation

In order to use the software model, the following, three input vectors were required: a temperature vector, a cooling load vector and a vector specifying the operation of the refrigeration system (i.e. day/night time operation). The TRY data files for the 2030s and the base period (1970) for Hull were downloaded from the website from the Centre for

Energy and the Environment, The University of Exeter (2010). This data is based on the weather generator introduced in Section 3.3 and contains probabilistic data derived from the UKCP09 (Eames *et al*, 2011). Amongst other data, these files contain hourly dry-bulb temperatures, which were used for the four temperature vectors (base period temperature, 10% probability, central estimate and 90% probability of future temperature).

Since the temperature data was only available as hourly data, the other input vectors were also hourly. As the refrigeration model was developed and tested with quarter hourly data, it was deemed advisable to test the software with hourly data. To this end the test vectors used for the calibration of the software model in Section 8.4.3 were averaged for every four values so that the hourly average for day and night operation for the six months was available (see Appendix for Matlab function developed). Figure 8.25, which was based on hourly data, shows a very similar pattern to Figure 8.23 inasmuch as most data remains within the ±10% error boundary. Also the model starts to systematically overestimate the power consumption from approximately 75% measured consumption onwards. The MBE of 0.527 kW and the $RMSE$ of 1.37 kW ($CV(RMSE)$ = 8.22%) are also very close to the values for 15 min data. The slight difference may be owing to the averaging of operation modes, as the programme can deal only with day or night time mode, but not with an input mixing these. Therefore, it can be concluded that using the software model with the hourly temperature data should yield valid results.

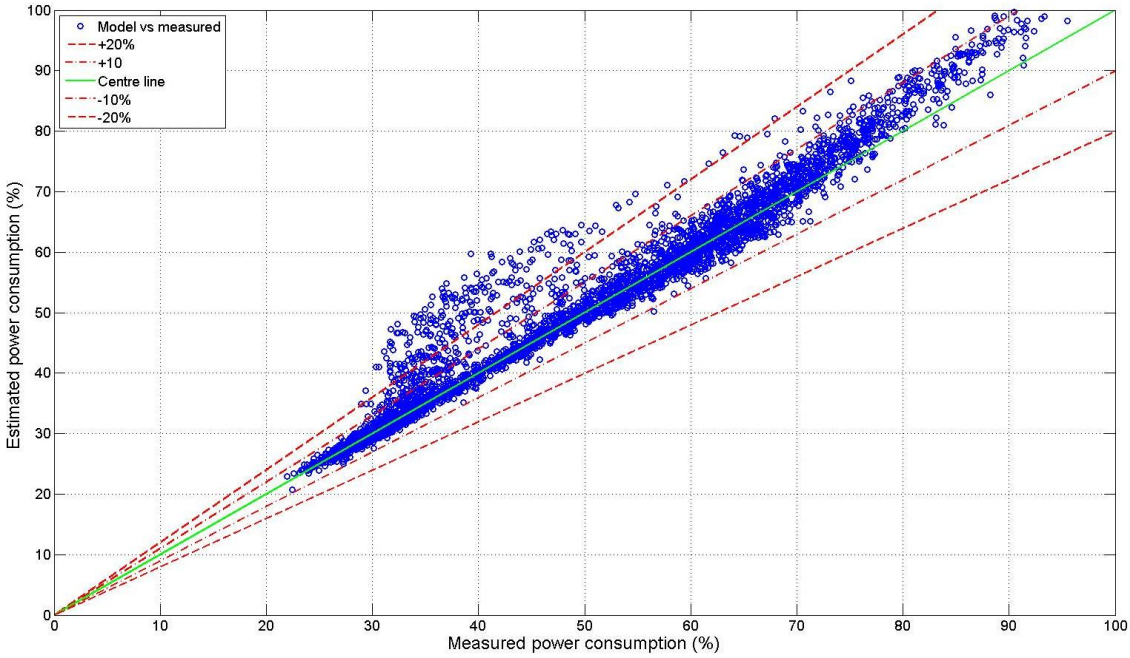

Figure 8.25: Scatter plot of the estimation from the model vs the measured data from the refrigeration system No. 1 with hourly data

In order to generate the four vectors for $\dot{Q}_e$, the relationships between the cooling load and the outside temperature and relative humidity were investigated. The relative humidity was considered because it has been shown that the inside humidity has an impact on the cooling load (Kosar *et al*, 2005). The humidity data for July 2014 (the warmest month in the data series) and for November 2014 (the coldest month in the data series) was averaged over 15 min intervals because the refrigeration loads were calculated in 15 min intervals, and then used in SPSS (IBM, 2012) to evaluate the regression model in Equation 8.46 separately for the night and day time operation.

$$\hat{\dot{Q}}_e = a_0 + a_1\,\vartheta_{outside} + a_2\,\vartheta_{outside}^2 + a_3\,RH_{out} + a_4\,RH_{out}^2 + a_4\,\vartheta_{outside}\,RH_{out}$$

Equation 8.46

This investigation suggested that there was no statistically significant relationship between the relative humidity and the cooling load for the day time operation. For the night time mode the predictive power with and without relative humidity was low. Therefore relative humidity was excluded as a predictor for $\dot{Q}_e$.

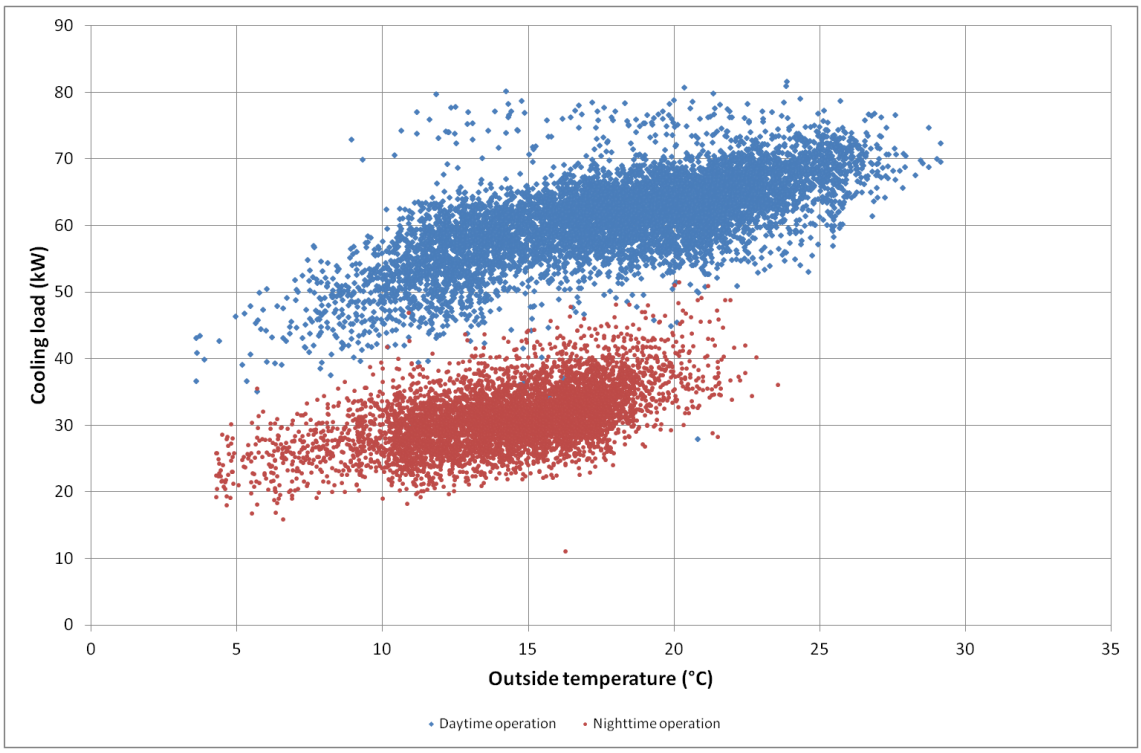

Figure 8.26: $\dot{Q}_e$ as a function of the outside temperature and operation mode

The data clouds in Figure 8.26 are for day and night time operations with outliers (e.g. due to stocking) having been removed. They show that there is an apparent divide between day time and night time operations. The scatter for the night time operation shows a medium

correlation with the temperature (correlation coefficient = 0.54). This is plausible as the refrigerated cases were covered to reduce the cooling load and the HVAC system was not in operation. Also, casual gain from other equipment was low as the light was switched off and staff and customers were not present. Therefore Equation 8.47 was used for the night time operation for the cooling load for all load vectors.

$$\hat{\dot{Q}}_e = 0.792 \frac{\text{kW}}{°\text{C}} \vartheta_{out} + 19.8 \text{ kW}$$

Equation 8.47

The linear model (with a correlation coefficient of 0.68) in Equation 8.48 for the day time operation was preferred to a third order polynomial equation because this model was used outside its data span. It was judged that a linear model gave more credible results, e.g. at the minimum temperature in the future weather files of -7.8°C a third order model suggested a cooling load of -41.0 kW and the linear model 36.1 kW.

$$\hat{\dot{Q}}_e = 0.971 \frac{\text{kW}}{°\text{C}} \vartheta_{out} + 43.7 \text{ kW}$$

Equation 8.48

8.5.2 Results

The results in Table 8.9 are for the base year 1970 and the TRY 2030 with three different likelihoods. For these probabilities the consumption figures represent the maximum value, e.g. for the 10% case this means that there is a 10% likelihood for the consumption to be equal to or less than this value if the relationship with the outside temperature is represented correctly.

Table 8.9: Simulation estimates of the annual electricity consumption change of the refrigeration system

	Base	**10%**	**Central**	**90%**
$\bar{\vartheta}_{outside}$ (°C)	10.0	10.5	11.7	13.0
Consumption (kWh)	124000	126000	132000	140000
Change (kWh)		2160	7960	16000
Change (%)		1.74	6.41	12.9

The temperatures and total consumption figures in Table 8.9 show a linear relationship suggesting that, for every degree of annual average temperature increase, the energy consumption of the refrigerating system raises by approximately 5330 kWh pa.

The results here are based on tools and data available and therefore the accuracy of the results is limited by these. For instance, the software model used has a limited accuracy.

Furthermore as a predictor for the cooling load, only the outside temperature was used as the outside relative humidity did not improve the predictive power of the model. The large data spread seen in Figure 8.26 indicates that other predictors may be more powerful or necessary. However, as both data sets (measured data and predicted climate variables) had only these two predictors in common, no other variables could be considered.

To compare the results for the climate change impact on the refrigeration system investigated here with the outcomes from the assessment of the whole supermarket in Hull absolute values for the predicted changes in electricity use for the supermarket and for both refrigeration systems have been calculated. Table 8.10 lists these figures for the 2030s and the medium emission scenario. Both sets of figures show that, for a rise in temperature, an increase in energy consumption can be expected. This table also indicates that most, if not all of this increase in supermarket electricity use may be attributed to the refrigeration systems. This is plausible as almost all other electrical equipment can be regarded as non-temperature sensitive and the air conditioning systems total 25 kW installed cooling capacity or 18% of the nominal refrigeration capacity of both refrigeration systems.

Table 8.10: Comparing the electricity consumption of the model for the complete supermarket in Hull with the model for the refrigeration systems installed there.

	Base		**10% probability**			**50% probability**			**90% probability**		
	Elec. (kWh)	$\vartheta_{outside}$ **(°C)**	**Change (kWh)**	**Change (%)**	$\vartheta_{outside}$ **(°C)**	**Change (kWh)**	**Change (%)**	$\vartheta_{outside}$ **(°C)**	**Change (kWh)**	**Change (%)**	$\vartheta_{outside}$ **(°C)**
Supermarket	561000		3110	0.554		9420	1.68		18600	3.32	
Temperature		9.35			10.1			11.2			12.4
Pack No 1	12400		2160	1.74		7960	6.41		16000	12.9	
Pack No 2	84700		1470	1.74		5430	6.41		10900	12.9	
Temperature		10.0			10.5			11.7			13.0

Figure 8.27 visualises the table data and shows more clearly the effect of the change point in the supermarket model. It also shows that, beyond the temperature of approximately 11.4°C, the increase in refrigeration energy requirements is generally higher than that of the whole supermarket. One of the reasons for this may be that two different data collection periods were used, 2012 for the whole supermarket model and June 2014 to November 2014 for the refrigeration models. This might be significant because it is possible that the supermarket was operated in a slightly different way (e.g. different building timer settings or opening times). Another cause of inconsistency could be that the temperature data was prepared differently (hourly for the refrigeration model and weekly

for the supermarket model). The impact of this can be seen when considering the temperature averages, also given in the table, which are lower for the whole supermarket data. When testing the software model it was also noticed that, for higher temperatures, the model tends to overpredict the energy use. A further reason may be owing to how the cooling load was treated. In the investigating of the whole supermarket, the supermarket was regarded as a “black box” and, therefore, the cooling load was implicitly included in the model, whereas the cooling load had to be separately estimated for the refrigeration model. On the other hand, it might be possible that other equipment uses less electricity at higher temperatures, but, as only a hot water heating with a gas boiler is installed and no electric heating, this seems unlikely.

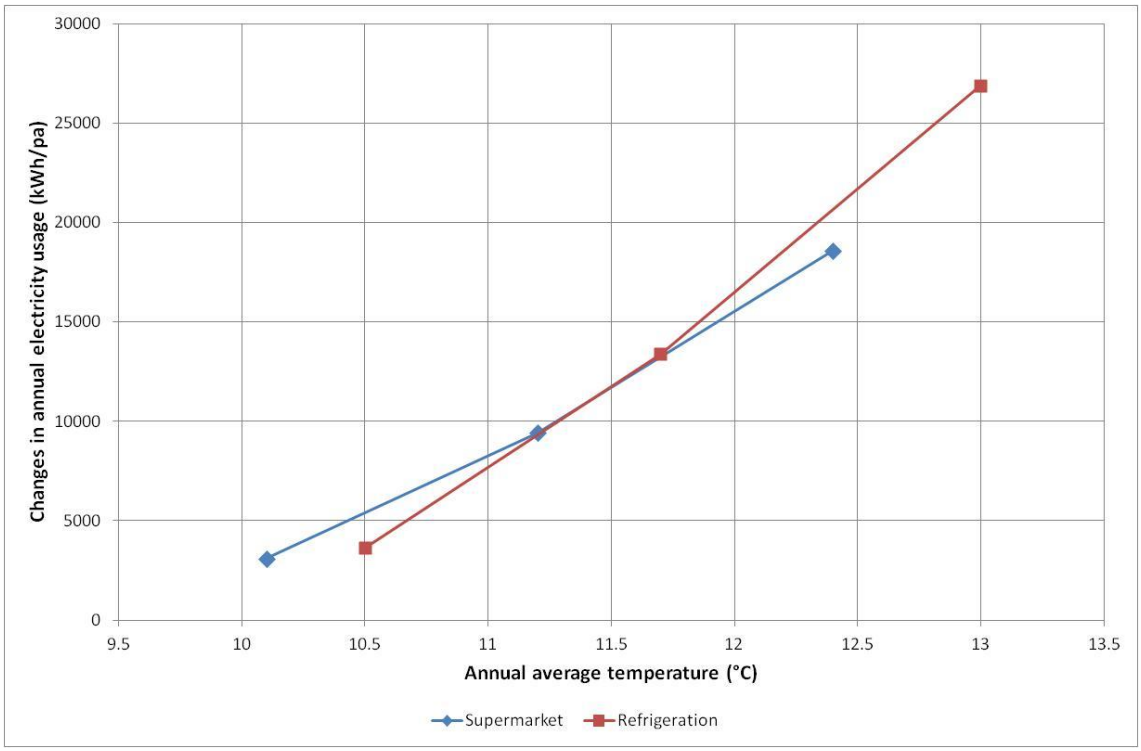

Figure 8.27: Comparing the estimates of absolute changes in annual electricity demand

A higher agreement could have been achieved by recalibrating the software model. However, it was not apparent that the simplifications used for the whole supermarket model had led to more accurate results. The section on climate change prediction also pointed out that those predictions had significant uncertainties attached to them. Therefore any investigation based on these predictions will not be able to compensate for them, but only add more to them. Taking these things into consideration it was not clear that new insight into the development of future energy consumption could have been gleaned for making these two models agree.

8.6 Improvements to condenser fan control

The air through the condenser removes the heat $\dot{Q}_c$ from the condenser. For a dry condenser an increase in $\dot{Q}_c$ can be met by either increasing the flow rate through the condenser or by increasing its temperature. Increasing the condenser temperature requires a rise in the compressor discharge pressure as indicted by Equation 8.17, which then in turn requires a larger work input to the refrigeration cycle by the compressor. This interdependency is well described by Manske *et al* (2001) who studied an industrial refrigeration system with an evaporative condenser. These authors pointed out that there was a trade-off between the power consumption of the compressor and the energy used by the fans. Contrary to Ge and Tassou (2000), who claim that the "fan power is only a small fraction of the total power consumption", it was found that, for the installed system, the maximum fan power is 95% of the maximum power of the compressors C1 and C4 (BITZER Kühlmaschinenbau GmbH, 2013).

The trade off between the compressor and condenser fan power seems to have been no thorough investigation performed for supermarket refrigeration systems. Some insight into this issue can be gleaned from work by Chan and Wu who investigated air cooled chillers. In one of their earlier works Chan and Yu (2002) modelled an air-cooled reciprocating chiller with a thermodynamic model and used it to investigate static head pressure and floating head pressure control. They found that for floating head pressure control the energy saved for running compressors as efficiently as possible is outweighed by the energy used to run more condenser fans. Three years later, Yu and Chan (2006) published work in which they included staged VSD condenser fans in their TRNSYS model. Their control algorithm included the staging of condenser fans in addition to speed control. The authors reported efficiency gains from the improved fan control which were dependent on the outside temperature and chiller load, hence they suggested using these as input parameters for fan controls. A later paper by Yu and Chan (2007), in which they employed their model to investigate a centrifugal chiller, includes a figure similar to Figure 8.23 and Figure 8.25 for compressor power. For their model the researchers reported that 95% of their data points were within the ±10% error limits.

Although work by Chan and Yu summarized in the previous paragraph suggests that the control strategy used in the Hull supermarket is sub-optimal, their results need to be verified for supermarket refrigeration systems. One reason for this is that refrigeration

systems generally have fewer condenser fans and they may be all controlled by the same VSD signal. A further reason is that, although these systems are comparable, their applications are different. Therefore this part of Chapter 8 studies the difference between a $COSP$ optimised supermarket refrigeration system and the software model of the installed system. Before this, a discussion on the difference between the COP and the $COSP$ is necessary to more fully appreciate the need to optimise the fan control. This is followed by a section describing how this improvement idea was implemented in the Matlab simulation. Results presented in the section after that indicate that the $COSP$ optimisation led to energy savings of approximately 4.5% for the data used in Section 8.3.

8.6.1 Difference between COP and $COSP$

The discussion below defines and contrasts the two ways of describing the efficiency of the refrigeration system mentioned in Section 8.2.1.5. The first is the coefficient of performance, which has the generic definition (ASHRAE, 1997, p 1.3):

$$COP \equiv \frac{\text{Useful refrigeration effect}}{\text{Net energy supplied from external sources}}$$

Equation 8.49

The denominator in this equation can be defined in a number of different ways. For instance, the same source (on page 1.8) analyses a theoretical single-stage cycle and equates the net supplied energy to the mass of the refrigerant multiplied by its enthalpy change. Obviously this does not take any compressor or motor losses into account. Probably this is why ASHRAE also gives compressor specific definitions of the energy (or rather power) supplied. In the handbook *HVAC Systems and Equipment* (ASHRAE, 2002, p 37.2), the power input is defined as either the electric power supplied to the motor terminals (for hermetic or semi-hermetic compressors) or as the mechanical power acting on the compressor shaft (for open compressors). This short discussion shows that (a) the well-known term COP may lead to misunderstandings as it can mean different things to different people, and (b) it does not consider any other energy requirements of the wider refrigeration system.

The performance figure $COSP$ can be used to clearly distinguish between the efficiency of the core refrigeration system, which may be characterized by a COP number, and the efficiency of the whole refrigeration plant. In other words, $COSP$ includes the additional

power consumption of equipment such as pumps and condenser fans as indicated in Equation 8.50 (Evans, 2008).

$$COSP = \frac{\dot{Q}_e}{E_{tot}} = \frac{\dot{Q}_e}{E_{comp} + E_{fan} + E_{other}}$$

Equation 8.50

It is also possible to create a relationship between those two efficiency coefficients as shown in Equation 8.51. For this equation it was assumed that E_{other} is much smaller than both E_{comp} and E_{fan} and, for this reason, can be neglected. Furthermore it was assumed that the compressor is semi-hermetic (as in the installed system) and therefore the COP equals $\dot{Q}_e/E_{comp}$.

$$COSP \cong \frac{COP}{1 + COP\,\frac{E_{fan}}{\dot{Q}_e}}$$

Equation 8.51

When analysing Equation 8.51 it is apparent that, when the fans are switched off, the COP is equal to the $COSP$. A less obvious result is that when $\dot{Q}_e$ (the cooling load) increases, the relative importance of the power use of the condenser fans diminishes. On the other hand, as the COP increases, so does the influence of fan power consumption. Figure 8.28 and Figure 8.29 visualize the results of this equation for one part load point ($\dot{Q}_e$ = 20% $\dot{Q}_{e,max}$) and for full load (the maximum fan power is assumed to be 10% of $\dot{Q}_{e,max}$). They show that the $COSP$ is influenced by the condenser fan, particularly under part-load conditions.

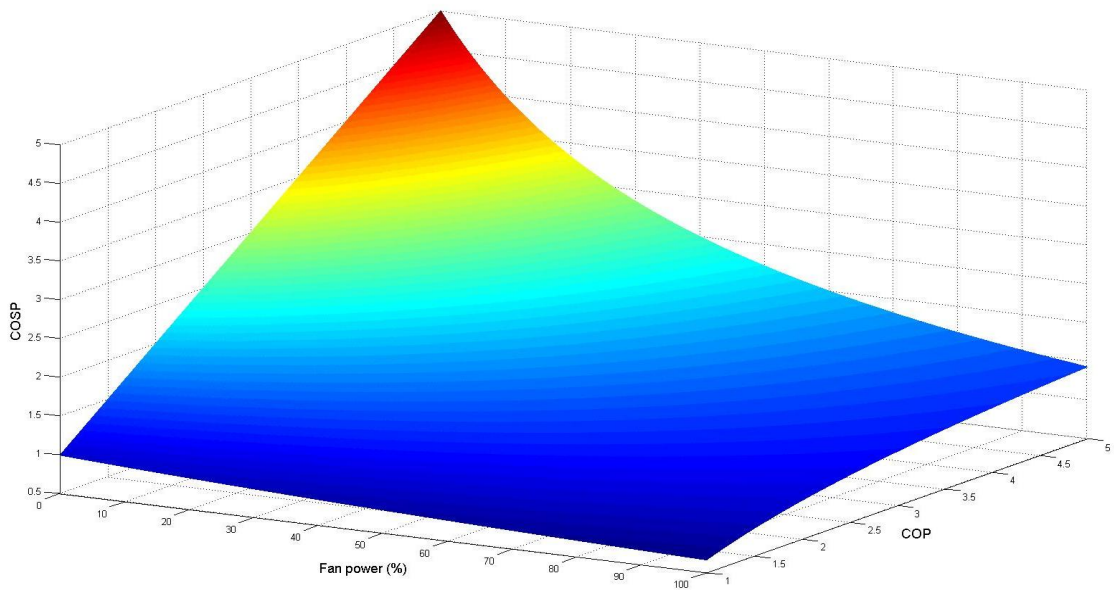

Figure 8.28: Surface of $COSP$ as a function of E_{fan} and COP for $\dot{Q}_e$ = 20% $\dot{Q}_{e,max}$

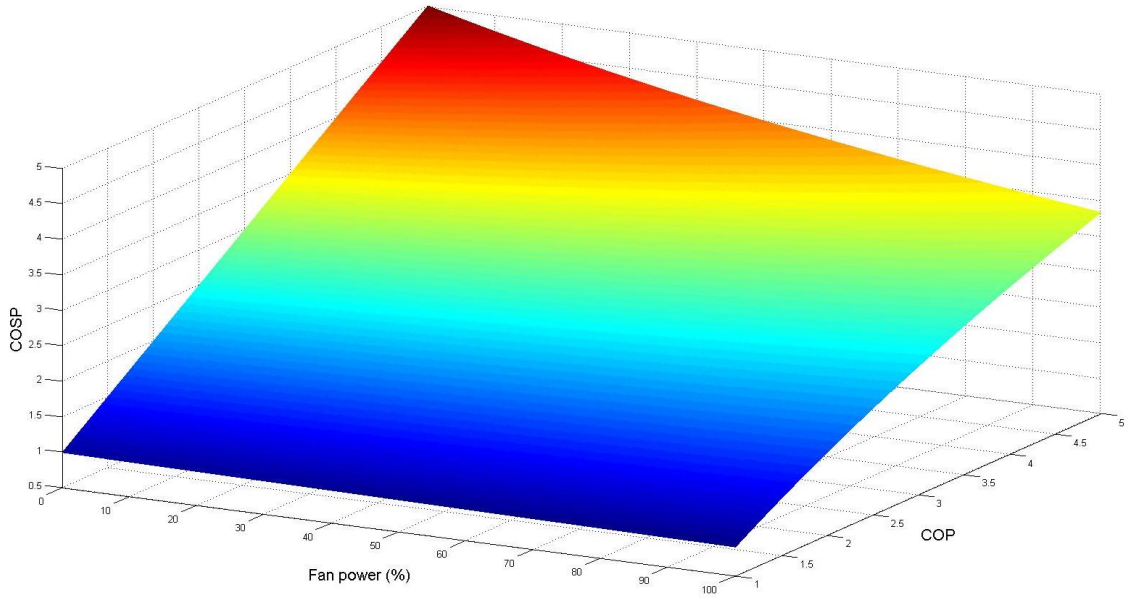

Figure 8.29: Surface of $COSP$ as a function of E_{fan} and COP for $\dot{Q}_e = 100\%\ \dot{Q}_{e,max}$

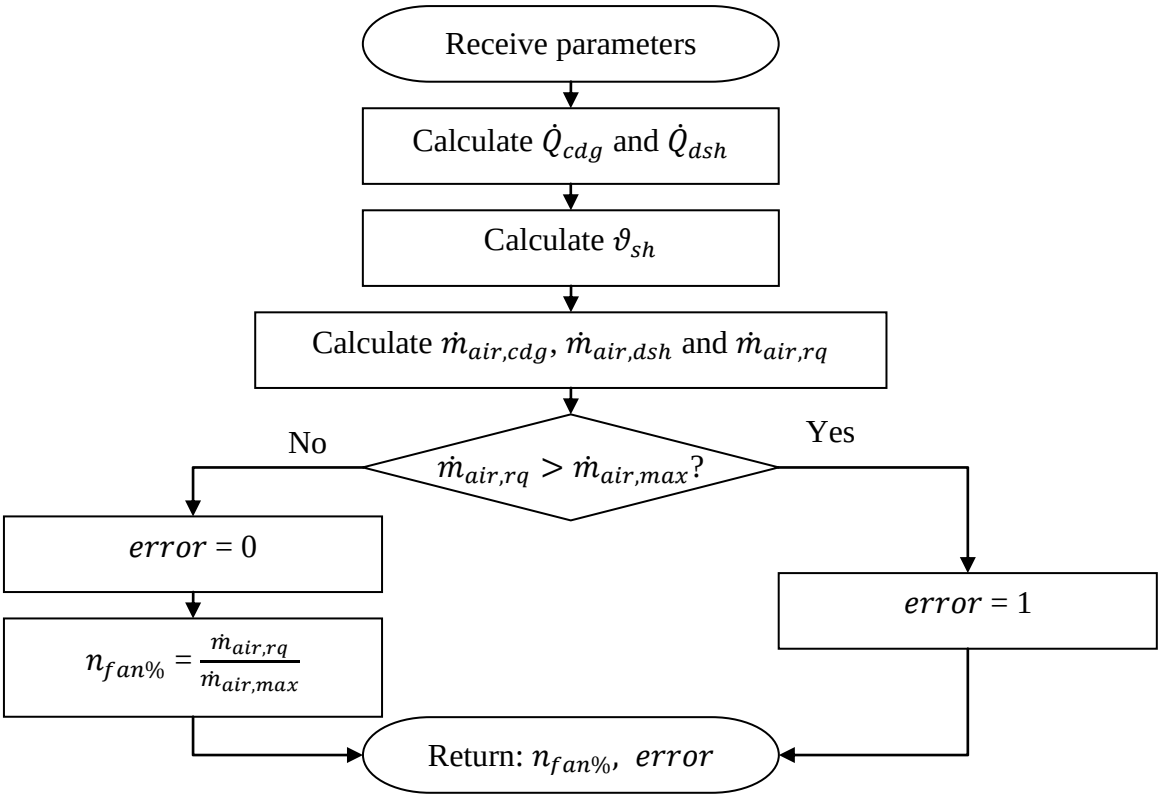

Figure 8.30: Flowchart for the condenser fan speed to maximise $COSP$

8.6.2 Controlling fans for maximum $COSP$

The flowchart for the Matlab function to calculate the necessary condenser fan speed is shown in Figure 8.30. This function takes the same parameters as inputs as the function described in 8.4.2.4, except for the variable 'day'. The function structure is simpler than the one displayed in the flowchart in Figure 8.20. For instance, there is no differentiation

between the day time and night time operations. Also the natural convective mode is not considered separately, because, as the heat rejected in this mode is quite small, the air requirements for this, computed by the Matlab function, are modest and the corresponding energy consumption is also small. If the required air flow, $\dot{m}_{air,rq}$, is greater than the maximum flow rate $\dot{m}_{air,max}$, an error is returned, otherwise the fan speed is calculated with Equation 8.52 and returned.

$$n_{fan\%} = \frac{\dot{m}_{air,rq}}{\dot{m}_{air,max}}$$

Equation 8.52

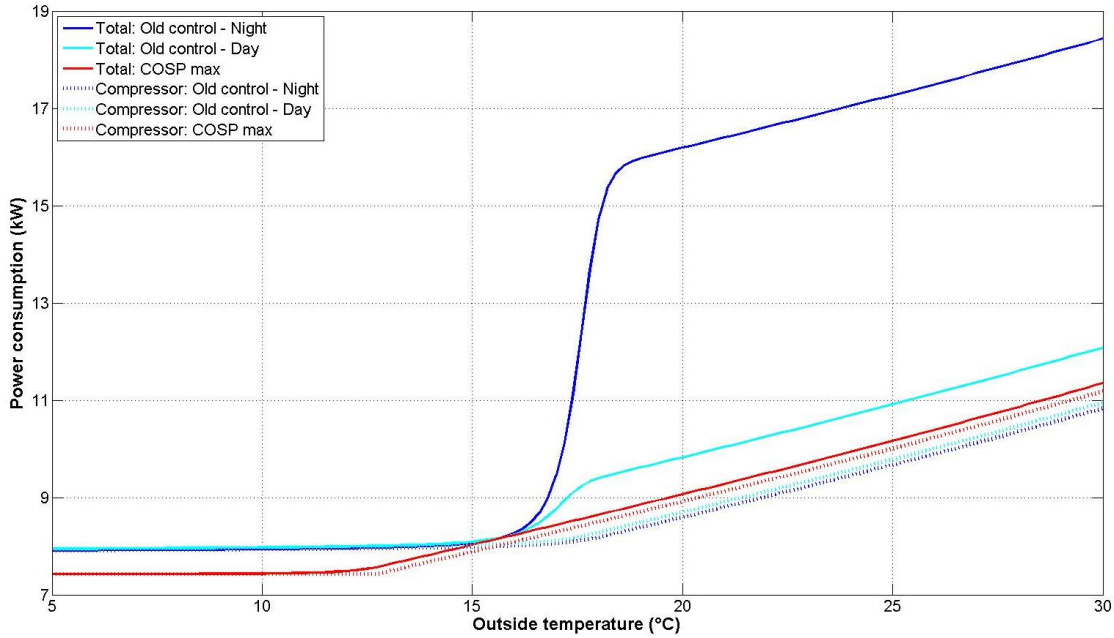

Figure 8.31: Comparing different fan control methods for a cooling load of 20 kW

The consumption of the refrigeration model was calculated for the new control method, for the day time and night time operation modes. The results for the cooling load of 20 kW are displayed in Figure 8.31. This graph contains lines for the total consumption (solid lines) and the compressor power (dotted lines). The total energy consumption for the new control method is below the old methods for the outside temperature to approximately 15°C. From approximately 16.5°C onwards the graphs for the total consumption spread out whilst the different compressor consumption lines remain close together. In this temperature range the compressor in the night time mode consumes the least power, closely followed by the day time mode. The dotted line for the new control indicates that compressor electricity consumption is somewhat higher. When examining the total consumption the results are reversed. The new approach is predicted to have an appreciably lower total energy use than both the day time and night time operation. For instance at 19°C the total consumption of

the system in night time mode is 16 kW, of which 7.6 kW, or 47.5%, is the condenser fan power. The day time mode uses about 9.6 kW and the new approach only 8.8 kW. In other words the lower compressor power (and therefore the higher COP) requires a higher total power input.

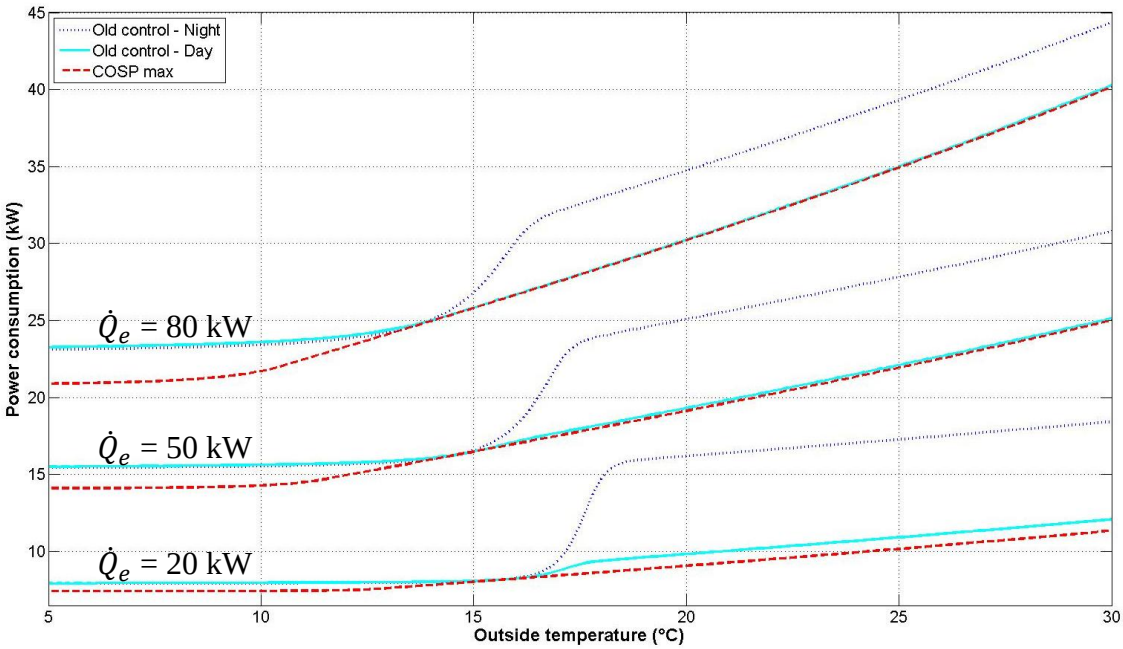

Figure 8.32: Comparing the total power consumption for cooling loads of 20 kW, 50 kW and 80 kW

The results for a $\dot{Q}_e$ of 20 kW, 50 kW and 80 kW are displayed in Figure 8.32. This graph shows that the range where all three approaches yield a comparable result moves toward the lower temperature range as cooling load increases. Below this range, the gap between the new approach and the old approaches increases with increasing cooling load. For the temperature range beyond this region the gap narrows and disappears almost completely for the day time operation at the highest refrigeration load. This agrees with higher requirements for the air flow rate for a higher load as more heat needs to be removed from the condenser.

8.6.3 Results of maximising $COSP$

The results presented below consider the $COSP$ (i.e. cooling load divided by total power consumption) for the three control methods: $COSP$ optimised control, day time and night time operations. The cooling loads of 20 kW, 50 kW and 80 kW were chosen so as to be able to compare the results of the software model with measurements from the installed system. These figures show that the $COSP$ of all three control approaches improves as the cooling load increases. For the original control methods the $COSP$ rises from just above 2.5

to approximately 3.5 for the minimum temperature. This spread agrees with Figure 8.11 and Figure 8.12 because the $COSP$ for the night time operation starts at approximately 2.5 and the day time $COSP$ reaches nearly 3.5 at the lower temperature range. Similar to Figure 8.11, the day time operation trace in Figure 8.34 for the mid range refrigeration load shows a change point at approximately 11.5°C. For the 50 kW and 80 kW cooling loads the day time $COSP$ in Figure 8.11 also shows agreement at the higher temperature range. This is reasonable because it can be expected that air infiltration into the supermarket of warmer air causes a higher cooling load.

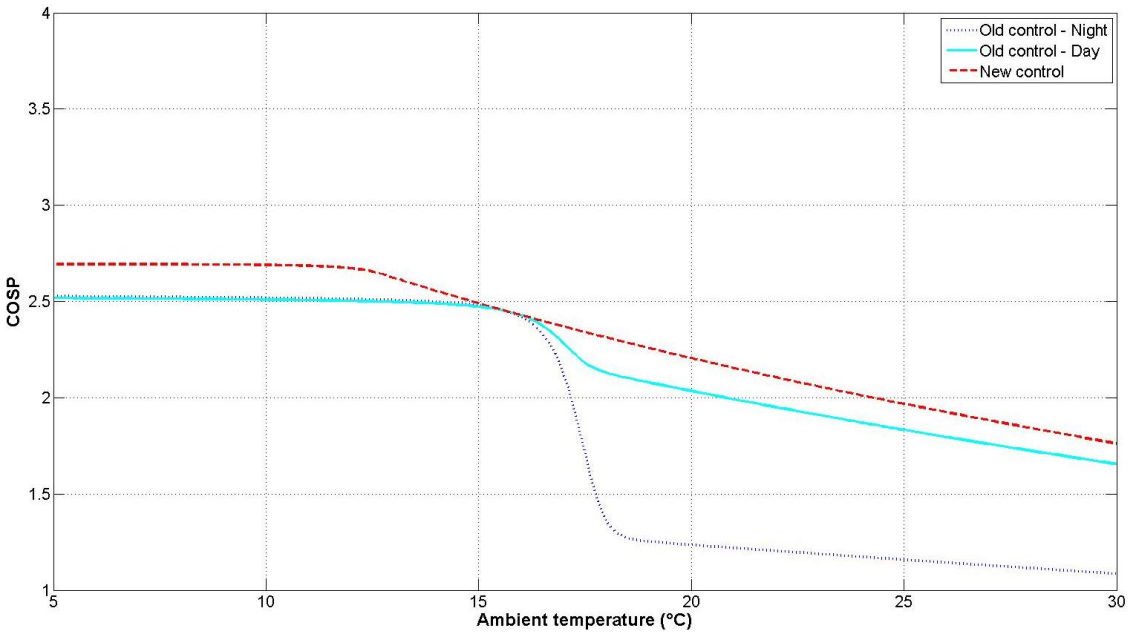

Figure 8.33: $COSP$ for all control methods for the cooling load of 20 kW

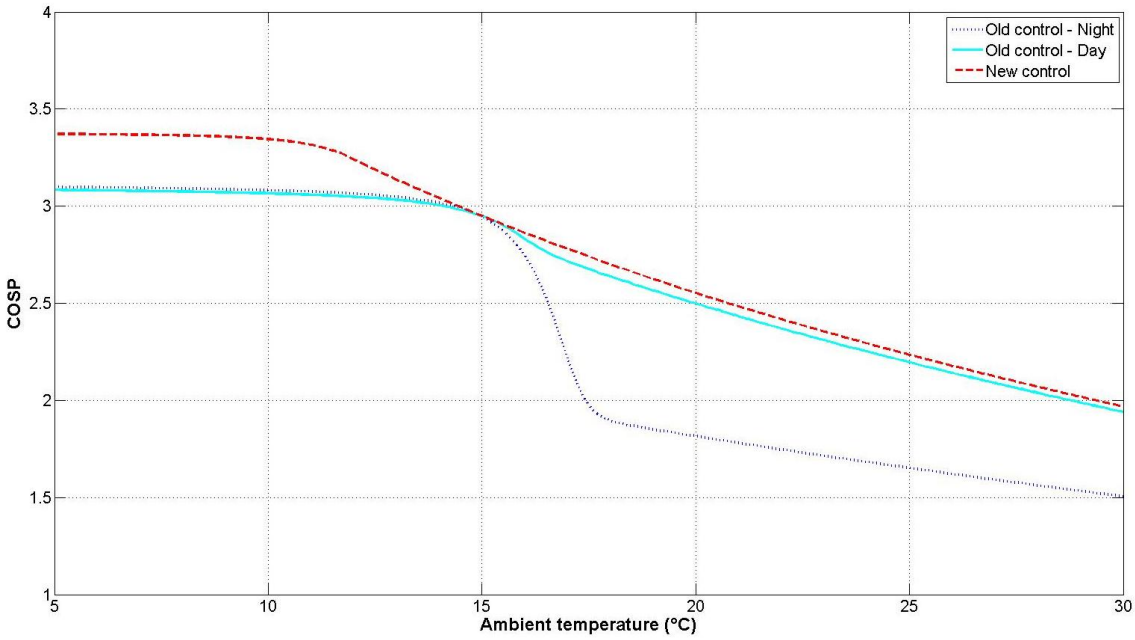

Figure 8.34: $COSP$ for all control methods for the cooling load of 50 kW

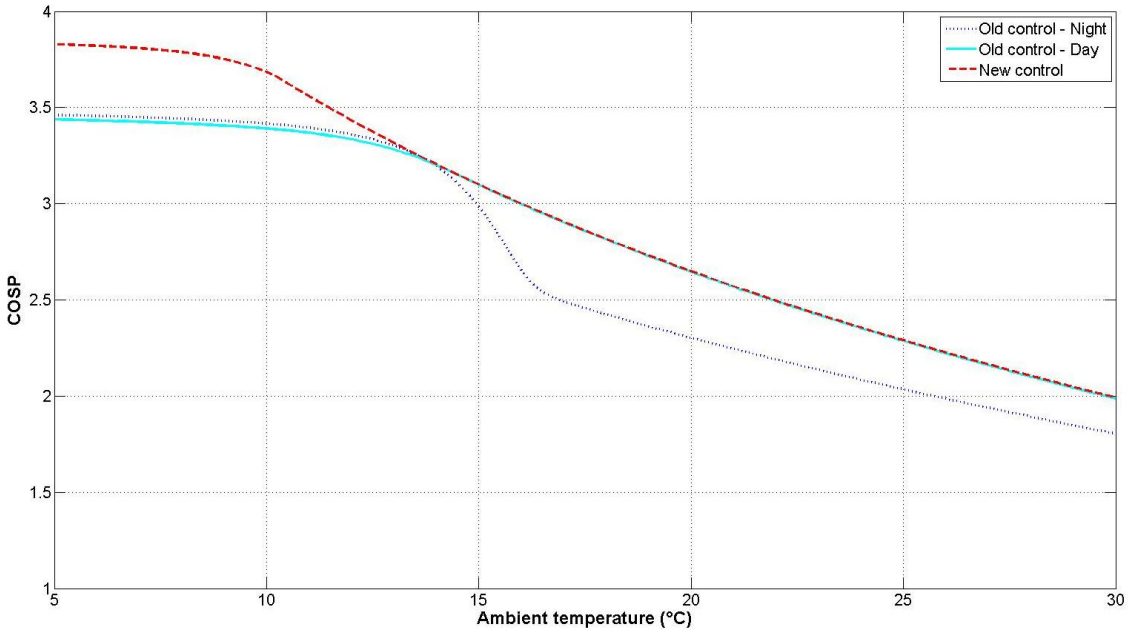

Figure 8.35: $COSP$ for all control methods for the cooling load of 80 kW

The graphs for the night time operation in Figure 8.33 to Figure 8.35 follow the general shape in Figure 8.12 albeit that the drop is not as steep. Also the slope after this decline is larger than in Figure 8.12. This may be owing to the inability of the software model to represent the large spread in the condenser fan data (seen in Figure 8.19).

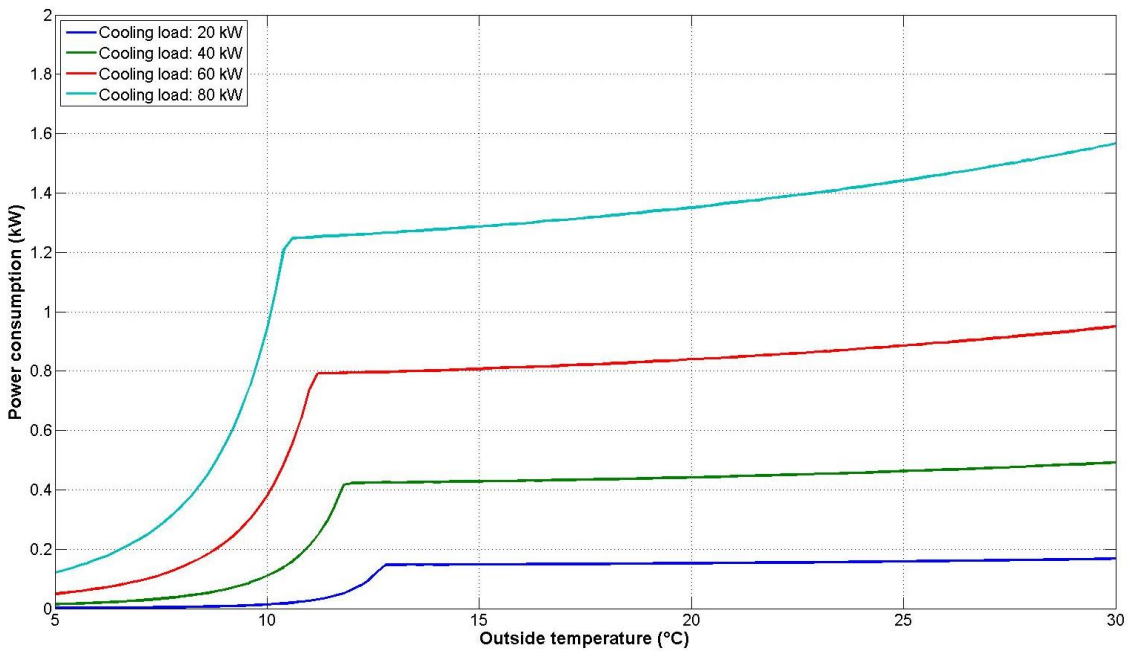

Figure 8.36: Fan power consumption for the $COSP$ maximised system for different cooling loads

The $COSP$ optimised system shows the best performance under all three cooling loads, albeit only marginally for the day time control mode for the highest cooling load case above 13.5°C. For all load cases the $COSP$ of the new control approach below the

temperature where the lines touch, is better than either the day time or the night time mode. This gap increases with rising cooling load. This is reversed for temperatures above this common point. There the gap between the original control methods and the $COSP$ optimised method narrows with increasing load. This is consistent with the discussion in Section 8.6.1, which suggested that the influence of the fan power on the overall system efficiency decreases as the cooling load increases.

The traces in Figure 8.36 relate to the power consumption of the $COSP$ optimised system and show that, as the cooling load increases, so does the fan power consumption. However, it always stays below the maximum power of 7.6 kW. It can also be seen that, although the temperature has some influence, the cooling load is the determining factor. All graphs show a 'kink' which corresponds to the point at which the minimum condenser pressure is no longer sufficient and needs to be increased to reject the required amount of heat.

The measured data from the installed refrigeration system was used to estimate the energy saving potential of the $COSP$ maximisation approach. The software model calculated an energy consumption of 78400 kWh for the six months from July 2014 to Nov 2014 with the original control method, and 74900 kWh with the new approach. The reduction of 3500 kWh represents an energy saving of approximately 4.5%.

8.6.4 Discussion and conclusion on $COSP$ maximisation

In this section the simplified equation relating the $COSP$ to COP and the power consumption of the condenser fans (see Equation 8.51) and its ramifications were compared with the software model. It was found that the insight gained by this simplified approach can be supported by the results from the software model.

This insight included appreciating the importance of the condenser fan power consumption on the overall efficiency. If the fan speed can be closely matched to the rejected heat, then the speed can be kept to a minimum. This, in turn, can have a significant impact on the overall power use because (a) the maximum fan power is comparable to the two smaller compressors of the installed system and (b) the power consumption rises by the power of three of the fan speed.

The work above also showed that it is possible to improve the $COSP$ by driving the compressor somewhat harder to allow the condenser fan to reduce its speed. This approach

was implemented in the Matlab model with an estimated energy reduction of 4.5% for the six months of the data set.

This idea should be taken forward to verify if the energy saving potential can also be achieved in practice. To do this the system may have to be modified to allow the measurement of the mass flow rate. In addition the control algorithm has to be modified to allow the calculation of the speed according to the heat rejection requirements.

8.7 Discussion and conclusions on the refrigeration system

This chapter concentrated on the investigation of the larger of the two refrigeration systems installed in the Hull supermarket mentioned in previous chapters in order to quantify the impact of the changing climate on the electricity consumption. The results predicted a temperature dependent rise in electricity use of between 1.7% (10% probability) and 12.9% (90% probability) with the central estimate being 6.4%. Furthermore the first principle model developed to answer this research question also allowed the investigation of a further question regarding the condenser fan controls. It was found that, based on the data set used for the model development, there was an energy saving potential of approximately 4.5%.

Errors and uncertainty of these findings arise from at least three different sources. The first of these is the approach chosen for model development including its assumption. For instance, the condenser fan control model approximated a large data spread with average values, which introduced errors. Other uncertainties stem from the way the cooling load for the base and future periods were estimated. The linear cooling load versus outside temperature models based on the measurement achieved only an r^2 of 0.46 for the day time operation and r^2 of 0.29 for the night time operation. Another source of uncertainty is the base year and future temperature data. This is explicitly acknowledged by stating consumption values for 10%, 50% and 90% temperature likelihoods and this approach gives rise to an 11 percentage point difference between the 10% and the 90% electricity values.

Apart from the modelling method chosen here, other research approaches are possible such as statistical models, similar to the supermarket models described in the previous chapters. However, as it was apparent that night time and day time were distinctly different early on in the investigation of the refrigeration system, a first principle model was chosen to be

able to explore and explain these differences. Some of the first principle models developed by other researchers use more sophisticated models for compressors (Ge and Tassou, 2000) or condensers (Arias and Lundqvist, 2005; Cecchinato *et al*, 2010a). Although these approaches may be more accurate they also introduce uncertainties, as these models also rely on "performance data published by the manufacturer" (Ge and Tassou, 2000) and "design experience and/or open literature correlations" (Cecchinato *et al*, 2010a) and this probably more so than the simplified approach chosen here, because more coefficients need to be determined. When comparing the results of the model here with the more detailed one by Yu and Chan (2007), one finds that the model by Yu and Chan seems to be similar in accuracy as the compressor model in their paper also has 95% of its data points within a ±10% error band. Therefore the model developed here can be considered adequate for its purpose so that an estimate of the magnitude of change in electricity use could be given and the differences in day time and night time operations be explained.

In this chapter a different approach to controlling the condenser fans was also investigated and it was shown that, for the data set used here, a $COSP$ optimised system uses 4.5% less energy than the approach used during the study period. Although this figure may not reflect the annual savings accurately because the data did not include winter months, it suggests that controlling a refrigeration system in a more holistic way will save energy. Further work on a real system would be beneficial to verify this conclusion.

9 Conclusions and further work

This thesis described how the research objectives mentioned in the introductory chapter were met. These aims were put into context in Chapters 2 to 4 which summarized existing knowledge on changes in energy consumption due to climate change, energy analysis tools and climate change uncertainties. How the first research goal of quantifying the influence of climate change and location on the energy use in supermarkets was investigated and the results of this investigation are detailed in Chapters 1 to 1. The chapter thereafter explained how a refrigeration software model was developed to meet the second objective of calculating the change in electricity consumption arising from the changing climate and how this model was used to study approaches to condenser fan controls. The research findings were discussed in Chapter 1 and in Section 8.7. Apart from comparing these results with each other, this chapter aims to put the research presented in the chapters above into the temporal context, present overall conclusions and suggest further work.

In order to appreciate the meaning of the predictions more fully it may be beneficial to highlight the three time periods involved. As this research investigated a change in climate, it compared variables (in particular temperature) over 30 year periods. The base period was from 1961 to 1990 and the '2030s' run from 2020 to 2049. If the average temperature occurs in the middle of these intervals, the estimated energy use changes will occur in two decades. The predictions have a base line which is about four decades prior to the time when the research was conducted (i.e. 2013/14). This means that at least some of the changes in energy use may have occurred already. Another point to consider is how the 2013/14 study period should be viewed. Is it the middle or the end of a 30 year climate period? If it is the end and, therefore, 1999 is about the midpoint, then it is possible to estimate how far the temperature has risen towards the predicted temperature rise for the 2030s. For instance, the work by Prior and Perry (2014), which used a bandwidth of 29 years for their smoothing algorithm, showed that a temperature rise from the base period (i.e. 1961-1990) to the latest period they studied (i.e. the period from 1982 to 2011) of approximately 0.6°C had occurred all over Great Britain (compared with the average central estimate of 1.8°C for the seven supermarket locations based on UKCP09). However, they also find that, for data towards the end of their period, this increase slowed down or even reversed so the exact increase both in magnitude and timing is extremely difficult to predict with any level of accuracy.

9.1 Overall conclusions

When examining gas data it is apparent that linear gas models are capable of explaining at least 83% of the variation in the analysed data. This examination also supports the conclusion that the gas use is mainly a function of outside temperature (that is, if the boiler is in operation). Regarding the parameters of these models, Chapter 1 has demonstrated that they can be explained based purely on a supermarket dimensions.

The study of the electricity consumption data showed that, for these data, non-linear models generally performed better than linear models. For four out of the seven supermarkets change point regression models improved the coefficient of determination by at least 13% over a simple regression model. The research here has also established that outside temperature is only one of the factors determining the electricity use in supermarkets. This is so because other electricity consumers, such as lighting, can be regarded as temperature independent and the use of kitchen equipment in the café areas is more stochastic in nature. The work here also showed that the model parameters are not just a function of the building geometry.

The major conclusion based on the climate science literature reviewed above is that climate change predictions have a high level of uncertainties. Sources of these uncertainties range from being unaware of natural phenomena or their influence on the climate to the lack of computer resources to modelling natural process in sufficient detail.

When combining the gas and electricity regression models with 1961-1990 climate data and predictions for the period from 2020 to 2049 the results showed an increase in electricity use and a reduction in gas consumption both in absolute and relative terms, or, in other words, the results predicted an overall reduction of energy usage.

The investigation into differences in location dependent energy use could not establish a link between any variation in operational procedures and differences in energy usage. These differences could be more credibility explained, in the case of gas average EUI_{wkly}, with the latitude and, in the case of the average EUI_{wkly} for electricity, with the total supermarket area.

Studying the refrigeration system in Hull showed that using simplifying assumptions yielded a model with a $CV(RMSE)$ with less than 10%. This model helped establish that

most of the additional electricity use due to climate change is owing to the refrigeration system. This section also demonstrated that a higher cooling load yielded a better $COSP$. Furthermore it showed that the method of controlling condenser fans employed during the study period can be improved and, thus, energy could be saved.

9.2 Further work

The work started here could be extended in a number of ways including further research into the condenser fan controls. This would start with using the software model developed in this work to investigate if widening the control band of ±0.5 bar (the setting during the period of investigation) would reduce the electricity use of the refrigeration system, followed by a verification with the installed system. The next step could be to develop an approach to estimating the cooling load in real-time, and then using the cooling load as an input to the condenser fan controller so that fan control can be optimised.

Another area of further work could concern the refrigeration model itself. This has been implemented in Matlab, but may benefit from being transferred to another software package, such as Simulink (The MathWorks, 2011), which is more geared towards simulating dynamic systems. This could be followed by developing better condenser models so that the de-superheating process can be better represented. Afterwards it could be investigated if and how gas coolers can be modelled in order to simulate, for example, transcritical CO_2 refrigeration systems.

The research with respect to whole supermarkets could be expanded by investigating how model parameters for both electricity and gas models can be estimated. The research indicated that, for gas consumption, only the building volume may suffice. However, the sample size needs to be increased in this building type and then broadened to include also other types of building (including buildings without a lobby). For the electricity model the dependency on the total area of supermarkets could be investigated. This could serve as a base line against which actual consumption could be compared with in order to detect energy inefficiencies.

Another strand of further research could include the construction of a reliable UK supermarket model (including refrigeration systems) in a building simulation software package as, so far, only a detailed US model is available (Deru *et al*, 2013). Such a model could be compared to a CFD model to explore possible stratification in supermarkets. This

work could suggest if there is an optimum ceiling height, or if combined heat and power plants or phase change material would be of benefit.

References

AL-HOMOUD, M. S. (2001) Computer-aided building energy analysis techniques. *Building and Environment,* 36**,** 421-433.

ALTHOUSE, A. D., TURNQUIST, C. H. & BRACCIONO, A. F. (1996) *Modern refrigeration and air conditioning,* Tinley Park, USA: The Goodheart-Willcox Company.

ANDERSON, C. H. (1993) *Retailing: Concepts, Stategy and Information,* Minneapolis/Saint Paul: West Publishing Company.

ANDERSON, D. R., SWEENEY, D. J. & WILLAMS, T. A. (2004) *Essential of Modern Business Statistics with Microsoft Excel,* London; Cincinnati, USA: Thomson; South-Western.

ANDERSON, D. R., SWEENEY, D. J. & WILLIAMS, T. A. (2003) *Modern Business Statistics with Microsoft Excel,* London; Cincinnati, USA: Thomson; South-Western.

ARIAS, J. (2005) *Energy Usage in Supermarkets: Modelling and Field Measurements.* Kungliga Tekniska Hogskolan (Sweden) DrTechn. Thesis, Kungliga Tekniska Hogskolan (Sweden).

ARIAS, J. & LUNDQVIST, P. (2005) Modelling and experimental validation of advanced refrigeration systems in supermarkets. *Proceedings of the Institution of Mechanical Engineers E, Journal of Process Mechanical Engineering,* 219**,** 149-149-156.

ARIAS, J. & LUNDQVIST, P. (2006) Heat recovery and floating condensing in supermarkets. *Energy and Buildings,* 38**,** 73-81.

ARORA, R. C. (2010) *Refrigeration and Air conditioning,* New Delhi: PHI Learning.

ASHRAE. (1997) *1997 ASHRAE HANDBOOK FUNDAMENTALS,* Atlanta, USA: ASHRAE.

ASHRAE. (2002) *2002 ASHRAE HANDBOOK, REFRIGERATION,* Atlanta, USA: ASHRAE.

ASHRAE. (2008) *2008 ASHRAE HANDBOOK, Heating, Ventilating, and Air-Conditioning SYSTEMS AND EQUIPMENT,* Atlanta, USA: ASHRAE.

ASHRAE. (2013) *2013 ASHRAE HANDBOOK FUNDAMENTALS,* Atlanta, USA: ASHRAE.

AZADEH, A., GHADERI, S. F., TARVERDIAN, S. & SABERI, M. (2007) Integration of artificial neural networks and genetic algorithm to predict electrical energy consumption. *Applied Mathematics and Computation,* 186**,** 1731-1741.

BAEDE, A. P. M., AHLONSOU, E., DING, Y. & SCHIMEL, D. (2001) The Climate System: an Overview. *In:* HOUGHTON, J. T.*, et al.* (eds.) *Climate Change 2001: The Scientific Basis.*

BAHMAN, A., ROSARIO, L. & RAHMAN, M. M. (2012) Analysis of energy savings in a supermarket refrigeration/HVAC system. *Applied Energy,* 98**,** 11-21.

BALTAZAR, J. C. & CLARIDGE, D. E. (2006) Study of cubic splines and Fourier Series as interpolation techniques for filling in short periods of missing building energy use and weather data. *Journal of Solar Energy Engineering,* 128**,** 226.

BEGGS, C. (2002) *Energy: Management, Supply and Conservation,* Oxford: Butterworth-Heinemann.

BELCHER, S. E., HACKER, J. N. & POWELL, D. S. (2005) Constructing design weather data for future climates. *Building Services Engineering Research & Technology,* 26**,** 49-61.

BELL, S., CORNFORD, D. & BASTIN, L. (2015) How good are citizen weather stations? Addressing a biased opinion. *Weather,* 70**,** 75-84.

BELZER, D. B., SCOTT, M. J. & SANDS, R. D. (1996) Climate change impacts on US commercial building energy consumption: An analysis using sample survey data. *Energy sources,* 18**,** 177-201.

BERGER, T., AMANN, C., FORMAYER, H., KORJENIC, A., POSPICHAL, B., NEURURER, C. & SMUTNY, R. (2014) Impacts of urban location and climate change upon energy demand of office buildings in Vienna, Austria. *Building and Environment,* 81**,** 258-269.

BITZER KÜHLMASCHINENBAU GMBH. (2013) *BITZER Software* [Online] (Version: 6.4.1.1210). Available from: www.bitzer.de/websoftware [Accessed: 7 Oct 2014].

BITZER KÜHLMASCHINENBAU GMBH. (2014) *COMPETENCE IN CAPACITY CONTROL,* Sindelfingen, Germany: Bitzer Kühlmaschinenbau.

BOOTH, A., PAPAIOANNOU, D. & SUTTON, A. (2012) *Systematic Approaches to a Successful Literature Review,* London: SAGE Publictions.

BOUCHER, O., RANDALL, D., ARTAXO, P., BRETHERTON, C., FEINGOLD, G., FORSTER, P., KERMINEN, V.-M., KONDO, Y., LIAO, H., LOHMANN, U., RASCH, P., SATHEESH, S. K., SHERWOOD, S., STEVENS, B. & ZHANG, X.

Y. (2013) Clouds and Aerosols. *In:* STOCKER, T. F., *et al.* (eds.) *Climate Change 2013: The Physical Science Basis. Contribution of Working Group I to the Fifth Assessment Report of the Intergovernmental Panel on Climate Change.* Cambridge and New York: Cambridge University Press.

BSI (2008) *Energy performance of buildings. Calculation of energy use for space heating and cooling,* London: BSI. BS EN ISO 13790:2008

BSI (2013) *Refrigerant compressors. Rating conditions, tolerances and presentation of manufacturer's performance data,* London: British Standards Institution. BS EN 12900:2013

BUILDING TECHNOLOGIES OFFICE. (2014) *Building Energy Software Tools Directory* [Online]. Washington: U.S. Department of Energy. Available from: http://apps1.eere.energy.gov/buildings/tools_directory/ [Accessed 28 July 2014].

BURT, S. (2009) *The Davis Instruments Vantage Pro2 wireless AWS – an independent evaluation against UK-standard meteorological instruments* [Online]. Available from: http://measuringtheweather.com/wp-content/uploads/2012/06/Davis-Vantage-Pro2-AWS-review-2009-c-Stephen-Burt.pdf [Accessed 01 Jan 2014].

CAPOZZOLI, A., MAZZEI, P., MINICHIELLO, F. & PALMA, D. (2006) Hybrid HVAC systems with chemical dehumidification for supermarket applications. *Applied Thermal Engineering,* 26**,** 795-805.

CAREL INDUSTRIES. (2012) E3V-U - Valvola di espansione elettronica / Electronic expansion valve / Détendeur électronique / Elektronisches Expansionsventil / Válvula de expansión electrónica. Padova, Italy: CAREL INDUSTRIES.

CARTALIS, C., SYNODINOU, A., PROEDROU, M., TSANGRASSOULIS, A. & SANTAMOURIS, M. (2001) Modifications in energy demand in urban areas as a result of climate changes: an assessment for the southeast Mediterranean region. *Energy Conversion and Management,* 42**,** 1647-1656.

CECCHINATO, L., CHIARELLO, M. & CORRADI, M. (2010a) A simplified method to evaluate the seasonal energy performance of water chillers. *International Journal of Thermal Sciences,* 49**,** 1776-1786.

CECCHINATO, L., CORRADI, M. & MINETTO, S. (2010b) Energy performance of supermarket refrigeration and air conditioning integrated systems. *Applied Thermal Engineering,* 30**,** 1946-1958.

CECCHINATO, L., CORRADI, M. & MINETTO, S. (2012) Energy performance of supermarket refrigeration and air conditioning integrated systems working with natural refrigerants. *Applied Thermal Engineering,* 48**,** 378-391.

ÇENGEL, Y. A. & BOLES, M. A. (2007) *Thermodynamics: An Engineering Approach,* Boston: McGraw-Hill Higher Education.

CHAN, A. L. S. (2011) Developing future hourly weather files for studying the impact of climate change on building energy performance in Hong Kong. *Energy and Buildings,* 43**,** 2860-2868.

CHAN, K. T. & YU, F. W. (2002) Applying condensing-temperature control in air-cooled reciprocating water chillers for energy efficiency. *Applied Energy,* 72**,** 565-581.

CHEN, L. (1991) *Developing a change-point principal component predictive model for energy use in a supermarket.* M S disertation, Texas A&M University.

CHOW, D., KELLY, M., WANG, H. & DARKWA, J. (2014) The effects of future climate change on energy consumption in residential buildings in China and retrofitting measures to counteract. *Journal of Energy Challenges and Mechanics,* 1**,** 1.

CHRISTENSEN, J. H., HEWITSON, B., BUSUIOC, A., CHEN, A., GAO, X., HELD, I., JONES, R., KOLLI, R. K., KWON, W.-T., LAPRISE, R., RUEDA, V. M., MEARNS, L., MENÉNDEZ, C. G., RÄISÄNEN, J., RINKE, A., SARR, A. & WHETTON, P. (2007) Regional Climate Projections. *In:* SOLOMON, S., *et al.* (eds.) *Climate Change 2007: The Physical Science Basis. Contribution of Working Group I to the Fourth Assessment Report of the Intergovernmental Panel on Climate Change.* Cambridge and New York: Cambridge University Press.

CHRISTENSON, M., MANZ, H. & GYALISTRAS, D. (2006) Climate warming impact on degree-days and building energy demand in Switzerland. *Energy Conversion and Management,* 47**,** 671-686.

CHUNG, W. (2011) Review of building energy-use performance benchmarking methodologies. *Applied Energy,* 88**,** 1470-1479.

CHUNG, W., HUI, Y. V. & LAM, Y. M. (2006) Benchmarking the energy efficiency of commercial buildings. *Applied Energy,* 83**,** 1-14.

CLARKE, J. A. (2001) *Energy simulation in building design,* Oxford: Butterworth-Heinemann.

COAKLEY, D., RAFTERY, P. & KEANE, M. (2014) A review of methods to match building energy simulation models to measured data. *Renewable and Sustainable Energy Reviews,* 37**,** 123-141.

COLLINS, L., NATARAJAN, S. & LEVERMORE, G. (2010) Climate change and future energy consumption in UK housing stock. *Building Services Engineering Research & Technology,* 31**,** 75-90.

CORRADO, V., MECHRI, H. E. & FABRIZIO, E. Building energy performance assessment through simplified models: application of the ISO 13790 quasi-steady state method. Proceedings of building simulation, 2007. 79-86.

COX, R. & BRITTAIN, P. (1996) *Retail Management,* London: Pitman Publishing.

CRAWLEY, D. B. Impact of climate change on buildings. 2003 CIBSE/ASHRAE Conference Building Sustainability, Value and Profit Conference, 24/09/03 - 26/09/03 2003 Edinburgh, UK.

CRAWLEY, D. B., LAWRIE, L. K., WINKELMANN, F. C., BUHL, W. F., HUANG, Y. J., PEDERSEN, C. O., STRAND, R. K., LIESEN, R. J., FISHER, D. E., WITTE, M. J. & GLAZER, J. (2001) EnergyPlus: creating a new-generation building energy simulation program. *Energy and Buildings,* 33**,** 319-331.

CRONIN, P., RYAN, F. & COUGHLAN, M. (2008) Undertaking a literature review: A step-by-step approach. *British Journal of Nursing,* 17**,** 38-43.

DATTA, D., TASSOU, S. & MARRIOTT, D. Application of neural networks for the prediction of the energy consumption in a supermarket. Proc. CLIMA 2000, 1997 Brussels. 98.

DATTA, D. & TASSOU, S. A. (1998) Artificial neural network based electrical load prediction for food retail stores. *Applied Thermal Engineering,* 18**,** 1121-1128.

DAVIES, J. H. & DAVIES, D. R. (2010) Earth's surface heat flux. *Solid Earth,* 1**,** 5-24.

DAY, A. R., JONES, P. G. & MAIDMENT, G. G. (2009) Forecasting future cooling demand in London. *Energy and Buildings,* 41**,** 942-948.

DAY, T. (2006) *Degree-days: Theory and application, TM41: 2006,* London: The Chartered Institution of Building Services Engineers.

DAZELEY, J. (2012) Supermarket Energy Retrofit *Twelfth International Conference for Enhanced Building Operations.* Manchester.

DE ROSA, M., BIANCO, V., SCARPA, F. & TAGLIAFICO, L. A. (2014) Heating and cooling building energy demand evaluation; a simplified model and a modified degree days approach. *Applied Energy,* 128**,** 217-229.

DE WILDE, P. & TIAN, W. (2009) Identification of key factors for uncertainty in the prediction of the thermal performance of an office building under climate change. *Building Simulation,* 2**,** 157-174.

DE WILDE, P. & TIAN, W. (2010) Predicting the performance of an office under climate change: A study of metrics, sensitivity and zonal resolution. *Energy and Buildings,* 42**,** 1674-1684.

DEFRA. (2006) Economic notes on UK grocery retailing. *In:* DEFRA (ed.). London: Stationery Office.

DENMAN, K. L., BRASSEUR, G., CHIDTHAISONG, A., CIAIS, P., COX, P. M., DICKINSON, R. E., HAUGLUSTAINE, D., HEINZE, C., HOLLAND, E., JACOB, D., LOHMANN, U., RAMACHANDRAN, S., DIAS, P. L. D. S., WOFSY, S. C. & ZHANG, X. (2007) Couplings Between Changes in the Climate System and Biogeochemistry. *In:* SOLOMON, S., *et al.* (eds.) *Climate Change 2007: The Physical Science Basis. Contribution of Working Group I to the Fourth Assessment Report of the Intergovernmental Panel on Climate Change.* Cambridge and New York: Cambridge University Press.

DERU, M., BONNEMA, E., DOEBBER, I., HIRSCH, A., MCINTYRE, M. & SCHEIB, J. (2011a) Thinking like a whole buiding: A Whole Foods Market new construciton case study. Golden, USA: National Renewable Energy Laboratory.

DERU, M., DOEBBER, I. & HIRSCH, A. (2013) Whole Building Efficiency for Whole Foods. *2013 ASHRAE Winter Conference.* Dallas.

DERU, M., FIELD, K., STUDER, D., BENNE, K., GRIFFITH, B., TORCELLINI, P., LIU, B., HALVERSON, M., WINIARSKI, D., ROSENBERG, M., YAZDANIAN, M., HUANG, J. & CRAWLEY, D. (2011b) U.S. Department of Energy Commercial Reference Building Models of the National Building Stock Golden, Colorado: National Renewable Energy Laboratory.

DESCLOITRES, J. (2002) *Satellite image of Great Britain and Northern Ireland in April 2002*. Wikimedia Commons: MODIS Land Rapid Response Team, NASA/GSFC.

DEVOTTA, S., SICARS, S., AGARWAL, R., ANDERSON, J., BIVENS, D., COLBOURNE, D., HUNDY, G., KÖNIG, H., LUNDQVIST, P., MCINERNEY, E., NEKSÅ, P. & EL-TALOUNY, A. (2005) Refrigeration. *In:* CALVO, E. & ELGIZOULI, I. (eds.) *IPCC/TEAP Special Report: Safeguarding the Ozone Layer and the Global Climate System.* Cambridge Cambridge University Press.

DING, G.-L. (2007) Recent developments in simulation techniques for vapour-compression refrigeration systems. *International Journal of Refrigeration,* 30**,** 1119-1133.

DOLINAR, M., VIDRIH, B., KAJFEŽ-BOGATAJ, L. & MEDVED, S. (2010) Predicted changes in energy demands for heating and cooling due to climate change. *Physics and Chemistry of the Earth, Parts A/B/C,* 35**,** 100-106.

DONG, B., CAO, C. & LEE, S. E. (2005) Applying support vector machines to predict building energy consumption in tropical region. *Energy and Buildings,* 37**,** 545-553.

DUCOULOMBIER, M., TEYSSEDOU, A. & SORIN, M. (2006) A model for energy analysis in supermarkets. *Energy and Buildings,* 38**,** 349-349.

EAMES, M., KERSHAW, T. & COLEY, D. (2011) On the creation of future probabilistic design weather years from UKCP09. *Building Services Engineering Research and Technology,* 32**,** 127-142.

EAMES, M., KERSHAW, T. & COLEY, D. (2012) A comparison of future weather created from morphed observed weather and created by a weather generator. *Building and Environment,* 56**,** 252-264.

ENVIRONMENT CANADA. (n.d.) *Data, Canadian Centre for Climate Modelling and Analysis* [Online]. Gatineau, Canada: Environment Canada. Available from: http://www.cccma.ec.gc.ca/data/data.shtml [Accessed 05 Jan 2015].

EUM, H.-I., GACHON, P., LAPRISE, R. & OUARDA, T. (2012) Evaluation of regional climate model simulations versus gridded observed and regional reanalysis products using a combined weighting scheme. *Climate Dynamics,* 38**,** 1433-1457.

EUROPEAN COMMISSION. (2002) Directive 2002/91/EC of the European Parliament and of the Council of 16 December 2002 on the energy performance of buildings. *Official Journal of the European Communities.*

EVANS, J. A. (ed.) (2008) *Frozen Food Science and Technology,* Oxford: Blackwell Publishing Ltd.

EVANS, J. A., HAMMOND, E. C., GIGIEL, A. J., FOSTERA, A. M., REINHOLDT, L., FIKIIN, K. & ZILIO, C. (2014) Assessment of methods to reduce the energy consumption of food cold stores. *Applied Thermal Engineering,* 62**,** 697-705.

FARAMARZI, R. (1999) Efficient display case refrigeration. *ASHRAE Journal,* 41**,** 46-46.

FELS, M. F. (1986) PRISM: An introduction. *Energy and Buildings,* 9**,** 5-18.

FLATO, G., MAROTZKE, J., ABIODUN, B., BRACONNOT, P., CHOU, S. C., COLLINS, W., COX, P., DRIOUECH, F., EMORI, S., EYRING, V., FOREST, C., GLECKLER, P., GUILYARDI, E., JAKOB, C., KATTSOV, V., REASON, C. & RUMMUKAINEN, M. (2013) Evaluation of Climate Models. *In:* STOCKER, T. F., *et al.* (eds.) *Climate Change 2013: The Physical Science Basis. Contribution of*

Working Group I to the Fifth Assessment Report of the Intergovernmental Panel on Climate Change. Cambridge and New York: Cambridge University Press.

FLATO, G. M. (2011) Earth system models: an overview. *Wiley Interdisciplinary Reviews: Climate Change,* 2**,** 783-800.

FOUCQUIER, A., ROBERT, S., SUARD, F., STÉPHAN, L. & JAY, A. (2013) State of the art in building modelling and energy performances prediction: A review. *Renewable and Sustainable Energy Reviews,* 23**,** 272-288.

FRANK, T. (2005) Climate change impacts on building heating and cooling energy demand in Switzerland. *Energy and Buildings,* 37**,** 1175-1185.

GE, Y. T. & TASSOU, S. A. (2000) Mathematical modelling of supermarket refrigeration systems for design, energy prediction and control. *Proceedings of the Institution of Mechanical Engineers. Part A. Journal of Power and Energy,* 214**,** 101-101-114.

GE, Y. T. & TASSOU, S. A. (2011) Performance evaluation and optimal design of supermarket refrigeration systems with supermarket model "SuperSim", Part I: Model description and validation. *International Journal of Refrigeration,* 34**,** 527-539.

GEA. (2012) *Global Energy Assessment – Toward a Sustainable Future,* Cambridge & New York and Laxenburg: Cambridge University Press and International Institute for Applied Systems Analysis.

GEA SEARLE. (2015) *Specification - MGC222H-EC855,* Fareham, UK: GEA Searle.

GOOGLE. (2009-2012) *Google Maps, Street View* [Online]. Available from: https://www.google.co.uk/maps/place [Accessed (Various dates) 2013].

GOOGLE. (2013) *Google Maps, Earth* [Online]. Available from: https://www.google.co.uk/maps [Accessed (Various dates) 2013].

GORDON, C., COOPER, C., SENIOR, C. A., BANKS, H., GREGORY, J. M., JOHNS, T. C., MITCHELL, J. F. & WOOD, R. A. (2000) The simulation of SST, sea ice extents and ocean heat transports in a version of the Hadley Centre coupled model without flux adjustments. *Climate Dynamics,* 16**,** 147-168.

GORDON, J. M. & NG, K. C. (2000) *Cool Thermodynamics: The Engineering and Physics of Predictive, Diagnostic and Optimization Methods for Cooling Systems,* Cambridge: Cambridge International Science Publishing.

GRAYSON, D. (2011) Embedding corporate responsibility and sustainability: Marks & Spencer. *Journal of Management Development,* 30 1017 - 1026.

GROSSBERG, S. (1988) Nonlinear neural networks: Principles, mechanisms, and architectures. *Neural networks,* 1**,** 17-61.

GUPTA, R. & GREGG, M. (2012) Using UK climate change projections to adapt existing English homes for a warming climate. *Building and Environment,* 55**,** 20-42.

GUT, J. A. W. & PINTO, J. M. (2003) Modeling of plate heat exchangers with generalized configurations. *International Journal of Heat and Mass Transfer,* 46**,** 2571-2585.

HACKER, J., BELCHER, S. & CONNELL, R. (2005) *Beating the Heat: keeping UK buildings cool in a warming climate,* Oxford: UKCIP.

HACKER, J., CAPON, R. & MYLONA, A. (2009) *TM48: Use of Climate Change Scenarios for Building Simulation: the CIBSE Future Weather Years (CIBSE Technical Memorandum),* London: Chartered Institution of Building Services Engineers.

HALL, J. (2007) Probabilistic climate scenarios may misrepresent uncertainty and lead to bad adaptation decisions. *Hydrological Processes,* 21**,** 1127-1129.

HEMINGWAY, P. & BRERETON, N. (2009) What is a systematic review? *What is...? series* [Online]. Available from: http://www.medicine.ox.ac.uk/bandolier/painres/download/whatis/syst-review.pdf [Accessed 28 Dec 2014].

HENDRON, R., LEACH, M., SHEKHAR, D. & PLESS, S. (2012) Advanced Energy Retrofit Guide: Practical Ways to Improve Energy Performance; Grocery Stores. Golden, USA: National Renewable Energy Laboratory (NREL).

HILL, F., EDWARDS, R. & LEVERMORE, G. (2012) Identification of changes needed in supermarket design for energy demand reduction *Twelfth International Conference for Enhanced Building Operations.* Manchester, UK.

HILL, F., EDWARDS, R. & LEVERMORE, G. (2014) Influence of display cabinet cooling on performance of supermarket buildings. *Building Services Engineering Research & Technology,* 35**,** 170-181.

HILL, F. & LEVERMORE, G. (2011) Impact of modelling protocols on supermarket energy demand. *Science Symposium 2012.* Powys: Graduate School of the Environment.

HONG, T., CHOU, S. & BONG, T. (2000) Building simulation: an overview of developments and information sources. *Building and Environment,* 35**,** 347-361.

HOWELL, R., ROSARIO, L. & BULA, A. Effects of indoor relative humidity on refrigerated display cases performance. Proceedings of CLIMA 2000 Conference. Brussells, Belgium, 1997.

IBM. (2012) *IBM SPSS Statistics 21 Core System User's Guide,* New York: IBM Corporation.

IEA HEAT PUMP CENTRE. (2012) Advanced Modeling and Tools for Analysis of Energy us in Supermarket Systems, Final Report. Boras: IEA Heat Pump Centre.

INCROPERA, F. P. & DEWITT, D. P. (1985) *Introduction to Heat Transfer,* New York: John Wiley & Sons.

IPCC. (2001) Climate Change 2001: The Scientific Basis. Contribution of Working Group I to the Third Assessment Report of the Intergovernmental Panel on Climate Change. *In:* HOUGHTON, J. T., *et al.* (eds.). Cambridge and New York: Cambridge University Press.

IPCC. (2007) Climate Change 2007: The Physical Science Basis. Contribution of Working Group I to the Fourth Assessment Report of the Intergovernmental Panel on Climate Change. *In:* SOLOMON, S., *et al.* (eds.). Cambridge and New York: Cambridge University Press.

IPCC. (2013) *Climate Change 2013: The Physical Science Basis. Contribution of Working Group I to the Fifth Assessment Report on the Intergovernmental Panel on Climate Change,* Cambridge and New York: Cambridge University Press.

ISAAC, M. & VAN VUUREN, D. P. (2009) Modeling global residential sector energy demand for heating and air conditioning in the context of climate change. *Energy Policy,* 37**,** 507-521.

ISO/IEC (2008) *Uncertainty of measurement -- Part 3: Guide to the expression of uncertainty in measurement (GUM:1995),* Genève: ISO.

JAKOB, C. & MILLER, M. (2003) Parameterization of physical processes, Clouds. *In:* HOLTON, J. R. (ed.) *Encyclopedia of Atmospheric Sciences.* Oxford: Academic Press.

JAMES, R. W. (1976) *Modelling and Control of Refrigeration and Air Conditioning Systems for Energy Conservation.* PhD thesis, University of Sheffield.

JENKINS, D. (2009) The importance of office internal heat gains in reducing cooling loads in a changing climate. *International Journal of Low-Carbon Technologies,* 4**,** 134-140.

JENKINS, D., LIU, Y. & PEACOCK, A. D. (2008a) Climatic and internal factors affecting future UK office heating and cooling energy consumptions. *Energy and Buildings,* 40**,** 874-881.

JENKINS, D. P. (2008) Using dynamic simulation to quantify the effect of carbon-saving measures for a UK supermarket. *Journal of Building Performance Simulation,* 1**,** 275-288.

JENKINS, G. J., MURPHY, J. M., SEXTON, D. M. H., LOWE, J. A., JONES, P. & KILSBY, C. G. (2009) UK Climate Projections: Briefing report. Exeter: Met Office Hadley Centre.

JENKINS, G. J., PERRY, M. C. & PRIOR, M. J. (2008b) The climate of the United Kingdom and recent trends. Exeter: Met Office Hadley Centre.

JONES, P., COMFORT, D. & HILLIER, D. (2009) Marketing Sustainable Consumption within Stores: A Case Study of the UK's Leading Food Retailers. *Sustainability,* 1**,** 815-826.

JONES, P., HARPHAM, C., KILSBY, C., GLENIS, V. & BURTON, A. (2010) *UK Climate Projections science report: Projections of future daily climate for the UK from the Weather Generator* [Online]. Available from: http://ukclimateprojections. metoffice.gov.uk/media.jsp?mediaid=87944&filetype=pdf [Accessed 18 April 2014].

JULIOUS, S. A. (2001) Inference and estimation in a changepoint regression problem. *Journal of the Royal Statistical Society: Series D (The Statistician),* 50**,** 51-61.

KALOGIROU, S. A. (2000) Applications of artificial neural-networks for energy systems. *Applied Energy,* 67**,** 17-35.

KATIPAMULA, S., REDDY, T. A. & CLARIDGE, D. E. (1998) Multivariate Regression Modeling. *Journal of Solar Energy Engineering,* 120**,** 177-184.

KHATTAR, M. K. & HENDERSON, H. I. (2000) Experiences with modelling supermarket energy use and performance. Stockholm: IEA Supermarket Refrigeration Workshop.

KISSOCK, J., REDDY, T. & CLARIDGE, D. (1998) Ambient-temperature regression analysis for estimating retrofit savings in commercial buildings. *Journal of Solar Energy Engineering,* 120.

KOSAR, D., DUMITRESCU, O. & ASHRAE. (2005) *Humidity effects on supermarket refrigerated case energy performance: A database review*.

KRARTI, M. (2011) *Energy audit of building systems: an engineering approach,* Boca Raton, FL: CRC press.

LAM, J. C., CHAN, R. Y. C. & LI, D. H. W. (2002) Simple regression models for fully air-conditioned public sector office buildings in subtropical climates. *Architectural Science Review,* 45**,** 361-369.

LAM, J. C., WAN, K. K. W., LAM, T. N. T. & WONG, S. L. (2010a) An analysis of future building energy use in subtropical Hong Kong. *Energy,* 35**,** 1482-1490.

LAM, J. C., WAN, K. K. W., LIU, D. & TSANG, C. L. (2010b) Multiple regression models for energy use in air-conditioned office buildings in different climates. *Energy Conversion & Management,* 51**,** 2692-2697.

LAM, T. N. T., WAN, K. K. W., WONG, S. L. & LAM, J. C. (2010c) Impact of climate change on commercial sector air conditioning energy consumption in subtropical Hong Kong. *Applied Energy,* 87**,** 2321-2327.

LEACH, M., HALE, E., HIRSCH, A. & TORCELLINI, P. (2009) Grocery Store 50% Energy Savings Technical Support Document. Technical Report NREL/TP-550-46101. Golden, USA: National Renewable Energy Laboratory.

LEBASSI, B., GONZÁLEZ, J. E., FABRIS, D. & BORNSTEIN, R. (2010) Impacts of Climate Change in Degree Days and Energy Demand in Coastal California. *Journal of Solar Energy Engineering,* 132**,** 031005-031005.

LI, D. H. W., YANG, L. & LAM, J. C. (2012) Impact of climate change on energy use in the built environment in different climate zones – A review. *Energy,* 42**,** 103-112.

LLOPIS, R., SÁNCHEZ, D., SANZ-KOCK, C., CABELLO, R. & TORRELLA, E. (2015) Energy and environmental comparison of two-stage solutions for commercial refrigeration at low temperature: Fluids and systems. *Applied Energy,* 138**,** 133-142.

LOVELAND, J. & BROWN, G. (1989) Impacts of Climate Change on the Energy Performance of Buildings in the United States. Oregon: Center for Housing Innovation, University of Oregon.

LUCAS, L. (2006) Using Refrigeration Equipment when facing Climate Change. French Experience. *Interlinked Challenges, Interlinked Solutions: Ozone Protection and Climate Change***,** 15.

MANSKE, K. A., REINDL, D. T. & KLEIN, S. A. (2001) Evaporative condenser control in industrial refrigeration systems. *International Journal of Refrigeration,* 24**,** 676-691.

MARKS AND SPENCER GROUP PLC. (2014) *Annual report and financial statements 2013,* London: Marks and Spencer Group plc.

MARSHALL, J. & PLUMB, A. (2008) *Atmosphere, ocean, and climate dynamics: an introductory text*, Burlington, MA: Elsevier Academic Press.

MATHWORKS. (2011) *MATLAB 7, Getting Started Guide*, The MathWorks: Natick, USA.

MATSUURA, K. (1995) Effects of climate change on building energy consumption in cities. *Theoretical and Applied Climatology*, 51**,** 105-117.

MAVROMATIDIS, G., ACHA, S. & SHAH, N. (2013) Diagnostic tools of energy performance for supermarkets using Artificial Neural Network algorithms. *Energy and Buildings*, 62**,** 304-314.

MEEHL, G. A., STOCKER, T. F., COLLINS, W. D., FRIEDLINGSTEIN, P., GAYE, A. T., GREGORY, J. M., KITOH, A., KNUTTI, R., MURPHY, J. M., NODA, A., RAPER, S. C. B., WATTERSON, I. G., WEAVER, A. J. & ZHAO, Z.-C. (2007) Global Climate Projections. *In:* SOLOMON, S., *et al.* (eds.) *Climate Change 2007: The Physical Science Basis. Contribution of Working Group I to the Fourth Assessment Report of the Intergovernmental Panel on Climate Change.* Cambridge New York: Cambridge University Press.

MET OFFICE. (2006) *Cloud types for observers, Reading the sky*, Exeter: Met Office.

MET OFFICE. (2013) *UK climate regions map* [Online]. Exeter: Met Office. Available from: http://www.metoffice.gov.uk/climate/uk/about/regions-map [Accessed 30 Aug 2013].

MET OFFICE. (n.d.) *UKCP09: Format of 25 km grid files* [Online]. Exeter: Met Offce. Available from: http://www.metoffice.gov.uk/climatechange/science/monitoring/ukcp09/download/gridformat25.html [Accessed 4 Sept 2013].

MONTGOMERY, D. C., PECK, E. A. & VINING, G. G. (2006) *Introduction to Linear Regression Analysis*, Hoboken: John Wiley & Sons.

MOORE, G. (2001) Corporate Social and Financial Performance: An Investigation in the U.K. Supermarket Industry. *Journal of Business Ethics*, 34**,** 299-315.

MULROW, C. D. (1994) *Systematic Reviews: Rationale for systematic reviews*.

MURPHY, J. M., SEXTON, D. M. H., JENKINS, G. J., BOORMAN, P. M., BOOTH, B. B. B., BROWN, C. C., CLART, R. T., COLINS, M., HARRIS, G. R., KENDON, E. J., BETTS, R. A., BROWN, S. J., HOWARD, T. P., HUMPHRY, K. A., MCCARTHY, M. P., MCDONALD, R. E., STEPHENS, A., WALLACE, C., WARREN, R., WILBY, R. & WOOD, R. A. (2009) UK Climate Projection Science Report: Climate change projections. Exeter: Met Office Hadley Centre.

MYLONA, A. (2012) The use of UKCP09 to produce weather files for building simulation. *Building Services Engineering Research and Technology,* 33**,** 51-62.

NAKICENOVIC, N., ALCAMO, J., DAVIS, G., VRIES, B. D., FENHANN, J., GAFFIN, S., GREGORY, K., GRÜBLER, A., JUNG, T. Y., KRAM, T., ROVERE, E. L. L., MICHAELIS, L., MORI, S., MORITA, T., PEPPER, W., PITCHER, H., PRICE, L., RIAHI, K., ROEHRL, A., ROGNER, H.-H., SANKOVSKI, A., SCHLESINGER, M., SHUKLA, P., SMITH, S., SWART, R., ROOIJEN, S. V., VICTOR, N. & DADI, Z. (2000) Special Report on Emissions Scenarios. A Special Report of Working Group III of the Intergovernmental Panel on Climate Change. Cambridge: Cambrige University Press.

NDOYE, M., MOUSSET, S., CARLIER, J. & ARROYO, G. Experimental study of the cold aisle phenomenon in supermarket display cabinets. 23rd IIR International Congress of Refrigeration, 2011.

NEELIN, J. D. (2011) *Climate Change and Climate Modeling,* Cambridge: Cambridge University Press.

NOAA/ESRL. (2014) *Mauna Loa CO2 monthly mean data* [Online]. NOAA/ESRL. Available from: ftp://aftp.cmdl.noaa.gov/products/trends/co2/co2_mm_mlo.txt [Accessed 2 June 2014].

NOZAWA, T., KENKYŪJO, K. K. & SENTĀ, C. K. K. (2007) *Climate change simulations with a coupled ocean-atmosphere GCM called the model for interdisciplinary research on climate: MIROC,* Tsukuba, Japan: Center for Global Environmental Research, National Institute for Environmental Studies.

OGLETHORPE, D. & HERON, G. (2010) Sensible operational choices for the climate change agenda. *The International Journal of Logistics Management,* 21**,** 538-557.

ORPHELIN, M., MARCHIO, D. & BECH, S. (1997) Significant parameters for energy consumption in frozen food area of large supermarkets. *CLIMA 2000.* Brussles.

OUEDRAOGO, B. I., LEVERMORE, G. J. & PARKINSON, J. B. (2012) Future energy demand for public buildings in the context of climate change for Burkina Faso. *Building and Environment,* 49**,** 270-282.

PEDERSEN, L. (2007) Use of different methodologies for thermal load and energy estimations in buildings including meteorological and sociological input parameters. *Renewable and Sustainable Energy Reviews,* 11**,** 998-1007.

PIACENTINI, M., MACFADYEN, L. & EADIE, D. (2000) Corporate social responsibility in food retailing. *International Journal of Retail & Distribution Management,* 28**,** 459-469.

PILLI-SIHVOLA, K., AATOLA, P., OLLIKAINEN, M. & TUOMENVIRTA, H. (2010) Climate change and electricity consumption—Witnessing increasing or decreasing use and costs? *Energy Policy,* 38**,** 2409-2419.

POPE, V. D., GALLANI, M. L., ROWNTREE, P. R. & STRATTON, R. A. (2000) The impact of new physical parameterizations in the Hadley Centre climate model: HadAM3. *Climate Dynamics,* 16**,** 123-146.

POPULA, L. (1991) *Mathematik für Ingenieure 2,* Braunschweig/Wiesbaden, Germany: Fridr. Vieweg & Sohn.

PORS, F. & KICIA, K. (2007) *[Quoted in:] Letters to the Editor: the inbox, The perils of prediction, June 2nd* [Online]. London: The Economist. Available from: http://www.economist.com/blogs/theinbox/2007/07/the_perils_of_prediction_june [Accessed 28/04/ 2015].

PRIOR, M. J. & PERRY, M. C. (2014) Analyses of trends in air temperature in the United Kingdom using gridded data series from 1910 to 2011. *International Journal of Climatology,* 34**,** 3766-3779.

RANDALL, D. A., WOOD, R. A., BONY, S., COLMAN, R., FICHEFET, T., FYFE, J., KATTSOV, V., PITMAN, A., SHUKLA, J., SRINIVASAN, J., STOUFFER, R. J., SUMI, A. & TAYLOR, K. E. (2013) Cilmate Models and Their Evaluation. *In:* STOCKER, T. F., *et al.* (eds.) *Climate Change 2013: The Physical Science Basis. Contribution of Working Group I to the Fifth Assessment Report of the Intergovernmental Panel on Climate Change.* Cambridge and New York: Cambridge University Press.

REICHLER, T. & KIM, J. (2008) How well do coupled models simulate today's climate? *Bulletin of the American Meteorological Society,* 89.

RIFFE, D. R. (1994) Is There a Relationship Between the Ideal Carnot Cycle and the Actual Ideal Carnot Cycle and the Acutual Vapor Compression Cycle? *International Refrigeration and Air Conditioning Conference.* Purdue: Purdue University.

RIVALIN, L., MARCHIO, D., STABAT, P., CACIOLO, M. & COGNÉ, B. (2014) Influence Of Building Zoning On Annual Energy Demand. *3rd International High Performance Buildings Conference.* Purdue, USA: Purdue University.

ROSENTHAL, D. H., GRUENSPECHT, H. K. & MORAN, E. A. (1995) Effects of global warming on energy use for space heating and cooling in the United States. *The Energy Journal,* 16**,** 77-96.

ROSHAN, G. R., OROSA, J. & NASRABADI, T. (2012) Simulation of climate change impact on energy consumption in buildings, case study of Iran. *Energy Policy,* 49**,** 731-739.

ROTMANS, J., HULME, M. & DOWNING, T. E. (1994) Climate change implications for Europe: An application of the ESCAPE model. *Global Environmental Change,* 4**,** 97-124.

ROWELL, D. P. (2006) A demonstration of the uncertainty in projections of UK climate change resulting from regional model formulation. *Climatic Change,* 79**,** 243-257.

RUCH, D., CHEN, L., HABERL, J. S. & CLARIDGE, D. E. (1993) A Change-Point Principal Component Analysis (CP/PCA) Method for Predicting Energy Usage in Commercial Buildings: The PCA Model. *Journal of Solar Energy Engineering,* 115**,** 77-84.

RUCH, D. & CLARIDGE, D. E. (1992) A four-parameter change-point model for predicting energy consumption in commercial buildings. *Journal of Solar Energy Engineering,* 114**,** 77-83.

RUCH, D. K. & CLARIDGE, D. E. (1993) A development and comparison of NAC estimates for linear and change-point energy models for commercial buildings. *Energy and Buildings,* 20**,** 87-95.

SCHRAPS, S. (2005) Energiekostenreduzierung in Supermärkten. *Kälte Klima Aktuell***,** 26-30.

SCHROCK, D. W. & CLARIDGE, D. E. Predicting energy usage in a supermarket. 6th Symposium on Improving Building Systems in Hot and Humid Climates, 1989. Dallas.

SCOTT, M. J., WRENCH, L. E. & HADLEY, D. L. (1994) Effects of Climate Change on Commercial Building Energy Demand. *Energy Sources,* 16**,** 317-332.

SEARLE MANUFACTURING COMPANY. (2008) *CCU-CO2-100, Walk in Condensing Unit for CO2 Cascade system,* Fareham: Searle Manufacturing Company.

SKOVRUP, M. J., JAKOBSEN, A., RASMUSSEN, B. D. & ANDERSEN, S. E. (2012) *CoolPack* (Version: 1.5). Available from: http://en.ipu.dk/Indhold/refrigeration-and-energy-technology/coolpack.aspx [Accessed: 2 Sept 2014].

STEHFEST, E., VUUREN, D. V., KRAM, T., BOUWMAN, L., ALKEMADE, R., BAKKENES, M., BIEMANS, H., BOUWMAN, A., ELZEN, M. D., JANSE, J., LUCAS, P., MINNEN, J. V., MULLER, M. & PRINS, A. G. (2014) *Integrated Assessment of Global Environmental Change with IMAGE 3.0 - Model description and policy application,* The Hague: PBL Netherlands Environmental Assessment Agency.

STOCKER, T. F., CLARKE, G. K. C., TREUT, H. L., LINDZEN, R. S., MELESHKO, V. P., MUGARA, R. K., PALMER, T. N., PIERREHUMBERT, R. T., SELLERS, P. J., TRENBERTH, K. E. & WILLEBRAND, J. (2001) Physical Climate Processes and Feedbacks. *In:* HOUGHTON, J. T., *et al.* (eds.) *Climate Change 2001: The Scientific Basis.* Cambridge and New York: Cambridge University Press.

STOCKER, T. F., QIN, D., PLATTNER, G.-K., ALEXANDER, L. V., ALLEN, S. K., BINDOFF, N. L., BRÉON, F.-M., CHURCH, J. A., CUBASCH, U., EMORI, S., FORSTER, P., FRIEDLINGSTEIN, P., GILLETT, N., GREGORY, J. M., HARTMANN, D. L., JANSEN, E., KIRTMAN, B., KNUTTI, R., KUMAR, K. K., LEMKE, P., MAROTZKE, J., MASSON-DELMOTTE, V., MEEHL, G. A., MOKHOV, I. I., PIAO, S., RAMASWAMY, V., RANDALL, D., RHEIN, M., ROJAS, M., SABINE, C., SHINDELL, D., TALLEY, L. D., VAUGHAN, D. G. & XIE, S.-P. (2013) Technical Summary. *In:* STOCKER, T. F., *et al.* (eds.) *Climate Change 2013: The Physical Science Basis. Contribution of Working Group I to the Fifth Assessment Report of the Intergovernmental Panel on Climate Change.* Cambridge and New York: Cambridge University Press.

STOECKER, W. F. & JONES, J. W. (1983) *Refrigeration and Air Conditioning,* New York: McGraw-Hill Higher Education.

STOVALL, T. K. & BAXTER, V. D. (2010) Modeling Supermarket Refrigeration with EnergyPlus™. *Heat Pump Centre*.

STREET, R. B., STEYNOR, A., BOWYER, P. & HUMPHREY, K. (2009) Delivering and using the UK climate projections 2009. *Weather,* 64**,** 227-231.

STRIBLING, D. (1997) *Investigation into the design and optimisation of multideck refrigerated display cases.* PhD, Brunel University.

SUZUKI, Y., YAMAGUCHI, Y., SHIRAISHI, K., NARUMI, D. & SHIMODA, Y. Analysis and modeling of energy demand of retail stores. Sydney, 14-16 November 2011 2011 12th Conference of International Building Performance Simulation Association.

TASSOU, S. A., GE, Y., HADAWEY, A. & MARRIOTT, D. (2011) Energy consumption and conservation in food retailing. *Applied Thermal Engineering,* 31**,** 147-156.

TASSOU, S. A., LEWIS, J. S., GE, Y. T., HADAWEY, A. & CHAER, I. (2010) A Review of Emerging Technologies for Food Refrigeration Applications. *Applied Thermal Energeering,* 30**,** 263-276.

THE MATHWORKS. (2011) Simulink® 7, User's Guide. Natick, USA: The MathWorks.

THE OPEN UNIVERSITY. (2002) *Environmental Science, Air and Earth,* Milton Keynes: The Open University.

THE UNIVERSITY OF EXETER. (2010) *Future weather files* [Online]. Exeter University of Exeter. Available from: http://emps.exeter.ac.uk/research/energy-environment/cee/research/prometheus/termsandconditions/futureweatherfiles/ [Accessed 10 March 2015].

THOMPSON, M., COOPER, I. & GETHING, B. (2015) The business case for adapting buildings to climate change: Niche or mainstream? Swindon: Innovate UK.

TIEDTKE, M. (1993) Representation of Clouds in Large-Scale Models. *Monthly Weather Review* 121**,** 3040-3061.

TRENBERTH, K. E., HOUGHTON, J. T. & FILOH, L. G. M. (1995) Greenhouse Gases and Aerosols. *In:* HOUGHTON, J. T., *et al.* (eds.) *Climate Change 1995, The Science of Climate Change, Contribution of Working Group I to the Second Assessment Report of the Intergovernmental Panel on Climate Change.* Cambridge and New York: Cambridge University Press.

TSO, G. K. F. & YAU, K. K. W. (2007) Predicting electricity energy consumption: A comparison of regression analysis, decision tree and neural networks. *Energy,* 32**,** 1761-1768.

UNDERWOOD, C. P. & YIK, F. W. H. (2004) *Modelling Methods for Energy in Buildings,* Oxford: Blackwell Science Ltd.

ÜRGE-VORSATZ, D., EYRE, N., GRAHAM, P., HARVEY, D., HERTWICH, E., JIANG, Y., KORNEVALL, C., MAJUMDAR, M., MCMAHON, J. E., MIRASGEDIS, S., MURAKAMI, S. & NOVIKOVA, A. (2012) Chapter 10 - Energy End-Use: Building. *Global Energy Assessment - Toward a Sustainable Future.* Cambridge University Press, Cambridge, UK and New York, NY, USA and the International Institute for Applied Systems Analysis, Laxenburg, Austria.

US DEPARTMENT OF ENERGY. (2013) EnergyPlus Engineering Reference.

VAN DER LINDEN, P. & MITCHELL, J. F. B. (eds.) (2009) *ENSEMBLES: Climate Change and its Impacts: Summary of research and results from the ENSEMBLES project.,* Exeter: Met Office Hadley Centre.

WAN, K. K. W., LI, D. H. W. & LAM, J. C. (2011a) Assessment of climate change impact on building energy use and mitigation measures in subtropical climates. *Energy,* 36**,** 1404-1414.

WAN, K. K. W., LI, D. H. W., PAN, W. & LAM, J. C. (2011b) Impact of climate change on building energy use in different climate zones and mitigation and adaptation implications. *Applied Energy*.

WANG, E. (2015) Benchmarking whole-building energy performance with multi-criteria technique for order preference by similarity to ideal solution using a selective objective-weighting approach. *Applied Energy,* 146**,** 92-103.

WANG, H. & CHEN, Q. (2014) Impact of climate change heating and cooling energy use in buildings in the United States. *Energy and Buildings,* 82**,** 428-436.

WANG, K., EISELE, M., HWANG, Y. & RADERMACHER, R. (2010) Review of secondary loop refrigeration systems. *International Journal of Refrigeration,* 33**,** 212-234.

WANG, S., YAN, C. & XIAO, F. (2012) Quantitative energy performance assessment methods for existing buildings. *Energy and Buildings,* 55**,** 873-888.

WARR, K. & SMITH, S. (1993) *Science Matters, Changing Climate,* Milton Keynes: The Open University.

WHITEHOUSE, L. (2006) Corporate social responsibility: views from the frontline. *JOURNAL OF BUSINESS ETHICS,* 63**,** 279-296.

WIGLEY, T. M. L. (2008) *MAGICC/SCENGEN 5.3: User manual (version 2),* Boulder, USA: National Center for Atmospheric Research.

WONG, S. L., WAN, K. K. W., LI, D. H. W. & LAM, J. C. (2010) Impact of climate change on residential building envelope cooling loads in subtropical climates. *Energy and Buildings,* 42**,** 2098-2103.

WORLD METEOROLOGICAL ORGANIZATION. (n.d.) *Climate Data and Data Related Products* [Online]. Geneva: World Meteorological Organization. [Accessed 05 Jan 2015].

WULFINGHOFF, D. R., RAWAL, R., GRAG, V. & MATHUR, J. (2011) *Energy Conservation Building Code Tip Sheet* [Online]. New Delhi: USAID ECO-III Project. Available from: http://eco3.org/wp-content/plugins/downloads-manager/

upload/Energy%20Simulation%20Tip%20Sheet%20(V-3.0%20March%202011).pdf.

XIANG, C. & TIAN, Z. (2013) Impact of climate change on building heating energy consumption in Tianjin. *Frontiers in Energy,* 7**,** 518-524.

XU, P., HUANG, Y. J., MILLER, N., SCHLEGEL, N. & SHEN, P. (2012) Impacts of climate change on building heating and cooling energy patterns in California. *Energy*.

YU, F. & CHAN, K. (2006) Advanced control of heat rejection airflow for improving the coefficient of performance of air-cooled chillers. *Applied Thermal Engineering,* 26**,** 97-110.

YU, F. W. & CHAN, K. T. (2007) Modelling of a condenser-fan control for an air-cooled centrifugal chiller. *Applied Energy,* 84**,** 1117-1135.

ZHAI, Z. (2006) Application of computational fluid dynamics in building design: Aspects and trends. *Indoor and Built Environment,* 15**,** 305-313.

ZHAI, Z., CHEN, Q., HAVES, P. & KLEMS, J. H. (2002) On approaches to couple energy simulation and computational fluid dynamics programs. *Building and Environment,* 37**,** 857-864.

ZHAO, H.-X. & MAGOULÈS, F. (2012) A review on the prediction of building energy consumption. *Renewable and Sustainable Energy Reviews,* 16**,** 3586-3592.

ZMEUREANU, R. & RENAUD, G. (2008) Estimation of potential impact of climate change on the heating energy use of existing houses. *Energy Policy,* 36**,** 303-310.

Appendix A – Review protocol

Review Question: What is known about the impact of different weather patterns on the energy consumption of supermarkets (in the UK)?

Background

According to figures from the DECC[6] the retail industry uses just under 2% of the total energy consumed in the UK. This is unlikely to decrease despite sustained efforts by this sector to improve their energy efficiency. The article published on the website of The Guardian[7] supports this evaluation as it explains that, although the big supermarket chains are committed to energy efficiency, most of them reported an increase in their energy use, which was mainly put down to their business growth.

A future cause of increased energy consumption may be a change in the prevailing weather pattern. The IPCC[8] suggests that it is almost certain that the weather will have more warm temperature extremes and a decrease in cold spells. This may mean that, while the heating efforts of supermarket decreases, the cooling efforts for both food refrigeration and room cooling may increase, thus leading to a net increase in the demand for energy. This may necessitate a re-negotiation of contracts with energy suppliers and a re-evaluation of the existing utility supply facilities, e.g. to ensure that the main electric incoming cable is capable of supplying sufficient electricity. In addition to this, supermarkets may have to investigate what further technical solutions can be employed to mitigate this increase, e.g. better insulation of certain refrigeration pipes, more rigorous maintenance of condensing units etc.

Although there has been some research conducted in this area[9] the reviewer is not aware of a recent systematic review. In particular, the impact of a change in the weather pattern has not been investigated. Also the quality of models used for predicting energy consumption needs to be looked at in order to identify the most useful one to comprehensively answer the consumption question with respect to different weather parameters (and not dry bulb temperature only).

---

[6] DECC (2012). *Energy consumption in the UK*. Available at www.decc.gov.uk/en/content/cms/statistics/publications/ecuk/ecuk.aspx. Accessed: 20/10/2012

[7] SULLIVAN, R. and GOULDSON A (2012) *Are there limits to energy efficiency for supermarkets?* Available at http://www.guardian.co.uk/sustainable-business/limits-energy-efficiency-supermarkets-retail. Accessed: 19/10/2012

[8] IPCC (2012). Summary for policy makers. In: *Managing the risks of extreme events and disasters to advance climate change adaptation*. [Field, C.B., V. Barros, T.F. Stocker, D. Qin, D.J. Dokken, K.L. Ebi, M.D. Mastrandrea, K.J. Mach, G.-K. Plattner, S.K. Allen, M. Tignor, and P.M. Midgley (eds.)]. A Special Report of Working Groups I and II of the Intergovernmental Panel on Climate Change. Cambridge University Press, Cambridge, UK, and New York, NY, USA, pp. 1-19

[9] E.g. ARIAS, J. 2005. *Energy Usage in Supermarkets: Modelling and Field Measurements.* Kungliga Tekniska Hogskolan (Sweden) DrTechn., Kungliga Tekniska Hogskolan (Sweden); GE, Y. T. & TASSOU, S. A. 2011. Performance evaluation and optimal design of supermarket refrigeration systems with supermarket model "SuperSim", Part I: Model description and validation. *International Journal of Refrigeration*, 34**,** 527-539. or DUCOULOMBIER, M., TEYSSEDOU, A. & SORIN, M. 2006. A Model for Energy Analysis in Supermarkets. *Energy and Buildings*, 38**,** 349-349.

Objectives
• Understanding the amount and quality of published literature available to assess the impact of the change in weather on the energy use of supermarkets • Identify any gaps in the existing literature.
Criteria for Inclusion and Exclusion of Studies:
Types of studies
• Mathematical models
Types of populations
• Supermarkets in the UK The review may also include: • Non-domestic buildings in the UK • Supermarkets outside the UK • Non-domestic buildings outside the UK
Types of intervention or exposure
The type of exposure that will be of interest here is the local weather. This is different from the local climate (i.e. the long term weather trend) and includes various parameters, e.g.: • Dry and wet bulb temperature • Relative humidity • Wind speed and direction • Atmospheric pressure • Global and horizontal solar radiation It is expected that the reviewed material will include mainly dry bulb temperature and relative humidity.
Types of outcome measures
Prediction of electricity consumption. Prediction of gas consumption. Or prediction of electricity and gas consumption
Setting/context (where applicable)
N/A
Search strategy for Identification of Studies
Electronic Databases to be used: • Web of Knowledge (Web of Science) • IEEE/IET Electronic Library

- BSOL – Full text British Standards
- Construction Information Service (CIS)
- ProQuest (incl ProQuest dissertations and theses, technology research database)
- TechXtra
- DART - Europe E-theses portal
- EThOS
- University of Sheffield star library
- Google Scholar
- Index to theses
- JSTOR
- Oxford Scholarship Online
- White Rose eTheses Online (WREO)
- White Rose Research Online (WRRO)
- Questia
- Academic Journals – Engineering
- Library catalogue of Sheffield Hallam University
- COS Conference Papers Index
- DOAJ
- ASHRE

Other Search methods:

- Hand search of list of references of included items
- Search citation index of included documents
- Hand searching the following magazines:
- Contemporary engineering science
- Building and energy
- Building and environment
- Applied energy
- Other magazines may be added as needed

The following websites will also be searched to locate any grey literature:

- Envirowise
- Carbon Trust
- Tesco
- Morrision
- Sainsburry's
- Asda
- Waitrose
- Co-op
- Marks and Spencer

Keywords in title and/or abstract:

1. Supermarket*
2. Hypermarket*
3. Store*
4. Retail*
5. Shop*
6. Non-domest*

7. Energy
8. Power
9. Electricity
10. Gas
11. Weather
12. Climate
13. Environment*
14. Model
15. Simulation
16. Refrigerat*
17. UK
18. Building simulation
19. 1 or 2 or 3 or 4 or 5 or 6 (operationalizing “supermarket”)
20. 7 or 8 or 9 or 10 (operationalizing “energy”)
21. 11 or 12 or 13 (operationalizing “weather”)
22. 14 or 15 (operationalizing “modelling”)
23. 19 and 20
24. 19 and 20 and 17
25. 19 and 20 and 21
26. 19 and 22
27. 19 and 22 and 17

As this review relates to supermarkets in the UK, the keywords will be in English only.

Because of technical advances, literature prior to 1981 will be disregarded.

Method of Review

Selection of studies

To determine whether to include a particular piece of literature the reviewer will read the title and the abstract/preface of all identified literature. A piece of literature will be included if it establishes a link between the energy consumption of a supermarket in the UK (or store etc) and at least one weather parameter. Literature establishing other links between energy consumption and supermarkets (e.g. footfall) may also be included. If less then 150 items are identified, then literature relating to supermarkets outside of the UK will be considered.

Literature relating to non-domestic buildings, but not explicitly studying supermarkets will be excluded.

Assessment of methodological quality

The quality assessment questions include:

- Has the model been verified?
- What is the average percentage error between the prediction of the model and the data used to verify it?
- Has a sensitivity analysis been performed?

Data Extraction
The following data will be extracted: • How many supermarkets (refrigeration systems) have been studied? • In which city/town are these supermarkets (refrigeration systems)? • What is the average consumption breakdown of refrigeration, HVAC and lighting? • What model has been used (Forward or reverse)? • How has the model been derived? • What is the error of the model? • What weather data has been included? • What is the source of the weather/climate data? • What is the relationship between the weather data (or other predictors) and the energy/electricity/gas consumption (in m^2)?
Data Synthesis
The reviewer will initially record the qualitative data in an Excel spreadsheet and then divide the literature into different weather phenomena studies and summarize their conclusions. If there is enough information on the models, the reviewer will perform a quantities study increasing the outside temperature from 13°C (about the UK average[10]) to 17 °C (not an impossible rise according to the IPCC[11]) and compare the change in energy consumption (supermarket size: 2800m^2, the average size of my sponsor supermarkets).
Timeframe

Milestone	Target date
Final protocol	24 Oct 2012
Literature search	05 Nov 2012
Study selection	26 Nov 2012
Data extraction and critical appraisal	17 Dec 2012
Data synthesis	31 Dec 2012
Conclusions	07 Jan 2013
Report writing	16 Jan 2013

[10] MET (n.d.) *Climate averages 1971–2000*. Available at www.metoffice.gov.uk/climate/uk/averages/19712000/areal/england.html. Accessed: 19/10/2012

[11] IPCC (n.d.) *Projection in future changes in climate – AR4 WG1 Summary for policy maker*. Available at http://www.ipcc.ch/publications_and_data/ar4/wg1/en/spmsspm-projections-of.html. Accessed: 19/10/2012

Feedback from Module Tutor or PhD Supervisor
Joint HAR6029 module co-ordinator Dear Martin, Thank you for sending through your review protocol- I think it is looking very good. You have set the scene well with the background section. Your question and inclusion/exclusion criteria is focused, and I like that you have specified up front what you will do in case of no/little UK literature. Your search approach is very thorough and you are searching a number of different sources and methods, which is very good practice. I think your search strategy itself is very good but have a couple of comments 1. Where possible, try and use Database Index terms in your search, however it may not be possible on the databases you are searching (at the moment you are using free-text terms incorporating truncation which is fine). 2. I think your step 20 is the set of results you want to use (at least initially). Some of the later steps in the strategy restrict the search too much. I'm not sure about including the steps 14 and 15 as this could be very restrictive. Similarly, if you are refining to UK literature, you need to include more synonyms (Great Britain, England, Scotland, Wales, Northern Ireland) so you don't miss anything. It all depends on how much literature is returned at step 20 though. In terms of quality assessment, do you know of any published checklists for models? If so, it might be worth using this here or explaining why you are using the criteria you have selected. In terms of data synthesis, it sounds like you will be doing a narrative review- so you should state this. It's looking very good and detailed, so just a few tweaks. Best wishes, Diana -- Joint HAR6029 module co-ordinator   PhD Supervisor (Prof Stephen Beck) Looks OK. Timeframe too tight! 6 months more realistic.

Appendix B – Summary table of analysis tools

Overview of some analysis and simulation tools for the energy consumption in buildings and some comments on

	Name	Description	Advantages	Disadvantages
Data-driven tools	Ratio based performance indicators	Provides a single figure for benchmarking or for pre-audit analysis	– Easy to calculate – Quick to use	– Normalization is limited – Requires large database if used for benchmarking
	Plot against time	Allows identification of general trends, base load and seasonal patterns	– Simple	– Allows only time dependent analysis
	Simple linear regression	Quantifies the relationship between two variables	– Versatile and simple technique	– Only one independent variable possible – Cause and effect not established
	Multiple regression analysis	Versatile tool for whole building energy use or analysis of individual equipment etc	– Flexible – Model parameters have physical meaning	– Cause and effect not established – May require statistical training
	Artificial neural networks	Consists of several connected layers to forecast short- and long-term energy use	– No prior knowledge of model structure required	– No indication of statistical signification – Parameters may have no physical meaning
	Support vector machine	Machine learning algorithm	– Solves non-linear problems effectively	– Complex modelling technique
Deterministic tools	Simplified building energy model	Uses simple heat balance equation to calculate heating and cooling loads	– Can be used for compliance test	– Limited by underlying assumptions
	Thermal network models	Discrete components form a network with temperature nodes	– Versatile	– Limited by discretization
	Computational fluid dynamics method	Uses a mesh of control volumes to simulate fluid flow	– Detailed simulation of fluid flows	– High computational load – Requires understanding of fluid dynamics
	Degree days	Uses balance point temperature to estimate heating or cooling loads	– Simple	– Only for steady state
	Building simulation software	Employed for simulating large buildings with complex HVAC systems	– Capable of modelling complex buildings	– One temperature per zone – Requires high level of expertise – Potentially very inaccurate

Appendix C – Site visit protocol

Site Visit Protocol - Glasgow

Date of visit: 6 May 2014

Name	ANNIESLAND SF	**Store manager**		**Coordinates**	
Number	0397	**Ops manger**		Lat	55.7432
Address	Great Western Road, Glasgow, G13 2TH	**Plan A champion**		Long	-2.8699
		Energy manager		Altitude	30 m (AMSL)
		Opening hours	Mo – Sa: 8:00 – 20:00		Su: 9:00 – 18:00
Store opened	Nov 2010	**Building approval**	?		

Building

Area	Longest length (m)	Longest width (m)	Area (m^2)	Others	Remarks
Total	51.3	39.5	1554.5	Volume: ca 12000 m^3	One floor
Sales floor	44.2	24.8	967.8	Lobby: 24 m^2	Incl. customer toilets
Café	17.4	6	104.4		
Stock	18.45	14.3	223		Incl. coldroom & IT, excluding boiler room
Offices & Staff area	26.5	5.9	156.35		
Plant	16	6.8	108.8		At ground level

Building timers

Name	Description	Day	On	Off	On	Off
Night cover				7:00	20:50	
Main bake			6:00	11:00		
Occu	Occupied alarm: Stock light					
M1	Master 1: Store trading times	Mo - Sa	8:00	20:00		
		Sun	9:00	18:00		
M23	Master 23: HVAC – non essential	Mo – Sa	8:00	16:00	18:00	20:00
		Sun	9:00	11:00	13:00	18:00
M24	Master 24: HVAC - essential	Mo – Sa	8:00	20:00		
		Sun	9:00	18:00		

Sales area

Name	Model	Power	No	Timer	Remarks
Staff	Full time equivalent		37.5		37.5 h/week
Light – Stocking	T5	49 W	57	Occu	
Light – Trading	T5	49 W	57	M1 -5min, 0	
Light – Trading	Twin spot lights	70 W	48	M1 -5min, 0	
Light	Hybrid R5	8 W	3	M1 -5min, 0	Bakery
Light	Recessed downlighter	2x26 W	98	M1 -5min, 0	Customer WC Lobby
Light	T5	28 W	90	M1 0, 0	Piped case
Light	T5	21 W	24	M1 0, 0	Mobile
Light	T8	30 W	28	M1 0, 0	Freezer
Air curtain	Diffusion Airboss 2000W	16 kW - HW	2	M23 -2, 0	Lobby
Unit heater	Diffusion SRW5/22	7.5 kW - HW	7	M23 -2, 0	
Cold aisle heater	GEA Searle, FAH-WC-1R1C-15	6 kW est - HW 0.72 kW - El	12	M23 -2, 0	
Fan	SAVLX63S-223	10 kW	1		Sales area, cold smoke
Fan	Saver, SAVAF250	300 W	1	M24 -5 min, 0	Customer WC
Refrigerated display unit	Lincoln (8ft = 2.44 m)	72 W	2		Produce
Refrigerated display unit	Lincoln (12ft = 3.66 m)	120 W	2		Produce
Refrigerated display unit	Brookland MK4 (5ft = 1.52 m)	54 W	8		
Refrigerated display unit	Brookland MK4 (6ft = 1.83 m)	56 W	1		
Refrigerated display unit	Brookland MK4 (8ft = 2.44 m)	72 W	2		
Refrigerated display unit	Brookland MK4 (14ft = 4.27 m)	126 W	1		
Refrigerated display unit	Brookland MK4 (18ft = 5.49 m)	162 W	1		
Refrigerated display unit	Brookland MK4 (36ft = 10.97 m)	324 W	2		
Refrigerated display unit	Brookland MK4 (38t = 11.58 m)	342 W	4		

Name	Model	Power	No	Timer	Remarks
Freezer	Constan - Symphony	2 kW	7		Incl lights (120 W)
Refrigerated display unit	Brooklands mobile		10		
Wine cooler	Caravell, CBC 800H MK2	700 W	1		
Ice cream freezer	Carrier – TF/TS 17	1.1 kW	1		
Tills	Pan Oston Dutch Florin		5		24h on (for updates)
Self check out			1		24h on (for updates)
Automatic door	Record		3		
Oven	Mono – FG158	7.5 kW	2		
Oven	Mono – DX (Eco-touch)	5 kW	1		Newly installed
Fridge-freezer	Williams, LJ1SA R1	400 W	1		Bakery
Bread slicer	Pico, 450 Jac	490 W	1		Bakery

Café area

Name	Model	Power	No	Timer	Remarks
Staff	Full time equivalent		6		37. 5h/week
Light – Stocking	T5	49 W	4	Occu	
Light – Trading	T5	49 W	4	M1 5 min, 0	
Light	PP9 Pendant	10 W	3	M1 0, 0	
Light	Recessed downlighter	2x26 W	4	M1 0, 0	
Light	Spot lights	35 W	4	M1 0, 0	
Refrigerated display unit	SD2 (1.5 m)	1.6 kW	1	M1 0, 0	Timer for lights
Refrigerator (small)	Delfield	220 W	2		
A/C: 4 way blow cassette	PLA-RP 125BA2	H: 11.9 kW C: 11.25 kW	2	M23 0, 0	
A/C: Wall mount	PKA-RP100KAL	H: 9.5 kW C: 9.2 kW	1	M23 0, 0	
Fan	SAVAF500	1.7 kW	1	M24 -5 min, 0	
Dishwasher	Hobart - AMXXS/31	6.15 - 15.9 kW	1		
Coffee Machines	Faema – Emblema	4.2-7 kW	2		
Microwave	Merrychef - 1925C45UK	3.12 kW	2		
Combination oven/microwave	Merrychef E3CXE	0.7/3 kW	1		
Hot water boiler	Bunn, Single	3 kW	2		
Coffee grinder	Matthew Algie, Eureka	85 W	2		

Name	Model	Power	No	Timer	Remarks
Flykiller	IF50	50 W	1		
Kettle	Marco - Aquarious 15	2.8 kW	1		
Warming Drawers	Wing	1 kW	1		Estimated
Icemaker	Scotsman, ACM56	0.4 kW	1		
Cash register		?	1		

Stock area

Name	Model	Power	No	Timer	Remarks
Ops staff	Full time equivalent		4.5		37.5 h/wk
Light	49W with reflector	58 W	18	PIR	Incl. Boiler room
Light	T5	49 W	2	?	Loading bay, outside
Light	T5	49 W	6	PIR	Coldroom
Outside lamps	Halogen,		?	?	
Light	LED		4	Door	Freezer
Coldroom evaporator	Searle DSR68-6MSHCO2P	104 W	2		1 from pack 1 1 from pack 2
Freezer evaporator	Searle KEC55-6	230 W	1		
Boiler	MHS Boiler – Ultramax R604	285.2 kW	1	M23 -2h, 0	Boiler room
Unit heater	Diffusion SRW5/22	7.5 kW	1	M23 -2, 0	
Air curtain	Diffusion Mirage 2000SC	20.6 kW	1	M23 -2h, 0	Loading bay
Fan	SAVAF400	1.2 kW	1	M24 -5min, 0	Stock area
Fan	OPUS60S-CR		1	M24 -5min, 0	Cleaner
Water Heater	Heatrae - Mega		1	M23 -2h, 0	Boiler room
Pump	Grundfoss – Twin impeller, 85D05965	2 x 1.1 kW	1	M23 -2h, 0	Boiler room
Shutter – Electric roller	Landlords		1		Loading bay
Scissor lift	Sara		1		Loading bay
Printer	HP 4350n	790 W	1		
Computer		150 W	2		incl screen, estim.
Fresh water booster pump	Grundfoss, CM 5-5	900 W	2		

Offices & Staff area

Name	Model	Power	No	Timer	Remarks
Office staff	Full time equivalent		2		37.5 h/wk
Light	Crompton - Modulay	4x14 W	29	Occu	
A/C: 4 Way blow cassette	PLA-RP100BA3	H: 9.5 kW C: 9.2 kW	1	M23 -2, 0	Admin office
A/C: 4 Way blow cassette	PLA-RP100BA3	H: 9.5 kW C: 9.2 kW	1	M23 -2, 0	Staff room
Fan	SAVAF315	730 W	1	M24 -5 min, 0	Staff WC
Fan	SAVAF500	1.7 kW	1	M24 -5 min, 0	General extract
Coffee machine	Crane – V4	2.3 kW	1		Catering unit
Chiller for cold water	Waterlogic	150 W	1		Catering unit
Microwave	Panasonic – NE1037	1.5 kW	2		Catering unit
Kettle	Russell Hobbs	3 kW	1		Catering unit
Toaster		2.2 kW	1		
Computer	Computer etc	150 W	6		
Printer	Different models	av 300 W	4		
Shredder			1		
Charging station			1		
Refrigerator, small	Gram, K 210 RG 3N	99 W	1		
Refrigerator, large	Gram. K 410 RG C 6N	103 W	1		

Plant area

Name	Model	Power	No	Timer	Remarks
Pack No 1 CCU-CO2-080	4DC-5.2Y 4PC-10.2Y 4J-13.2Y	5.29 kW 6.41 kW 12.5 kW	1 1 1		From drawings because no keys available
Pump Station No 1	MSH-CO2-Pump-400V	4 kW	1		Estimated (incl pump)
Condenser		1.7 kW	4		
Condenser No 1	MGC222H-09-EC3	1.9 kW	4		
Pack No 2 CCU-060-CO2	4EC-4.2Y 4DC-5.2Y 4NCS-12.2Y	4.39 kW 5.29 kW 11.15 kW	2 1 1		
Pump Station No 2	MSH-CO2-Pump-400V	4 kW	1		Estimated (incl pump)
Condenser		1.7 kW	2		
Condenser No 2	MXA123H-90-EC3	1.9 kW	2		
Freezer Condenser	Searle NSQ18-3LS-C	3.7 kW	1		
AHU	Systemair KK 062 ST20 40kW LPHW	40kW HW 2.4 kW - El	1	M23 -5 min, 0	Full fresh air AHU + LPHW heating coil and G4 filter
A/C: Condenser	Mitsubishi	8.3 kW	1	M23	

Name	Model	Power	No	Timer	Remarks
	PUHZ-RP250YKA	(max)		-5 min, 0	
A/C: Condenser	Mitsubishi PUHZ-RP100YKA	5 kW (max)	3	M23 -5 min, 0	
Condensing unit	Rivacold, Hum140Z0312/04	3.26 kW	2		For cooling refrigeration packs

Sensor

ID	Description	Controlling	Location	Type
S1	Outside temp	HVAC Plant	Outside north facing wall	PT1000 Sontay TT 531/E External
S6	Salesfloor temp	Unit heater No2-1	Horticulture area	PT1000 Fortune 300 mm Pendant
S7	Salesfloor temp	Unit heater No2-2 to 2-4	Food area	PT1000 Fortune 300 mm Pendant
S8	Salesfloor temp	Unit heater No2-5 to 2-7	Tills area	PT1000 Fortune 300 mm Pendant
S12	Café temp	AC 1-1 and 1-2	Café seating area	PT1000 Fortune 300 mm Pendant

Site Visit Protocol - Gateshead

Date of visit: 7 May 2014

Name	GATESHEAD TEAM VALLEY SF	**Store manager**		**Coordinates**	
Number	0433	**Ops manger**		Lat	54.923
Address	Team Valley RP Gateshead NE11 0BD	**Plan A champion**		Long	-1.620
		Energy manager		Altitude	13.7m (AMSL)
		Opening hours	Mo –We, Sa: 8 – 20:00 Th, Fr: 8:00-21:00		Su: 10:30 – 16:30
Store opened	Aug 2011	**Building approval**	?		

Building

Area	Longest length (m)	Longest width (m)	Area (m^2)	Others	Remarks
Total	54.29	16.75	1726.7	Volume ca 7800 m^3	Both floor, staircases and lift
Sales floor	54.29	16.75	931.8	GF: 771.1 m^2, FF: 160.7 m^2	Incl. customer toilets No lobby
Café	13.7	13.71	204.3		1st floor
Stock	21.7	16.3	261.75		Incl. coldroom & IT, excl. boiler room
Offices & Staff area	13.3	13.8	159		
Plant	10	7.9	79.1		1st floor

Building timers

Name	Description	Day	On	Off	On	Off
Night cover				6:00	Closing + 45 min	
Main bake			6:00	10:00		
Occu	Occupied alarm: Stock light					
M1	Master 1: Store trading times	Mo – We, Sa	8:00	20:00		
		Th - Fr	8:00	21:00		
		Sun	10:30	16:30		
M27	Master 27: HVAC – non essential	Mo – We, Sa	7:30	16:00	18:00	19:30
		Th - Fr	7:30	16:00	18:00	20:30
		Sun	10:00	16:00		
M28	Master 28: HVAC - essential	Mo – Sa	8:00	20:00		
		Sun	10:30	16:30		

Sales area

Name	Model	Power	No	Timer	Remarks
Staff			35		37.5 h/week
Light – Stocking	T5	49 W	69	Occu	
Light – Trading	T5	49 W	70	M1 -5min, -5min	
Light – Trading	Single spot light	35 W	7	M1 -5min, -5min	
Light - Trading	Twin spot light	70 W	70	M1 -5min, -5min	Off which 12 1st floor
Light	Hybrid R5	8 W	2	M1 -5min, -5min	Bakery
Light	Recessed downlighter	2x26 W	8	M1 -5min, -5min	Customer WC
Light	2DE luminaire	14W (est)	2	M1 -5min, -5min	Stair case
Light	T5	21 W	54	M1 0, 0	Piped cases & mobile
Light	T5	28 W	29	M1 0, 0	Piped cases & mobile
Light	T8	30 W	16	M1 0, 0	Freezer
Air curtain	Diffusion Airboss 2000W	13.7 W - HW	1	M28 0, 0	Entrance door (no lobby)
Unit heater	Diffusion SRW5/22	7.5 kW – HW 150W - El	2	M28 0, 0	Sales area
A/C: 4 way blow cassette	PLA-RP125BA2	H: 11.9 kW C: 11.25 kW	2	M27 0, 0	Sales area – ground floor
A/C: 4 way blow cassette	PLA-RP100BA3	H: 9.5 kW C: 9.2 kW	2	M27 0, 0	Sales area – first floor
Cold aisle heater	GEA Searle, FAH-WC-1R1C-15	6 kW est - HW 0.72 kW - El	12	M28 0, 0	
Cold aisle heater	Diffusion, WH18/4 HOCH	5.3 kW – HW 34 W - El	1	M28 0, 0	
Fan	AX63AA-463A	4 kW	1		Sales area, cold smoke
Fan	AX560-453A	1.5 kW	1		Sales area, cold smoke
Fan	NALAF250	130 W	1	M27 0, 0	Customer WC
Refrigerated display unit	Lincoln (8 ft = 2.44 m)	72 W	2		Produce
Refrigerated display unit	Lincoln (12 ft = 3.66 m)	120 W	2		Produce
Refrigerated display unit	Lincoln (20ft = 6.1 m)	192 W	1		Produce

Name	Model	Power	No	Timer	Remarks
Refrigerated display unit	Brookland MK4 (5 ft = 1.52 m)	54 W	6		
Refrigerated display unit Mobile	Brookland MK4 (8 ft = 2.44 m)	72 W	2		Mobile
Refrigerated display unit	Brookland MK4 (8 ft = 2.44 m)	72 W	1		
Refrigerated display unit Mobile	Brookland MK4 (6 ft = 1.83 m)	56 W	2		Mobile
Refrigerated display unit	Brookland MK4 (14 ft = 4.27 m)	126 W	3		
Refrigerated display unit	Brookland MK4 (26 ft = 7.92m)	234 W	4		
Refrigerated display unit	Brookland MK4 (30 ft = 9.14 m)	270 W	2		
Wine cooler	Caravell, CBC 800H MK2	700 W	1		
Freezer	Constan - Symphoney	2 kW	4		
Ice cream freezer	Carrier – TF/TS 17	1.1 kW	1		
Tills	Pan Oston Dutch Florin		4		
Selfcheck out			5		
Automatic door	Record		1		
Oven	Mono – BX	7.5 kW	2		Bakery
Freezer	Williams, LJ1SAR1	400 W	1		Bakery
Breadslicer	Pico, 450 Jac	490 W	1		Bakery

Café area

Name	Model	Power	No	Timer	Remarks
Staff	Full time equivalent		18		37.5 h/week
Light	T5	49W	16	Occu	Incl 3 in kitchen
Light	T5	49W	15	M1 -5, -5	Incl 4 in kitchen
Light	PP9 Pendant	10W	6	M1 -5, -5	
Light	1x58W c/w reflector	58W	7	M1 -5, -5	
Light	Recessed downlight	2x26W	4	M1 -5, -5	
Refrigerated display unit	SD2 (1.5 m=5 ft)	1.6 kW	2	M1 -5, -5	
Fridge	Williams	310 W	4		
Fridge	Defrige	340 W	1		
Freezer	Williams	345 W	1		
A/C: 4 way blow cassette	PLA-RP 100BA3	H: 9.5 C: 9.2	2	M27 0, 0	
Fan	NALAF500	1.7 kW	1	M27 0, 0	Extractor
Dishwasher	Horbart – AMXXS/31	10 - 15.9 kW	1		

Name	Model	Power	No	Timer	Remarks
Coffee Machines	Faema – Emblema	4.2-7 kW	3		
Kettle	Marco - Aquarious 15	2.8 kW	1		
Hot water boiler	Bunn, Single	3 kW	1		
Blender	Magrini, Vitamix	85 W	2		
Microwave	Merrychef – 1925c	3.12 kW	2		
Insectocutor	IF50 S/S	50W	1		
Oven/Microwave	Merrycheff –eikon e4	3.2 kW/1.5 kW	2		
Warming Drawers	Wing	1 kW	1		Estimated
Icemaker	Scotsman, ACM56	0.4 kW	1		
Fridge	Delfried, Willams	217 W	2		
Coffee grinder	Matthew Algie, Eureka	85 W	2		
Cash register			3		

Stock area (incl Goods in)

Name	Model	Power	No	Timer	Remarks
Ops staff	Full time equivalent		10		37.5 h/week
Light	1x49W c/w reflector	49 W	31	PIR	Off which 10 ground floor
Light	T5 49 W	49 W	8	PIR	Cold room
Light	Bulkhead	18 W	7	Switch	
Cold room Evaporator	Searle DSR62-6ALCO2P	75 W	1		Pack 1
Cold room Evaporator	Searle DSR51-6	75 W	1		Condensing unit
Freezer Evaporator	Searle KEC45-6	230 W	1		Condensing unit
Boiler	MHS Boiler – Ultramax R603	242 kW	1		Boiler room
Unit heater	Diffusion SRW5/22	7.5kW – HW	1	M28 0, 0	
Air curtain	Diffusion Mirage 2000SC	20.6kW	1	M28 0, 0	Loading bay
Fan	NALAF315	730 W	1		Stock & cleaners
Fan	NALAF400	1.2 kW	1		Stock area
Water Heater	Heatrae – Mega	24.3 kW	1		Boiler room
Pump	Grundfoss – UPS	650 W	1		Boiler room
Shutter – Electric roller	Landlords		1		Loading bay
Scissor lift	Sara		1		

Offices & Staff area

Name	Model	Power	No	Timer	Remarks
Office staff	Full time equivalent		2		37.5 h/week
Light	T5	49 W	5	Occu	Stair case
Light	T8 Recessed modular	4x14 W	33	PIR	
Light	Recessed downlighter	2x26W	4	PIR	

Name	Model	Power	No	Timer	Remarks
A/C: Wall mounted	PAK-RP35HAL	H: 3.5 kW C: 3.2 kW	1	M27 0, 0	Admin office
A/C: 4 Way blow cassette	PLA-RP35BA	H: 3.5 kW C: 3.2 kW	1	M27 0, 0	Staff room
Fan	NALAF250	330 W	1	M27 0, 0	Staff WC
Fan	NALAF315	730W	1	M27 0, 0	General
Coffee machine	Crane – V4	2.3 kW	1		Catering unit
Chiller for cold water	Waterlogic, F4FW	150 W	1		Catering unit
Microwave	Panasonic, NE1037	1.5 kW	2		Catering unit
Toaster	Russell Hobbs	2.2 kW	1		
Printer		300 W	2		Estimated
Photocopier			1		
Shredder			1		
Charging station		150 W	2		
Refrigerator (small)	Gram, K 210 RG 3N	99 W	1		Catering unit
Refrigerator (large)	Gram. K 410 RG C 6N	103 W	1		Catering unit

Plant area

Name	Model	Power	No	Timer	Remarks
Light	2DE Luminaire	16 W	8		
Light	Recessed downlighter	2x26 W	6		
A/C: Condenser	Mitsubishi PUHZ-RP250YKA	12.4 kW	1	M27 0, 0	
A/C: Condenser	Mitsubishi PUHZ-RP200YKA	11.2 kW	2	M27 0, 0	
A/C: Condenser	Mitsubishi PUHZ-RP35VHA4	2.5 kW	2	M27 0, 0	
AHU	System Air – KW100 ST200 42 kW LPHW	42 kW - HW 2.13 kW	1	M27 0, 0	Supply AHU complete with LPHW heater & filter
Refrigeration Pack Searle CCU-CO2-100	4CC-6.2Y 4J-13.2Y 4G-20.2Y 4TCS-8.2Y	6.36 kW 12.5 kW 17.12 kW 8.17 kW	1 1 1 1		
Pump Station	MSH-CO2-Pump-400V	4 kW	1		Estimated (Incl pump)
Condenser		1.7 kW	4		
Condenser unit – Cold room	Searle, SCQ27-1MX-A-CU	1.7 kW	1		Cold room
Condenser unit - Freezer	Searle, NCQ24-3LS-D2W1	4.8 kW	1		

Sensor

ID	Description	Controlling	Location	Type
S1	Outside temp	HVAC Plant	Outside north facing wall	PT1000 Sontay TT 531/E External
S6	Salesfloor temp	Unit heater No2-1 & H2-2	Tills area	PT1000 Fortune 300 mm Pendant
S7	Salesfloor temp	Unit heater No2-3 to 2-4	General merchandise	PT1000 Fortune 300 mm Pendant
S12	Café temp	AC 12	Café seating area	PT1000 Fortune 300 mm Pendant

Site Visit Protocol - Washington

Date of visit: 7 May 2014

Name	WASHINGTON GALLERIES SF	**Store manager**		**Coordinates**	
Number	S0420	**Ops manger**		Lat	54.900
Address	Washington Tyne and Wear NE38 7SD	**Plan A champion**		Long	-1.532
		Energy manager		Altitude	66m (AMSL)
		Opening hours	Mo – Sa: 8 – 20:00		Su: 10:30 – 16:30
Store opened	May 2011	**Building approval**	?		

Building

Area	Longest length (m)	Longest width (m)	Area (m^2)	Others	Remarks
Total	GF: 44.8 FF: 22.8	GF:19.7 FF: 19.7	GF: 883 FF: 439	Volume: ca 7090 m^3	Two floors
Sales floor	41.7	19.7	650	Lobby: 26 m^2	Incl. customer toilets
Café	20.2	4. 6	93		
Stock	22.3	15.3	268.4		incl. coldroom & IT, excluding boiler room
Offices & Staff area	13.3	10.4	140		
Plant	12.2	4.7	60		1st floor

Building timers

Name	Description	Day	On	Off	On	Off
Night cover			6:30 – 7:00	20:30 - 20:45		
Main bake			6:30	9:30		
Occu	Occupied alarm					
M1	Master 1: Store trading times	Mo - Sa	8:00	20:00		
		Sun	10:15	18:30		
M13	Master13: HVAC – non essential	Mo-Fr	8:30	16:00	18:00	19:00
		Sa	8:30	18:00		
		Sun	11:00	16:00		
M14	Master14: HVAC – essential	Mo-Fr	8:00	20:00		
		Sa	8:00	19:00		
		Sun	10:30	18:30		

Sales area

Name	Model	Power	No	Timer	Remarks
Staff	Full time equivalent		19		37.5 h/week
Light – Stocking	T5	49 W	44	Occu	
Light – Trading	T5	49 W	45	M1 0, 0	
Light – Trading	Single spot light	35 W	94	M1 0, 0	
Light	Hybrid R5	8 W	3	M1 0, 0	Bakery
Light	Recessed down lighter	2x26 W	13 8	M1 0, 0 M1 0, 0	Customer WC Lobby
Light	2DE luminary	14W (est)	2		Stair case
Light	T5	28 W	22	M1 0, 0	Piped cases
Light	T8	30 W	8	M1 0, 0	Freezer
Light	T5	21 W	31	M1 0, 0	Piped cases
Air curtain	Diffusion Airboss 2000W	16 kW - HW	2	M13 0, -0.5	Lobby
Unit heater	Diffusion SRW5/22	7.5 kW - HW	4	M13 0, -0.5	
Cold aisle heater	Gea Searle, FAH-WC-1R1C-15	6 kW est - HW 0.72 kW	10	M14 0, -1	
Fan	NALT-200L	125 W	1	M13 0, -0.5	Sales area
Fan	NALT-250	130 W	1	M13 0, -0.5	Customer WC
Refrigerated display unit	Lincoln (8ft = 2.44 m)	72 W	4		
Refrigerated display unit	Brookland MK4 (5ft = 1.52 m)	54 W	10		
Refrigerated display unit	Brookland MK4 (10ft = 3.05 m)	90 W	7		
Refrigerated display unit	Brookland MK4 (38ft = 11.6 m)	350 W	3		
Wine cooler	Caravell, CBC 800H MK2	700 W	1		
Ice cream freezer	Carrier – TF/TS 17	1.1 kW			
Freezer	Constan - Symphoney	2 kW	4		
Tills	Pan Oston Dutch Florin		3		
Self check out			4		
Automatic door	Record		3		
Oven	Mono – BX	7.5 kW	2		Bakery
Oven	Mono - DX	5 kW	1		Bakery
Freezer	Williams, LJ1SAR1	400 W	1		Bakery
Breadslicer	Pico, 450 Jac	490 W	1		Bakery

Café area

Name	Model	Power	No	Timer	Remarks
Staff	Full time equivalent		6		37.5 h/week
Light	T5	49 W	6	Occu	
Light	T5	49 W	6	M1 0, 0	
Light	PP9 Pendant	10 W	3	M1 0, 0	
Light	Recessed downlight	2x26 W	5	M1 0, 0	
Light	Spot lights	35 W	9	M1 0, 0	
Refrigerated display unit	SD4-150E (1.5m)	1.6 kW	1		
A/C: 4 way blow cassette	PLA-RP 140BA2	H: 13.6 kW C: 12.9 kW	1	M13 0, 0	
Fan	NALAF500	1.7 kW	1	M14 0, 0	Extractor
Dishwasher	Horbart - AMXXS/31	10 - 15.9 kW	1		
Hot water boiler	Bunn, Single	3 kW	2		
Blender	T&G2 Magrini	1.2 kW	1		
Warming Drawers	Wing	1 kW	1		Estimated
Insectocutor	IF50 S/S	50W	1		
Refrigerator	Dellfield, RS10100U	250 W	3		
Combination oven/microwave	Merrychef E3CXE	0.7/3 kW	1		
Microwave	Merrychef, 1925C	3.12 kW	1		
Blender	Magrini, Vitamix	85 W	1		
Coffee grinder	Matthew Algie, Eureka	85 W	2		
Kettle	Marco - Aquarious 15	2.8 kW	1		
Coffee Machines	Faema – Emblema	4.2-7 kW	2		
Icemaker	Scotsman, ACM56	0.4 kW	1		
Fridge					
Cash register			1		

Stock area

Name	Model	Power	No	Timer	Remarks
Ops staff	Full time equivalent		7		37.5 h/week
Light	1x49 W c/w reflector	49 W	FF: 21 4 6 6	PIR PIR	 Downstairs Coldroom Staircase
Lights	Bulkhead	18 W	8	Switch	Freezer
Air curtain	Diffusion Mirage 1500SC	17.16 kW	1	M13 0, -0.5	Loading bay
Unit heater	Diffusion SRW5/22	7.5 kW - HW	1	M13 0, -0.5	1st floor
AHU	Systemair	25 kW - HW	1	M14	Full fresh air

	KK 25 kW LPHW	1.33 kW (electric)		0, 0	AHU with LPHW heating coil and G4 filter
Fan	NALAF315	730 W	1	M13 0, -0.5	Stock area
Coldroom Evaporator	Searle DSR62-6CO2P	104 W	1		
Coldroom Evaporator	Searle DSR51-6	192 W	1		
Freezer Evaporator	Searle KEC70-6L	231 W	1		
Boiler	MHS Boiler – Ultramax R603	237 kW	1	M14 0, -1	Boiler room
Pump	Grundfoss, T040	900 W	1		Boiler room
Pump	Siemens, 1101	3 kW	1		Boiler room
Lift - Goods	OTIS, ND8905		1		Boiler room
Water Heater	Heatrae – Mega	24.3 kW	1		Boiler room
Pressurisation Unit	Lowara Mini v series		1		Boiler room
Pump	Grundfoss – TPE	1.1 kW (?)	2		Boiler room
Shutter – Electric roller	Landlords		1		Loading bay
Scissor lift	Sara		1		
Printer	HP 4350n	790 W	1		
Computer		150 W	2		incl screen, estim.
Fresh water booster pump	Grundfoss, CM 5-5	900 W	2		

Offices & Staff area

Name	**Model**	**Power**	**No**	**Timer**	**Remarks**
Office staff	Full time equivalent		3		37.5 h/week
Light	Crompton - Modulay	4x14W	32	Occu	
Fan	NALAF250	330 W	1	M13 0, -0.5	Staff WC
Fan	NALT-100L	75 W	1	M13 0, -0.5	Spare office
Water cooler	Waterlogic, F4FW	150 W	1		Catering Unit
Kettle	Russell Hobbs, 13949	3 kW	1		Catering Unit
Microwave	Panasonic, NE1037	1.5 kW	2		Catering Unit
Coffee Machines	Crane, V4	2.3 kW	1		Catering Unit
Toaster	Russell Hobbs	2.2 kW	1		
Refrigerator (small)	Gram, K 210 RG 3N	99 W	1		Catering unit
Refrigerator (large)	Gram. K 410 RG C 6N	103 W	1		Catering unit
Shredder	HSM, Securo B32		1		
Computer		150 W	6		
Printer		300 W	3		estimated
Photocopier			1		
Charging station	Different models	av 100 W	5		estimated

Plant area

Name	Model	Power	No	Timer	Remarks
Light	Bulk head	18 W	8		
A/C: Condenser	PUHZ-RP140YKA	4.36 kW	1	M13 0, 0	
R404A pack Searle, CCU100	4CC-6.2Y 4J-13.2Y 4G-20.2Y 4TCS-8.2Y	6.36 kW 12.5 kW 17.12 kW 8.17 kW	1 1 1 1		
Pump Station	Star, CCU-CO2-HSG	3 kW	1		Nikkiso BR22D-A3
Condenser		1.7 kW	4		
Condenser unit - Freezer	Searle, NCQ24-3LS-D2W1	4.8 kW	1		
Condenser unit – Cold room	Searle, SCQ27-1MX-A-CU	1.7 kW	1		

Sensor

ID	Description	Controlling	Location	Type
S1	Outside temp	HVAC Plant	Outside north facing wall	PT1000 Sontay TT 531/E External
S6	Salesfloor temp	Unit heater No2-1 & H2-2	Tills area	PT1000 Fortune 300 mm Pendant
S7	Salesfloor temp	Unit heater No2-3 to 2-4	General merchandise	PT1000 Fortune 300 mm Pendant
S12	Café temp	AC 12	Café seating area	PT1000 Fortune 300 mm Pendant

Site Visit Protocol - Hull

Date: 2 Nov 2012 (and 4 July 2014)

Name	ANLABY HULL SF	**Store manager**		**Coordinates**	
Number	0374	**Ops manger**		Lat	53.748
Address	Springfield Way Hull, HU10 6RJ	**Plan A champion**		Long	-0.425
		Energy manager		Altitude	6 m (AMSL)
		Opening hours	Mo: 9:00 – 18:00 Tu – Sa: 8 – 20:00		Su: 10:00 – 16:00
Store opened	July 2010	**Building approval**	?		

Building

Area	Longest length (m)	Longest width (m)	Area (m^2)	Others	Remarks
Total	57.3	31.8	1822	Volume: ca 13700 m^3	One floor
Sales floor	40.9	32.6	1192	Lobby: 26 m^2	Incl. customer toilets
Café	16.5	7	115.5		
Stock	14.5	21.5	301		Incl. coldroom & IT, excluding boiler room
Offices & Staff area	16.7	10	167		
Plant	11.2	9.98	111.8		At ground level

Building timers

Name	Description	Day	On	Off	On	Off
Night cover				6:30	20:00	
Main bake			6:00	10:00		
Occu	Occupied alarm: Stock light					
M1	Master 1: Store trading times	Mo – Fr	8:00	20:00		
		Sun	10:00	16:00		
M8	Master 23: HVAC – non essential	Mo – Sa	7:30	16:00	18:00	19:30
		Sun	9:00	11:00	13:00	18:00
M9	Master 24: HVAC - essential	Mo – Sa	7:30	18:00	18:00	19:30
		Sun				

Sales area

Name	Model	Power	No	Timer	Remarks
Staff	Full time equivalent		23		37.5h/week
Light – Stocking	T5	49 W	63	Occu	
Light – Trading	T5	49 W	78	M1	
Light – Trading	Twin spot lights	35 W	112	M1	
Light	T5	49W	57		Refrigeration
Light	T8	30W	12		
Light	Hybrid R5	8 W	3	M1	Bakery
Light	Recessed downlighter	2x26 W	9 8	M1	Customer WC Lobby
Air curtain	Diffusion Airboss 2000W	13.7 kW - HW	2		Lobby
Unit heater	Diffusion SRW5/22	7.5 kW - HW	5		
A/C: Condenser	Mitsubishi PLA_PRRPBA2	H: 11.9 kW C: 11.5 kW	3	M1	
Fan	SAVLX56P-273	10 kW			Sales area, cold smoke
Fan	Saver, SAVAF250	300 W	1	M8	Customer WC
Refrigerated display unit	Lincoln (16ft = 4.9 m)		2		Produce
Refrigerated display unit	Lincoln (8ft = 2.44 m)		2		Produce
Refrigerated display unit	Brookland MK4 (5ft = 1.52 m)		10	M1	Case light timer
Refrigerated display unit	Brookland MK4 (8ft = 2.44 m)		4	M1	Case light timer
Refrigerated display unit	Brookland MK4 (18ft = 5.47 m)		1	M1	Case light timer
Refrigerated display unit	Brookland MK4 (36ft = 10.97m)		5	M1	Case light timer
Refrigerated display unit	Brookland Mobile (6ft = 1.83m)		5	M1	Case light timer
Freezer	Constan - Symphony	2 kW	3 (5)	M1	Case light timer
Wine cooler	Caravell, CBC 800H MK2	700 W	1		
Tills	Pan Oston Dutch Florin		5		24h on (for updates)
Self check out			5		24h on (for updates)
Automatic door	Record		3		
Oven	Mono – BX	7.5 kW	2		Bakery Main bake
Fridge-freezer	Williams, LJ1SA R1	400 W	1		Bakery
Breadslicer	Pico, 450 Jac	490 W	1		Bakery

Café area

Name	Model	Power	No	Timer	Remarks
Staff	Full time equivalent		8		37.5h/week
Light – Stocking	T5	49 W	6	M1	
Light – Trading	T5	49 W	9	M1	

Name	Model	Power	No	Timer	Remarks
Light	PP9 Pendant	10 W	4	M1	
Light	Recessed downlighter	2x26 W	5	M1	
Light	Spot lights	35 W	4	M1	
Refrigerated display unit	SD2 (1.5m)		1	M1	Timer for lights
Refrigerator (small)	Delfield, RS 10100	250 W	2		
A/C	PLA-RP100BA3	H: 9.5 C: 9.2	2	M8	
Fan	SAVAF500	1.7 kW	1	M8	
Dishwasher	Hobart - AMXXS/31	6.15 - 15.9 kW	1		
Coffee Machines	Faema – Emblema	4.2-7 kW	2		
Microwave	Merrychef - 1925C45UK	3.12 kW	1		
Hot water boiler	Bunn, Single	3 kW	2		
Coffee grinder	Matthew Algie, Eureka	85 W	2		
Flykiller	IF50	50 W	?		
Kettle	Marco - Aquarious 15	2.8 kW	1		
Warming Drawers	Wing	500 W	1		
Cash register		?	1		
Icemaker	Scotsman, ACM56	0.4 kW	1		
Blending station	Vitamax, T&G VM0122	1.5kW	1		

Stock area

Name	Model	Power	No	Timer	Remarks
Ops staff	Full time equivalent		5		37.5h/wk
Light	T5	49 W	27	PIR	Incl. Boiler room
Light	T5	49 W	6	PIR	Coldroom
Outside lamps	Halogen	?	5		Outside
Light	LED		3	Door	Freezer
Coldroom evaporator	Searle DSR62-6AL CO2P	75 W	1 1		1 from pack 1 1 from pack 2
Freezer evaporator	Searle ?	? W	1		
Boiler	MHS Boiler – Ultramax R604?	285.2 kW	1	M8 -2h, 0	Boiler room
Unit heater	Diffusion SRW5/22	7.5 kW - HW	2	M8	
Air curtain	Diffusion Mirage 2000SC	20.6 kW	1	M8 -2h, 0	Loading bay
Fan	SAVAF500	1.1 kW	1	M9	Stock area
Fan	OPUS95D-CR	100W	1	M9	Cleaner
Water Heater	Heatrae - Mega		?	M8 -2h, 0	Boiler room
Pump	Grundfoss – Twin impeller 85D05965	2 x 1.1 kW	?	M8 -2h, 0	Boiler room
Shutter – Electric roller	Landlords		1		Loading bay
Scissor lift	Sara		1		Loading bay

Offices & Staff area

Name	Model	Power	No	Timer	Remarks
Office staff	Full time equivalent		3		37.5h/wk
Light	Crompton - Modulay	4x14 W	25	Occu	
A/C: 4 Way blow cassette	PLA-RP35BA	H: 3.5 C: 3.3	1	M8	Admin office
A/C: 4 Way blow cassette	PLA-RP35HAL	H: 3.5 C: 3.3	1	M8	Staff room
Fan	SAVAF315	300W	1	M9	Staff WC
Fan	SAVAF400	1.1 KW	1	M9	General extract
Door			1		Goods in
Coffee machine	Crane – V4	2.27 kW	1		Catering unit
Chiller for cold water	Waterlogic	150 W	1		Catering unit
Microwave	Panasonic – NE1037	1.5 kW	2		Catering unit
Kettle	Russell Hobbs				Catering unit
Computer	Computer etc	150 W	4		
Printer	Different models	av 300 W	1		
Shredder			1		
Charging station		150 W	1		
Refrigerator (small)	Gram, K 210 RG 3N	99 W	1		
Refrigerator (large)	Gram. K 410 RG C 6N	103 W	1		

Plant area

Name	Model	Power	No	Timer	Remarks
Pack No 1 CCU-080-CO2	4J-13.2Y-40P 4PCS-10.2Y-40P 4DC-5.2Y-40P	15 kW 12 kW 4.5 kW	1 1 2		
Pump Station No 1	MSH-CO2-Pump-400V	4 kW	1		
Condenser		1.7 kW	4		
Condenser No 1	MGC222H-09-EC3	1.9 kW	4		
Pack No 2 CCU-060-CO2	4NCS-12.2Y-40P 4DC-5.2Y-40S 4EC-4.2Y-40S	13.3 kW 4.5 kW 6 kW	1 1 2		
Condenser		1.7 kW	2		
Pump Station No 2	MSH-CO2-Pump-400V	4 kW	1		
Condenser No 2	MXA123H-90-EC3	1.9 kW	2		
Freezer Condenser	Searle NSQ18-3LS-C	3.7 kW	1		
AHU	Systemair MRLT031X 65kW LPHW	2.4 kW (electric) 65kW - HW	1	M8	Full fresh air AHU with LPHW coil and G4 filter
A/C: Condenser	Mitsubishi PUHZ-RP125VKA	5 kW(max)	1	M8	
A/C: Condenser	Mitsubishi	2.5 kW(max)	2	M8	

Name	Model	Power	No	Timer	Remarks
	PUHZ-RP35VKA				
A/C: Condenser	Mitsubishi PUHZ-RP200VKA	10.5 kW(max)	1	M8	
A/C: Condenser	Mitsubishi PUHZ-RP250YKA	ca 12 kW(max)	3	M8	
Condensing unit	GEA Searle, NSQ15-3LS-A3WI	3.1 kW	1		

Sensor

ID	Description	Controlling	Location	Type
S1	Outside temp	HVAC Plant	Outside north facing wall	PT1000 Sontay TT 531/E External
S2	Salesfloor temp	Unit heater No2-1	Sales floor rear area	PT1000 Fortune 300mm Pendant
S3	Salesfloor temp	Unit heater No2-2 to 2-4	Sales till area	PT1000 Fortune 300mm Pendant
S8	Salesfloor temp	Unit heater No2-5 to 2-7	Café revive area	PT1000 Fortune 300mm Pendant

Site Visit Protocol - Leicester

Date: 3 July 2014

Name	LEICESTER THURMASTON SF	**Store manager**		**Coordinates**	
Number	0386	**Ops manger**		Lat	52.684
Address	Thorpe Lane Leicester LE4 8GP	**Plan A champion**		Long	-1.088
		Energy manager		Altitude	72 m (AMSL)
		Opening hours	Mo – Sa: 8:00 – 20:00		Su: 9 – 16:30
Store opened	Nov 2010	**Building approval**	?		

Building

Area	Longest length (m)	Longest width (m)	Area (m^2)	Others	Remarks
Total	48	28	1640	Volume: 9210 m^3	Two floors
Sales floor	48	28	899	Lobby: 20.25 m^2	Incl. customer toilets
Café	17	6	101		
Stock	24	18.5	390		Incl. coldroom & IT, excluding boiler room
Offices & Staff area	17.5	9.2	200		
Plant	3.2	3.2	10.4	On roof	First floor

Building timers

Name	Description	Day	On	Off	On	Off
Night cover				6-7:00	20:00	
Main bake			6:00	10:00		
Occu	Occupied alarm: Stock light					
M1	Master 1: Store trading times	Mo - Sa	08:00	20:00		
		Sun	09:00	16:30		
M8	Master 8: HVAC staff zone	Mo – Su	04:00	18:00		
M9	Master 9: HVAC sales zone	Mo – Sa	08:00	16:00		
		Sun	08:00	15:00		

Sales area

Name	Model	Power	No	Timer	Remarks
Staff	Full time equivalent		26		37.5h/week
Light – Stocking	T5	49 W	77	Occu	
Light – Trading	T5	49 W	78	M1 0, 0	
Light – Stocking	T5	49 W	7	Occu	Stair case
Light – Trading	Spot lights	35 W	81	M1 0, 0	
Light	T5	28 W	63		Refrig. shelves
Light	T5	21 W	8		Refrig. shelves
Light	T8	30 W	24		Freezer
Light	Recessed downlighter	2x26 W	9 6	M1 0, 0	Customer WC Lobby
Air curtain	Diffusion Savanna 2000 high cap	20 kW - HW	2	M9 0,0	Lobby
Unit heater	Carrier 42 GW008	6.7 kW - HW	4	M9 0,0	
Cold aisle heater	GEA Searle, FAH-WC-1R1C-15	6 kW est - HW 0.72 kW	9	M9 0,0	
Fan	AXC 800-9/31 6	3 kW	1		Sales area, cold smoke
Fan	Saver, KVKEF250	265 W	1	M9 0,0	Customer WC
Refrigerated display unit	Lincoln (8ft = 2.44m)	72 W	2		Produce
Refrigerated display unit	Lincoln (18ft = 5.5m)	162 W	2		Produce
Refrigerated display unit	Brookland MK4 (5ft = 1.52m)	54 W	8		
Refrigerated display unit	Brookland MK4 (6ft = 1.83m)	56 W	4		Mobile
Refrigerated display unit	Brookland MK4 (26ft = 8m)	234 W	7		
Refrigerated display unit	Brookland MK4 (28ft = 8.5m)	238 W	1		
Freezer	Constan - Symphony	2 kW	6		
Wine cooler	Caravell, CBC 800H MK2	700 W			
Ice cream freezer	Carrier – TF/TS 17	1.1 kW	1		
Tills	Pan Oston Dutch Florin		4		24h on (for updates)
Self check out			4		24h on (for updates)
Automatic door	Record		3		
Oven	Mono – BX	7.5 kW	2		Bakery
Fridge-freezer	Williams, LJ1SA R1	400 W	1		Bakery
Breadslicer	Pico, 450 Jac	490 W	1		Bakery
Computer		150 W	2		

Café area

Name	Model	Power	No	Timer	Remarks
Staff	Full time equivalent		5		37.5h/week
Light – Stocking	T5	49 W	5	Occu	
Light – Trading	T5	49 W	6	M1 0, 0	
Light	PP9 Pendant	10 W	4	M1 0, 0	
Light	Recessed downlighter	2x26 W	4	M1 0, 0	
Light	Spot lights	35 W	18	M1 0, 0	
Refrigerated display unit	SD2 (1.5m)		1		Timer for lights
Refrigerator	Delfield	217 W	2		
Refrigerator	Williams, Ha135SA	279 W	1		
Refrigerator (small)	Delfield	220 W	2		
A/C: 4 way blow cassette	PLA-RP 71 BA	H: 6.8 kW C: 6.5 kW	2	M9 0,0	
Fan	MUB 042 500 DV-K2	1.5 kW	1	M9 0,0	
Dishwasher	Hobart - AMXXS/31	6.15 - 15.9 kW	1		
Coffee Machines	Faema – Emblema	4.2-7 kW	2		
Microwave	Merrychef - 1925C45UK	3.12 kW	1		
Combination oven/microwave	Merrychef E3CXE	0.7/3 kW	1		
Hot water boiler	Bunn, Single	3 kW	1		
Coffee grinder	Matthew Algie, Eureka	85 W	1		
Flykiller	IF50	50 W	1		
Kettle	Marco - Aquarious 15	2.8 kW	1		
Warming Drawers	Wing	1 kW	1		
Icemaker	Scotsman, ACM56	0.4 kW	1		
Cash register		?	1		

Stock area

Name	Model	Power	No	Timer	Remarks
Ops staff	Full time equivalent		4.5		37.5h/wk
Light	T5	49 W	GF: 6 FF: 19	PIR	Incl. Boiler room
Light	T5	49 W	6		Coldroom
Light	T5	49 W	3		Loading bay, outside
Outside lamps	Halogen	150 W	7		Estimated
Light	LED		4	Switch	Freezer
Coldroom evaporator	Searle DSR51-6	75 W	2		1 from pack 1 1 from pack 2
Freezer evaporator	Searle	50 W	1		
Boiler	MHS Boiler – Ultramax	285.2 kW	1		Boiler room

Name	Model	Power	No	Timer	Remarks
	R603				
Unit heater	Diffusion SRW 5/50	10 kW - HW	1	M9 0, 0	FF
Air curtain	Diffusion Mirage 1500W	16 kW	2	M9 0, 0	Loading bay
Fan	KVKE 315 EC	300 W	1	M9 0, 0	GF: Goods in
Fan	MUB 042 450	580 W	1	M9 0, 0	FF: Stock room
Fan	OPUS60S-CR	50 W	1	M9 0, 0	Cleaner
Water Heater	Heatrae - Mega		1	M9 0, 0	Boiler room
Heating pump	Grundfoss	1.1 kW	2	M9 0, 0	Boiler room
Shutter – Electric roller	Landlords				Loading bay
Scissor lift	Sara				Loading bay
Fresh water booster	Grundfoss	1.1 kW	2		Loading bay
AHU	Modulair	28kW – HW 1.5 kW (est)	1		Loading bay, sealing
Computer		150 W	2		
Printer		300 W	2		

Offices & Staff area

Name	Model	Power	No	Timer	Remarks
Office staff	Full time equivalent		2.5		37.5h/week
Light	Down lighter	55 W	14	PIR	
Light	Recessed downlighter	2x26 W	9	PIR	
Light	T5	49 W	3	PIR	
A/C: 4 Way blow cassette	PLA-RP50BA	H: 5.1 kW C: 4.6 kW	1	M9 0, 0	Admin office
A/C: 4 Way blow cassette	PLA-RP60BA	H: 5.05 kW C: 5.5 kW	1	M9 0, 0	Staff room
Fan	KVKE 250 EC	265 W	1	M9 0, 0	Staff WC
Fan	KVKE 200 EC	157 W	1	M9 0, 0	General extract
Fan	KVKE 160 EC	100 W	2	M9 0, 0	Staff & spare
Door			1		Goods in
Coffee machine	Crane – V4	2.3 kW	1		Catering unit
Chiller for cold water	Waterlogic	150 W	1		Catering unit
Microwave	Panasonic – NE1037	1.5 kW	2		Catering unit
Computer	Computer etc	150 W	7		Incl 1 TV
Printer	Different models	av 300W	3		
Shredder			1		
Charging station		120 W	2		

Name	Model	Power	No	Timer	Remarks
Refrigerator (small)	Gram, K 210 RG 3N	99W	1		
Refrigerator (large)	Gram. K 410 RG C 6N	103W	1		

Plant area

Name	Model	Power	No	Timer	Remarks
Pack No 1 CCU-CO2-100	4CC-6.2Y-40S 4TCS-8.2Y-40P 4J-13.2Y-40P 4G-20.2Y-40P	6.5 kW 8.2 kW 12.5 kW 17.12 kW	1 1 1 1		
Pump Station No 1	MSH-CO2-Pump-400V	3 kW	1		
Condenser No 1	MGC222H-09-EC3	1.9kW	4		
Freezer Condenser	Searle NSQ15-3LS-C	3.1kW	1		
A/C: Condenser	Mitsubishi PUHZ-RP50VHA4	2.5 kW	1	M8 0, 0	
A/C: Condenser	Mitsubishi PUHZ-RP60VHA4	3.7 kW	1	M8 0, 0	
AC: Condenser	Mitsubishi PUHZ-RP140YKA	7.7 kW	1	M9 0, 0	
Condensing unit	Searle, SCQ31-1MX-A-CU	1.8 kW	2		For cooling refrigeration packs

Sensor

ID	Description	Controlling	Location	Type
	Outside temp	Boiler		

See drawing

Site Visit Protocol - Newbury

Date of visit: 20 May 2014

Name	PINCHINGTON LN NEWBURY SF	**Store manager**		**Coordinates**	
Number	0387	**Ops manger**		Lat	51.385
Address	Pinchington Lane Newbury RG14 7HU	**Plan A champion**		Long	-1.318
		Energy manager		Altitude	123.9m
		Opening hours	Mo – Fr: 8:00 – 20:00 Sa: 8:00 - 19:00		Su: 10:00 – 16:00
Store opened:	Nov 2010	**Building approval:**			

Building

Area	Longest length (m)	Longest width (m)	Area (m^2)	Others	Remarks
Total	54.3	17.7	1912 (inc stairs)	Volume: 8266m^3	Two floors
Sales floor	46.3	17.7	1190	No lobby	Both floors Incl. customer toilets
Café	15	17.7	219.6		
Stock	18.8	17.7	199		Incl. coldroom and IT, excluding boiler room
Offices & Staff area	10.6	13.9	145		
Plant	6.4	6.1	40		At ground level

Building timers

Name	Description	Day	On	Off	On	Off
Night cover				6:00	20:00	
Main bake			6:00	9:30-10:00		
Occu	Occupied alarm: Stock light					
M1	Master 1: Store trading times	Mo - Fr	8:00	20:00		
		Sa	8:00	19:00		
		Sun	10:00	16:00		
M8	Master 8: HVAC - Essential	Mo-Fr	8:00	20:00		
		Sa	8:00	19:00		
		Sun	10:00	16:00		
M9	Master 9: HVAC – non essential	Mo – Fr	7:30	16:00	18:00	19:30
		Sa	7:30	16:00	18:00	18:30
		Sun	9:30	16:00		

Sales area

Name	Model	Power	No	Timer	Remarks
Staff	Full time equivalent		33		37.5h/week
Light – Stocking	T5	49 W	51 16	Occu	Ground floor 1st floor
Light – Trading	T5	49 W	52 17	M1 0, 0	Ground floor 1st floor
Light	Twin spot lights	70 W	49 16	M1 0, 0	Ground floor 1st floor
Light	Single spot lights	35 W	7	M1 0, 0	Ground floor
Light	Hybrid R5	8 W	3	M1 0, 0	Bakery
Light	Recessed downlighter	2x26 W	10 5	M1 0, 0	Customer WC Others
Light	T8	30 W	12	M1 0, 0	Freezer
Light	T5	21 W	4	M1 0, 0	Piped case
Light	T5	28 W	51	M1 0, 0	Piped case
Light	T5	36 W	28	M1 0, 0	Piped case
Air curtain	Diffusion Airboss 1550W	9.66 kW - HW	2	M9 0, 0	Lobby
Unit heater	Diffusion SRW5/22	7.5 kW - HW	2	M8 0, 0	Ground floor
A/C: 4 Way blow cassette	PLA-RP71BA2	H: 8.55 kW C: 6.8 kW	2	M9 0, 0	Ground floor
A/C: 4 Way blow cassette	PLA-RP71BA2	H: 8.55 kW C: 6.8 kW	2	M9 0, 0	1st floor
Cold aisle heater	GEA Searle, FAH-WC-1R1C-15	6 kW est - HW 72 W - Elec	10	M9 0, -5 min	
Fan	SAVLX56P-273	12 kW	1	M8 0, 0	Sales area, cold smoke
Fan	Saver, SAVAF250	300 W	1	M8 0, 0	Customer WC
Refrigerated display unit	Lincoln (10ft = 3 m)	100 W	4		Produce
Refrigerated display unit	Brookland MK4 (5ft =1.52 m)	54 W	8		
Refrigerated display unit	Brookland MK4 (6ft = 1.83 m)	56 W	2		
Refrigerated display unit	Brookland MK4 (16ft = 4.9 m)	144 W	2		
Refrigerated display unit	Brookland MK4 (26ft = 7.9 m)	234 W	2		
Refrigerated display unit	Brookland MK4 (28ft = 8.5 m)	252 W	4		
Refrigerated	Brookland MK4	378 W	1		

Name	Model	Power	No	Timer	Remarks
display unit	(42ft = 12.8 m)				
Freezer	Constan - Symphoney	2 kW	3		
Wine cooler	Caravell, CBC 800H MK2	700 W	1		
Ice cream freezer	Carrier – TF/TS 17	1.1 kW	1		
Tills	Pan Oston Dutch Florin		5		Also FF
Self check out			5		
Automatic door	Record		1		
Oven	Mono – FG158	7.5kW	2		Bakery
Fridge-freezer	Williams, LJ1SA R1	400 W	1		Bakery
Bread slicer	Pico, 450 Jac	490 W	1		Bakery

Café area

Name	Model	Power	No	Timer	Remarks
Staff	Full time equivalent		10		37.5h/week
Light – Stocking	T5	49 W	17	Occu	
Light – Trading	T5	49 W	17	M1 0, 0	
Light	T5	49 W	6	M1 0, 0	
Light	PP9 Pendant	10 W	4	M1 0, 0	
Light	Recessed downlighter	2x26 W	5	M1 0, 0	
Light	Spot lights	35 W	6	M1 0, 0	
Light	Twin spot lights	70 W	7	M1 0, 0	
A/C: 4 way blow cassette	PLA-RP 125BA2	H: 11.9 kW C: 11.5 kW	3	M9 0, 0	
AC: Wall mounted	PKA-RP100KAL	H: 9.55 kW C: 9.2 KW	1	M9 0, 0	
Refrigerator	Delfield RS 101001	217 W	5		
Refrigerator	Delfield RS 101001-FM83	279 W	1		
Refrigerator	Delfield RS 20700	340 W	1		
Refrigerator	Delfield RS 21400	370 W	1		
Refrigerated display unit	SD2 (1.2m)	1.6 kW	1		
Fan	SAVAF500	1.7kW	1	M8 0, 0	
Dishwasher	Horbart – AMXXS/31	10 - 15.9 kW	1		
Coffee Machines	Faema – MA17427	4.2-7 kW	2		
Microwave	Merrychef - 1925C45UK	3.12 kW	2		
Oven	Merrychef E3CXE	4.3 kW	2		
Hot water boiler	Soft heat SHBREW1	3 kW	1		
Coffee grinder	Matthew Algie, Eureka	85 W	2		
Flykiller	IF50	50W	1		
Icemaker	Scotsman, ACM56	0.4 kW	1		
Kettle	Marco - Aquarious 15	2.8 kW	2		
Blender	Magrini, Vitamix	85 W	2		

Icemaker	Scotsman, ACM56	0.4 kW	1		
Cash register			3		

Stock area

Name	Model	Power	No	Timer	Remarks
Ops staff	Full time equivalent		7.5		37.5h/week
Light Incl. Boiler room	T5	49 W	7 21	PIR PIR	Ground floor 1st floor
Light	T5	49W	6	PIR	Coldroom
Outside lamps	Son floodlight	70W	4	Photocell	
Light	LED (large)		4	PIR	Freezer
Coldroom evaporator	Searle DSR62-6ALCO2P	75 W	1		Pack 1
Cold room Evaporator	Searle DSR51-6	75 W	1		Condensing unit
Freezer evaporator	Searle KEC55-6	75 W			Condensing unit
Fan	SAVAF315	730 W	1	M8 0, 0	
Fan	SVAVF500	1.7 kW	1	M8 0, 0	
Unit heater	Diffusion SRW5/22	7.5kW - HW	2	M8 0, 0	GF: 1, FF: 1
Boiler	MHS Boiler – Ultramax R603	237.2 kW	1	M8 -2 h, +0.5 h	Boiler room
Pump	Grundfoss – Twin impeller 85D05965	2 x 1.1kW	1		Boiler room
Scissor lift	Sara		1		Loading bay
Computer		150 W	2		
Printer		300 W	1		
Charger		150 W	3		

Offices & Staff area

Name	Model	Power	No	Timer	Remarks
Office staff	Full time equivalent		2.5		37.5h/week
Light	Crompton - Modulay	4x14 W	3 27	PIR PIR	Ground floor 1st floor
Light	T5	49 W	7	Occu	Stair case
A/C: 4 Way blow cassette	PLA-RP35BA	H: 9.5 kW C: 9.2 kW	1	M8 0, 0	Staff room
A/C: Wall mount	PKA-RP35HAL	H: 3.5 kW C: 3.3 kW	1	M8 0, 0	Admin office
Fan	SAVAF250	330 W	1	M8 0, 0	General extract
Fan	SAVAF315	730 W	1	M8 0, 0	Staff WC
Coffee machine	Crane – V4	2.3 kW	1		Catering unit
Chiller for cold water	Waterlogic	150 W	1		Catering unit

Name	Model	Power	No	Timer	Remarks
Microwave	Panasonic – NE1037	1.5 kW	2		Catering unit
Kettle	Russell Hobbs	3 kW	1		Catering unit
Computer	Computer etc	150 W	5		
Printer	Different models	av 300 W	3		
Shredder	HSM		1		
Charging station		120 W	1		
Refrigerator (small)	Gram, K 210 RG 3N	99 W	1		Switched off
Refrigerator (large)	Foster EPRO G600H	349 W	1		

Plant area

Name	Model	Power	No	Timer	Remarks
Pack No 1 CCU-CO2-100	4CC-6.2Y-40S 4TCS-8.2Y 4PC-10.2Y 4J-13.2Y	6.4 kW 8.2 kW 9.37 kW 12.5 kW	1 1 1 1		Inside plant area
Condenser		1.7 kW	4		
Pump Station No 1	MSH-CO2-Pump-400V	4 kW	1		Inside plant area
Condenser Unit No 1	NSQ18-3LS-C2W	3.7 kW	1		Outside plant area
Condenser Unit No 2	N2DQ90-3MS-E3W	10.2 kW	1		Outside plant area
A/C: Condenser	Mitsubishi PUHZ-RP250YKA	ca 12.4 kW(max)	1		Outside plant area
A/C: Condenser	Mitsubishi PUHZ-RP140YKA	7.7 kW	2		Outside plant area
A/C: Condenser	Mitsubishi PUHZ-RP125YKA	5.6 kW	1		Outside plant area
A/C: Condenser	Mitsubishi PUHZ-RP100YKA	4.7 kW	1		Outside plant area
A/C: Condenser	Mitsubishi PUHZ-RP35VHA4	2.7 kW	2		Outside plant area
AHU	Systemair KK 100 ST200 54kW LPHW	2.2kW – Elec 54 kW - HW	1	M9 0, 0	Inside plant area
Fresh water booster pump	MHI404 -1/E/1-230-50-2	0.75 kW	2		Inside plant area

Sensor

ID	Description	Controlling	Location	Type
	Outside temp	HVAC Plant		PT1000 Sontay TT 531/E External
	Salesfloor temp	Unit heater No 2	General merchandise	PT1000 Fortune 300 mm Pendant

Site Visit Protocol - Exebridge

Date of visit: 21 May 2014

Name	EXEBRIDGE EXETER SF	**Store manager**		**Coordinates**	
Number	5295	**Ops manger**		Lat	50.717
Address	Unit 4 Exeter Bridges Retail Park Exeter, EX4 1AH	**Plan A champion**		Long	-3.538
		Energy manager		Altitude	10m
		Opening hours:	Mo – Sa: 8:00 – 20:00		Su: 11:00 – 17:00
Store opened:	Dec 2011	**Building approval:**			

Building

Area	Longest length (m)	Longest width (m)	Area (m^2)	Others	Remarks
Total	54.39	26.65	1444	Volume: 10440m^3	Height only appr.
Sales floor	36.8	26.65	790.2	Lobby: 24.2m^2	Incl customer WC
Café	15.5	6.8	114.6		
Stock	17	20.2	210		Incl cold rooms Excl boiler room
Offices & Staff area	17	10.6	150		
Plant	Two plant areas: one mezzanine floor (incl boiler): 24.2m^2 , one outside: 19.9m^2				

Building timers

Name	Description	Day	On	Off	On	Off
Night cover				6-7:00	20:45	
Main bake			6:00	10:00		
Occu	Occupied alarm: Stock light					
M1	Master 1: Store trading times	Mo - Sa	8:00	20:00		
		Sun	11:00	17:00		
M4	External loading bay light	Mo - Th	5:30	9:00		
		Fr	5:00	8:00		
		Sa	5:30	9:00		
		Su	7:00	9:00		
M26	Master 26: HVAC	Mo - Sa	7:30	16:00	18:00	19:30
		Sun	10:30	16:00		

Sales area

Name	Model	Power	No	Timer	Remarks
Staff	Full time equivalent		23		37.5 h/week
Light – Stocking	T5	49 W	52	Occu	
Light – Trading	T5	49 W	52	M1 0, -10 min	
Light	T5	28 W	45	M1 0, 0	Piped cases
Light	T5	21 W	14	M1 0, 0	Mobile cases
Light	T8	30 W	24	M1 0, 0	Freezer
Light	Twin spot lights	70 W	47	M1 0, 0	
Light	Single spot lights	35 W	6	M1 0, 0	
Light	Hybrid R5	8 W	4	M1 0, 0	Bakery
Light	Recessed downlighter	2x26 W	8 13	M1, 0, 0 PIR	Lobby Customer WC
Air curtain	Diffusion Airboss 2000W	16 kW - HW	2	M26 -15min, 0	Lobby
Unit heater	Diffusion SRW5/22	7.5 kW - HW	4	M26 -15min, 0	
Ducted unit heater	Diffusion, HWW27 18-4B	5.4 kW - HW	1	M26 -15min, 0	
Cold aisle heater	GEA Searle, FAH-WC-1R1C-15	6 kW est - HW 0.72 kW	12	Not active	
Fan	SAVLX63S-223	10kW	1		Sales area, cold smoke
Fan	Nuaire, NALAF 150	100 W	1	M26 0, 0	Customer WC
Refrigerated display unit	Lincoln (8 ft = 2.44 m)	72 W	2		Produce
Refrigerated display unit	Lincoln (12 ft = 3.66 m)	120 W	2		Produce
Refrigerated display unit	Brookland MK4 (5 ft =1.52 m)	54 W	10		
Refrigerated display unit	Brookland MK4 (6 ft = 1.83 m)	56 W	1		
Refrigerated display unit	Brookland MK4 (8 ft = 2.44 m)	72 W	5		
Refrigerated display unit	Brookland MK4 (18 ft = 5.49 m)	162 W	1		
Refrigerated display unit	Brookland MK4 (22 ft = 6.71 m)	198 W	4		
Refrigerated display unit	Brookland MK4 (24 ft = 7.32 m)	216 W	4		
Refrigerated display unit	Brookland MK4 (36ft = 10.97 m)	324 W	1		

Name	Model	Power	No	Timer	Remarks
Freezer	Constan - Symphoney		6		Incl lights (120 W)
Wine cooler	Caravell, CBC 800H MK2	700 W	1		
Ice cream freezer	Carrier – TF/TS 17	1.1 kW	1		
Tills	Pan Oston Dutch Florin		3		24h on
Self check out			6		24h on
Automatic door	Record		3		
Oven	Mono – FG158	7.5kW	2		Bakery
Fridge-freezer	Williams, LJ1SA R1	400W	1		Bakery
Bread slicer	Pico, 450 Jac	490W	1		Bakery

Café area

Name	Model	Power	No	Timer	Remarks
Staff	Full time equivalent		7		37.5 h/week
Light	T5	49W	8	Occu	
Light	T5	49W	8	M1 0, -10 min	
Light	PP9 Pendant	10W	4	M1 0, -10 min	
Light	Recessed downlighter	2x26W	5	M1 0, -10 min	
Light	Spot lights	35W	8	M1 0, -10 min	
Refrigerated display unit	SD2 (1.5m)	36 W	1	M1 0, -10 min	
Refrigerator (small)		200 W	3		
A/C: 4 way blow cassette	PLA-RP 125BA2	H: 11.9 kW C: 11.25 kW	2	M26 0, 0	
Fan	Nuaire, SAVAF500	1.7 kW	1	M26 0, 0	
Dishwasher	Horbart - AMXXS/31	6.15 - 15.9 kW	1		
Coffee Machines	Faema – MA17689		2		
Coffee Machines	Faema – Emblema	4.2-7 kW	2		
Microwave	Merrychef - 1925C45UK	3.12 kW	1		
Oven	Merrychef E3CXE	0.7/3 kW	1		
Hot water boiler	Soft heat SHSTAT1	3 kW	1		
Coffee grinder	Matthew Algie, Eureka	85 W	1		
Flykiller	IF50	50W	1		
Kettle	Marco - Aquarious 15	2.8 kW	1		

Name	Model	Power	No	Timer	Remarks
Icemaker	Scotsman, ACM56	0.4 kW	1		
Cash register		?	1		

Stock area

Name	Model	Power	No	Timer	Remarks
Ops staff	Full time equivalent		5		37.5 h/week
Light	T5	49 W	24	PIR	Incl. Boiler area
Light	T5	49 W	4	M4 0, 0	Loading bay, outside
Outside lamps	Son floodlights	70W	3		
Light	T5	49 W	8	PIR	Coldroom
Light	Bulk head	18 W	8	Switch	Freezer
Coldroom evaporator	Searle DSR68-6MSHCO2P Searle DSR42-6 AL	50 W 50 W	1 1		1 from pack 1 1 from pack 2
Freezer evaporator	Searle KEC55-6	75 W	1		
Boiler	MHS Boiler – Ultramax R603	237.2 kW	1	M1 -2h, -0.5h	Boiler area (Mezzanie)
Unit heater	Diffusion SRW5/22	7.5kW - HW	1	M26 0, 0	
Air curtain	Diffusion Mirage 2000SC	20.6kW - HW	1	M26 0, 0	Loading bay
AHU	Systemair	29 kW - HW 1.5 kW (fan)	1	M26 0, 0	
Fan	Nuaire, NALAF400	1.2 kW	1	M26 0, 0	Stock area
Fan	Nuaire, NALAF150	100 W	1	M26 0, 0	Cleaner
Water Heater	Heatrae - Mega	?	1		Boiler area (Mezzanine)
Pump	Grundfoss – 96430300	1.15 kW			Boiler area (Mezzanine)
Pump	Grundfoss	50 W	1		Boiler area (Mezzanine)
Cold water booster pump		750 W	2		
Shutter – Electric roller	Landlords		1		Loading bay
Scissor lift	Sara		1		Loading bay
Computer		150 W	2		
Printer	HP Laser Jet 4350n	800 W	1		
Charging stations		150 W	2		Estimated

Offices & Staff area

Name	Model	Power	No	Timer	Remarks
Office staff	Full time equivalent		1		37.5 h/week
Light	Crompton - Modulay	4x14W	32	PIR	
A/C: 4 Way blow cassette	PLA-RP35BA	H: 3.3 kW C: 3.5 kW	1	M26 0, 0	Admin office
A/C: 4 Way blow cassette	PLA-RP35BA	H: 3.3 kW C: 3.5 kW	1	M26 0, 0	Staff room
Fan	Nuaire, NALAF200	230 W	1	M26 0, 0	Staff WC
Fan	Nuaire, NALAF250	330 W	1	M26 0, 0	General extract
Coffee machine	Crane – V4	2.3 kW	1		Catering unit
Chiller for cold water	Waterlogic	150 W	1		Catering unit
Microwave	Panasonic – NE1037	1.5 kW	2		Catering unit
Computer	Computer etc	150 W	6		
Printer	Different models	av 300W	2		
Shredder			1		
Charging station		150 W	4		Estimated
Refrigerator (large)	Gram. K 410 RG C 6N	103W	1		
Toaster		2.2 kW	1		
Photo copier		400 W	1		Estimated

Plant areas (one in building, one outside)

Name	Model	Power	No	Timer	Remarks
Pack No 1 Searle, MSO100 - CO2-HX	4DC-5.2Y 4G 20.2 4CC-6.2Y-40.2S 4TCS-8.2Y 4J-13.2Y	5.3 kW 6.7 kW 8.2 kW 12.5 kW	1 1 1 1		
Pump Station No 1	MSH-CO2-Pump-400V	3 kW	1		
Condenser		1.7 kW	4		
Condenser No 1	MGC224H-EC465	1.9kW	4		
Freezer Condenser	Searle NDQ45-3MS-C	5.1 kW	2		
A/C: Condenser	Mitsubishi PUHZ-RP250YKA	ca 11.7 kW(max)	2		
A/C: Condenser	Mitsubishi PUHZ-RP35VHA4	2.4 kW	2		
Condensing unit	Searle, NSQ18-3LX-C	3.7 kW	1		For cooling refrigeration packs

Sensor

ID	Description	Controlling	Location	Type
S1	Outside temp	HVAC Plant	Outside north facing wall	PT1000 Sontay TT 531/E External
S6	Till area space temperture	Unit heater No2-1, 2	Sales Tills area	PT1000 Fortune 300 mm Pendant
S7	Sales GM area temperature	Unit heater H2-3, 4	Sales GM Area	PT1000 Fortune 300 mm Pendant
S14	Café space temperature	AC 1	Café revive area	PT1000 Fortune 300 mm Pendant

Appendix D – Matlab programmes

```
%%%%%%%%%%%%%%%%%%%%%%%%%%%%%%%%%%%%%%%%%%%%%%%%%%%%%%%%%%%%%%%%%%
%
% This script calculates estimates for future energy consumption in
% supermarkets. It is part of the PhD project
%
%%%%%%%%%%%%%%%%%%%%%%%%%%%%%%%%%%%%%%%%%%%%%%%%%%%%%%%%%%%%%%%%%
%% Tidy
clear
clc

disp('Started')

%% Import data
Mdl=importdata('C:\Users\bao_mading\Documents\MATLAB\Supermarket.xlsx');
TPbs=mth2wk(Mdl.data(:,2)); % Generating weekly data from monthly
TP10=mth2wk(Mdl.data(:,3));
TP50=mth2wk(Mdl.data(:,4));
TP90=mth2wk(Mdl.data(:,5));

gB0=Mdl.data(1,6); % Gas model intercept
gB1=Mdl.data(1,7); % Gas model slope

eCP=Mdl.data(1,8); % Electricity model change point
eB0=Mdl.data(1,9); % Electricity model intercept before CP
eB1=Mdl.data(1,10); % Electricity model slope before CP
eB0_a=Mdl.data(1,11); % Electricity model intercept after CP
eB1_a=Mdl.data(1,12); % Electricity model slope after CP

gMSres=Mdl.data(1,13); % Mean of square of gas data residuals
elMSres=Mdl.data(1,14); % Mean of square of electricity data residuals


%% Calculating gas consumption
Gbs=gB1*TPbs+gB0; % Weekly consumption
G10=gB1*TP10+gB0;
G50=gB1*TP50+gB0;
G90=gB1*TP90+gB0;

TotGbs=sum(Gbs); % Annual consumption
TotG10=sum(G10);
TotG50=sum(G50);
TotG90=sum(G90);

%% Calculating electricity consumption

% Weekly consumption
if eCP~=0 % If change point model
    for i = 52:-1:1

        if TPbs(i) < eCP
            Ebs(i)=eB1*TPbs(i)+eB0;
        else
            Ebs(i)=eB1_a*TPbs(i)+eB0_a;
```

```
        end

        if TP10(i) < eCP
            E10(i)=eB1*TP10(i)+eB0;
        else
            E10(i)=eB1_a*TP10(i)+eB0_a;
        end

        if TP50(i) < eCP
            E50(i)=eB1*TP50(i)+eB0;
        else
            E50(i)=eB1_a*TP50(i)+eB0_a;
        end

        if TP90(i) < eCP
            E90(i)=eB1*TP90(i)+eB0;
        else
            E90(i)=eB1_a*TP90(i)+eB0_a;
        end

    end
else % If not change point model
    Ebs=eB1*TPbs+eB0;
    E10=eB1*TP10+eB0;
    E50=eB1*TP50+eB0;
    E90=eB1*TP90+eB0;
end


TotEbs=sum(Ebs); % Annual consumption
TotE10=sum(E10);
TotE50=sum(E50);
TotE90=sum(E90);


%% Error estimate
t = 2; % for 95% confidence and 40 df (50 not in table)
c = 1+1/52;

% Base year temperature error
Sx=sum(TPbs);
Sxx= sum(TPbs.^2) - Sx^2/52;
gasErVc=t*sqrt(gMSres*(c+(TPbs-Sx)/Sxx));
elErVc=t*sqrt(elMSres*(c+(TPbs-Sx)/Sxx));
gasErbs=sqrt(sum(gasErVc.^2));
elErbs=sqrt(sum(elErVc.^2));


% Future 10% temperature error
Sx=sum(TP10);
Sxx= sum(TP10.^2) - Sx^2/52;
gasErVc=t*sqrt(gMSres*(c+(TP10-Sx)/Sxx));
elErVc=t*sqrt(elMSres*(c+(TP10-Sx)/Sxx));
gasEr10=sqrt(sum(gasErVc.^2));
elEr10=sqrt(sum(elErVc.^2));


% Future 50% temperature error
Sx=sum(TP50);
```

```
Sxx= sum(TP50.^2) - Sx^2/52;
gasErVc=t*sqrt(gMSres*(c+(TP50-Sx)/Sxx));
elErVc=t*sqrt(elMSres*(c+(TP50-Sx)/Sxx));
gasEr50=sqrt(sum(gasErVc.^2));
elEr50=sqrt(sum(elErVc.^2));

% Future 90% temperature error
Sx=sum(TP90);
Sxx= sum(TP90.^2) - Sx^2/52;
gasErVc=t*sqrt(gMSres*(c+(TP90-Sx)/Sxx));
elErVc=t*sqrt(elMSres*(c+(TP90-Sx)/Sxx));
gasEr90=sqrt(sum(gasErVc.^2));
elEr90=sqrt(sum(elErVc.^2));

%% Calculating change in consumption

gasChange10 = (TotG10-TotGbs)/TotGbs; % Relative increase gas
gasChange50 = (TotG50-TotGbs)/TotGbs;
gasChange90 = (TotG90-TotGbs)/TotGbs;

gasChange10Er = sqrt(gasEr10^2+gasErbs^2)/TotGbs; % Relative error of gas
increase
gasChange50Er = sqrt(gasEr50^2+gasErbs^2)/TotGbs;
gasChange90Er = sqrt(gasEr90^2+gasErbs^2)/TotGbs;

elChange10 = (TotE10-TotEbs)/TotEbs; % Relative increase electricity
elChange50 = (TotE50-TotEbs)/TotEbs;
elChange90 = (TotE90-TotEbs)/TotEbs;

elChange10Er = sqrt(elEr10^2+elErbs^2)/TotEbs; % Relative error of
electricty increase
elChange50Er = sqrt(elEr50^2+elErbs^2)/TotEbs;
elChange90Er = sqrt(elEr90^2+elErbs^2)/TotEbs;

%% Calculating change in temperature

avTpbs = mean(TPbs);
avTp10 = mean(TP10);
avTp50 = mean(TP50);
avTp90 = mean(TP90);

tpChange10 = (avTp10-avTpbs)/avTpbs;
tpChange50 = (avTp50-avTpbs)/avTpbs;
tpChange90 = (avTp90-avTpbs)/avTpbs;

%% Wrting results back into Excel workbook - Sheet 2

% Headers
col_header={'Week No','Temp_base (°C)','Elec_base (W/m2)','Gas_base
(W/m2)',...
    'Temp_10% (°C)','Elec_10% (W/m2)','Gas_10% (W/m2)',...
    'Temp_50% (°C)','Elec_50% (W/m2)','Gas_50% (W/m2)',...
    'Temp_90% (°C)','Elec_90% (W/m2)','Gas_90% (W/m2)',...
    '','','Change 10%','Error 10%','Change 50%','Error 50%','Change
90%','Error 90%'};
row_header1={'Average';'Total use';'Total error'};
row_header2={'Electricty (%)';'Gas(%)';'Temperture (%)'};

% Data
```

```
xlsData1=[[1:52]' TPbs' Ebs' Gbs' TP10' E10' G10' TP50' E50' G50' TP90'
E90' G90'];
xlsData2=[avTpbs, mean(Ebs), mean(Gbs), avTp10, mean(E10), mean(G10),...
    avTp50, mean(E50), mean(G50), avTp90, mean(E90), mean(G90),;...
    0, TotEbs, TotGbs, 0, TotE10, TotG10, 0, TotE50, TotG50, 0, TotE90,
TotG90;...
    0, elErbs, gasErbs, 0, elEr10, gasEr10, 0, elEr50, gasEr50, 0, elEr90,
gasEr90];
xlsData3=100*[elChange10, elChange10Er, elChange50, elChange50Er,
elChange90, elChange90Er;...
    gasChange10, gasChange10Er, gasChange50, gasChange50Er, gasChange90,
gasChange90Er];
xlsData4=100*[tpChange10,0,tpChange50,0,tpChange90];

% Writing to Excel
xlswrite('C:\Users\bao_mading\Documents\MATLAB\Supermarket.xlsx',col_head
er,'Sheet2','A1')
xlswrite('C:\Users\bao_mading\Documents\MATLAB\Supermarket.xlsx',row_head
er1,'Sheet2','A55')
xlswrite('C:\Users\bao_mading\Documents\MATLAB\Supermarket.xlsx',row_head
er2,'Sheet2','O2')
xlswrite('C:\Users\bao_mading\Documents\MATLAB\Supermarket.xlsx',xlsData1
,'Sheet2','A2')
xlswrite('C:\Users\bao_mading\Documents\MATLAB\Supermarket.xlsx',xlsData2
,'Sheet2','B55')
xlswrite('C:\Users\bao_mading\Documents\MATLAB\Supermarket.xlsx',xlsData3
,'Sheet2','P2')
xlswrite('C:\Users\bao_mading\Documents\MATLAB\Supermarket.xlsx',xlsData4
,'Sheet2','P4')

disp('Finished')
% END OF PROGRAMME
```

```
function wkData=mth2wk(mthData)
% Generates weekly data by interpolating between monthly data points

if length(mthData)~=12
  error('Vector needs to contain 12 monthly values')
end

mth=1:14;
mthData2=[mthData(end) mthData' mthData(1)];
wkd=linspace(1,length(mth),56); % to have Dec and Jan and oposite end
wkDatad=interp1(mth,mthData2,wkd);
wkData=wkDatad(3:54);

end %End of function mth2wk
```

```
%%%%%%%%%%%%%%%%%%%%%%%%%%%%%%%%%%%%%%%%%%%%%%%%%%%%%%%%%%%%%%%%%%%%%%%%%%%%
%
%    REFRIGERATION SYSTEM MODEL (M&S Hull, Anlaby: Pack 1)
%
%    20/02/15: Started (MB)
%    24/02/15: Fixed bug - saw tooting at higher temperature (Tcd-dT<Tamb)
%              Finished version 1.0
%    25/02/15: Version 1.1: Change the way h3 and the n_fan of the old
%              contorl is calculated
%    01/03/15: Version 1.2: Finished testing, tweekt E_comp equation to
%    overlay well on measured data
%    04/03/15: Version 1.3: E_comp relates now simulation results to
%    measurements => Better fit
%   21/04/15: Renumbering of enthalpies
%
%%%%%%%%%%%%%%%%%%%%%%%%%%%%%%%%%%%%%%%%%%%%%%%%%%%%%%%%%%%%%%%%%%%%%%%%%%%%

% This script emulates the R404A side of the pack 1 of the refrigeration
% system installed in the M&S supermarket in Hull, Anlaby.

%% Main Cell
clear all

% VARIABLE DECLARATION

c_rf = 0.8917; % [kJ/kg/K]: Average heat constant in superheat region
% dS [kJ/kg/K]: Enthalpy change in vapour region
h5 = 363.29; % [kJ/kg]: Specific enthalpy at evaporator out
% h1 [kJ/kg]: Specific enthalpy as suction port of compressor
% h2 [kJ/kg]: Specific enthalpy at discharge port of compressor
% h2d [kJ/kg]: Specific enthalpy at start of isothermal condensing
% h3 [kJ/kg]: Specific enthalpy at outlet of condenser
% dh_HX [kJ/kg]: Specific enthalpy change through HX
% m_dot [kg/s]: Refrigeration mass flow rate
% op_mode [-]: day time = 1, night time = 0
% p_c [bar_g]: (vector) Condenser pressure
p_e = 3.5; % p_e [bar_g]: Evaporator pressure
% E_comp [kW]: Energy consumption of compressor
% E_fan_n [kW]: Energy consumption of fan with new control algorithm
% E_fan_od [kW]: Energy consumption of fan old control algorithm - day
% mode
% E_fan_on [kW]: Energy consumption of fan old control algorithm - night
% mode
% E_n [kW]: (Matrix) Total energy consumption for new algorithm
% E_o [kW]: (Matrix) Total energy consumption for old algorithm
% eps [-]: Average effectiveness of HX
eta = 1; %[-]: Efficiency of compressors
% i [-]: Loop index for p_c loop
% j [-]: Loop index for T_on loop
% k [-]: Loop index for Qdot_e loop
maxE_fan = 7.6; %[kW]: Maximum power consumption of all condenser fans
% Qdot_e [kW]: (vector) Refrigeration effect
% Tamb [°C]: Ambient temperature
% T_c [°C]: Average condensing temperature
T_e = -8.8; % [°C]: Temperature of saturated vapour at evaporator out
% T_on [°C]: (vector) Air temperature onto the compressor

% Qdot_e=[30 60]; day=0;
Qdot_e = 20:1:80;
day = 0; % Night time operation test
```

```
% Qdot_e = [55 60 65]; day = 1; % Day time operation test
T_amb = 5:0.1:30;
p_c = 9:0.01:18.5;
% p_c=[9:18.5];
clc
disp ('Programme started')

% CALCULATIONS
% Loops
for k = length (Qdot_e):-1:1;% Refrigeration load loop
  for j = 1:length (T_amb) % Air onto condenser loop
    for i = 1:length (p_c)% Condenser pressure loop

      % Enthalpies
      eps = -0.000055278132 * Qdot_e(k)^2 + 0.001676007808 * Qdot_e(k) +
0.857278155966;
      T_c = -0.0722 * p_c(i)^2 + 4.6862 * p_c(i) - 19.142;
      dh_HX = eps * c_rf *(T_c - T_e);
      h1 = h5 + dh_HX;
      % dS = 0.003407 * h1 + 0.3864;
      a=0.12397*h1-24.793;
      % h0 = 159.18*dS^2-296.71*dS+397.47;
      h2 = a*log((p_c(i)+1)/4.5)+h1;
      h2d = -0.069930 * p_c(i)^2 + 2.8095 * p_c(i) + 357.35;
      h3 = -0.081402 * p_c(i)^2 + 6.8432 * p_c(i) + 169.91;
      m_dot = Qdot_e(k)/(h1-h3);

      % Energy consumption of compressor
      E_comp(i) = 1.91*m_dot * (h2 - h1)+3.1;

      % - Energy consumption of fans and total consumption
      [n, pc_sm] = n_old(p_c(i),h2,h2d,h3,T_c,T_amb(j),m_dot,day);
      if pc_sm ~= 1
        oE_fan(i) = maxE_fan * n^3;
      else
        oE_fan(i) = 9e99; %High values to avoid false minimums
      end
      oE (i) = oE_fan(i) + E_comp(i);

      [n, pc_sm] = n_new(p_c(i),h2,h2d,h3,T_c,T_amb(j),m_dot);
      if pc_sm ~= 1
        nE_fan(i) = maxE_fan * n^3;
      else
        nE_fan(i) = 9e99; %high values to avoid false minimums
      end
      nE (i) = nE_fan(i) + E_comp(i);

    end

    % Find minimum new control
    [nMinE_tot(k,j),nc_min]=min(nE);
     nMinE_fan (k,j) = nE_fan(nc_min);
     nMinE_comp (k,j)= nMinE_tot(k,j)-nMinE_fan (k,j);

    % Find minimum old control
    [Dummy, c_temp] = min (oE_fan); % To start search after high value
    [oMinE_comp(k,j),oc_min]=min(E_comp(c_temp:length(E_comp)));
    oc_min=oc_min+c_temp-1; % index relative to start of sensible fan
values
    oMinE_fan (k,j) = oE_fan(oc_min);
```

```
    oMinE_tot (k,j) = oE(oc_min);

  end

end
disp ('Finished calculating :-)')

%% OUTPUT

% Preparing output
for l = length(Qdot_e):-1:1;
  COPo(:,l)=Qdot_e(l)./oMinE_tot(l,:)';
end

figure(1); plot(T_amb,COPo(:,1),'r',T_amb,COPo(:,2:end),'r','linewidth',
2.5)
title(['Maximum COP - Cooling load: from ',num2str(Qdot_e(1)),' kW to
',num2str(Qdot_e(end)),' kW'],'FontSize',20)
grid on
xlabel('Ambient temperature (deg C)','FontSize',18)
ylabel ('COP','FontSize',18)

figure(2); plot(T_amb,nMinE_tot(1,:),'r',T_amb,nMinE_comp(1,:),'c--
',T_amb,nMinE_tot(2:end,:),'r',T_amb,nMinE_comp(2:end,:),'c--
','linewidth', 2.5)
title(['Maximum COSP - Cooling load: from ',num2str(Qdot_e(1)),' kW to
',num2str(Qdot_e(end)),' kW'],'FontSize',20)
grid on
xlabel('Ambient temperature (deg C)','FontSize',18)
ylabel ('Power (kW)','FontSize',18)
legend ('Total power','Compressor power')

figure(3); plot(T_amb,oMinE_tot(1,:),'r',T_amb,oMinE_comp(1,:),'c--
',T_amb,oMinE_tot(2:end,:),'r',T_amb,oMinE_comp(2:end,:),'c--
','linewidth', 2.5)
title(['Maximum COP - Cooling load: from ',num2str(Qdot_e(1)),' kW to
',num2str(Qdot_e(end)),' kW'],'FontSize',20)
grid on
xlabel('Ambient temperature (deg C)','FontSize',18)
ylabel ('Power (kW)','FontSize',18)
legend ('Total power','Compressor power')

figure
surf(oMinE_tot);

disp ('Finished :-)')
% END OF PROGRAMME
```

```
function [n, err] = n_old(p_c,h2,h2d,h3,T_cdg,T_on,m_rf,day)
%%%%%%%%%%%%%%%%%%%%%%%%%%%%%%%%%%%%%%%%%%%%%%%%%%%%%%%%%%%%%%%%%%%%%%%%%%%%
%
%    REQUIRED AIR MASS FLOW RATE (OLD CONTROL)
%
%    22/02/15: Started (MB)
%    23/02/15: Finished version 1.0 (MB)
%
%%%%%%%%%%%%%%%%%%%%%%%%%%%%%%%%%%%%%%%%%%%%%%%%%%%%%%%%%%%%%%%%%%%%%%%%%%%%

% This function calculates the required mass flow rate when the fans are
% controlled with the old control algorithm, i.e.
% n_% = 0 for p_c < 9.5 bar_g
% n_% = (p_c-9.5) / 100 for 9.5 bar_g <= p_c <= 10.5 bar_g (max 53% for
day)
% n_% = 100% (night) or 53% (day) for p_c > 10.5 bar_g

% VARIABLE DECLARATION
c_air = 1.006; % [kJ/kg/K]: Specific heat constant of air
% day [-]: 1 if refrigeration system in day time operation mode
dT = 2; %[K]: Temperature difference between average condenser
temperature
% dT_air [K]: Temperature difference between air on and off condenser
% and air off the condenser
err = 0; % [-]: Error variable, 1 if insufficient air through condenser
% h2 [kJ/kg]: Specific enthalpy at discharge port of compressor
% h2d [kJ/kg]: Specific enthalpy at start of isothermal condesing process
% h3 [kJ/kg]: Specific enthalpy at outlet of condenser
% m_arq [kg/h]: Air mass flow rate required to reject heat from condenser
% m_rf [kg/s]: Refrigeration mass flow rate
max_m_fan = 33.7148; %[kg/s]: Maximum mass flow rate through condenser
%                    (maxV_fan * roh = 28 m3/s * 1.2014 kg/m3)
n = 0; % [-]: Speed of fans
roh = 1.2041; %[kg/m3] Average density of air
% T_cdg [°C]: Average condensing temperature
% T_on [°C]: Air temperature onto the condenser
% T_sh [°C]: Superheat temperature at h2
Q_air = 15; % [kW]: Heat removed through air passing through condenser
%                 Default value for convective mode, i.e. n = 0
% Qdot_c [kW]: Total heat reject by condenser
% Qdot_cdg [kW]: Heat rejected during condensing of the refrigerant
% Qdot_sh [kW]: Heat reject during de-superheating the refrigerant

% CALCULATIONS

Qdot_c = m_rf * (h2-h3); %Heat rejected by condenser
Qdot_cdg = m_rf * (h2d - h3); %Heat rejected by condensing part
Qdot_sh = Qdot_c - Qdot_cdg; %Heat rejected by de-superheating part

T_sh = 0.0049022 * p_c^2 + 0.00011216 * h2^2 + 6.6677 * p_c + 1.02716 *
h2 -0.013191 * p_c * h2 - 401.16;

mair_cdg = Qdot_cdg / c_air / (T_cdg - dT - T_on);
mair_sh = Qdot_sh / c_air / ((T_sh + T_cdg)/2 - dT - T_on);
m_arq = mair_cdg + mair_sh;
dT_air = Qdot_c / m_arq / c_air;

if p_c > 10.5
   if day == 1
      n = 0.53;
```

```
   else
      n = 1;
   end
Q_air = n * max_m_fan * c_air * dT_air;
end

if (p_c >= 9.5 && p_c <= 10.5)
   if day == 1
     n = 0.53/(1+0.25*exp(-15*(p_c-10)));
   else
     n = 1/(1+0.25*exp(-15*(p_c-10)));
   end
Q_air = n * max_m_fan * c_air * dT_air;
end

if Qdot_c > Q_air | (T_cdg-dT) < T_on
  err = 1;
  n = -1;
end

%END FUNCTION
end
```

```
function [n, err] = n_new(p_c,h2,h2d,h3,T_cdg,T_on,m_rf)
%%%%%%%%%%%%%%%%%%%%%%%%%%%%%%%%%%%%%%%%%%%%%%%%%%%%%%%%%%%%%%%%%%%%%%%%%%%%
%
%    REQUIRED AIR MASS FLOW RATE (NEW CONTROL)
%
%    23/02/15: Started (MB)
%
%%%%%%%%%%%%%%%%%%%%%%%%%%%%%%%%%%%%%%%%%%%%%%%%%%%%%%%%%%%%%%%%%%%%%%%%%%%%

% This function calculates the required mass flow rate and returns the
speed
% if it is 1 or less otherwise the error variable becomes 1.

% VARIABLE DECLARATION
c_air = 1.006; % [kJ/kg/K]: Specific heat constant of air
dT = 2; %[K]: Temperature difference between average condenser
temperature
err = 0; % [-]: (o/p) Error variable, 1 if insufficient air through
%              condenser
% h2 [kJ/kg]: (i/p) Specific enthalpy at discharge port of compressor
% h2d [kJ/kg]: (i/p) Specific enthalpy at start of isothermal condensing
% h3 [kJ/kg]: (i/p) Specific enthalpy at outlet of condenser
% m_arq [kg/h]: Air mass flow rate required to reject heat from condenser
% m_rf [kg/s]: (i/p) Refrigeration mass flow rate
max_m_fan = 33.7148; %[kg/s]: Maximum mass flow rate through condenser
%                    (maxV_fan * roh = 28 m3/s * 1.2014 kg/m3)
n = -1; % [-]: (o/p) Speed of condenser fans as fraction of full speed
% T_cdg [°C]: (i/p) Average condensing temperature
% T_on [°C]: (i/p) Air temperature onto the condenser
% T_sh [°C]: Superheat temperature at h2
% Qdot_c [kW]: Total heat reject by condenser
% Qdot_cdg [kW]: Heat rejected during condensing of the refrigerant
% Qdot_sh [kW]: Heat reject during de-superheating the refrigerant

% CALCULATIONS
% - Enthalpies
Qdot_c = m_rf * (h2-h3);
Qdot_cdg = m_rf * (h2d - h3);
Qdot_sh = Qdot_c - Qdot_cdg;

T_sh = 0.0049022 * p_c^2 + 0.00011216 * h2^2 + 6.6677 * p_c + 1.02716 *
h2 -0.013191 * p_c * h2 - 401.16;

% - Required air mass flow rate
mair_cdg = Qdot_cdg / c_air / (T_cdg - dT - T_on);
mair_sh = Qdot_sh / c_air / ((T_sh + T_cdg)/2 - dT - T_on);
m_arq = mair_cdg + mair_sh;

if m_arq > max_m_fan | (T_cdg-dT) < T_on
  err = 1;
else
  n = m_arq / max_m_fan;
end

%END FUNCTION
end
```